

DISS. ETH Nr. 26178

STRUCTURAL BUILD-UP FOR DIGITAL FABRICATION WITH
CONCRETE – MATERIALS, METHODS AND PROCESSES

A thesis submitted to attain the degree of

DOCTOR OF SCIENCES of ETH ZURICH

(Dr. sc. ETH Zürich)

presented by

LEX REITER

M.Sc. ETH in Bauingenieurwissenschaften, ETH Zürich

born on 19.01.1989

citizen of Luxembourg

accepted on the recommendation of

Prof. Dr. Robert J. Flatt, examiner

Prof. Dr. Richard A. Buswell, co-examiner

Prof. Dr. Viktor Mechtcherine, co-examiner

Dr. Timothy Wangler, co-examiner

2019

Contents

CONTENTS	I
LIST OF FIGURES.....	IV
LIST OF TABLES.....	VI
ABSTRACT	VII
ZUSAMMENFASSUNG.....	VIII
CHAPTER 1 INTRODUCTION.....	1
1.1. General introduction	1
1.2. Open questions in digital fabrication with concrete.....	4
1.3. Objective of the thesis.....	6
1.4. Structure of the manuscript	7
CHAPTER 2 THE ROLE OF EARLY AGE STRUCTURAL BUILD-UP IN DIGITAL FABRICATION WITH CONCRETE.....	9
Abstract	10
2.1. Introduction	10
2.2. Types of material evolution in digital fabrication	11
2.2.1. Building processes in digital fabrication	11
2.2.2. Macroscopic buildup requirements	14
2.3. Physico-chemical concepts of structural build-up.....	17
2.3.1. Definitions	17
2.3.2. Mechanisms responsible for structuration.....	18
2.3.3. Characterization methods for structuration	20
2.4. Manipulating structural build-up.....	22
2.4.1. Thickening vs. acceleration	22
2.4.2. Controlling the structuration rate	25
2.5. Examples in digital fabrication processes.....	26
2.5.1. Practical considerations for thickener and activator choice.....	26
2.5.2. Structuration during material delivery	27
2.5.3. Process scaling.....	28
2.5.4. Dealing with variability	30
2.6. Conclusions	31
CHAPTER 3 PROCESS AND RHEOLOGY MODELS FOR STRUCTURING MATERIALS	32
List of symbols	33
Abstract	35
3.1. Introduction	36
3.2. Material evolution providing resistance	38
3.2.1. Capturing the yield stress evolution at rest.....	38
3.2.2. Evolution of instantaneous yield stress.....	39
3.2.3. Yield stress and build-up variations.....	42
3.3. Stability criteria	44
3.3.1. Requirement for self-support.....	44
3.3.2. Self-weight induced buckling	46

Contents

3.3.3. Interactions with supporting elements	51
3.3.4. Material changes to be avoided	55
3.4. Linking stability criteria to processes	56
3.4.1. Slip-forming process	56
3.4.2. Layered extrusion	65
3.4.3. Digital casting	70
3.4.4. Coatings.....	72
3.4.5. Shotcrete and precision spraying	73
3.5. Conclusions	74
CHAPTER 4 CONTINUOUS CHARACTERISATION METHOD FOR YIELD STRESS OF FRESH CONCRETE AT REST	76
Abstract	77
4.1. Introduction	77
4.2. Materials and methods	80
4.3. Understanding penetration experiments in concrete and soil	81
4.3.1. A soil mechanics approach to fresh concrete	81
4.3.2. Penetration in soil mechanics	84
4.3.3. Bearing capacity factors for conical penetration tests.....	86
4.3.4. Penetration and compressive strength in fresh concrete	89
4.4. Discontinuous and continuous methods on cement pastes	92
4.4.1. Fast penetration	92
4.4.2. Slow penetration	95
4.4.3. Complementary methods	97
4.4.4. Yield stress from experimental methods.....	98
4.5. Continuous penetration in mortars	101
4.6. Discussion	104
4.6.1. Slow penetration test for yield stress characterisation.....	104
4.6.2. Measuring recommendations	105
4.6.3. Checklist for measurements.....	107
4.6.4. Application to mortars used for digital fabrication	107
4.6.5. Effect of hydration	108
4.7. Conclusion.....	110
CHAPTER 5 DISTINGUISHING FLOCCULATION AND HYDRATION EFFECTS ON STRUCTURATION	111
Abstract	112
5.1. Introduction	113
5.2. Materials and Methods	114
5.3. Model system for study of flocculation	116
5.3.1. Retarding cement hydration	116
5.3.2. Changes to pore solution	118
5.3.3. Changes to hydrates	123
5.3.4. Competitive adsorption	124
5.3.5. Rheological consequences of sucrose addition	126
5.4. Structuration from flocculation	127
5.4.1. Measuring at different times in the induction period.....	127
5.4.2. Changing the solid volume fraction.....	128

Contents

5.4.3. Changing the interstitial viscosity.....	130
5.5. Structuration from hydration	131
5.5.1. Measuring at different times from induction to acceleration period	131
5.5.2. Yield stress at long resting times.....	132
5.5.3. Relating structural build-up to the rate of hydration.....	133
5.6. Discussion	135
5.6.1. Understanding sucrose retardation.....	135
5.6.2. Understanding flocculation.....	140
5.6.3. Understanding structural build-up from hydration.....	142
5.6.4. Consequences for building processes.....	143
5.7. Conclusions	144
CHAPTER 6 SET ON DEMAND SYSTEMS FOR DIGITAL FABRICATION WITH CONCRETE	147
Abstract	149
6.1. Goals for the set on demand system	150
6.2. Concepts for hydration control.....	151
6.2.1. Fundamentals of hydration	151
6.2.2. Types of mineral binders.....	151
6.2.3. Delaying the time of hydration onset.....	153
6.2.4. Causing onset and accelerating cement hydration	154
6.3. Setting on Demand.....	155
6.3.1. Achieving the strength requirements.....	155
6.3.2. Negating retardation on demand.....	156
6.3.3. Acceleration on demand	160
6.4. Practical aspects.....	165
6.4.1. Set on Demand processes at work	165
6.4.2. Mixing chamber	166
6.4.3. Dealing with time dependent effectiveness of activators	168
6.4.4. Applying Set on Demand systems	169
6.5. Conclusions	170
CHAPTER 7 CONCLUSIONS AND OUTLOOK.....	171
7.1. Main outcome.....	171
7.2. Importance of structural build-up	173
7.3. Outlook	173
REFERENCES.....	180
ACKNOWLEDGEMENTS	196
APPENDIX.....	198
CURRICULUM VITAE	201

List of figures

Figure 2.1: Setups to control concrete hardening for layered extrusion.....	12
Figure 2.2: Setup to control concrete hardening for slipforming.....	13
Figure 2.3: Macroscopic material evolution for a single layer and subsequent layers and failure modes associated.....	16
Figure 2.4: Time scales of structural buildup in concrete for digital fabrication	19
Figure 2.5: Examples of measurement methods for structural build-up.	21
Figure 2.6: Relation of long-term structural build-up to hydration.....	25
Figure 2.7: Practical implications, residence time distribution in long delivery pipes	28
Figure 2.8: Practical implications, achievements in contour length changes.....	30
Figure 3.1: Qualitative changes in mineral binders with occurring structuration	39
Figure 3.2: Estimated relative yield stress increase for a cement paste.....	42
Figure 3.3: Yield stress evolution of a mortar activated at two different times after water addition.....	43
Figure 3.4: Vertical element and the associated loading and yield stress.....	45
Figure 3.5: Shear stress and storage modulus normalised to storage modulus at rest and yield stress.	46
Figure 3.6: Supported vertical building element loaded horizontally and subjected to its own weight.	46
Figure 3.7: Supporting elements	52
Figure 3.8: Friction in the building process, when a formwork is moved upwards.....	54
Figure 3.9: Formwork pressure with increasing material level in formwork.....	55
Figure 3.10: Weight of concrete in formwork, friction on formwork walls, yield stress and coordinate system.	57
Figure 3.11: Size of formwork and relationship to hydrodynamic radius.....	58
Figure 3.12: Characterization of yield stress and process range by measurement of friction and formwork pressure.	61
Figure 3.13: Friction and formwork pressure measurements for slip-forming rate.....	62
Figure 3.14: Yield stress evolution as designed for slip-formin and yield stress requirements.	65
Figure 3.15: Yield stress calculated from penetration tests and compressive strength and requirements	68
Figure 3.16: Dependence of shape of cylinder for the buckling mode.....	69
Figure 4.1: Mechanical behaviour of drained and undrained soils	84
Figure 4.2: Steps of the penetration test and kinematic shear failure surface.....	89
Figure 4.3: Estimation of ratio of penetration stress and compressive stress.....	92
Figure 4.4: Fast penetration. Dependence of depth and container geometry	93
Figure 4.5: Fast penetration for the same geometry at different times.	94
Figure 4.6: Slow penetration, repetitions and comparison to flat tip	96
Figure 4.7: Vane measurements at constant strain rate	97
Figure 4.8: Measurements penetration force and yield stress calculated from vane test and uniaxial compression.....	99
Figure 4.9: Slow penetration evolution for different mortars	102
Figure 4.10: Yield stress from compressive strength.....	102

List of figures

Figure 4.11: Yield stress calculated from slow penetration tests and compared to discrete measurements.....	103
Figure 4.12: Yield stress on mortars as used for layered extrusion, slip-forming and casting (SCC).	108
Figure 5.1: Heat rate as a function of hydration time for increasing sucrose dosage	117
Figure 5.2: Adsorption of sucrose in Portland cement pore solution	119
Figure 5.3: Adsorption isotherm of sucrose in a calcium hydroxide suspension and Ca concentration in CH pore solution.....	120
Figure 5.4: Ion concentration in pore solution of the major ions Ca, K, Na, S (being SO ₄) and OH and of the minor ions Al, Fe, Mg and Si by ICP.....	122
Figure 5.5: Saturation index of pore solutions with respect to portlandite, C-S-H, gypsum and syngenite, following a method described in[211]. Values larger than 0 indicate oversaturation and indicate that this phase can form.....	123
Figure 5.6: Mass loss 200-350°C and CH formed	124
Figure 5.7: Heat rate in cement pastes containing both sucrose and CH	125
Figure 5.8: Apparent viscosity evolution in pastes with a w/c 0.4 during a pre-shear and structuration at rest.....	126
Figure 5.9: Evolution of structural build-up at rest and at low heat rate.....	128
Figure 5.10: Shear elastic modulus as a function of resting time for five cement solid volume fractions in a retarded system.....	130
Figure 5.11: Storage modulus evolution with added PEG at increasing dosage	131
Figure 5.12: Storage modulus evolution at rest, capturing structural build-up.....	132
Figure 5.13: Shear stress and storage modulus after 20 minutes at rest measured by oscillation sweep.....	133
Figure 5.14: Structuration on the left axis compared to the rate of hydration by isothermal calorimetry on the right axis.....	134
Figure 5.15: Storage modulus after 20 minutes compared to the heat rate	134
Figure 5.16: Calcium concentration from figure 5.4.....	138
Figure 6.1: Ternary binder diagram.....	153
Figure 6.2: Set on Demand application concept with a retarded concrete batch and an activator, pumped into a mixing reactor	155
Figure 6.3: Heat release of cement pastes retarded with a PCE based superplasticizer with the subsequent addition of bentonite.....	156
Figure 6.4: Heat release rate of OPC mortar retarded with sucrose and containing PCE based superplasticizer, and activated 1h after water addition.....	158
Figure 6.5: Heat release of a binary binder paste, consisting of the main phases C ₁₂ A ₇ and hemihydrate	160
Figure 6.6: Strength build-up of the mortar from figure 6.4 in the first 2 hours since activation.	162
Figure 6.7: Fabrication of 2.7m high articulated columns, by layered extrusion	163
Figure 6.8: Heat release rate of an OPC paste and heat release rate of a CAC mortar....	164
Figure 6.9: Heat release rate of a CAC mortar and strength build-up qualitatively measured by ultrasound travel speed.....	165
Figure 6.10: Extruders likely containing mixing chambers in use at XTreE, Sika, Baumit	167
Figure 6.11: Mixing chambers in use at ETH for the processes slipforming, layered extrusion and spraying	168

List of tables

Table 3.1: Low and high limit for yield stress in slip-forming	64
Table 4.1: Bearing capacity factors according for a 2D-wedge.....	86
Table 4.2: Ratio of penetration stress to compressive stress for a 2D-wedge and equivalent bearing capacity factor for a conical tip.....	91
Table 4.3: Best fit bearing capacity factor for mortars with different aggregate volume fraction.....	104
Table 4.4: Best fit bearing capacity factor for a large range of accelerated mortars.	108

Abstract

With the emergence of digital fabrication technologies employing concrete, a new set of challenging and demanding questions has arisen with respect to material control. In these new technologies, more emphasis lies on early age strength and its development, as many processes require concrete to sustain its own weight and subsequently, as more layers are placed, it has to sustain the weight of concrete placed on top. This is notably the case in layered extrusion and in slipforming. This thesis studies how multiple of these criteria have to be fulfilled in combination, which is giving a common framework for the study of physical requirements for building materials.

As shown in this thesis, achieving such strength build-up is achievable by controlling hydration rate. To make this work, the dichotomy of needing a long open time for processing concrete for multiple hours, while having the occurrence of hydration at the time of placing for strength build-up, needs to be overcome. For this goal, a set on demand approach has been devised, in which hydration is triggered in a mixing chamber just before placing and we have applied this for multiple processes, these being slipforming, layered extrusion and coatings. This thesis also shows different approaches of combinations of set retarders and set accelerators, that can be combined into said set on demand systems, and studies some of their fundamental mechanisms of action, allowing direct analysis of rheological consequences of flocculation and hydration processes. With a more direct link established between yield stress increase and hydration rate, a more effective link from hydration to building processes has been established.

To measure the effect of set on demand systems on strength build-up at rest (after placing) a simple to use continuous measurement method involving penetration is developed, which intends to close the gap of reliable and easy measurement techniques for structuration, a property catching increasing attention in digital fabrication with concrete. This is intended to both allow effective development and quality control measurements during processing.

Zusammenfassung

Mit der Entwicklung von Herstellungsmethoden der digitalen Fabrikation mit dem Werkstoff Beton, treten eine Reihe von neuen und anspruchsvollen Herausforderungen bezüglich Steuerung und Kontrolle von Materialeigenschaften auf. Bei diesen neuen Technologien rücken Eigenschaften wie Frühfestigkeit und dessen Entwicklung mit der Zeit stärker ins Zentrum des Interesses, da Beton bei vielen Herstellungsprozessen vom Zeitpunkt des Auftragens sein eigenes Gewicht tragen muss und diese Last danach mit zunehmender Anzahl an Schichten weiter steigt. Dies trifft insbesondere beim 3D-Druck und beim Gleitschalungsbau zu. Diese Doktorarbeit untersucht wie mehrere solche Bedingungen vom Material in einem gegebenen Prozess gleichzeitig erfüllt werden müssen und erarbeitet daraus die physikalischen Anforderungen für einen Baustoff für eine Reihe von Prozessen.

Diese Doktorarbeit zeigt, dass die Anforderungen an die Frühfestigkeitsentwicklung durch Steuerung der Hydratation von Zement erfüllt werden können. Um dies mit einem Bauprozess in Einklang zu bringen, müssen die gegenläufigen Anforderungen von einer mehrstündigen Topfzeit für die Verarbeitung des Materials und der Festigkeitsentwicklung durch Hydratation zum Zeitpunkt des Auftragens gleichzeitig erfüllt werden können. Dafür wurde eine «Set on Demand» Lösung (Abbinden bei Bedarf) erarbeitet, bei der die Hydratation kurz vor dem Auftragen in einem Mischreaktor ausgelöst wird. Dies wurde dann auf die Herstellungsprozesse Gleitschalungsbau, 3D-Druck und das Spritzen von Beschichtungen angewendet. In dieser Arbeit werden zusätzlich mehrere Möglichkeiten von Kombinationen von Verzögern und Beschleunigern für solche «Set on Demand» Systeme gezeigt, sowie deren fundamentaler Wirkweisen mit einer direkten Analyse der Auswirkungen von Flokkulation und Hydratation auf die Fliesseigenschaften im Zeitraum der Bauprozesses. Diese direktere Verbindung von Fließgrenze und Hydratationsprozess erlaubt es den Herstellungsprozess und Hydratation effizienter zu Verbinden.

Um den Effekt der Hydratation auf die Festigkeitsentwicklung in Materialien nach dem Auftragszeitpunkt effizient zu messen wurde zudem eine einfach zu benutzende kontinuierliche Messmethode durch Penetration entwickelt. Dadurch soll die

Zusammenfassung

Verfügbarkeit von einfachen und zuverlässigen Methoden zur Ermittlung von Strukturbildung (Frühfestigkeitsentwicklung) verbessert werden, damit diese wichtige Eigenschaft bei der Produktentwicklung und Qualitätskontrolle von Herstellungsprozessen und Baumaterialien besser berücksichtigt werden kann.

Chapter 1 Introduction

1.1. General introduction

With the ongoing digitalisation our notion of functionality, space and design is rapidly evolving. The boundaries of what is possible are rapidly expanding, providing solutions to desires that were not possible to realise only a few years back. In architecture and construction, the introduction of advanced design, construction and planning tools keeps expanding these possibilities allowing to imagine novel structures, details, functional elements and building procedures. An empowering act for architects and designers is the capability of merging the traditional workflow steps into a framework giving control over geometry, functionality and fabrication processes. This is being referred to as “file to factory” [1] or “digital fabrication” [2], [3]. In this way an architect may inform the geometry with features of the fabrication process, improving and enriching the design, not only ornamentally, but also functionally.

The pursuit of this dream is a gigantic undertaking, requiring advancements in understanding and technology in many research fields involving among others architecture, robotics, automation, processing, structural engineering, materials with all disciplines working towards the common goal of integration of their knowledge into construction technologies. Within this community, material scientists and technologists can take an active role, enabling the “possible” and eliminating the “not yet possible” and the “truly impossible”. With respect to concrete processing the desires arising from digitalisation are closely linked to geometrical capabilities, a notion called design space, the desire being to build construction elements that cannot be moulded or for which moulding is complex, costly or environmentally unsustainable [4]–[6]. Just as important is the notion of bespoke fabrication, the capability to build a different geometry every time in a controlled way, allowing specialised adapted solutions for every object built and if possible at no added costs. This enables to have local architectural, functional and material control, leading to mechanical and functionally optimised structures, something referred to as “form follows function”. In this sense digital fabrication enables the production of lean, efficient structures by placing material where it is needed, saving materials and resources and is not purely driven by artistic expression. Digital fabrication

Introduction

can however also become competitive for some regular or mass-produced cast geometries if substantial cost savings can be achieved, for instance by eliminating formwork.

Be it for regular or bespoke fabrication these novel building processes naturally involve an increasing complexity for the fabrication step. In concrete technology, this increased complexity comes in the form of more simultaneous requirements, ever more difficult to achieve in a given concrete. This difficulty comes together with significant variability in concrete raw ingredients, both as a function of time, for materials from the same source, and as a function of the source, which has direct consequences for the narrowness of achievable properties. For this reason, in depth understanding of the levers that allow control over concrete properties and processing are indispensable for efficient and evidence-based development. By studying the requirements of processes, knowing how to achieve them with the underlying physical and chemical processes, rather than offering only individual solutions, more universally valid descriptions can help transferring advancement to other applications.

Given the variability of raw ingredients, only very few properties of concrete can be reliably achieved without much understanding of the material system and without pre-trials. Specifically, after mixing, concrete must be “soft” enough to be moulded and must later harden within a specified time frame. Beyond this, in mix design targeted properties can be defined and achieved with concrete additives. With these additives many degrees of freedom are opened, an important one for digital fabrication being the strength build-up in placed concrete. Starting from rheology considerations, in particular yield stress and its evolution, this topic embeds early hydrations kinetics, merging topics that can traditionally be decoupled. Controlling it represents a main challenge for digital fabrication and is a core topic of research in this PhD.

Driven by the interest in processes relying on early age strength, a specific subject of increasing significance is the capability to use strength build-up to place material layer by layer. This requirement can manifest itself in various embodiments, including the capability for material to self-support. It may also require to limit negative effects, such as formwork pressure and friction along a temporary formwork. More clearly, for layered

Introduction

extrusion placed layer should not collapse when additional layers are placed on top [7], [8]. In slip-forming, a balance between low friction and fast yield stress evolution needs to be ensured in the formwork [9]. The common ground for the material evolution in these applications and independently of the building process is the self-recurring nature of concrete processing (layer by layer or at least involving a defined vertical building rate) and the need for every placed layer to show similar and process-defined structural build-up rates. Beyond the self-recurrence, the properties of concrete just before and after placement are vastly different, the first ideally shows not significant evolution, remaining fluid for an extended time-period, while the second increases strength rapidly. These conflicting requirements mean that without the long open time, many batches of concrete need to be prepared in rapid succession, otherwise, in absence of fast strength increase, vertical building rates become severely limited. Sourced from the same batch, a trigger is therefore needed to make the transition from the long open time to a rapid structural build-up [10].

Quantitatively it is well known that strength build-up on long timescales, beyond the interest of most fabrication processes, is proportional to hydration and is related to the filling by hydrates of an initially more open microstructure[11]. On the shorter timeframe of processing, where concrete can be brought to flow, strength build-up is a combined evolution of the flocculation of a cementitious matrix, due to attractive interparticle forces and of the growth of hydration products[12]. The timescales in which the contributing phenomena dominate the mechanical behaviour are however less well understood, as are the quantitative contributions, scaling between structuration and hydration, dependency on packing and the effect of admixtures. This is being studied in chapter 5. One reason for this lies in the lack of simple mechanical measuring techniques in these initial stages of hydration and this is being studied in chapter 4.

Generally, structural build-up and the process requirements can be linked to hydration reactions. It is known from shotcrete applications, that introducing a set accelerator causes rapid precipitation of hydration products [13]. Such admixtures can be added during processing to trigger hydration, an approach further explained in chapter 6. In the range of other chemical compounds, such as cross-linking epoxies, the use of two-component systems with a resin and its hardener is common. In the same way,

we can think of concrete during the open time as the resin and of its set accelerator as the hardener. Both components only react when brought in contact, enabling their combination to achieve the required strength increase upon placing.

1.2. Open questions in digital fabrication with concrete

Being a nascent research field, advanced building processes with concrete are undergoing rapid improvements. Contributions are coming from many different areas of expertise, this being often driven by processing, robotics, architectural design and structural (reinforcement) considerations [14]–[17]. All too often, the building material is taken for granted at first, with much of the focus being put on using mortar and concrete formulations initially designed for other applications. The logic behind this is to focus on what is perceived as inherent primary challenges: such as in the processing timeframe driving machines and introducing reinforcement; and at later stages hardened state properties, including the impact of layer interfaces, and general mechanical performance. Time and again these approaches sooner or later stumble over the problem of controlling materials properties and their variability. Rather than designing mix designs specifically for processing equipment, taking a more universal approach using the physical and chemical processes underlying material properties can be a useful tool to control material properties. In chapter 3 this thesis lays out processing requirements, in chapter 5 it distinguishes the contributing underlying mechanisms, joins the hydration and strength build-up and demonstrates the structuration control in multiple processes in chapter 6.

In research, for lack of adequate methods and models, strength evolution at early age is not systematically associated with the design space possibilities of the used building process, apart from some exceptions [8], [18]. Not knowing material properties, process requirements and their interplay, turns such fabrication processes “close to blind empirical experimentation” with a high sensitivity to material variability. This gap needs to be closed with simple to use tools and contributing to this represents another objective of this thesis with a method introduced in chapter 4.

Beyond this, starting process development from existing concrete formulations and excluding the degrees of freedom offered by the material system adjustments

Introduction

(tailoring rheology and hydration) carries the distinct risk of optimising building processes towards local minima characterized by poor performance and low robustness. This point can be illustrated by the case of layered extrusion (the research field with most activity), for which in order to build somewhat high components (around half a meter height) in one go, mortar formulations with high instantaneous yield stress need to be processed. This requires strong pumping equipment, but more importantly, specialised printing nozzles and the placing of materials susceptible to fracturing. All of this leads to the need for feedback control to account for layer settlement and stigmatises questions about interface bonding. In contrast, by having a much lower yield stress that increases rapidly after placing and by placing layers slightly wider than the extruder nozzle diameter, most of these challenges can be resolved and less powerful equipment can be used. However, the needed depth of insight into material chemistry and its relation to processing is more substantial. This thesis will provide examples of how achieving this does indeed enable the more efficient processing option described above and is described in chapter 6. For this binder chemistry and admixtures working mechanisms are investigated and new measurement methods are developed.

More broadly, the right choice of set accelerator and cementitious matrix for each application is essential. This is complicated by the discrepancy between the strength build-up needs of current applications involving set accelerators and the ones in development in digital fabrication with concrete. Indeed, set accelerators for regular concrete are generally effective only after some time of the order of 1 hour as concrete needs to be cast. This is too slow for the type of strength build-up required for advanced building processes. On the other hand, shotcrete accelerators react immediately with concrete and lead to a thickening within seconds of contact [13]. This is only useful if homogenisation of concrete and accelerator does not need to be perfect at the time that concrete leaves the processing equipment, with some homogenisation occurring on impact. In processes for digital fabrication other than shotcrete, proper homogenisation and controlled outflow are a must. For this reason, the contact between accelerator and concrete for homogenisation before placing needs to be of the order of 30 seconds, which is difficult to achieve with shotcrete accelerators. To solve this, we have developed and used specialised equipment in collaborative projects that are introduced in chapter 6.

1.3.Objective of the thesis

The objective of this thesis is to enable the implementation of advanced building processes, in which early age strength build-up after placing is essential, these being layered extrusion, slip-forming, digital casting and spraying. Rather than taking material evolution as a given, I place a particular focus on controlling strength build-up through hydration control.

For this purpose, I express the rheological requirements to prevent failure in the above processes within a common theoretical framework, defining the required time evolutions of yield stress for concrete at rest. For characterisation of this yield stress time evolution, a characterisation method is developed giving continuous measurements in real time and being based on mechanical shearing. Such a method can serve in processes as a quality or feedback control tool, eliminating uncertainty of material variability.

This thesis more specifically examines the contributions of flocculation and hydration to the structural build-up to neat cement pastes and the modifications caused by the set retarder sucrose to the cementitious system. This is done with the premise of finding the time-scales in which these phenomena occur and how they can be quantitatively harnessed.

To fulfil the contradictory rheological requirements of the building processes such as extended open time before concrete placing and a rapid increase of strength for placed concrete, choices to reach these yield stress evolution goals are devised. This will be achieved by delayed hydration onset, a concept called Set on Demand. For the tailoring of hydration kinetics and structural build-up to the manufacturing process, I combined different binder systems and admixtures for set retardation and acceleration into multiple Set on Demand compositions, for multiple processes.

1.4. Structure of the manuscript

This manuscript is structured as follows:

Chapter 2 presents the state of the art. It deals with the role of structural build-up in digital fabrication with concrete and is based on a journal article written as first author for a special issue of Cement and Concrete Research on the subject of concrete in digital fabrication. It is separated into 4 main parts, describing broadly the types of material evolution needed for digital fabrication, the physico-chemical concepts underlying structural build-up, the manipulation of structural build-up and practical implications on building processes. As such it connects the subjects dealt with in more detail in the following chapters.

Chapter 3 studies the rheological requirements of the building processes as studied in digital fabrication with concrete for cases where structural build-up can be technologically beneficial. In this chapter I use a general mechanics approach for modelling of the stability of structures during processing. In the first part, the material evolution required to provide a resistance to failure is determined. The related failure case is studied in the second part as a stability criterion. In the last part, the material resistance and its time evolution are brought together with a combination of different stability criteria for each process studied. With this, the required structural build-up for the placed concrete can be derived for a given process, geometry and building rate.

Chapter 4 studies a continuous characterisation method for structural build-up in concrete at rest. The chapter applies a soil mechanical model developed for foundation stability on a continuous penetration test to calculate the yield stress of concrete at rest. The yield stress derived from the theoretical approach is then compared to yield stress measurements conducted with Vane and compression tests from which yield stress can be calculated with existing models. An important outcome is the linear scaling of yield stress with the penetration force and the agreement with the theoretical analysis. Based on this, I show that the characterisation method is suited as a simple continuous measurement for quality control of concrete placed in digital fabrication.

Introduction

Chapter 5 studies the contributions of flocculation and hydration on the structural build-up of cement pastes at rest. For this purpose, by adding sucrose (a potent set retarder) a model cement system is created in which flocculation is not significantly modified, while the hydration onset is strongly delayed. With the model cement characterisations insight into the physico-chemical working mechanism of sucrose is also gained. By carefully choosing modifications to the cement system, fully new insights into the kinetics of colloidal interactions are gained as well as a link between hydration occurring at rest and structural build-up in the same timeframe. This provides the physical basis for structural build-up control by control of hydration.

Chapter 6 analyses the possibilities for modifying hydration kinetics with set retarders and accelerating admixtures as well as by changes to the cementitious system itself. It explains how retardation can be achieved, how it may be negated, and how to accelerate it with admixtures or by blending different cements. These concepts are then combined into a two-component system, based on two non-reacting or strongly retarded materials where at least one is cementitious. Upon intermixing of these components hydration begins, along the line of what I defined above as Setting on Demand. Finally, strategies for modifying hydration kinetics to match the requirements of various digital fabrication processes are devised.

Chapter 7 presents the general conclusions and outlook of this thesis. The main outcome and a highlight of the importance of structural build-up are given in a concise way. The scope of the outlook is more broadly written, trying to anticipate the potentials and challenges of structural build-up as well as process scaling questions for Set on Demand materials.

Chapter 2 The role of early age structural build-up in digital fabrication with concrete

This chapter has been previously published as first author in the journal *Cement and Concrete Research*, where it appeared as part of the special issue for Digital concrete 2018.

L. Reiter, T. Wangler, N. Roussel, and R. J. Flatt, “The role of early age structural build-up in digital fabrication with concrete,” *SI Digit. Concr. 2018*, vol. 112, pp. 86–95, Oct. 2018.[19].

It is entirely written by Lex Reiter under the guidance of Timothy Wangler, Nicolas Roussel and Robert J Flatt.

Abstract

The advent of digital fabrication for concrete calls for advancing our understanding of the entanglement of processing technology, rheology, admixture use and hydration control, in addition to developing novel measurement and control techniques. We provide an overview of recently proposed building processes, defining the type and range of yield stress evolution that they require for successful building. In doing so, we explain which mechanisms are at stake and how their consequences can be measured.

Controlling the structural build-up of concrete with the precision required by digital processes will be at the heart of future progress. For this, chemically controlling cement hydration of concrete is essential and we provide an overview of admixtures, focusing on “set on demand” solutions, concluding that activators should be added as closely to the delivery point as possible. Advantages and limitations are discussed and showcased using recent successes in process scaling and material and process control.

2.1.Introduction

Digitalisation is reaching out to revolutionise a host of industries, among them the construction industry and concrete technology. No longer limited to the rapid prototyping of small scale models, additive manufacturing is now being realized in construction scale applications [20], [21]. Digitalisation in concrete technology comes with the promise of integration of design, planning and construction processes as well as increased automation and rationalisation of building processes [22], savings on labour costs and formwork and increased workspace safety [23], [24]. Additionally, the use of robots can compensate for the increased difficulty in precisely materialising the non-standard complex geometries that architects can design and plan with their panoply of digital design tools [25]. The extension of what we can imagine, design and plan has opened up a highly innovative playground for new and rethought building processes with new challenges for concrete processing and early age mechanics.

In this new age, concrete pumping will be the backbone of automation in construction. High-resolution geometrical features and low precisely controlled process rates will limit the maximum aggregate size, by limiting the cross-sections of pumping systems and extruders. Concrete compositions will thus have higher proportions of

matrix material and the limited aggregate size will reduce the aggregate packing fraction further [26]. Optimising material use, eliminating formworks or integrating additional functionality into building elements can however offset the induced additional material costs .

Faced with automation, the need for precise placing, and limitations of traditional formworks, the paradigms “Harder, Better, Faster, Stronger” formerly at the heart of technological development and linked primarily to hardened concrete properties are now complemented by the new paradigms of precision, control, resilience and compliance, linked overwhelmingly to processing and fresh concrete properties.

This means that the efforts in bringing the up-and-coming building processes, as described in the following section, into practical use will revolve around *precisely controlling* concrete processing, flow behaviour, placing, activation and hardening, ensuring *resilience* of the building processes and of the material against deterioration and complying with building codes (especially incorporation of reinforcement)[16], process boundaries and economic considerations.

This paper provides an overview of recently proposed building processes, their requirements of yield stress evolution, how such evolutions can be measured and which physico-chemical mechanisms are underlying them. In addition, the paper shows levers to modify yield stress evolution and discusses practical consequences for the design of these digital building processes.

2.2.Types of material evolution in digital fabrication

2.2.1.Building processes in digital fabrication

The technologies associated with digital fabrication, of which a summary can be found in [28] pose particular new challenges for control of rheology [26]. Some of these new technologies, in particular 3d-printing by layered extrusion, slipforming and form filling in weak formworks, additionally require the concrete to quickly become self-supporting upon placing (at rest), in order to keep the shape stability or limit formwork pressure.

The role of early age structural build-up in digital fabrication with concrete

In the case of layered extrusion (also known by the names Contour Crafting, 3d concrete printing or cementitious ink printing), layers of concrete, mortar or cement paste are extruded and placed by means of an actuated gantry or robotic arm [14], [22], [29]–[31]. The concrete is required to stay in place instantaneously upon extrusion and to build enough strength to sustain the subsequently placed layers on top of it. Setups featuring methods to control hardening rates are illustrated in figure 2.1.

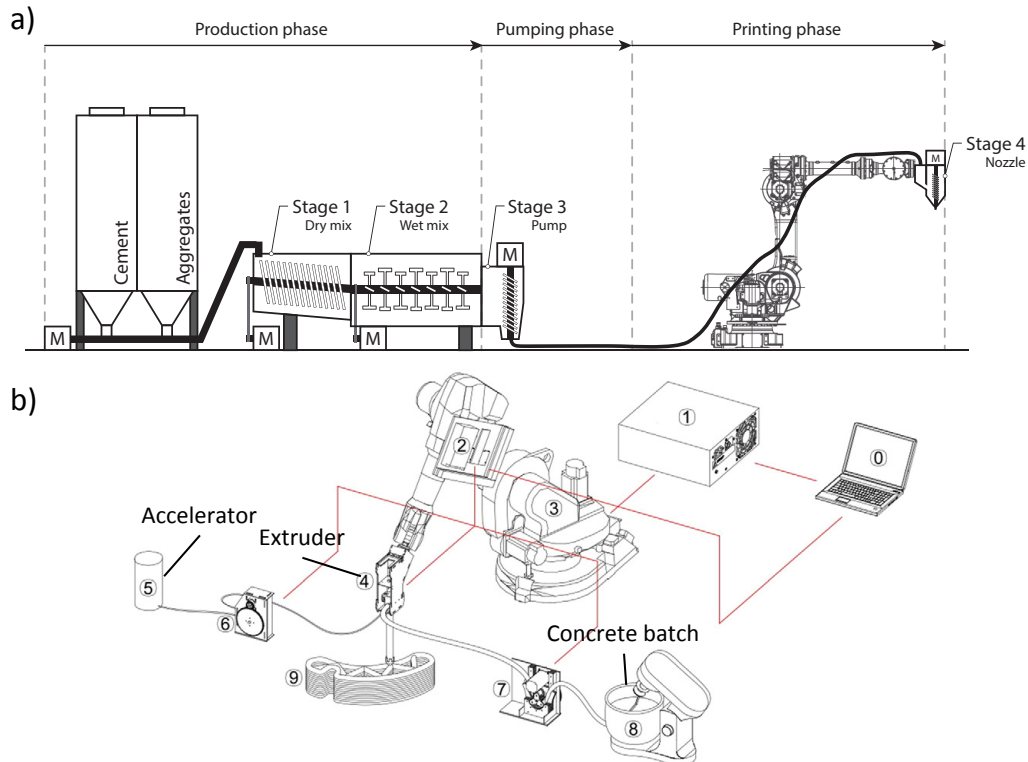


Figure 2.1: Setups to control concrete hardening for layered extrusion.

a) Setup in which hardening is controlled by continuous concrete preparation and pumping, controlling the age at the extruder [32].

b) Setup in which hardening is controlled by continuously pumping concrete from a batch and an accelerator into an extruder tool, in which they are mixed before exiting the nozzle [31].

In the case of slipforming (also called Smart Dynamic Casting when digitally controlled), a self-compacting concrete is cast into an actuated formwork that is lifted during filling [33]. Upon placing, the concrete should spread evenly inside the formwork, without segregating, bleeding or layering. Then, the placed concrete, must gain it strength and be strong enough to support the mass above it by the time it is released from the upward moving formwork [34]. A setup featuring a method to control hardening rates for slipforming is illustrated in figure 2.2.

The role of early age structural build-up in digital fabrication with concrete

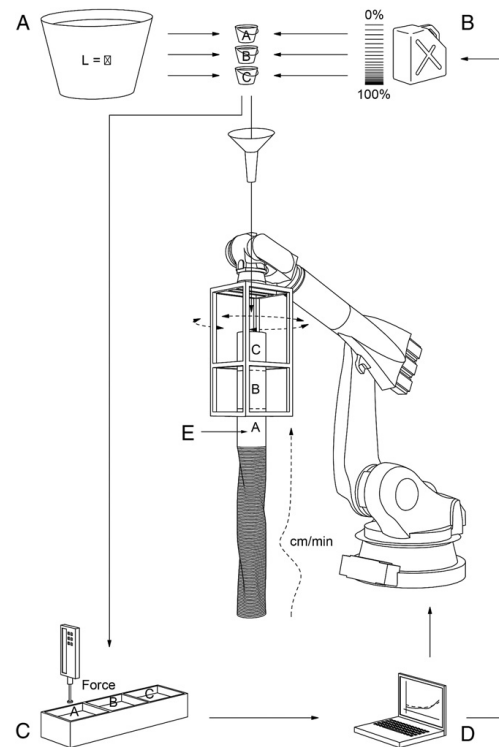


Figure 2.2: Setup to control concrete hardening for slipforming, in which hardening rates are controlled by incrementally mixing parts of a heavily retarded concrete batch with an accelerator and pouring the resulting concrete into the formwork and monitoring the hardening rate offline using penetration measurements as input for robotic feedback[33].

The only physical differences in terms of concrete processing characteristics are that, in layered extrusion, the concrete is at rest from the time of extrusion and self-supporting immediately, while, in slipforming, it is at rest from the time of casting and self-supporting when exiting the formwork. In terms of technological process characteristics however, layered extrusion is a pressure driven extrusion process, while slipforming is a gravity driven one, with respective major benefits to freedom of shape for layered extrusion and the possibility to insert reinforcement through the open top of the formwork for slipforming.

When it comes to filling formworks, recent developments indicate the interest to fill concrete or grout into formworks produced with other additive manufacturing techniques such as binder jetting [26], [35], fused deposition modelling [36] or concrete with textiles [37]. This provides a means to integrate reinforcement, eliminate possible layering issues and ultimately obtain a concrete element more similar mechanically and durability-wise to one built with non-digital processes, thus facilitating acceptance with

respect to existing building codes. When these formworks are weak, the pressure exerted on the formwork by the cast concrete can break them. One possibility to solve this challenge is to limit the formwork pressure by slowly casting a thixotropic concrete [38].

2.2.2. Macroscopic buildup requirements

In all of the above applications and as illustrated in figure 2.3, the concrete yield stress/strength should evolve faster than the hydrostatic pressure of subsequently placed concrete. In layered extrusion and slipforming one would generally target constant vertical building rates. Thus, the yield stress should at least evolve linearly over time throughout the timescale of construction, with a similar evolution for every layer with respect to the time of placing (unless the contour length changes significantly with height). This requirement is elaborated below first for layered extrusion and then slipforming.

In layered extrusion the yield stress for a single layer at the time of extrusion should be at least in the range of 150 Pa, sufficient to self-support a typical layer height of 1cm and prevent flow off. For every layer placed on top, the yield stress should increase at least according to the additional weight, in order to prevent flow out of the lower layers [26], [28], [39]. If the yield stress of the first layer is substantially above the minimum needed at the time of extrusion, but that it increases only slowly with time, then the lower layer will eventually flow under the weight of cumulated layers, something that is indeed often observed. When this occurs, many processes must wait for setting to occur, before continuing with fresh material. This poses a constraint on the size of the batches of concrete that can be prepared and on the building rate, and introduces the possibility of a poorly bonded interface between layers, as discussed later. In layered extrusion, compositions offering high yield stress evolution/thixotropy or including viscosity-modifying admixtures are often used. The use of these materials is convenient, as thixotropic build-up can be reversed by pumping, eliminating issues with starting and stopping process operation, and provide a reproducible yield stress evolution. However, the strength gain that they offer is limited and constrains building heights. In contrast, systems in which set accelerators are added shortly before placing have reported build heights of 2m [31]. Recently, the buckling of slender layered extrusion walls has been reported [40], [41], introducing a process requirement for the evolution of material

stiffness in relation to the structure slenderness. In particular, the higher the slenderness the more the yield stress must depart from a linear increase.

In slipforming, the yield stress at the time of casting should be in the range of 20 Pa (self-compacting) and it must then transition to self-support the vertical stress at the formwork exit to prevent flow out (approximately 3'000-5'000 Pa – equivalent to a formwork height of 40cm). In addition to strength considerations, friction along the sliding formwork is to be considered, as the process is gravity driven. Friction is related to yield stress and formwork surface, while the driving force is related to formwork volume. When the average yield stress in the formwork increases beyond a critical value related to the ratio of surface to volume, friction can overcome the concrete weight and lead to fracturing. Thus, the yield stress at the formwork exit should stay within a lower and an upper bound. With large surface to volume ratios (small cross-sections), these boundaries approach each other, requiring more precise hardening control. After extrusion, the yield stress has to increase at least at the same rate as the building rate. All these requirements - the existence of an upper strength limit at the time of extrusion, the narrow process boundaries, the yield stress increase in the formwork by two orders of magnitude and the progressive strength increase after - have made it necessary to control hardening rates with a high accuracy in terms of repeatability and evolution of the hardening rates. In Smart Dynamic Casting, this is achieved by pumping concrete from a large and massively retarded batch and by incrementally activating the pumped material chemically to obtain the desired yield stress evolution [42]–[44].

The role of early age structural build-up in digital fabrication with concrete

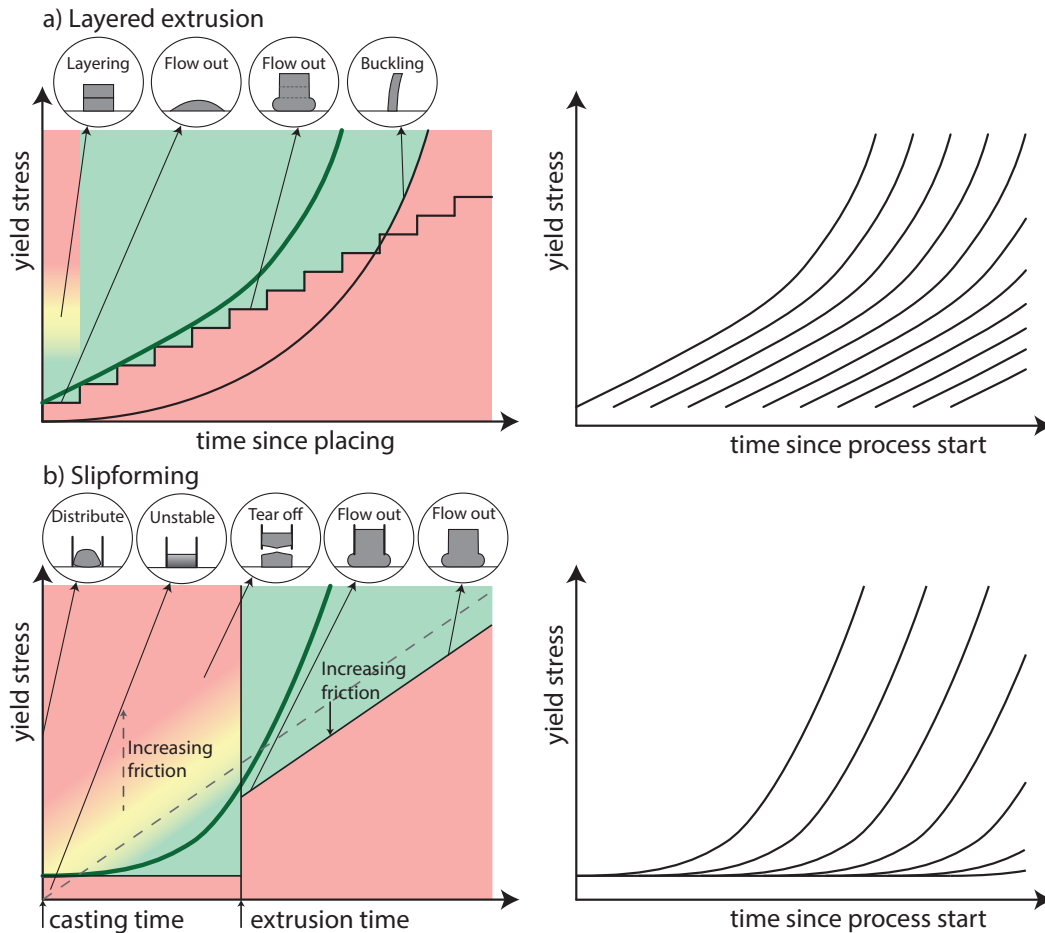


Figure 2.3: Macrocscopic material evolution for a single layer (bold green) and subsequent layers and failure modes associated (black). The green range represents the optimal conditions, yellow the range in which processing is possible but detrimental effects exist and red are conditions in which processing fails.

a) Yield stress evolution required for layered extrusion as a function of age after placing, taking into account the process limiting factors: layering, flow out and buckling for a single layer (left figure) and subsequent layers (right figure).

b) Yield stress evolution required for slipforming as a function of age after placing and after extrusion, taking into account the process limiting factors: instability, tear off and flow out for a single layer (left figure) and subsequent layers (right figure).

In the above, we have examined boundary conditions needed for vertical build up. An additional boundary is the possible formation of cold joints/lift lines. They can form from the layer-based process in layered extrusion or from very low casting rates in slipforming and form filling. It was reported that layering can severely affect mechanical cohesion between layers for self-compacting concrete when time between layers was too long [45]. How severe this is must depend on many factors. Recent studies have demonstrated the potential for strength loss can be rather severe, although this is very likely material dependent [46], [47]. Questions about how broadly this finding applies,

what the physical nature underlying cold joint formation is and how processing changes such as temperature or humidity variations will affect it, are nevertheless still to be answered. Additionally, the question about whether cold joints can compromise durability needs to be addressed. Most critically, for reinforced structures it is chloride transport and carbonation rates that must be examined. For unreinforced structures, for which digital fabrication represents an important potential, the ingress of water or salt solutions could be problematic in term of freeze thaw damage or sulphate attack. To attenuate these risks cold joint formation could be avoided by providing a certain degree of intermixing between subsequently placed layers as effectively applied for self-compacting concretes [45]. For this to be effective the strength of a placed layer should not increase too much before the next one is placed.

2.3. Physico-chemical concepts of structural build-up

2.3.1. Definitions

Fresh concrete behaves as solid when the applied stress is below a critical shear stress, called the yield stress, and behaves as liquid above this value. Concrete hence belongs to the family of yield stress fluids and this behaviour is regularly approximated by physical models such as the Bingham or Herschel-Bulkley model [48], [49]. Often concrete resistance to flow is time-dependent. This means that, at rest or for low shear rates, the shear stress to initiate or sustain flow increases because of the build-up of a stress-transferring structure, while it breaks down as flow rates increase. This is called thixotropy or structuration. Definitions and quantification techniques for thixotropy are especially ambiguous and often capture a range of flow rates and a particular shear rate history. For digital fabrication processes, concrete should not flow after placing and the yield stress evolution at rest is of importance. In order to capture this, we will use the terminology of structuration, which shall describe the time evolution of yield stress for a concrete at rest.

When concrete is sheared, the structure it has built at rest is broken and this can happen in different steps with characteristic grades of deformation, called critical strains. The lowest critical strain is of the order of 0.01%. It is situated at the end of the linear-elastic range and has been associated with the early hydrates forming at the contact points of aggregated cement grains and can be captured by non-destructive fine

oscillation or ultrasound experiments. The second critical strain is of the order of a few %. It relates to the peak shear stress/yield stress and has been associated with colloidal interactions [50]. In structuring concrete, yield stress, critical strain and elastic modulus are all time-dependent. However, the critical strains show a more limited evolution beyond a critical hydration degree [51].

For structuring concrete, competing models can predict formwork pressure [52], [53], some of which introduce a thixotropy factor A_{thix} describing a constant increase of yield stress per time unit. While intrinsically useful to estimate the possible building height, such a linear evolution is only observed in some cases and on limited time-scales.

2.3.2. Mechanisms responsible for structuration

All of the terms mentioned above are physical descriptions of fluid-mechanical behaviours and are a priori not associated with a particular underlying physical or chemical process.

Because space between sand and aggregates is saturated with matrix material, the yield stress of concrete used in digital fabrication is governed by the behaviour of the cement paste. For cement pastes, attractive interactions between cement grains leading to flocculation, and the growth of hydration products at the contact points between cement grains are the main mechanisms leading to yield stress as illustrated in figure 2.4. While flocculation is a reversible phenomenon with a short time scale, the growth of hydration products is irreversible and takes more time, partly explaining that the structuration behaviour can be reversed at early age through mixing [50]. This difference in time scales can lead to a partition of both phenomena, introducing a regime of maximum flocculation, when hydration kinetics are slow. Admixtures can influence the flocculation and hydration kinetics and are discussed in section 2.4.

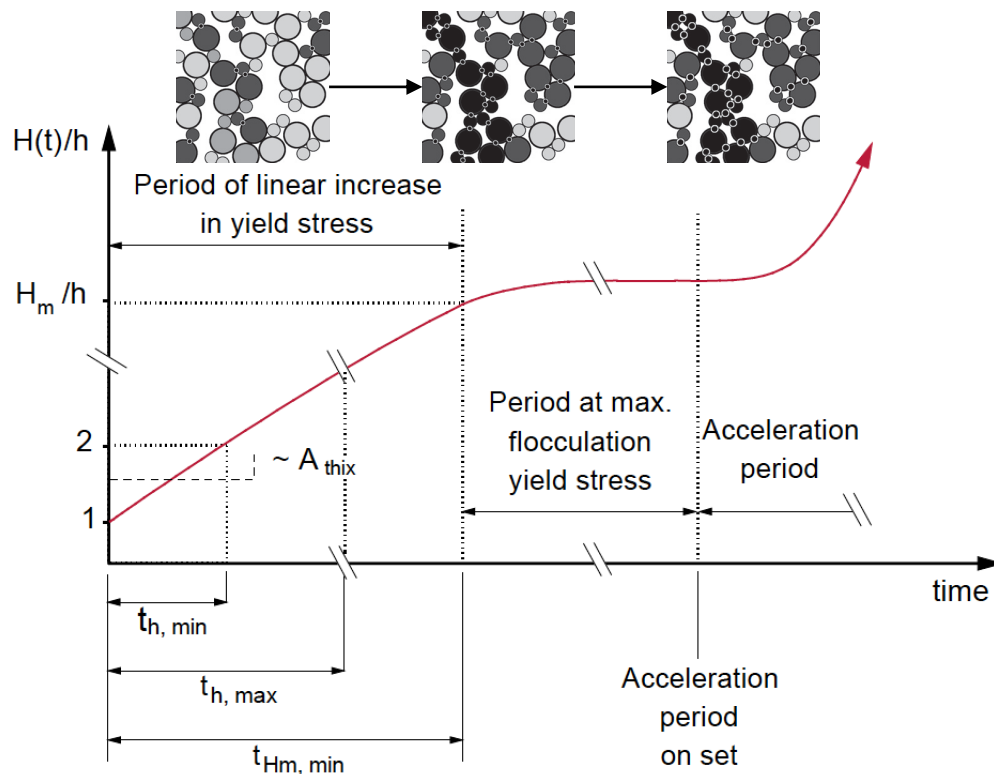


Figure 2.4: Time scales of structural buildup in concrete for digital fabrication scaled as possible building height relative to the possible building height immediately upon placing. Immediately upon placing flocculation leads to a supporting structure of cement grains of limited strength. Over longer timeframes the growth of hydration products at the grain contact points dominates the structural buildup. Modified from [28], [50].

The primary factors affecting the yield stress due to flocculation in a dense suspension are the inter-particle force that strongly relates to the number of contacts between particles and the inter-particle distance at the contact points [54]–[57]. This is influenced by a host of parameters such as the water to cement ratio and steric hindrance of molecules such as superplasticisers adsorbed on the cement [58].

The primary factor affecting the yield stress due to hydration is the rate at which hydration products are formed. The formation rate is time dependent, with low rates during the induction period and increasing rates during the acceleration period, the transition being the onset of hydration. Hydration products not only bond grains together, directly building a supporting structure, they additionally provide additional surface onto which admixtures can adsorb. Over time, this reduces the specific surface coverage of admixtures affecting also flocculation [55]. It should be noted that hydration is a combined mechanism involving dissolution of anhydrous cementitious phases into an aqueous phase, and nucleation and growth of hydrates from it. Growth surfaces, pore

solution composition and admixture adsorption strongly affect hydration kinetics and are the lever for modifying hydration with admixtures, but possible negative side effects should not be forgotten, some of which are addressed in section 2.5.1.

2.3.3.Characterization methods for structuration

Techniques qualified to measure yield stress evolution should ideally be continuous or allow multiple discontinuous measurements and should reliably determine mechanical properties. Additionally, for digital fabrication, the measurement range of interest lies between the requirement for a single layer (approx. 150Pa) and that of a building element (approx. 100kPa) [26], [28]. Measuring techniques must also be validated in mixes containing inclusions at least as large as those of the concrete considered (aggregate size and/or fiber lengths). Additionally and when possible, the sample should be processed and measured in-line. When this is not possible, or when calibration measurements are needed, samples must be measured off-line. In such situations, it is essential for them to be prepared, conditioned and processed in the way that best represents production conditions (temperature, resting times, shear rate history, etc.).

Penetration tests with a sufficiently large needle have the potential to measure strength in the needed range. That such measurements may quantitatively relate to yield stress was first reported on the basis of a combination of experimental measurements on cement paste and numerical simulations [59]. More recently, this conclusion was substantiated and broadly strengthened by using an ensemble of mechanical measurements on mortars at early age [51]. A significant result of this work was to establish that, at very early age, failure is localised at shear bands and tensile and compressive strength are of similar magnitude, while this ratio diverges in the course of hydration towards the ratio of about 1:10 known for hardened concrete, with the occurrence of distributed cracks. Measurements used for robotic feedback in slipforming are shown in figure 2.5 a).

Compression and squeeze flow tests are done by directly loading a sample layer with a force to simulate the loading with subsequently extruded layers. This is shown in figure 2.5 b). They have been carried out between two plates at the process rate of

interest to detect failure and have been related to yield stress at the time of failure [39]. It should be considered that, in an extrusion process, subsequent layers have similar yield stress and stiffness, while, in the experiment, the sample is constrained between stiff plates. Predicting the failure not for a single layer but for an extruded structure renders the use of cylinders with an aspect ratio of 2 preferable ($H=2D$). Alternatively, the loading rate can be modified. This method has potential as a simple failure prediction method for quality control.

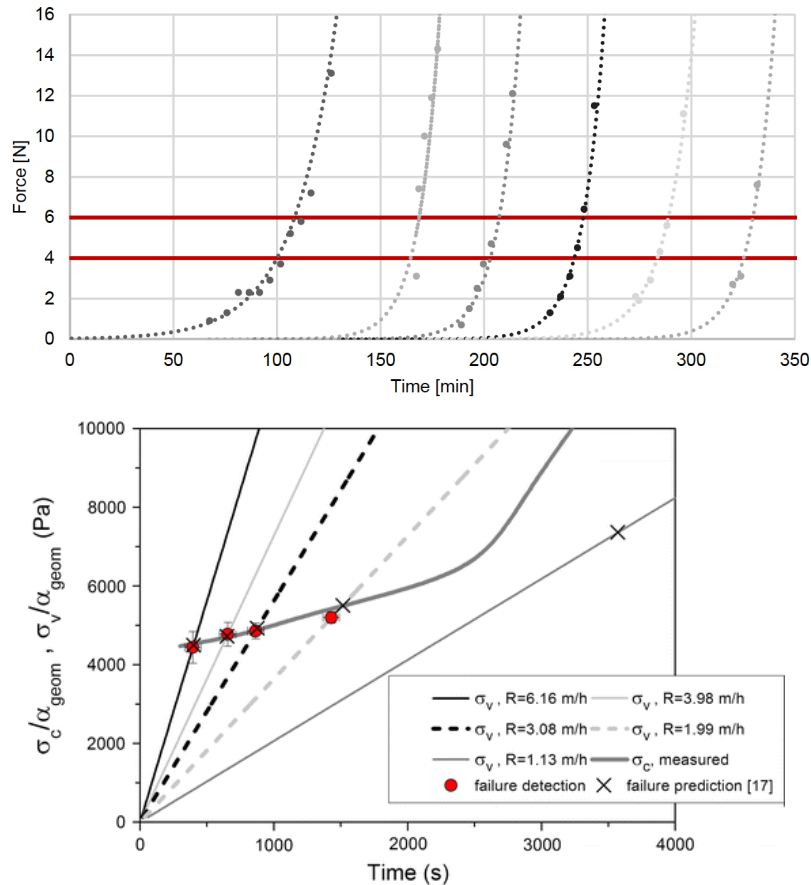


Figure 2.5: Examples of measurement methods for structural build-up.

a) Penetration force measurements used in slipforming as input for robotic feedback. The red lines indicate the upper and lower process boundaries, dotted lines represent concrete batches accelerated at different times. Reproduced from [60].

b) Squeeze flow measurements with different loading rates, simulating the layer buildup (straight lines). The stress at the detection of failure could be related to the measured yield stress evolution. Reproduced from [39].

Vane measurements can cover a broad range of yield stresses and instruments exist for mortars [61]. However, measuring yield stress evolution remains difficult as the peak shear stress that is of interest is situated in a transient flow regime (structural breakdown). Consequently, *a priori* only one point can be taken per sample. While

approaches involving multiple discontinuous measurements have been studied [62], caution should be exhibited concerning the exact level of structuration from one measurement to the next. In addition for yield stresses exceeding a critical value, shear localisation and fracturing occur, which leads to a permanent change of measuring conditions[63].

Calorimetric measurements or even thermocouples allow for monitoring the rate of hydration and could have the potential of providing information on the rate of strength increase. However, as the heat release is low in the stages of greatest interest, and even more so in mortars than in pastes, such measurements are only of limited interest. Very importantly, they do not provide information on the physical interactions between particles responsible for the flocculation controlling the stability of the first layers. Some of these underlying questions are discussed in the work of Mantellato [55].

Ultrasound can measure dynamic shear moduli, a property that is frequency dependent in concrete at early ages. By measuring multiple frequencies, it should be possible to assess the static elastic modulus, which is of interest for the process analysis. With this in hand and assuming that the critical deformation does not depend on material age, a normalised strength evolution could be estimated directly from the modulus change. If absolute values of strength are however needed, then a calibration must be carried out. In the most advantageous case, only an initial independent strength measurement, for example with a penetrometer could be used, provided once again that the critical deformation does not evolve with time. In view of this, it is expected that some strength ranges may not be reliably or robustly quantified by ultrasound, something that reported data appears to corroborate by a lack of agreement with penetration tests between 1kPa and 50kPa [59].

2.4.Manipulating structural build-up

2.4.1.Thickening vs. acceleration

Two independent methods to manipulate the yield stress evolution exist. The first category consists of agents that “thicken” the concrete upon deposition. These additives can either increase the ratio of instantaneous yield stress to apparent viscosity (helping in the processing line) and/or enhance the thixotropy upon deposition (increase yield

stress at short times). For thixotropic admixtures, several action mechanisms are conceivable, such as: providing bridging flocculation, desorbing/interacting with superplasticisers, absorbing/consuming water or increasing the viscosity of the interstitial fluid [64]–[66].

A first category of additives is chemically inert and does not directly impact cement hydration. These admixtures modify the flocculation behaviour of concrete, increasing the “effective” solid content and the number of contacts between cement particles, providing bridging between particles. They are however limited in strength to the range of colloidal interactions. VMAs, most importantly welan and diutan gum, can have very pronounced thixotropy during a few minutes after placing, but not cellulose ether [67] as reported in [68]–[70]. Additionally, if no admixtures adsorbing on clay are present, nanoclays can offer an immediate stiffening due to flocculation that is especially useful for shape stability [71], [72].

Another group of chemically inert additives induce yield stress changes that are irreversible. These additives can be added in-line and should be considered as activators. Such additives can increase the effective solid content or consume organic admixtures. For example, swelling clays strongly increase the yield stress of concrete containing polycarboxylate superplasticisers [73]–[76]. This effect comes from side chain intercalation within the clays and cannot be reversed by shear. Such effects can indirectly impact cement hydration if the adsorbed admixtures affect cement hydration [77], [78].

Additionally, if set retarding admixtures are present, admixtures consuming the retarders can be used to trigger the onset of hydration. This is possible with montmorillonite for PMA superplasticisers [77] and with portlandite for sucrose. In the case of sucrose, it is proposed that sucrose migrates through solution from cement surfaces to the surface of portlandite [79].

Accelerators directly modify the hydration kinetics of concrete and consist of admixtures that either accelerate hydration and/or cancel retardation. Three main groups of accelerators are available. The first increases the concentration of ions in the pore solution, enhancing the precipitation kinetics of hydrate phases, but possibly also

The role of early age structural build-up in digital fabrication with concrete

directly or indirectly affecting the dissolution of anhydrous phases [80], [81]. They consist mostly of inorganic salts, most prominently calcium chloride and calcium nitrate, but organic salts such as TEA also exist [82].

The second group of accelerators have compositions pertaining to those used for shotcrete accelerators [83]–[85], [82]. They typically act on the aluminates and lead to a fast formation of ettringite. This alone will stiffen the mix very rapidly, but also provide additional surface for consuming retarders and/or favouring the growth of hydrates. Depending on the system, such accelerators can lead to flash set through sulphate depletion, which can have negative effects on long-term strength development [86], [87]. We therefore expect that a balance must be found between benefitting from aluminate reactivity in terms of short-term structuration while mitigating their possible negative effect on silicate hydration.

The third group of accelerators consists of seeds that offer C-S-H surfaces for this phase to grow faster [88], [89]. Such seeds do not have as radical of an effect as the previously mentioned accelerators, but they act on silicate hydration, do not lead to sulphate depletion and are thus beneficial for a faster development of long-term strength. These accelerators strongly change the slope of the acceleration period in addition to reducing the induction period. This can result in very narrow operating time, making any process exploiting the liquid-to-solid transition very delicate.

Blended cements are interesting from the perspective of reducing the environmental impact of the concrete used. However, they are generally slower to reach specific strength. This calls for using higher accelerator dosages, which may partially overhaul their environmental benefit. Additionally, blended cements introduce a higher level of complexity and compositional variability, in particular in the case of cement containing fly-ash. Therefore, it is rather recommended to withhold from using such cements in early development stages and start implementing them once the main process requirements start to be under control.

2.4.2. Controlling the structuration rate

Manipulating the structural build-up can involve changing the time of onset for structuration and/or the rate of structuration after the onset. The time of onset can be manipulated by prolonging the induction period by using set retarding admixtures such as sugars, sulfonates and superplasticisers, of which the mechanisms are discussed in more detail by Marchon et al [56].

The irreversible structural build-up after onset relates to hydration rate and to admixture type and dosage. This is illustrated in figure 2.6 with curves showing the storage/elastic modulus gain versus the heat rate increase after the onset. Mantellato [55] has obtained similar results with superplasticiser and could even produce a master curve accounting for the polymer structure and dosage [55]. There is therefore very useful and probably quite general information to be gained from that type of data.

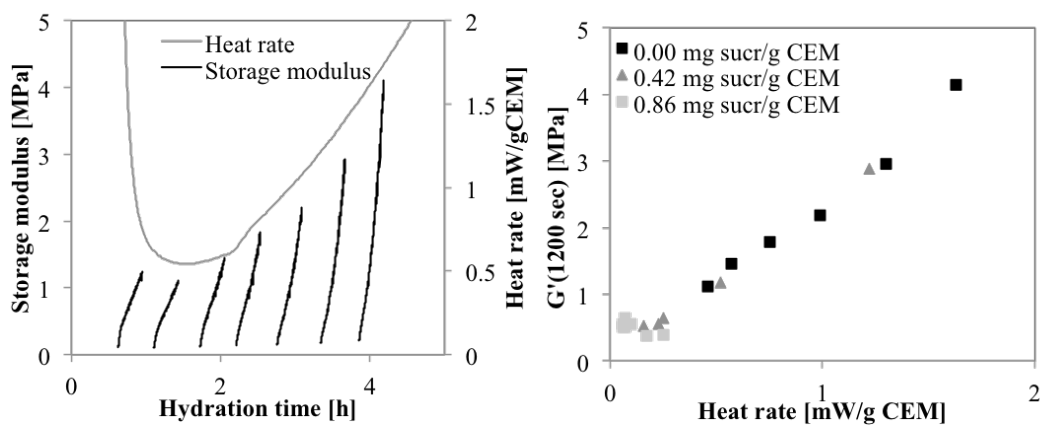


Figure 2.6: Relation of long-term structural build-up to hydration. a) The evolution of elastic modulus is measured on samples placed at different times using small amplitude oscillation strain. b) The elastic modulus after 20 minutes relates well with rate of hydration product growth as measured with isothermal calorimetry for multiple cement pastes retarded to different extent by sucrose [43].

Controlling the structuration rate after onset can be achieved by modifying the rate of hydration, typically in the acceleration phase of cement hydration. With this in mind, we must consider that each layer must follow the same kinetics, but that successive layers are placed at different times. Consequently, because the hydration rate increases in the acceleration phase, using a single concrete batch would lead to low structuration rates for the lower layers and higher ones for the upper layers [43]. This contradicts the target of having a constant structuration rate in each layer and greatly complicates

processing requirements. To overcome this and obtain similar behaviour of all layers, the use of “set on demand” systems should be considered. These are characterized by the use of a non-reacting chemically retarded base mix that is activated with set accelerators, which can be added shortly before material delivery to the base mix by using an inline mixing reactor. Alternatively, the continuous production of fresh material or the use of multiple successive small batches can be implemented.

2.5.Examples in digital fabrication processes

2.5.1.Practical considerations for thickener and activator choice

Not all admixtures triggering structural build-up introduced in section 2.4 can be used with ease technologically. In the domain of thickeners, any admixture mainly absorbing water is useful only if added dry and inline, introducing difficulties of precise dosing and dispersion in a closed system. On the other hand, admixtures directly enhancing flocculation or acting by bridging flocculation can be introduced easily into the base mixture. In general, thickeners are useful processing aids, as they enhance the structuration rate for the first layers, while attenuating difficulties associated with pumping a high yield stress concrete.

In the domain of accelerators, all admixtures are added inline and require inline mixing and accurate dosing, which favours fluid over powder addition. They trigger and/or enhance the kinetics in the acceleration phase, giving faster strength gain. As such they are especially useful when many layers are placed. When using admixtures cancelling retardation by desorbing set retarders, either large quantities of water are introduced as in the case of clay suspensions, or prohibitive admixture quantities are required as in the case of portlandite suspensions. Additionally, they do not enhance the hydration rate compared to a composition without set retarders, rendering them comparably slow.

Difficulties with the set accelerators described in section 2.4.1 are rather linked to the specific product type used. Inorganic salts are cost effective and can be added efficiently as high concentration solutions, reducing the yield stress in the mixer only to a minor extent. There are however open questions about the maximum dosage at which they may be used. *A priori*, one may expect that the bonding of such compounds to AFm

phases, as for calcium nitrates, may represent an upper bound [90]. Beyond this, typical problems occurring with soluble salts may develop over the long term if exposed to rising damp or moisture cycles [91]–[93]. Research on such questions would be needed. Beyond this, many of these accelerators can lead to steel corrosion [94], [95]. While more is known on this subject, it none-the-less deserves further attention, in particular in the cases of nitrates.

Shotcreting accelerators usually act immediately upon addition and provide very fast structuration rates, which can clog delivery lines. These enhance ettringite precipitation, activating C_3A reaction, which can lead in addition to sulphate depletion, causing a suppression of the hydration of silicates [86], [96]. Being a secondary phase, the quantity, mineralogy and morphology of aluminates is usually not, or poorly controlled in cement. Side effects of this are controlled in cement production by adjusting the sulfate content, but this can reduce the robustness of the cement and can be used to explain cement-admixture incompatibilities [97].

Concerning crystallization seeds, their main drawback in digital concrete is the associated high content of water and superplasticizer [88]. Indeed, this can reduce the yield stress at the time of addition by about 2 orders of magnitude. Starting from a concrete that can be pumped to the inline mixer without entraining uncontrollable quantities of air, this yield stress drop can easily lead to segregation.

A logical consequence of the various limitations of such accelerators is that a combination of solutions could potentially be more effective. This is however, beyond the scope of this review, but is addressed in a research paper in preparation by most of the present authors.

2.5.2. Structuration during material delivery

It is important to think of structural buildup during material delivery, as structuration in the delivery line can be technologically needed to reach a sufficient yield stress upon placing. Therefore, the amount of time a given portion of the material spends in the delivery system (the residence time) is an important parameter, particularly after an activator has been added. Here we consider as an example the case of layered extrusion [14]. In this process, the structuration occurs just at the pipe exit when the

The role of early age structural build-up in digital fabrication with concrete

material is at rest, or it can start in the pipe, depending on if and when the addition of activator or thickener has taken place. If structuration takes place too late, the material will potentially not sustain its own weight over any meaningful height. More specifically, in long pipes, the concrete rheology at the nozzle will then depend strongly on the processing rate and will largely dictate it. In a process such as Smart Dynamic Casting, self-compaction (low yield stress) is required at the outflow, and this can give rise to flow rate profiles in pipes that naturally give variable residence time distributions, as seen in Figure 2.7, which leads to variable concrete age within the delivery line. This can lead to potentially problematic conditions at the outflow.

These considerations give rise to the design paradigm of introducing thickeners and activators as closely to the delivery point as possible, reducing residence time changes when scaling the process flow rate.

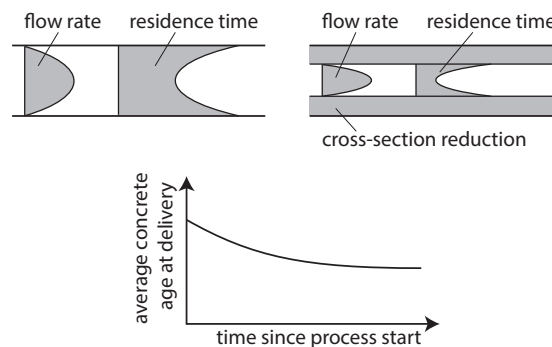


Figure 2.7: Practical implications and challenges of structural buildup control for processing and manufacturing. Residence time distribution in long delivery pipes. Structuring compositions with low yield stress during pumping show residence time gradients within a pipe cross-section, which can lead to partial clogging and modifies the average age of concrete being delivered during processing.

2.5.3. Process scaling

Being designed with the goal of realising complex structures, layered extrusion faces the challenge of variable contour length within a printed object. In layered extrusion with other materials this is typically addressed by keeping the same process flow rate as well as horizontal velocity if not mandated otherwise by mechatronics [98] and by varying the print time for each layer as well as the vertical building rate. With concrete this is *a priori* possible but, as structuration is more time dependent, the age difference of successive layers is of high importance. In analogy to section 2.2.2, shortening layer contour length shortens age differences and leads to flow off of lower layers and vice

versa, longer contour length promotes layering. In addition, it should be kept in mind that starting and stopping operation and volumetric process rate changes are challenging for reasons discussed in the previous section.

Approaches to overcome this challenge introduce an additional degree of freedom in this interaction. An easy solution is to optimise the composition for the longest layer and discard the material that is not needed. Optimising the composition for the shortest layer and printing layers of different thickness would also be possible. In such a case, the same amount of material and the same time would be used for each layer, addressing layering problems. Yet another solution is to keep the residence time in the delivery line constant despite the changing process rate, by changing the delivery line volume and to master the structuration rate by adapting the activator concentration or the temperature so that contour length becomes a free parameter.

In layered extrusion, with contour lengths as short as a few cm up to several tens of meters, estimated ranges in processing rates of between 0.01 – 10 L/min are reported for different compositions. However, it is only more recently that substantial contour length variation has been reported within one print, with approximately a factor 3 within a printed object [99]. In slip forming, cross-section variations within a structure have been varied by a factor 4, corresponding in the specific case to processing rates between 0.1 and 0.4 L/min. Throughout different trials the processing rate range was broader, ranging between 0.05 and 0.8 L/min, but this necessitated differently sized mixing reactors and mortar compositions. Highlights of such successes are shown in figure 2.8.

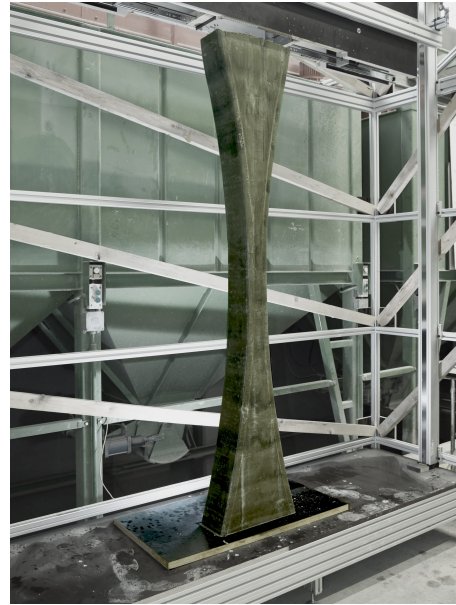


Figure 2.8: Practical implications and challenges of structural build-up control for processing and manufacturing. Achievements in contour length changes in the case of layered extrusion for a piece contracted by Zaha Hadid Architects [99] and of cross-section area for slipforming [42]. Reproduced from [99] and [42].

2.5.4. Dealing with variability

Concrete properties vary significantly as a function of composition and environmental conditions and especially temperature. This is seen as a major challenge for onsite digital fabrication. Moreover, concrete properties can also only be controlled to a limited degree as the used products have an underlying variability in composition, so that performance control is also a challenge in prefabrication sites with well-controlled temperature. For these reasons, whether for prefabrication or on-site production, process control methods will be necessary for successful adoption of digital fabrication in industry. This will have to involve real-time measurements that can dictate production rate and/or accelerator delivery for example.

In digital concrete flow properties, instantaneous yield stress upon placing and structuration are to be controlled precisely, simultaneously and throughout production. To become cost effective, digital fabrication must do this through highly automated monitoring including proper feedback loops, something that appears to still require a lot of work in most cases.

Speculative solutions can involve measuring the yield stress and flow rate before and after activation. In food processing, similar problems are addressed by ultrasound profilometry and pressure difference measurements along a pipe [100], [101]. For concrete the coupling with penetrometer measurements from an initial portion of the mix appears a useful calibration protocol. The power consumption of a stirrer in a mixing reactor could also be monitored and related to an apparent viscosity, as done for concrete mixing [102]. In layered extrusion and after placing, offline or in-situ test samples involving a method as described in section 2.3.3 or contact-less visual methods may be used to measure settlement or creep. For slipforming, a combination of friction and formwork pressure measurements has already been proposed, used and related to the upper and lower processing limits at the extrusion time as introduced in section 2.2.2. This was manually used as input for process control [42].

We expect that, for digital fabrication to gain acceptance for large-scale applications, it will be necessary for such measurements to be performed in real-time and to deliver reliable values of the physical parameters controlling the production outcome. Only in this way will it be possible to effectively adjust mix composition or processing rate to react to the numerous perturbations expected in real situations and on a daily basis. Without this, digital fabrication will probably have to target more marginal markets, where cost benefits may be large and can cover the extra overhead needed to guarantee seamless production.

2.6. Conclusions

Controlling the structural build-up of digital concrete to the degree of precision required by the digital processes will be at the heart of future progress in the nascent field of additive manufacturing with cementitious materials. Chemically controlling the hydration of concrete, either by continuous material preparation or with set accelerators, can provide a rate increasing structural build-up that would not limit the building time of a process. In addition, we show that thickener and activator use in practice is limited by a host of secondary effects. We also show that accelerators should be added as closely to the delivery point as possible, as well as recent successes and limitations in process scaling and material control. Finally, we discuss opportunities to implement feedback techniques in order to take into account material variability.

Chapter 3 Process and rheology models for structuring materials

This chapter is a summary of different contributions to the development of set on demand fabrication processes within the collaborative framework of the NCCR digital fabrication. In this chapter, the evolution of strength of cement pastes, mortar and concrete is considered a given. The way this strength can be measured is explained in chapter 4, while the origin of its evolution is covered in chapter 5 and the way to achieve it is to be found in chapter 6.

Readers should keep in mind that modelling approaches for materials are idealisations of actual material behaviour and should serve as a pragmatic basis for understanding. With this in mind, this chapter attempts to lay a conceptual framework facilitating deeper understanding developed in the subsequent chapters.

The sections involving stability criteria and slip-forming have previously been published as co-author in similar form in [9], [103] as well as a journal paper in preparation [104] (Section 3.4.1 is based on this analysis). The sections involving stability criteria and layered extrusion are part of a journal paper in preparation as first author [105] (Section 3.4.2 is based on this analysis). In each case, the original analysis in the published papers has been the contribution of Lex Reiter and this is what is presented here.

List of symbols

Rheology:

τ_0	Yield stress
$\dot{\tau}_0$	Rate of yield stress increase
τ_{00}	Instantaneous yield stress
τ_{rel}	Relative change of instantaneous yield stress
t	Time since material is at rest
t_{ACC}	Time at which acceleration occurred with respect to process
$\alpha, \alpha_1, \alpha_2$	Factor of yield stress increase
β	Exponent of yield stress increase
A_{thix}	Linear structuration rate
E	Young's modulus
E_0	Young's modulus at bottom of structure
G	Shear modulus
ν	Poisson ratio
γ_{cr}	Critical strain
f_y	Compressive strength

Material composition:

ϕ	Solid volume fraction
ϕ_s	Solid volume fraction at start of hydration
$\phi_{c,s}, \phi_{c,f}$	Solid volume fraction of cement grains at start and end of hydration
ϕ_{max}	Maximum random close packing fraction
ϕ_0	Percolation threshold
ξ_H	Degree of hydration
ρ	Density

Geometry of structure:

H	Height of structure
z	Vertical position in structure
L	Beam length
b	Layer width of placed layer
d	Thickness of applied layer
d_L	Thickness of an individual applied layer
r	Center radius of hollow cylinder
ϕ_1, ϕ_2	Support element diameter
s_1, s_2, l_1, l_2	Support element separation/length
ξ_z	Relative position in a structure
I	Second moment of area
A	Cross-section area
r_{hy}	Hydrodynamic radius

Loading and resistance:

g	Gravity
q	Horizontal load
v	Vertical building rate
c	Stiffness of lateral support
C	Vertical load of self-weight

Process and rheology models for structuring materials

w	Horizontal displacement of structure
w_H	Nominal horizontal displacement
σ_{cr}	Euler stress
ϵ	Coefficient of buckling length
Π	Sum of potentials
τ_{fr}	Frictional stress
α_{fr}	Coefficient of friction
σ_h	Formwork pressure
e	Disturbed zone

Failure criteria:

$\tau_{0,min}$	Minimum yield stress for strength-based failure
$\tau_{0,def}$	Minimum yield stress for low deformations
$E_{0,min}$	Minimum Young's modulus for global stability
$E_{0,local}$	Minimum Young's modulus for local stability

Specific to processes:

σ_{VE}, σ_{VM}	Vertical stress in position E and M
τ_{0E}, τ_{0M}	Yield stress in position E and M
ψ	Friction number
F_{fr}	Measured friction force on formwork
σ_{hM}	Formwork pressure in position M
z_E, z_M	Position of points E and M
δ	Amplification factor for stiffness
ξ_R	Reinforcement fraction
E_R, E_C	Elastic modulus of reinforcement and concrete
α_{pen}	Factor relating yield stress and penetration force
F_{pen}	Measured penetration force
σ_R	Formwork strength

Abstract

Structural build-up and rheology control of cementitious materials is a make-or-break requirement of many advanced building processes, such as slip forming, layered extrusion, digital casting, shotcrete and coatings. These building processes need substantial strength/yield stress gain from the time of placing onwards, owing to different requirements, such as early age loading.

We argue that how narrowly strength evolution has to be controlled during the timeframe of processing depends on the building process and that this can be estimated by combining rheological models for concrete with process specifics. This gives a processing range, defined as a property range, in which placing and manufacturing can occur and which has direct implications on the shapes that can be built. Main lessons learnt are:

- For self-support linear strength buildup is required. If layer deformations need to be limited, limiting the loads to shear stresses as low as 1/3 of yield stress can give a simple approximative rule to limit structural breakdown.
- At larger building heights, layer stability/buckling is shown to limit building rates, due to a H^3 scaling.
- Supports such as rigid reinforcement can substantially lower yield stress requirements as a function of the surface of supporting material that opposes the flow of concrete.
- In formworks, pressure can be limited with a sufficiently fast structural buildup.
- In shotcrete, owing to large shear rates on previously placed material, an instantaneous yield stress increase is required.
- As opposed to other processes, coatings should have their pore water bound in hydration products, either by decreasing the rate of drying or by rapidly growing hydrates.

3.1.Introduction

In many manufacturing processes in industry, fluid to solid transitions are used to produce goods. This concerns any form of forging, moulding, pressing, extrusions or more recently printing, be it powder bed printing [106], or fused deposition modelling (FDM) [20], [21]. Generally, these materials solidify by a temperature drop (e.g. polymer filament in FDM printing), which is a parameter external to the material and the transitions can occur quickly.

Mineral binders form a special group of materials in this respect as their fluid to solid transition is a consequence of processes occurring in the material, strongly affected but usually not controlled by temperature changes, and occurring more subtly over longer time periods (hours rather than seconds). At early age, mineral binders are rigid particle suspensions governed by flocculation and involving effects of gravity, Van der Waals colloidal interactions and Brownian motion. Over longer timescales mineral binder rheology and strength development is governed by hydration and the growth of hydration products. Hydration can be accelerated by heating, however at large flow rates or in large cross-sections this may take specialised solutions, such as inductive heating of metallic particles[10], [15].

For the strength build-up, we consider that there exists a common physico-chemical origin of strength build-up, which is discussed in chapter 5. For the work presented here, we consider that build-up takes place with characteristic kinetics and timescales that are introduced in our analysis.

In most applications of concrete, control of hardening or even precise control of workability is not required, as concrete is usually cast in moulds, involving vibration for placing or more advanced self-compacting formulations. In addition, concrete is typically not loaded until moulds are removed after several days. In advanced building processes studied in the realm of digital fabrication [14], [15], [28] this is no more the case, many and sometimes conflicting requirements are put on concrete, both in terms of flow behaviour and strength build-up.

Concrete exhibits substantial batch-to-batch variations and this adds to the difficulty of controlling advanced building processes [19]. For this reason, it is important to know how sensitive these are to rheology and build-up and how large the range of tolerable properties can be. Additionally, measurement techniques for build-up are not yet accurate enough to give precise model input parameters. Because of this, rather than approaching the process modelling with as precise as possible models, simplified approaches will be employed in order to provide realistic estimates and study scaling relationships. For digital fabrication, understanding how the strength gain over time affects the possibilities offered by different building processes is an important first step when it comes to using strength characterisation measurements on concrete.

In a broader sense, the generalised approach proposed to studying building processes with concrete may also be applied to similar material systems that also rely on strength build-up over rather long timescales. This includes other mineral binders such as gypsum and geopolymers, but also materials relying on other chemical reactions like crosslinking in polymers, foaming or gelation. Additionally, we can include materials relying on drying as earth and clay. In all these cases there is a characteristic process creating a yield stress material for which characteristic strength gain kinetics determine the range of shapes that can be produced.

3.2. Material evolution providing resistance

3.2.1. Capturing the yield stress evolution at rest

Here yield stress suspensions formed of mineral binders, saturated in matrix material and adequate for pumping are considered [19], [26]. Upon hydration and at rest (no applied deformations) their yield stress increases rather linearly with the amount of hydration products formed (see chapter 5) [43], [50], [107]. Such cement pastes transition to frictional materials at higher degree of hydration (see chapter 4)[51], [108].

As the rate of hydration is not a constant throughout the building process, models describing yield stress should be able to capture this. At the same time, the model needs to capture systems with:

- no substantial hydration in the induction period (constant yield stress or very slowly increasing),
- a rate increase owing to the “autocatalytic” nature of hydration product growth upon the onset of hydration [109],
- a rate decrease, either by a rate-decreasing hydration step or by physical interactions, such as flocculation[50], in some cases amplified by viscosity modifying admixtures[68], [110], [111].

Yield stress fluid models such as Bingham model [48], [49] are applied in a widespread field of applications with τ_{00} being the instantaneous concrete yield stress. Extensions to the Bingham model including structural build-up, such as by Ovarlez and Roussel [38] involving a linear build-up using a thixotropy factor A_{thix} and by Lecompte and Perrot et al.[112] involving an extension to longer resting times and being based on growth of hydration products.

Without considering the physico-chemical origin of build-up an empirical approach of a power law time-dependent behaviour can be chosen and applied to the process related critical time periods. This can capture mechanisms of different kinetics, for example rate increasing ($\beta > 1$), rate decreasing ($0 < \beta < 1$) and constant (α or $\beta =$

0) ones with a simplified representation of the yield stress evolution at rest (see figure 3.1):

$$\tau_0(t) = \tau_{00} + \alpha t^\beta \quad (1)$$

Equation (1) can be simplified to αt^β if yield stress at placing is low compared to long-term build-up or to $\tau_{00} + \alpha t$ if specifically, linear build-up is observed. Approximations of this nature have the sole purpose of capturing and describing process relevant changes in adequate time frames and their choice can be intertwined with the studied process timeframe.

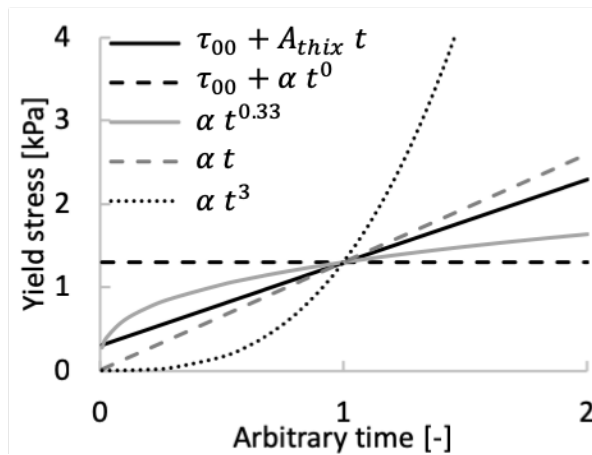


Figure 3.1: Qualitative changes in mineral binders with occurring structuration using (1).

Any onset of flow is associated with reaching the yield stress, generally described by the Tresca criterion and this being the main stress difference in a section of material or by the von Mises criterion. Reality is more complex, involving a partial structural breakdown, creep and large plastic deformations before yield stress is reached [50], together with a strongly localised shearing in a thin shear surface [113]–[115].

3.2.2. Evolution of instantaneous yield stress

The intent of this section is to provide a first to second order approach to studying the change of instantaneous yield stress in relation to hydration, so as to offer a tool for formulation choices and general understanding. A more advanced derivation can be found in [112] or specifically for superplasticised pastes results in [55], [116] can be used. As such, the present derivation does not intend to capture all phenomena precisely.

Instantaneous yield stress is related to the solid volume fraction ϕ of particles (relating to the number of contact points between particles) and to admixtures such as superplasticizer adsorbed on cement, reducing particle interactions[117]. Models such as YODEL [118], [119] or Zhou [120] can be used as descriptions of interparticle forces creating a yield stress fluid. Furthermore, Mantellato [55], [116] showed that the initial rise of yield stress in the induction period of superplasticised pastes, is dictated by a combination of two factors: The increase in the number of contact points and the reduction of the surface coverage. Mantellato also showed that the volume fraction dependence of yield stress is an exponential function and that in presence of superplasticizers, volume fraction changes cannot account for the initial rise in yield stress.

Ignoring the presence of superplasticizers and given the different approaches and models used in literature, a simple power law scaling factor is used here, describing the relationship between solid volume fraction and instantaneous yield stress:

$$\tau_{00}(\phi) = \alpha\phi^{\beta\phi} \quad (2)$$

In the range of interest (ϕ between 0.4 and 0.56), for the model of Zhou a general scaling exponent β_ϕ of 6.1 is found, while YODEL has the same exponent at low solid volume fraction (ϕ between 0.4 and approximately 0.46) and diverges when approaching the maximum volume fraction. The results of Mantellato (ϕ between 0.4 and approximately 0.55 and including cases with superplasticizer) show an exponent of 14.1. Storage modulus and yield stress measurements at long resting times of a flocculated cement paste with no occurring hydration presented in chapter 5 appear to confirm this solid content scaling, giving an exponent of 14.9 (ϕ between 0.42 and 0.50), while similar measurements by Mostafa et al [121] give a scaling exponent of 6.8 (ϕ between 0.36 and 0.48).

Being matrix saturated, mortars and concrete are treated here in the same way as cement pastes. The materials used start with a solid volume fraction $\phi_s = \phi_{c,s} + \phi_{f,s}$ defined by the content of cement, filler and water and neglecting early hydration products from reactions occurring immediately at water contact.

With increasing degree of hydration of the main phases, the solid volume fraction increases, reaching the percolation volume fraction (named here maximum volume fraction ϕ_{max}) and beyond this increasing further[108]. The change of volume fraction with occurring hydration can be expressed in terms of degree of hydration, neglecting that hydration of different phases is occurring at separate times. It can be considered for simplicity that the cement volume fraction for pure OPC $\phi_{c,s}$ increases to $\phi_{c,f} = 2.14 \phi_{c,s}$ at full hydration [11]. This may be adapted, considering the main hydration step in the timeframe of processing, distinguishing systems dominated by ettringite formation and ones dominated by silicate hydration.

The solid content with increasing degree of hydration ξ_H is:

$$\phi(\xi_H) = (1 - \xi_H)\phi_s + \xi_H\phi_{c,f} \quad (3)$$

In absence of admixtures affecting rheology, the maximum attractive interparticle force, curvature radius of particles and particle size distribution, which influence interparticle interaction are expected to change to a minor degree at the onset of hydration, despite early age particles increasing the specific surface substantially [116], [122]. For a given binder and including fillers, the maximum volume fraction may be increased compared to a simple cement by the filler effect. A typical value for ϕ_{max} found for cement pastes is 0.57[118]. ϕ_{max} is considered to increase to a minor degree with increasing degree of hydration, despite changes to PSD and changing shape of average particles.

To compare the effect of hydration, the relative yield stress increase τ_{rel} under a changing solid content may be expressed as:

$$\tau_{rel} = \frac{\tau_{00}(\phi)}{\tau_{00}(\phi_s)} \quad (4)$$

Using equations (3) and (4), the relative yield stress increase can be calculated based on the degree of hydration as shown in figure 3.2. It appears that no matter which model or experimental data is used, at very low degree of hydration, below 10%, only a

minor instantaneous yield stress increase is expected. It shows that at early age, most interactions occur at rest and are not dictated by solid content changes, but rather by hydration product growth at contact points [50].

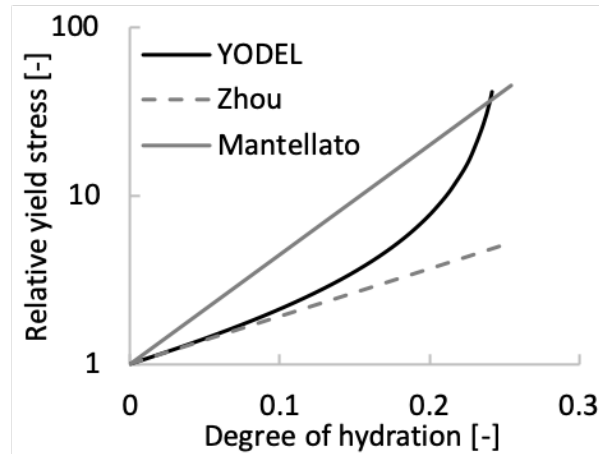


Figure 3.2: Estimated relative yield stress increase for a cement paste with a water to cement ratio of 0.4 ($\phi_{max}=0.57$ max packing).

If any meaningful instantaneous yield stress increase is required in a building process, the best path of action appears to be the consumption of superplasticizer by forming hydration products, namely ettringite (acting on interparticle forces), the design of mix compositions very close to the maximum packing fraction (acting on the difference of $\phi_{max} - \phi_s$), and the use of fast hydration steps forming hydration products with high water binding potential, namely ettringite (acting on ξ_H) or a combination of the above.

3.2.3. Yield stress and build-up variations

Variations to both the yield stress at the time of placing or to the yield stress increase upon placing may occur during the processing timeframe. For the time of placing, this is largely linked to permanent changes occurring to the concrete as it waits for processing (evolution of instantaneous yield stress)[116], [123]. For the yield stress increase upon placing, this is also linked to the state of concrete at the time of processing and additionally to how efficient an optionally used activator is. Depending on the time of its addition with respect to concrete water addition large changes can occur [103], [104].

If yield stress increase is to be precisely controlled for long timescales, but varies substantially with the time of activator addition (figure 3.3), then taking into account the time at which an activator is added t_{ACC} gives the following relationship (α_1, α_2 being factors describing yield stress increase):

$$\tau_0 = (\alpha_1 t_{ACC} + \alpha_2) t^\beta \quad (5)$$

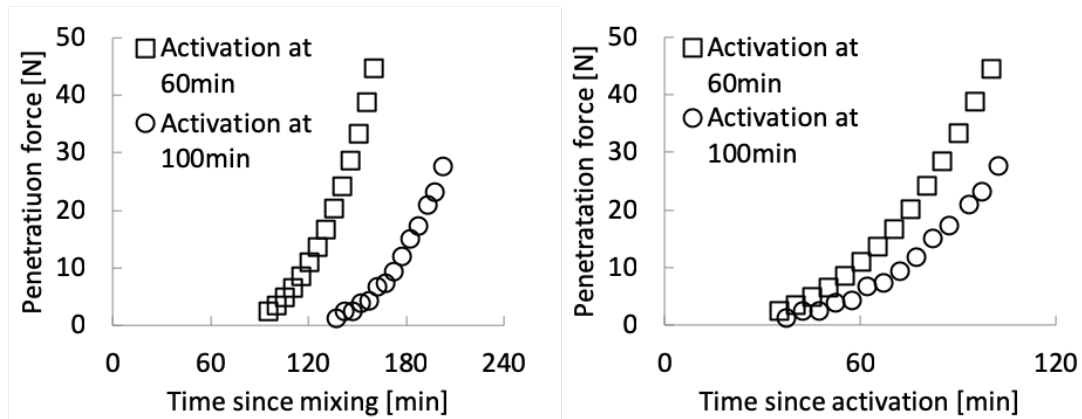


Figure 3.3: Yield stress evolution (as penetration force) of a mortar activated at two different times after water addition. (left) Evolution with respect to process, (right) Evolution of a specific sample with respect to its time of placing. At later activation time, the yield stress evolves slower in this instance, leading to a factor $\alpha_1 < 0$ (data provided by Anna Szabo)[104].

3.3. Stability criteria

Through the definition of stability criteria, descriptions of types of phenomena that can lead to failure or undesired side-effects are proposed. The criteria listed here should be seen as a non-exhaustive overview of phenomena encountered in advanced building processes with concrete. These criteria are defined independently of the specific building process, in which multiple criteria are combined and conceptualized as loads, to which the material resists.

3.3.1. Requirement for self-support

A vertical element of height H (figure 3.4) built with a yield stress fluid is not collapsing, if the yield stress at every point z along its height is higher than the shear stress from hydrostatic pressure [18], [28], [124]:

$$\tau_0(z) \geq \frac{\rho g}{\sqrt{3}} z = \tau_{0,min}(z) \quad (6)$$

For a constant vertical building rate, the yield stress should increase over long timescales at least with the rate:

$$\frac{\tau_0(z)}{z} \geq \frac{\tau_{0,min}(z)}{z} = \frac{\rho g}{\sqrt{3}} \quad (7)$$

Example: In order to build a structure of 1m height in 1h with mortar (2300kg/m³), for the pure self-support criterion, the yield stress at the bottom needs to reach $\tau_0 = \frac{\rho g H}{\sqrt{3}} = 13kPa$ and the linear yield stress increase needs to be at least: $\frac{\rho g v}{\sqrt{3}} = 13kPa/h$.

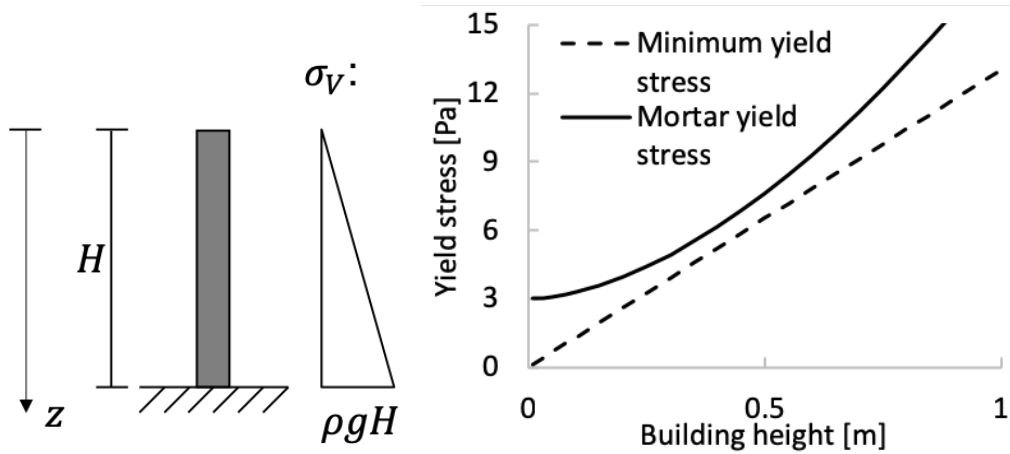


Figure 3.4: (left) Vertical element and the associated loading. (right) Material yield stress and requirement for a given vertical building rate showing in the example a need for yield stress increase beyond a height of approximately 20cm.

However, for loading close to the yield stress, substantial deformations can occur before failure[26], [125]. This can be described as a partial structural breakdown. Indeed, partial structural breakdown occurs from very low stress and much of the structure is damaged, when yield stress is reached (figure 3.5)[50]. It should be kept in mind that in addition to simple breakdown under load, with the stepwise application of layers and possible printing pressure applied on previous layers, loads high enough to cause damage to the structural build-up can occur with every layer applied, so the material is not perfectly at rest and the effective strength build-up is slowed by successive damaging[123]. The interplay of these parameters is of considerable complexity and a research topic on its own.

For applications, large layer deformations are undesired, be it only to prevent cumulative placing errors due to excessive layer settlement. For this reason, rather than considering purely collapse, limiting the deformations can give a useful engineering approach covering also the mechanical failure. At a typical shear stress to yield stress ratio of 1/3, cement pastes having been at rest for a long time, behave largely as linear elastic materials involving only minor structural breakdown, small deformation (figure 3.5) and showing high stiffness under shear. Thus, increasing the yield stress requirement by a factor 3x should remove most of the layer settling and structural breakdown, without needing knowledge of thixotropic history. In the example above, yield stress should now increase to 39 kPa and to 39 kPa/h.

$$\tau_{0,def}(z) \geq 3 \frac{\rho g}{\sqrt{3}} z \quad (8)$$

For changing geometries, analytical approaches quickly reach limitations, however the more general form of a yield stress criterion using the Tresca or von Mises criterion for any position and orientation in the material can be used together with the time-dependent yield stress of equation (1).

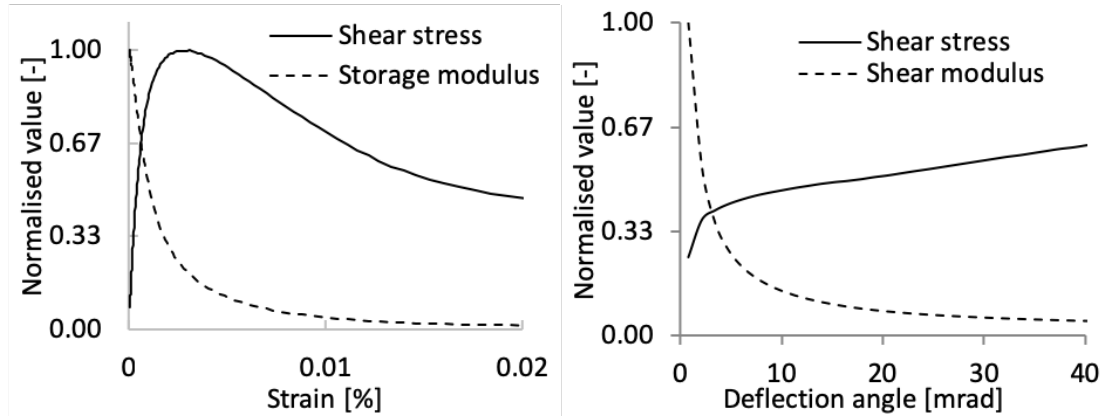


Figure 3.5: Shear stress and storage modulus normalised to storage modulus at rest and yield stress. (left) Strain oscillation for a cement paste at rest for 20min (chapter 5). (right) Rotational Vane measurement for a cement paste at rest for 60min with storage modulus as relationship of stress to strain (chapter 4).

3.3.2. Self-weight induced buckling

For slim structures or ones built of soft material, failure can additionally occur from buckling [40], [41]. Provided, that layer deformations can be considered small (no plastic deformations) and that the applied concrete behaves linear-elastically in this range, then buckling occurs ideally at the Euler/bifurcation load [126].

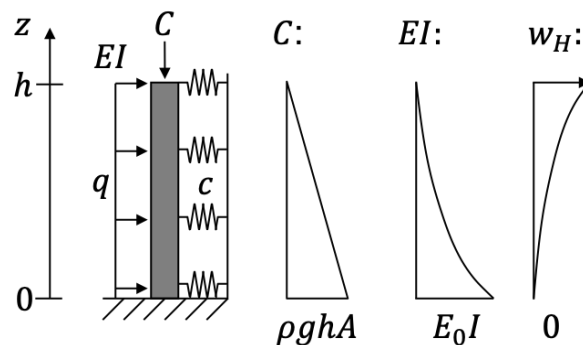


Figure 3.6: Supported vertical building element loaded horizontally and subjected to its own weight. The material has a gradient of stiffness.

For linear elastic materials it is well established that structures are more prone to buckling with increasing slenderness. Calculating the Euler load is straightforward for structures with a constant Young's modulus and a constant normal load. For axially loaded slim structures of an ideal wall of rectangular shape of length L , width b , height H and Young's modulus E , an upper limit for the critical stress σ_{cr} can be calculated from the Euler load [26]:

$$\sigma_{cr} = \frac{\pi^2 E i^2}{(\epsilon H)^2} \text{ with } I = \frac{b^3 L}{12}, A = bL, i^2 = \frac{I}{A} \text{ and } \epsilon = 2 \quad (9)$$

A simplified approach as a first order scaling for a self-supporting wall, neglecting stress and stiffness gradients in the wall and assuming that the stress increases with building height according to $\sigma_{cr} = \rho g H$ can be used in combination with the Euler load (9). It is found that E should scale with height with exponent 3.

$$E_{0,min} \propto \rho g \frac{H^3}{i^2} \quad (10)$$

The correct solution of Greenhill for elastic self-buckling of a beam of constant Young's modulus [127] agrees with the derived general scaling:

$$E_{0,min} = 0.1276 \frac{\rho g H^3}{i^2} \quad (11)$$

Accounting for the gradient in materials properties

To account for gradients, the generalized differential equation describing beam stability as a function of vertical load C , lateral supports c and a bending load q (compare figure 3.6) writes as [126]:

$$(EI w'')'' + (C w')' + c w = q \quad (12)$$

with w the displacement along the beam length, E the elastic modulus, I the second moment of area, C the normal load, c the stiffness of an elastic continuous support and q a load perpendicular to the beam direction.

In early age concrete and for buckling under self-weight, all terms of the differential equation (12) may vary along the beam length, making a closed analytical solution of buckling impossible.

When only scaling relationships are of interest, the parameters may be separated into unit-carrying factors ($\tilde{E}, \tilde{C}, \tilde{c}, \tilde{q}, \tilde{w}$) and unitless functions ($\check{E}, \check{C}, \check{c}, \check{q}, \check{w}$). For example, the displacement may be expressed as: $w = \tilde{w} \cdot \check{w}$. With this, the differential equation becomes:

$$\frac{\tilde{E}I\tilde{w}}{H^4} \cdot \frac{\partial^2 \left(\frac{\check{E}(\partial^2 \check{w})}{\partial \xi^2} \right)}{\partial \xi^2} + \frac{\tilde{C}\tilde{w}}{H^2} \cdot \frac{\partial \left(\frac{\check{C}(\partial \check{w})}{\partial \xi} \right)}{\partial \xi} + \tilde{c}\tilde{w} \cdot \check{c}\check{w} = \tilde{q} \cdot \check{q} \quad (13)$$

All differentiated unitless functions compute to unitless factors. In the case of an unsupported beam without perpendicular load ($c=q=0$), constant cross-section, and self-weight ($\tilde{C} = \rho gHA$) equation (13) gives the relationship:

$$\frac{\tilde{E}I}{H^4} = \lambda \frac{\rho gHA}{H^2} \Rightarrow E_{0,min} \propto \frac{\rho gAH^3}{I} \quad (14)$$

This scaling is valid independent of the evolution of E and of the boundary conditions determining \check{w} the unitless shape of the displacement leading to buckling, the variation only affects the factor λ . In addition, this scaling shows that for high beams, the minimum required Young's modulus in the first layer scales with H^3 even if gradients are present. Considering constant vertical building rates and starting from low Young's moduli, placed concrete is required to evolve over time with t^3 on long timescales.

Quantifying the Young's modulus requirement

In order to quantify the Young's modulus requirement, the energy-based formulation of inner and outer potentials can give useful insight. The sum of potentials in a vertical unsupported element as above writes:

$$\Pi = \int_0^H E(z) \cdot I \cdot (w'')^2 - C(z) \cdot (w')^2 dz \quad (15)$$

With this expression (15), buckling is not occurring as long as the second derivative of the potential by the displacement (lowest energy state occurring at no horizontal displacement):

$$\frac{\partial^2 \Pi}{\partial w^2} > 0 \quad (16)$$

As opposed to the differential equation, the energy-based expression allows using approximated expressions for E , c , C and w . Assuming a constant vertical building rate the Young's modulus evolution writes as:

$$E(z) = \alpha \cdot (H - z)^\beta = E_0 \cdot (1 - \xi_z)^\beta \quad (17)$$

An approximation of the buckling shape that fulfils the boundary conditions ($w(0) = w'(0) = EIw''(H) = (EIw''(H))' = 0$) can be found with:

$$w(\xi) = w_H \cdot \left(\frac{1}{3} \xi^4 - \frac{4}{3} \xi^3 + 2\xi^2 \right) \quad (18)$$

Using these approximations of Young's modulus (17) and failure shape (18), the minimum requirement for the Young's modulus for an ideal wall is then:

$$E_{0,min} = \frac{(\beta+5)}{40} \cdot \frac{\rho g H^3}{i^2} \quad (19)$$

For a constant Young's modulus ($\beta = 0$) this solution is very close to the solution of Greenhill [127] (pre-factor 0.125 compared to 0.1276). The exponent of yield stress increase appears to have a minor effect on the pre-factor (increasing from 0.125 to 0.2 for $\beta = 3$). With small adaptations, an instantaneous yield stress can be considered in the power law expression. It is however important to see that the scaling with t^3 will make the initial situation just after deposition irrelevant for high building heights as the stiffness increase has to be fast.

It also is important to state again that this approach is limited to cases in which buckling occurs without any substantial plastic deformations beforehand, for idealized

shapes and that Young's modulus in early age concrete can be decreased for loading close to the strength limit involving potentially large deformations.

Critical strain

Fundamentally for concrete at early age, yield stress and stiffness/shear modulus do not scale directly [50]. In fact, they measure different behaviours (see figure 3.5). Yield stress indicates the maximum shear stress sustainable, while shear modulus characterises the deformation response to low shear stresses, before flow occurs. In most cases we will consider that stiffness scales with yield stress for small deformations and at long timescales. This is a reasonable assumption, as linearity is a good approximation in systems where interactions are governed by hydration products and it gives the relationship [50]:

$$G(t) = \gamma_{cr} \tau_0(t) \quad (20)$$

Measuring such a critical strain is difficult. Derivations from mechanical tests have limited validity due to a strong shear localization[50], [113] in a shear zone, characterized by structural breakdown in a thin shear surface and large local shear strain. The range of possible values is large and depends on the measuring procedure and particle interactions. The lowest possible value for critical strain is by considering the structural breakdown of a cement paste after a long period of rest by strain sweep oscillations and comparing yield stress to storage modulus at rest, giving $\gamma_{cr} \approx 0.01$ [%] (compare figure 5 and [107], [128]). Alternatively, stiffness may be measured directly from compression tests or from yield displacements [129], [130]. Typical deformations for this are of the order of 2-4% [50] [51] but can reach 10% with some viscosity modifiers [131].

The critical strain is directly connected to the slenderness, deciding if a structural element fails through strength (8) or stability criteria (19):

$$\gamma_{cr} = \frac{\tau}{G} = \frac{2(1+\nu)}{\sqrt{3}} \frac{f_y}{E} = \frac{380(1+\nu)}{\sqrt{3}(\beta+5)} \frac{i^2}{H^2} \quad (21)$$

This scaling (21) distinguishes if a structure would rather fail by mechanical loading or by self-weight induced buckling and shows that the critical deformation should be small for a high structure. This means that in absence of hydration, admixtures increasing the interparticle distance (especially PCEs) or creating long range bridging interactions (some VMAs) [131] may cause buckling failure at lower building height. On the contrary, after hydration starts, the effect of PCEs on average interparticle distances is expected to decrease quickly, decreasing critical strain. Relationship (21) does not per se define the height at which the structure fails, as this depends not only on the strength but additionally on the load.

Determining the critical strain from printing experiments using equation (21) can give a valuable approximation of characteristic strain and can help in the understanding of changes occurring to characteristic strain over the manufacturing timeframe. Using the above relationship, the Young's modulus and compressive strength relationship $\frac{f_y}{E}$ experimentally determined by Wolfs et al[40] ($E(t = 0)=78$ kPa, $f_y(t = 0)=6.0$ kPa), the critical strain in this experimental study is 11%, a very large value when considering elastic deformations. With this value a critical building height of 13cm is expected and the observed one is 20cm, predicting the correct type of failure, despite very large critical strain.

3.3.3. Interactions with supporting elements

Leaky formwork

Supporting elements holding concrete in place such as formworks are common. Other elements such as reinforcement cages, mats or other forms of meshed materials may also act as supporting elements (figure 3.7)[9], [132]. How well such supports can hold back concrete, firstly depends on their own strength and rigidity and secondly on their geometry. In the simplest approach, if the gaps are smaller than the largest grain to pass the perforated mold, flow-out is entirely prevented. For larger gaps, fiber induced clogging can be employed as a technological solution [133].

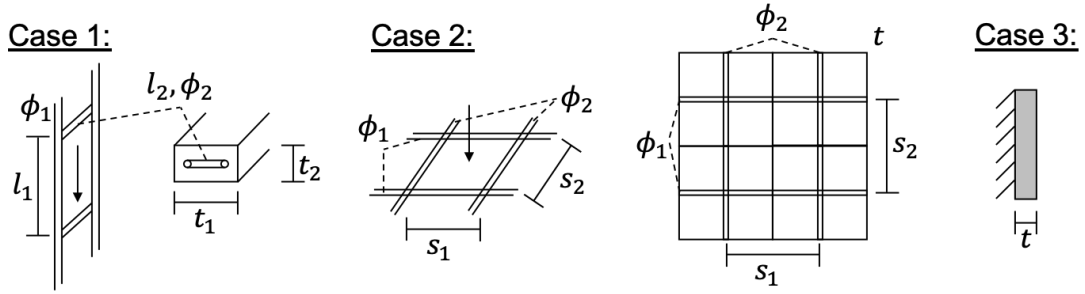


Figure 3.7: Supporting elements. In case 1 the main reinforcement is parallel to the direction of concrete flow, in the case 2 all reinforcement opposes flow. In case 3 concrete needs to stick on a wall.

For gaps substantially larger than the largest grain of concrete, supporting elements can still have beneficial effects. For flow occurring through a perforated grid, the grid resists the flow. Depending on the direction of flow with respect to the support, the flow opposing stress differs, being τ_0 parallel to reinforcement and being $n\tau_0$ for supports opposing flow. The factor n is not derived for a Bingham fluid, but is in the range of 3, close to the value for a sphere [134] when using the approach in [135]. The resistance to flow in such formwork gives a requirement for material yield stress as follows:

$$\text{Case 1: } l_1 = 0.15\text{m}, \phi_{1,2} = 12\text{mm}, l_2 = 0.05\text{m}, t_1 = 0.07\text{m}, t_2 = 0.1\text{m}$$

$$\tau_0(\pi\phi_1 l_1 + n\pi\phi_2 l_2) \geq \rho g l_1 t_1 t_2 \rightarrow \tau_0 > 2090\text{Pa} \quad (22)$$

$$\text{Case 2: } s_{1,2} = 0.04\text{m}, \phi_{1,2} = 4\text{mm}, t = 0.03\text{m}$$

$$\tau_0(n\pi\phi_1 s_1 + n\pi\phi_2 s_2) \geq \rho g s_1 s_2 2d \rightarrow \tau_0 > 720\text{Pa} \quad (23)$$

In addition, the presence of supporting material can substantially lower the yield stress requirement during placing. This is the same consideration as above, with the difference that the asserted shear surface does not occur on the support but along the general surface formed by the supporting material. A particular example of this is the cover needed for reinforcement. In this case the yield stress required to support the cover thickness d (case 3) reduces to values as low as:

$$\tau_0 = \rho g d \quad (24)$$

Given the competition of both processes (23) and (24), the concrete yield stress required in the presence of supports is dominated by cover thickness for dense meshes

and by flow through meshes for wide meshes with the transition in a regular mesh occurring at: $s = n\pi\phi$

Friction

Friction is understood as the shear stress exerted by mortar along a formwork wall. In the interface layer, concrete is a heterogeneous material, due to its large aggregate size to surface roughness, a fully covered interface surface needs to be rich in paste material. In many cases it is considered in literature that shear stress at the interface is equivalent to concrete yield stress [38]. In the case of pumping, a lubrication layer is observed at the interface [136], [137], especially for densely packed matrices.

On a microstructural level, friction on a slowly sliding interface such as a formwork in slip-forming, is a priori caused by a normal stress applied by solid particles on the formwork wall, as well as a possible adhesion. In absence of cohesive bonds with the formwork, friction should be proportional to the source of this normal stress. Three states need to be distinguished, friction without formwork movement (studied in [38]), at the beginning of slip (structural breakdown of interface layer) and continuous slip [9] (compare static and dynamic cases in figure 3.8).

At low yield stress (compared to industrial slip-forming) pore water pressure is positive. In the continuous phase, the interface layer is continuously damaged and normal stress of particles on the formwork should be governed by hydrodynamic interactions. It is experimentally observed that the friction at slip start can be as much as 3x higher than in the continuous regime [9], [104]. In the range of negative pore water pressure, observed at the transition from plastic to elastic behaviour, substantially higher friction is shown by Fossa [138]. This could be explained by a positive pressure applied between particles and formwork interface.

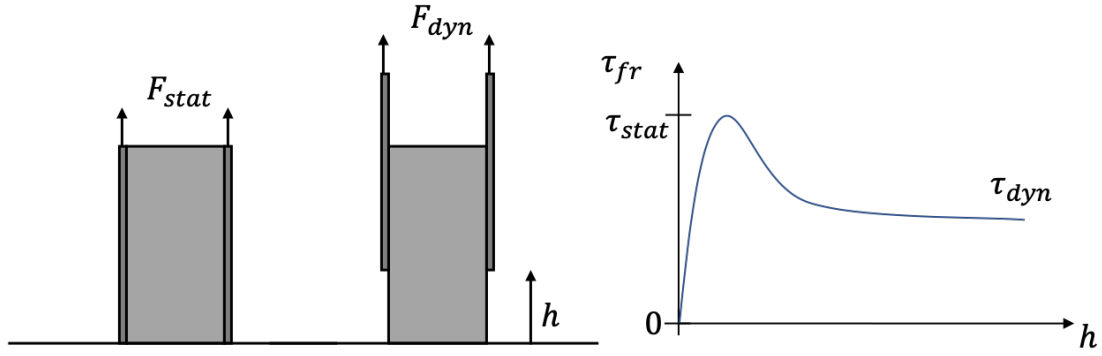


Figure 3.8: Friction in the building process, when a formwork is moved upwards.

In the range of positive pore water pressure, it appears reasonable to relate friction along the formwork wall to the mortar yield stress including a pre-factor:

$$\tau_{Fr}(t) = \alpha_{Fr} \tau_0(t) \quad (25)$$

This coefficient of friction α_{Fr} should depend on many different parameters, among which the particle packing (defining how dissimilar the concrete and the interface layer are) and the shear history (defining if the interface layer has been damaged by shearing). The latter one is of particular interest in slip-forming, where substantially higher friction is observed at start-up than during slipping.

Formwork pressure

The pressure exerted by concrete on a formwork has been the matter of a large body of research. Formwork pressure measurement techniques exist [139], [140]. Many competing models can predict formwork pressure [141], [52], [38], [53], among which the one of Ovarlez and Roussel [38] is using a yield stress fluid approach. They consider the strength build-up of concrete at rest and a reduced vertical pressure due to friction along the formwork wall. Once casting is finished or if it is slow, the formwork pressure decreases over time [139], [142] (compare figure 3.9).

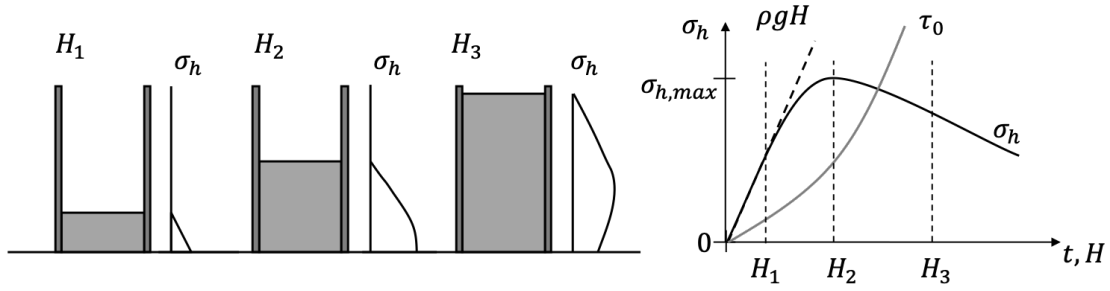


Figure 3.9: Formwork pressure with increasing material level, following a linear increase at the rate of hydrostatic pressure as the filling level increases and reaching a maximum value, due to structural build-up.

The vertical pressure is defined in a cylinder of radius r_{hy} by, using the power law yield stress evolution and considering a zone of structural damaging e . For a plastic material, vertical and horizontal pressures can be set equal at the time of casting and by extension at a later stage ($K=1$):

$$\sigma_h = \sigma_v = \rho g H - \frac{2\alpha_{fr}}{r_{hy}} \int_0^{H-e} \tau_0(z) dz \quad (26)$$

By integrating the power law yield stress evolution, the horizontal pressure is put in relation to the yield stress at the formwork bottom $\tau_0(t_{bot})$:

$$\sigma_h = \rho g H - \frac{2(H-e)\alpha_{fr}}{(\beta+1)r_{hy}} \tau_0(t_{bot}) \quad (27)$$

3.3.4. Material changes to be avoided

Segregation/Bleeding

In concrete/mortar a minimum yield stress is required in order to avoid dense large particles from sedimentation to the bottom and to prevent excess pore water from bleeding to the free surface. This minimum yield stress depends on the packing of particles [143], bleeding being strongly hindered by the presence of aggregates [144]. For low aggregate solid content, it is the sedimentation of the largest aggregate that needs to be prevented, while for denser packing close to the percolation limit, the squeezing of cement paste between approaching aggregates is an adequate criterion [135].

Water loss/evaporation

For any concrete directly exposed to air, evaporation occurs, removing some of the water necessary for hydration. This is especially important in applications involving large surface to volume ratios, such as coatings, as well as cases where drying can occur between the application of successive layers as this can lead to weak layer interfaces[45] [46], [47].

Generally, as long as the matrix is water saturated evaporation occurs at a constant rate. At the transition to granular a transition to a mechanism at lower rate occurs[145].

In order to prevent evaporation or its negative effects, either drying needs to be reduced, by changing the environment (lower temperature, higher humidity, less wind), by changing the mix design (drying rate reducing admixtures) or by hydration kinetics (binding water in hydration products quicker).

3.4. Linking stability criteria to processes

3.4.1. Slip-forming process

In digitally controlled slip-forming (Smart Dynamic Casting – SDC)[9], [33], [34], [44], [51], [103], [104], [146] a self-compacting concrete is cast into and distributes in a formwork that is simultaneously lifted. This is very similar to traditional slip-forming, but differs in the formulation and strength range at slipping [138]. Segregation needs to be avoided, defining the yield stress requirement at the time of casting. While the concrete stays in the formwork, it builds strength to support itself at the time of extrusion. As it is lifted, the concrete shears along the formwork, typically along an interface layer.

The main challenge for slip-forming is self-support of the concrete upon extrusion, without tearing caused by friction[9], [103], [104]. Buckling, as shown in the following, is not a major concern in the presence of reinforcement, as its Young's modulus is orders of magnitude larger than the one of fresh concrete, providing high resistance by embedding. Evaporation is also not a major concern before the time of extrusion, as the layer in contact with air is regularly covered by subsequent layers.

The competition between friction and yield stress

For the process, the integral of the spatially variable shear stress τ_{fr} along the formwork surface is responsible for the total friction (see figure 3.10). This depends on many parameters, such as formwork material, material evolution, surface geometry, process rate, and material microstructure.

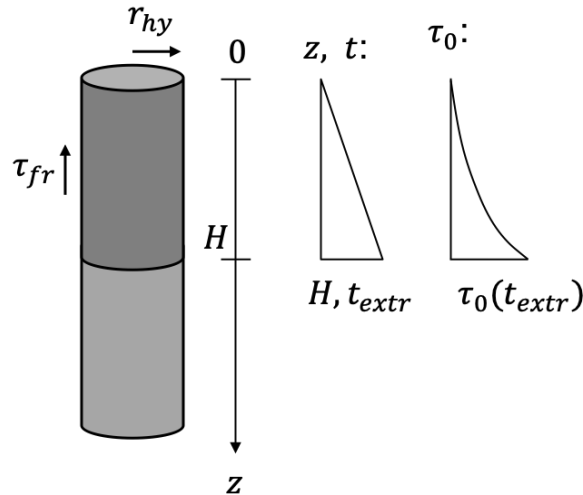


Figure 3.10: Weight of concrete in formwork (dark grey), friction on formwork walls, yield stress and coordinate system.

The ratio of formwork volume to surface is an important parameter and it can be expressed as hydrodynamic radius r_{hy} (equation 28), treating any shape of formwork as a cylinder [103]. For geometries with small hydrodynamic radius (thus large surface to volume), friction affects the process more in relative terms. Typical values for hydrodynamic radius as used in the project Smart Dynamic Casting (SDC) are shown in the following.

$$r_{hy} = \frac{2 \cdot Volume}{Surface} \tag{28}$$

Examples of geometries studied in SDC (figure 3.11):

Columns: $r_{hy} = \frac{2 \cdot a \cdot b}{2a + 2b}$, with $a = b = 150mm \Rightarrow r_{hy} = 75mm$

Mullions: $r_{hy} = \frac{2 \cdot a \cdot b}{2a + 2b}$, with $a = 100mm, b = 70mm \Rightarrow r_{hy} = 41mm$

Folded structures: $r_{hy} = \frac{2 \cdot 2 \cdot a \cdot t}{4 \cdot a} = t$, with $t = 25mm \Rightarrow r_{hy} = 25mm$

Process and rheology models for structuring materials

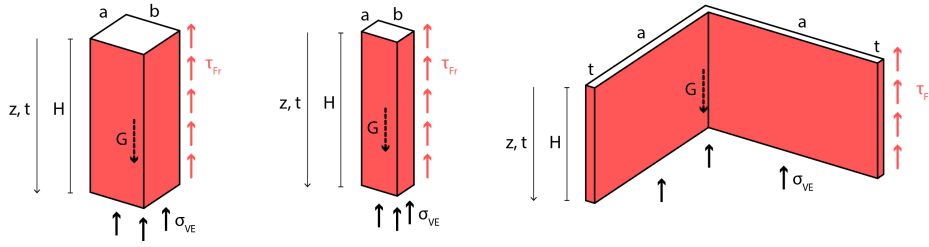


Figure 3.11: Size of formwork and relationship to hydrodynamic radius, ranking the formwork typologies according to difficulty [103].

The force balance between the hydrostatic pressure ρgH of concrete in the formwork and the cumulated friction of concrete along the formwork allows for calculating the vertical stress σ_{vE} at the extrusion point:

$$\sigma_{vE} = \rho gH - \frac{2}{r_{hy}} \int_0^z \tau_{Fr}(z) dz \quad (29)$$

Conservatively, risk of fracture can be excluded if compressive stress is present at the extrusion point, giving an upper limit associated with friction:

$$\sigma_{vE} > 0 \quad (30)$$

At the exit point E, the horizontal stress is zero. The yield stress at this point $\tau_{0,E}$ needs to at least support the main stress difference, giving a lower limit associated with yield stress:

$$\tau_{0,E} > \tau_{0,E,min} = \frac{\sigma_{vE}}{2} \quad (31)$$

These failure criteria limit the vertical stress allowed by the slip-forming process to positive values (no cracking caused by tensile stresses) (30) and values lower than twice the yield stress $\tau_{0,E}$ at the time of extrusion t_{Extr} (no flow according to Tresca criterion) (31):

$$0 \leq \sigma_{vE}/2 \leq \tau_0(t_{Extr}) \quad (32)$$

Assuming that in any point of the formwork, friction $\tau_{Fr}(t)$ is proportional to the concrete yield stress (25) (evidenced within the range of interest for SDC by [104]) and that the yield stress evolves according to a power law scaling with time t since concrete placing, then the following relationship is found:

$$\tau_{Fr}(t) = \alpha_{Fr} \tau_0(t) = \alpha_{Fr} \alpha t^\beta \quad (33)$$

The stress balance (29) can be reformulated with (33) and integrated over time, assuming constant velocity and making the substitution $dz = v dt$:

$$\sigma_{VE} = \rho g H - \frac{2}{r_{hy}} \int_0^{t_{Extr}} \tau_{Fr}(t) v dt = \rho g H - \frac{2v\alpha_{Fr}\alpha}{r_{hy}(1+\beta)} t_{Extr}^{1+\beta} \quad (34)$$

Using the failure criteria (32), the range of the relative balance of weight and yield stress can be described with a dimensionless quantity referred to here as the friction number ψ representing the effect of friction.

$$\psi = \frac{H\alpha_{Fr}}{r_{hy}(1+\beta)} \quad (35)$$

The friction number involves only the coefficient of friction α_{Fr} , the hydrodynamic radius r_{hy} , the power law exponent of yield stress evolution β and the formwork height H and defines the process window by limiting the range of yield stress:

$$\psi \leq \frac{\rho g H}{2 \tau_0(t_{Extr})} \leq 1 + \psi \quad (36)$$

In summary, equation (36) states that material exiting the formwork needs a minimum yield stress to prevent flow-out and has to cause as low friction as possible to avoid crack formation. When the friction number is larger than 1, requirements related to material control become substantially harsher. The compressive strength at the time of extrusion has to be lower than the hydrostatic pressure, while it is required to evolve at the rate of vertical building after extrusion. In addition, as the friction number increases, the upper and lower relative limits of hydrostatic pressure to compressive

strength ratio approach each other, thus narrowing the range of acceptable yield stresses at the time of extrusion.

Taking the friction number (35) the effect of a change of power law exponent in the yield stress evolution or hydrodynamic radius on friction and the process window can be quantified as:

$$R_{\beta} = \frac{\psi_2}{\psi_1} = \frac{(1 + \beta_1)}{(1 + \beta_2)} ; R_{r_{hy}} = \frac{\psi_2}{\psi_1} = \frac{r_{hy,1}}{r_{rh,2}}$$

It is evident that slip-forming difficulty is directly proportional to the inverse of hydrodynamic radius. Empirical experience in [103] shows that the SDC process is excessively difficult to keep robust from a friction number of $\psi = \frac{0.3m \cdot 0.13}{0.025m(1+1.5)} \simeq 0.62$ onwards.

Beyond the extrusion time, yield stress needs to increase at a rate of :

$$\dot{\tau}_0 = \frac{\rho g v}{\sqrt{3}} \quad (37)$$

Using process criteria for control

The measurement of the cumulative friction F_{fr} (compare figure 3.12) can be used to calculate the vertical stress σ_{VE} at the exit point E and this can be combined with equation (30). This has been studied using load cells holding the formwork, measuring weight changes and can be used robustly [9], [44] as a process criterion (with A the cross-section area exiting the formwork):

$$\sigma_{VE} = \rho g H - \frac{F_{fr}}{A} > 0 \quad (38)$$

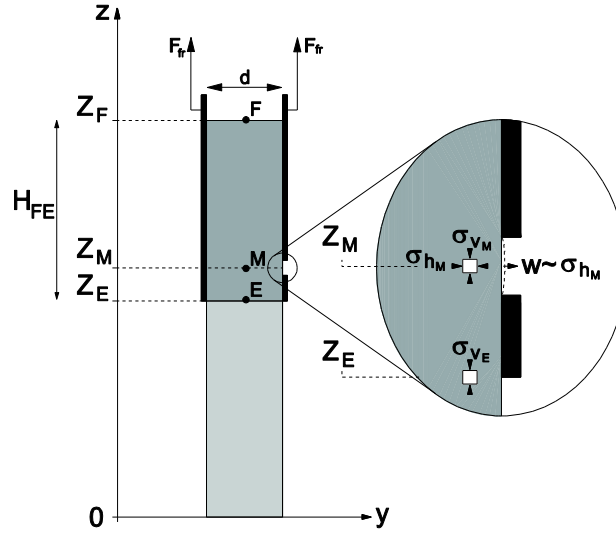


Figure 3.12: Characterization of yield stress and process range by measurement of friction and formwork pressure [9]. The formwork is filled to the height H_{FE} , friction force F_{fr} occurs along the formwork interface, vertical stress at the exit point is σ_{VE} and formwork pressure is σ_{hM} .

Similarly, the strength criterion at the exit point can be combined with a formwork pressure measurement or other method performed at a point M close to the exit. The mortar yield stress τ_{0M} at the measurement point M can be estimated by the formwork pressure measurement σ_{hM} and an estimation of the vertical stress σ_{VM} :

$$\tau_{0M} = \frac{\sigma_{VM} - \sigma_{hM}}{2} \quad (39)$$

Knowing the exponent of yield stress evolution between points E and M and the vertical stress at these points from friction measurements, the acceptable formwork pressure σ_{hM} can be calculated with:

$$\frac{\tau_{0E}}{\tau_{0M}} = \left(\frac{z_E}{z_M}\right)^\beta > \frac{\sigma_{VE}}{\sigma_{VM} - \sigma_{hM}} \quad (40)$$

Considering a vertical stress similar in points E and M, the above criteria (38) and (40) simplify to a singular criterion:

$$\frac{\sigma_{hM}}{1 - \left(\frac{z_M}{z_E}\right)^\beta} + \frac{F_{fr}}{A} \leq \rho g H \quad (41)$$

For typical values in the range of continuous slip (compare figure 3.13) as found in [9], equation (41) is valid by a small margin, indicating that processing is possible.

$$\frac{1500 \text{ Pa}}{1 - \left(\frac{0.35}{0.40}\right)^{2.2}} + 2000 \text{ Pa} = 7.9 \text{ kPa} \leq \rho g H = 9.0 \text{ kPa}$$

However especially in the first phase of slipping, when friction and formwork pressure measurements are high, this approach estimates unsafe conditions.

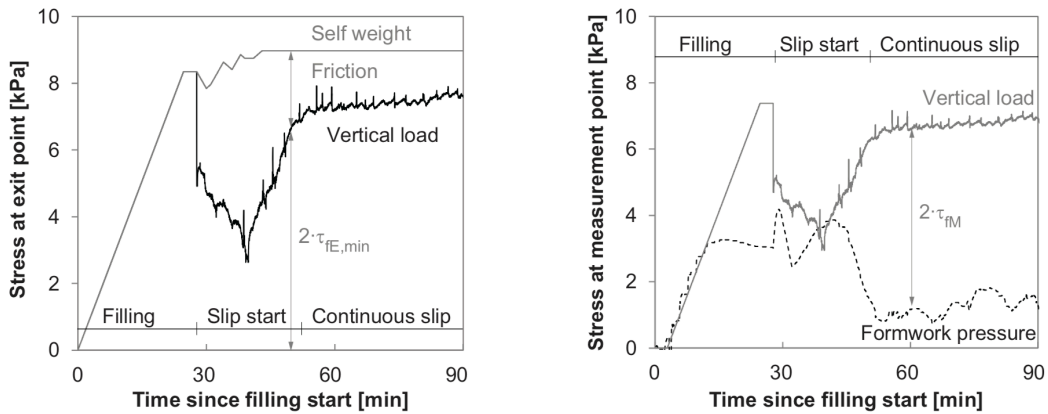


Figure 3.13: Friction and formwork pressure measurements for a typical slip-forming rate during the filling, the slip start and continuous phases [9].

The presence of reinforcement

Reinforcement in slip-forming can be fed through the formwork, allowing the construction of standard reinforced elements. Such reinforcement is beneficial as it has high strength and can hold concrete at its surface (see section 3.3.3). For a column as used in SDC development (square section of length 0.15m, longitudinal reinforcement 4xD12 and stirrups D6@100, $l_2 = 0.4m$), this resistance lowers the required yield stress at the low deformation limit according to equation (22) after extrusion independently of building height, indicating that in presence of reinforcement yield stress growth is not critical (compare also to figure 14):

$$\tau_0 \geq 3 \frac{\rho g a^2 l_1}{\pi(4\phi_v l_1 + 3\phi_H l_2)} = 4.0 \text{ kPa} \quad (42)$$

With increasing building height, reinforcement is also highly beneficial to prevent buckling due to its high Young's modulus. Indeed, the presence of $\xi_R = 1\%$ of

reinforcement amplifies the Young's modulus of the composite structure if full embedment is achieved by a factor δ given below in equation (43). By considering at the same time a high yield stress and low critical deformation (20 kPa and 0.1%), using equation (21) the Young's modulus is conservatively (with respect to the amplification δ) in the range of $E_C = 50\text{MPa}$.

$$\delta = \frac{\xi_R E_R + (1 - \xi_R) E_C}{E_C} = \frac{0.01 \cdot 205 \text{ GPa} + 0.99 \cdot 0.05 \text{ GPa}}{0.05 \text{ GPa}} \approx 42 \quad (43)$$

The same relationship applies also to shear states, such as applied shear or torsion at the extrusion point, significantly increasing the force or torque required to deform the concrete at the extrusion point. An increase of this magnitude in conjunction with shear fracturing was observed when reinforcement was introduced to elliptical formworks twisted during slipping. This behavior severely limits the possibility to locally deform concrete during extrusion and has led to the development of formworks where the deformation is applied at the time of filling [9].

Desired material evolution

The above relationships can be used to study the building process of a typical reinforced column ($a=b=0.15\text{m}$) using a typical yield stress evolution ($\beta=2$) and a building rate of $1\text{cm}/\text{min}$ in a formwork of 0.4m height. With these parameters the desired yield stress range can be calculated.

Based on empirical experience, the correct starting point for slipping is in the range of a penetration force F_{pen} of 6N (formula and more details in chapter 4) and this translates to a yield stress using the pre-factor α_{pen} :

$$\tau_0 = \alpha_{pen} \cdot F_{pen} = 774 \frac{\text{Pa}}{\text{N}} \cdot 6\text{N} = 4.6 \text{ kPa} \quad (44)$$

The yield stress needs to be reached at an age of 40min , the time when the formwork is full. This gives the following empirically desired evolution using (1):

$$\tau_0 = 2.88 \frac{\text{Pa}}{\text{min}^2} t^2 \rightarrow \alpha = 2.88 \frac{\text{Pa}}{\text{min}^2} \quad (45)$$

Using the above calculated hydrodynamic radius (28) of $r_{hy} = 0.075m$ and taking the measured friction from figure 3.13 in continuous slipping (2000 Pa), the vertical pressure in equation (34) is used to calculate the coefficient of friction α_{fr} (assuming linearity of yield stress and friction):

$$\frac{2H\alpha_{Fr}\tau_0}{r_{hy}(1+\beta)} = 2000Pa \rightarrow \alpha_{fr} = 0.12 \quad (46)$$

Using equation (46), the friction number (35) is: $\psi = \frac{0.4m \cdot 0.12}{0.075m(1+2)} = 0.21$

Reformulating equation (36) to calculate the yield stress range at the time of extrusion quantifies how well the empirical finding relates to the predicted range (equation (44)).

$$\frac{\rho g H}{2(1+\psi)} \leq \tau_0(t_{Extr}) \leq \frac{\rho g H}{2\psi} \quad (47)$$

Table 3.1: Low and high limit for yield stress in slip-forming. All continuous cases are valid; however, the slip start for folded structures is not possible with the predefined material.

Geometry – State	r_{hy} [m]	α_{Fr} [-]	ψ [-]	Low limit [kPa]	High limit [kPa]
Column – Start	0.075	0.12·3	0.63	2.75	7.04
Column – Continuous	0.075	0.12	0.21	3.73	21.5
Folded – Start	0.025	0.12·3	1.89	1.54	2.35
Folded – Continuous	0.025	0.12	0.63	2.75	7.04

For the slip start, friction observed in figure 3.13 is approximately 3 times larger at the start than in the continuous state and the hydrodynamic radius decreases by the factor 3 from columns to folded structures. The results of these other cases are summarized in table 3.1. Generally, the slip start is the most critical part in slip-forming, involving the narrowest gap and without change of formulation, a process adequate for a large section may be difficult to implement for a substantially smaller formwork (column to folded). In the particular case of slip start, confinement of material inside the lifted

section allows to have a 3-dimensional normal stress, reducing the yield stress requirement and thus widening the yield stress range for a short timeframe.

A summary of the described requirements (8), (37), (42) and (47) is given in figure 3.14, with the yield stress range at the start of slipping at a height of 0.4m and the strength requirements beyond extrusion time, taking into account the reduced vertical loading due to friction.

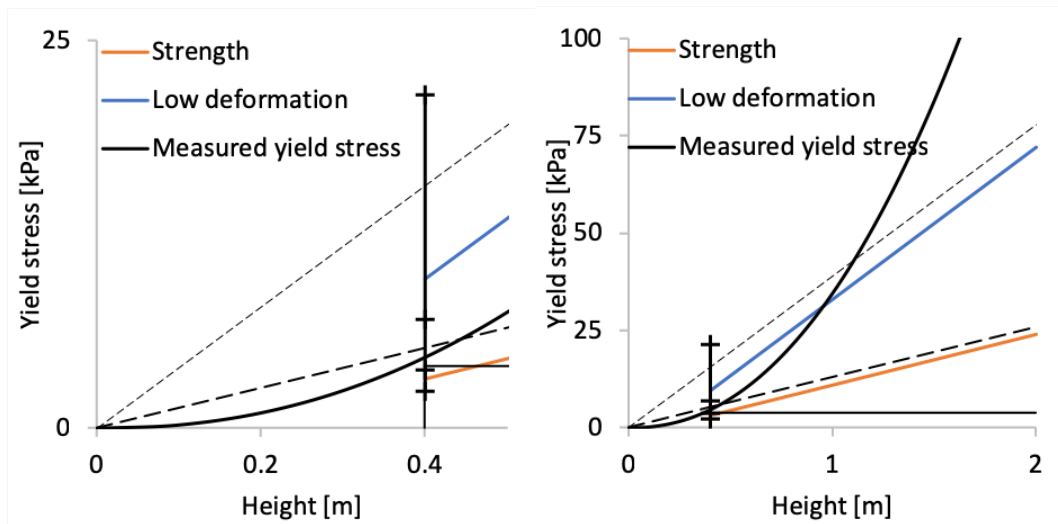


Figure 3.14: Yield stress evolution as designed for slip-forming (black curve) and yield stress requirements (blue for low deformations and orange for strength criterion). At the time of extrusion (vertical black line), yield stress needs to stay within a narrow gap (delimited by dashes) this gap being more restricted at the start-up (two inner dashes), than during continuous slipping (two outer dashes).

3.4.2. Layered extrusion

Layered extrusion is a building process that has received substantial attention in the last years [14], [18], [22], [26], [28]–[31], [147]. In this process, the concrete needs to be self-supporting from the time of placing and should increase its strength at a sufficient rate to support subsequently placed layers [19], [26] and limit layer deformations (see section 3.3.1). To achieve this, accelerators or fast hardening formulations have been studied [31], [147], [148]. The stiffness increasing at a similar rate as the strength, on longer timescales, buckling can be the dominating failure criterion (see section 3.3.2) as experimentally observed by Wolfs et al [40] and studied by Roussel [26] and in more depth by Suiker [41].

The strength and global buckling requirements (6), (8) and (19), more generally valid for any type of building process will be used here in addition to the more specific requirement of preventing localised buckling.

Local buckling

For vertical bodies more complex than a singular wall section, in addition to global buckling, sections of the element can show buckling failure. Suiker gives the example of clamped wall sections in a hollow rectangular element [41]. In this instance the wall sections are supported in the corners of the frame. Such behavior can in general be approached as a distributed spring resistance c in a beam (as in figure 3.6) as in equation (11).

In a similar fashion, the local stability of a hollow cylinder can be approximated by writing its differential equation [149]:

$$\nabla(D \nabla w) + (\sigma_V b w')' + \frac{Eb}{r^2} w = -\nu \sigma_V \quad (48)$$

Using again the expression of the sum of potentials (14) for the hollow cylinder a requirement can be defined to prevent local buckling in a hollow cylinder:

$$\begin{aligned} \Pi &= \int_0^{2\pi} \int_0^H (D \nabla w^2 + \frac{Eb}{r^2} w^2 - \sigma_V w'^2) r dz d\theta, \text{ with } w = w_H \cdot \tilde{w}, \text{ with:} \quad (49) \\ E &= E_0(1 - \xi_z)^\beta \text{ and } D = \frac{b^3 E}{12(1 - \nu^2)} \text{ and } \tilde{w} = (1 - \cos(\epsilon \xi_z)) \sin \theta \text{ and} \\ \epsilon &= \frac{\pi}{2} \text{ and } \frac{d^2 \Pi}{dw^2} > 0 \end{aligned}$$

For these conditions (49) and for linear gradient, the Young's modulus needs to increase according to the following scaling (details in appendix):

$$E_{0,local} \geq \frac{0.368 \rho g H}{0.178 \left(\frac{b}{H}\right)^2 - 0.022 \left(\frac{b}{r}\right)^2 + 0.0034 \left(\frac{Hb}{r^2}\right)^2 + 0.041 \left(\frac{H}{r}\right)^2} \quad (50)$$

It appears that in the presence of supports, for example the rotational symmetry providing $\frac{Eb}{r^2} w$ in a hollow cylinder, the requirement to prevent buckling locally is much reduced by the introduction of geometric details acting as distributed supports. To exemplify this positive effect, the Young's modulus requirement $E_{0,local}$ tends towards zero at infinite building height. Local buckling is thus only relevant on cylindrical bodies in a certain height range, or by consideration of the recurring nature of the printing process, in a limited upper section of the print. For the boundary case of an infinitely large radius R , the criterion converges to the case of a straight wall and the pre-factor of the local stability criterion for linear increase of E is 0.172, when the value predicted by the quantification for global buckling (19) of such straight wall is 0.150. This shows that despite a set of approximations, the main features of local and global stability phenomena can be captured in a simple to apply way.

For a generalized understanding of the phenomenon of local failure by self-weight induced buckling, the differential equation describing the presence of a distributed spring (11) can again be divided into unit-carrying factors and unitless functions, resulting again in a generalized form of Young's modulus with the same trend at large height as for the cylinder (50). This shows that local buckling failure is for any shape a phenomenon that can occur at low building height, but is rather not relevant for tall elements ($H \rightarrow \infty$).

$$E_{0,local} \geq \frac{c_1 \rho g H^3 A}{c_2 I + c_3 H^4} \quad (51)$$

From penetration force to vertical building rate

Taking the measured penetration force evolution [105], converted to yield stress (corrected for depth dependency as done in chapter 4 and [150]) and the known vertical building rate (2.8 m/h), the measured yield stress of the bottom layer can be related to the current building height (see figure 3.15). This allows a direct comparison of the measured strength compared to the required one, given the before mentioned criteria of strength (6), deformation (8), global (19) and local stability (50).

In the building process with a Set on Demand material, every layer evolves in a similar manner compared to its time of activation/placing. Because of the recurring nature of the building process, if the material placed in the first layer (or into a testing

sample before printing is started) fulfils the yield stress requirements during the fabrication time, then every layer placed above also fulfils the requirements [19].

Figure 3.15 shows on the same graph the yield stress evolution of a set activated mortar measured by penetration (as introduced in chapter 4) and the process requirements. Both measurement and requirements (low deformation with eq. (8), strength with eq. (6), local buckling with eq. (50) and global buckling with eq. (19)) are shown as a function of building height using in the case of the measured yield stress evolution the vertical building rate of the hollow cylinder of 2.8 m/h as conversion factor from time to height. The cylindrical column is built in the experiment at a rate of 2.8 m/h, with a center radius 0.15m and a layer width of 32mm, mortar density is 2300 kg/m³. The requirements are fulfilled both for the strength requirement (6) and the less clearly defined deformation limiting requirement (8). Buckling criteria are assessed using a conservative critical strain of 4% as input (compared to 2.5% as approximated by Roussel et al [12]). In this approach, buckling does not occur within the first 2.5m and indeed in the printing experiment in question it did not over the printed height of 1m. With the same critical deformation, it also appears that local buckling cannot occur before plastic collapse for this particular geometry (evident as no intersection exists between blue and black dashed curves) and that local buckling is irrelevant once the structure has reached a certain height (here 12cm).

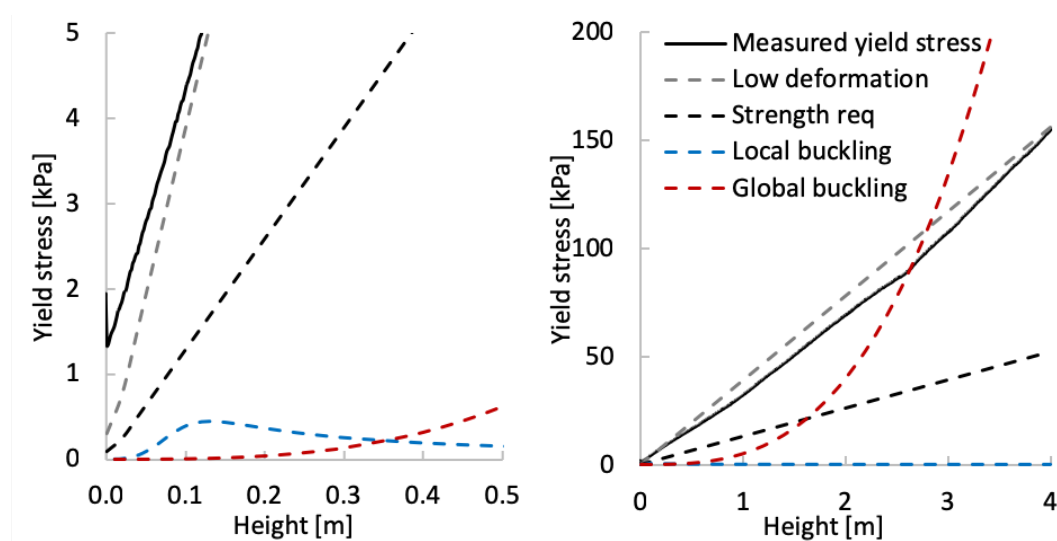


Figure 3.15: Yield stress calculated from penetration tests and compressive strength and requirements (assuming a critical deformation of 4%). From these results a building height of at least 2.5m in one piece appears to be possible (in approximately 1h). [105]

Effect of shape, a cylindrical hollow body

In figure 3.16 the same relationships (eq. (6), (8), (19), (50)) are used for hollow cylinders of a given height and a changing radius. This shows in which range, which requirement is critical, again assuming a critical deformation of 4% and two different column heights. The dashed line shows the experimentally tested radius. At low height (1m), the strength-based criteria are dominating (6) and (8), while at high height (3m) global buckling (19) becomes the dominant contributor (similar case as straight wall).

It is also evident that cylindrical shapes are an ideal testing case for studying strength-based criteria and for benchmarking material formulations with respect to vertical building rates, as buckling is not a relevant loading case within any currently meaningful building height. This is especially evident when comparing the buckling requirements (19) in the intermediate radius range of 0.15m and 1m to the requirements for long single-filament wall sections ($r \rightarrow \infty$) and slim columns ($r \rightarrow 0$) in (50).

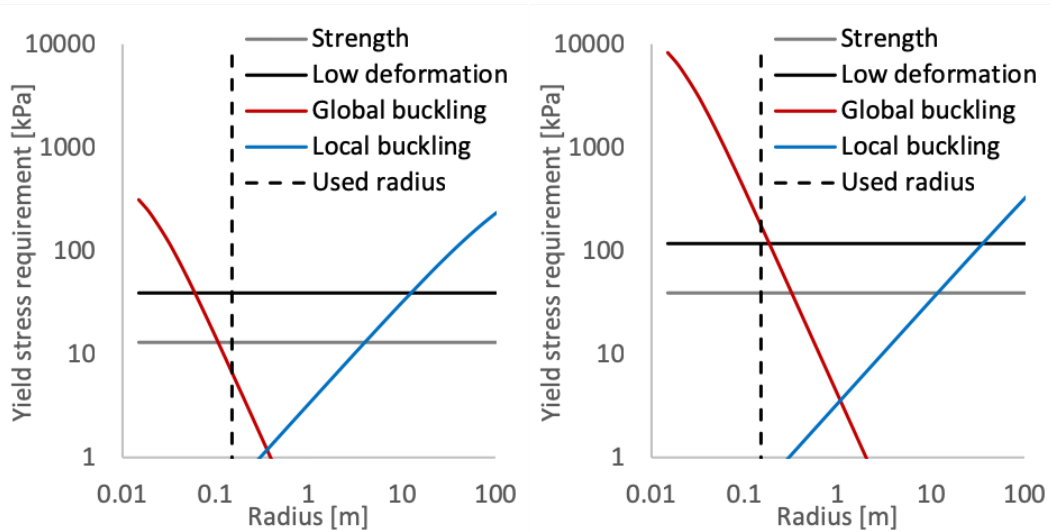


Figure 3.16: Dependence of shape of cylinder for the buckling mode. (left) $H=1m$, (right) $H=3m$. The used radius is 0.15m. [105]

Buckling for geometries in practice

The scaling of self-weight induced buckling (19) with $1/i^2$ means that there are substantial benefits from cross-connecting layers with zigzagging strands [26] such as done in some examples of layered extrusion [22], [31] as this significantly increases the ratio I/A . The scaling shows that this can only expand the possible height not eliminate

the limitation. Alternatively, 3d-printing projects are placing concrete in a discontinuous approach, printing layers until the process needs to be stopped to allow for hydration to stiffen the structure, then subsequent placing can continue.

From this work, it appears that only a strong rate increasing mechanism providing a t^3 evolution and significant immediate strength increase can be used. It appears thus that set accelerators can provide sufficient quantitative strength increase efficiently and only a rate increasing set accelerator leading directly to the main hydration reactions can solve the problem of self-weight induced buckling.

Approaches to concrete extrusion: soft or stiff?

Without an activation system, strength buildup is eventually limiting the achievable layer count, either by strength or stability requirements. In order to place as many layers as possible without activation, formulations involving high solid content and very high initial yield stress are used to avoid layer settlement. This involves some processing disadvantages, for example filament tearing at deposition, processing at substantially higher pressure and a risk of weak layer interfaces [14], [26]. When designing for this approach in conjunction with activation, strong mixing reactors are required, adding to cost and weight.

With a mortar formulation designed with an activation system in mind, a formulation with lower yield stress and lower aggregate solid content can be chosen, strongly reducing pumping pressure, risk of clogging, size and weight of mixing reactors and providing a means of pressing mortar on previously placed and still soft layers. Additionally, owing to fast strength build-up, layer settling is expected to only occur in the uppermost layers and layer settling can be compensated without a feedback system by choosing a pumping rate slightly higher than warranted by the process (printing a filament wider than the nozzle).

3.4.3.Digital casting

In digital casting, the goal is to limit formwork pressure (see section 3.3.3) in order to fill weak formworks [35], [36] or to prevent the outflow from permeable formworks[132]. In this approach, formwork pressure from equation (26) needs to be

limited to the formwork strength σ_R and for this, the yield stress needs to increase in the following way [38]:

$$\tau_o(t_{bot}) \geq \frac{(\beta+1)(\rho g H - \sigma_R) r_{hy}}{2 \alpha_{fr}(H-e)} \quad (52)$$

It appears that on long timescales (large H), the yield stress only needs to conservatively reach a value depending on the formwork geometry:

$$\tau_{o,min}(H \rightarrow \infty) = \frac{(\beta+1)\rho g r_{hy}}{2\alpha_{fr}} \approx \frac{2 \cdot 2300 \cdot 9.8 \cdot 0.2}{2 \cdot 0.33} Pa = 13.7 kPa \quad (53)$$

Assuming instead of stress transfer through friction, rather a sustainable normal stress difference by the Tresca criterion can give a criterion in which stress is not necessarily applied on the formwork. Such a criterion writes as:

$$\sigma_h = \rho g H - 2\tau_o \quad (54)$$

In this way, the yield stress needs to linearly increase with the filling height, allowing early on only an applied pressure of the same size as formwork strength σ_R . The required evolution does not depend on the formwork geometry and is generally conservative compared to equation (53) for high formworks.

$$\tau_{o,min} = \frac{\rho g H - \sigma_R}{2} \quad (55)$$

Reaching the required yield stress predicted in equation (53) with a set activated concrete formulation as in figure 3.15 appears trivial, however equation (53) assumes that vertical stress transfer occurs in the formwork material. As the target application involves very weak formworks, not strong enough to take over the vertical stress in the formwork material resulting from friction along the formwork wall and it not necessarily being ductile, using equation (53) for digital casting may be risky. Instead, equation (54) with harsher demands on material evolution has the advantage that formwork friction is not required for self-support, potentially allowing leaner formworks if this criterion is fulfilled.

3.4.4.Coatings

Coatings are thin covering layers. They have many different purposes, one particular interesting one for digital fabrication as a stiffening material for fabrics [37], [151]. Their large surface to volume ratio renders them prone to drying (see section 3.3.4). For cementitious coatings, the competition of surface drying to water binding by hydration is the main effect to consider for the hardening of such coatings.

In standard conditions (20°C, 50%RH) the drying rate of a cement paste is in the range of 80g/m²/h. For coating layers of thickness 2mm, typical coating mixtures may contain 520 g water/m² at a solid volume fraction of approximately $\phi = 0.5$ (wc=0.32). In these conditions the evaporation rate is 15%/h of the initial water.

The rate of drying can be considered constant (water film on surface) as long as the solid volume fraction is smaller than close packing $\phi_{max} \approx 0.6$. This should mark the transition to rate decreasing evaporation and can be calculated from (4). Knowing the hydration products forming, the transition occurs at a degree of hydration $\xi_H = 0.175$, according to equation:

$$\phi_{max} = (1 - \xi_H)\phi + \xi_H 2.14\phi \quad (56)$$

Reaching a degree of hydration of 17.5% in an OPC (500 J/g) the cumulative heat release of 88 J/g is needed, typically reached after 9h of hydration. As a solid content of 0.6 marks the transition, this is reached by evaporation at an equivalent wc-ratio of 0.283, reached after evaporation of 11% of the initially present water, thus after 45min. From this it becomes obvious that OPC hydration is not quick enough for thin coatings in outside conditions.

By consuming enough pore water to transition quickly to an undersaturated matrix, the amount of evaporated water can be limited. This involves specialised fast setting mineral binders forming ettringite as the main hydration products (faster kinetics and large quantity of bound water), something introduced later in chapter 6.4. Water retention admixtures could also be used in this context[144].

3.4.5. Shotcrete and precision spraying

In shotcrete [152] and precision spraying applications a concrete or mortar, often containing fibers, is sprayed onto a support and has to remain in place. The applied layers are usually built up gradually, but a typical minimum thickness of a single layer needs to be supported from the time of application. For the applied concrete mainly empirical requirements are found in literature, such as rebound, achievable build-up and torque measurements [153]–[156], but no common process description. Considering only static loading the required yield stress can be directly calculated from the layer thickness d using equation (24).

$$\tau_{00} = \rho g d \quad (58)$$

It has to be stressed that in spraying the impact pressures are substantial and it causes some intermixing with previous layers as well as evacuation of entrained air. Upon application of successive layers, the impact forces are expected to partially breakdown the yield stress of the previous layers. It is known, that upon mixing of mortars in the induction period and at the beginning of hydration, vigorous mixing can bring a mortar at rest for a long time back to a similar yield stress as after previous mixing [123]. For this reason, it is expected that instead of the yield stress for the applied layer, the instantaneous yield stress for the first placed material has to reach the value required for the entire thickness d_L already applied:

$$\tau_{00} = \rho g d_L \quad (59)$$

Alternatively, when this cannot be achieved in terms of processing (evacuating entraining air), substantially accelerating concrete hardening, to increase the instantaneous yield stress after mixing is an option and this is best achieved by growing large quantities of hydration products, increasing the yield stress by solid content increase. The most effective shotcrete accelerators (Al-salts) do this very effectively by forming large quantities of ettringite [13], [157]–[159]. Qualitatively this type of yield stress increase can be understood as a consequence of increasing packing (lowering air content or increasing solid content) and can be described by YODEL, Zhou or the results of Mantellato (see section 3.2.2). Finally, if supports are present, these can also be beneficial, provided they have sufficient strength to take the entire concrete weight.

3.5. Conclusions

Structural build-up and rheology control of cementitious materials is a make-or-break requirement of many advanced building processes, such as slip forming, layered extrusion, digital casting, shotcrete and coatings. The common ground of these building processes is the need for a substantial strength/yield stress gain from the time of placing onwards, owing to different requirements, such as early age loading or drying.

How narrowly strength evolutions have to be controlled during the timeframe of processing may differ depending on the building process and can be estimated using rheological models for concrete and applying them to processes. This gives a processing range, defined either as a property range or a timeframe, in which placing and manufacturing can occur and with direct implications on the shapes that can be built.

For self-support, linear strength buildup is required. If layer deformations need to be limited, limiting the loads to shear stresses as low as $1/3$ of yield stress can give a simple approximative rule to limit structural breakdown. At larger building heights, layer stability/buckling limits building rates, due to a H^3 scaling. Supports such as rigid reinforcement can substantially lower yield stress requirements as a function of the surface of supporting material that opposes flow of concrete. Similarly, the presence of formwork lowers initial yield stress requirements.

The ideal strength build-up kinetics of concrete are strongly informed by the individual building process under study. For slip-forming it appears advantageous to have exponential kinetics in order to keep friction in the formwork as small as possible. In layered extrusion, at least linear strength increase is needed from the start and on long timescales rate increasing one. In digital casting, at least a linear strength increase is needed to prevent formwork failure, starting at a low yield stress. For coatings, it is essential to bind as much mixing water as possible, warranting fast hydration processes. In spraying instantaneous yield stress increase is necessary, involving a quick but not necessarily sustained increase of solid content.

As yield stress increase is largely proportional to hydration product growth (chapter 4), processes requiring merely a linear strength buildup, can take advantage of

Process and rheology models for structuring materials

activation systems offering a short-term precipitation and growth of hydration products. In contrast, processes needing an exponential strength buildup require rate accelerating hydration kinetics, something that generally is found after the onset of the main hydration peak of cement.

Chapter 4 Continuous characterisation method for yield stress of fresh concrete at rest

This chapter describes a measurement method for yield stress evolution of fresh concrete at rest.

The results of this chapter are intended to be published as journal publication under the same name:

Lex Reiter, Timothy Wangler, Nicolas Roussel, Robert J Flatt, “Continuous characterisation method for yield stress of fresh concrete at rest”, in preparation.

Further the results from chapter 4.4 have been submitted for a non-peer reviewed conference paper:

Lex Reiter, Timothy Wangler, Nicolas Roussel, Robert J Flatt, “Continuous characterisation method for structural buildup”, RheoConf2, 2019

In both cases, the papers are entirely written by Lex Reiter under the guidance of Timothy Wangler, Nicolas Roussel and Robert J. Flatt

Abstract

Digital fabrication processes with concrete require a specific yield stress evolution after placing that is similar for each layer. To account for variability in hydration and hardening kinetics, measuring techniques of yield stress for concrete at rest are necessary.

Continuous and point-wise penetration are here compared to more common methods such as the uniaxial compression and vane test, from which a yield stress can be computed. For yield stresses computed from the vane test and uniaxial compression, the same hardening kinetics can be observed over multiple scales as for penetration tests, allowing to scale the penetration force with yield stress.

Penetration tests with a conical tool moving at a slow rate are adequate to measure the structural build-up of both cement pastes and mortars over time on a single sample. Modelling penetration as a geo-mechanical soil stability problem predicts the relationship of penetration resistance to yield stress for plastic and frictional materials. The soil mechanical approach predicts that the factors relating yield stress and compressive to penetration stress change at early age. This change is expected to occur at the transition from plastic to frictional behaviour and depends on the internal friction angle. In typical systems with ordinary Portland cement, the measurements indicate a validity range of 1-100kPa and as low as 100Pa with consideration of depth dependency. This range is of greatest interest for structural build-up in digital fabrication with concrete during production.

4.1.Introduction

With the advent of new fabrication methods associated with the integration of design and fabrication using digital tools, novel and demanding building processes pose challenges to cementitious materials [14], [15], [19], [26]. Especially in layered extrusion and robotically controlled slip-forming, the yield stress of concrete needs to be assessed throughout production. At the time of placing, yield stress needs to be robust, at rest (time after placing) it needs to increase at a specific rate.

The required precision in terms of initial yield stress and its build-up is substantially higher than in traditional processes. Indeed, a too high yield stress upon placing can lead to weak layer interfaces, to filament tearing or to insufficient form filling. In contrast, a too low yield stress can lead to flow off or segregation. After placing, a too slow yield stress increase can lead to flow off and at later ages to buckling, while a too fast increase can cause filament tear-off in slip-forming [8], [19].

An important distinction from traditional casting processes is the emphasis on so-called “green” strength evolution or structuration of fresh concrete at rest. Variability in hydration and hardening kinetics can be a result of compositional and environmental variability that can compromise process robustness. In order to take such variations into account, measuring techniques of yield stress for concrete at rest are necessary.

Characterization methods for concrete have extensively dealt with flow behaviour, the onset and end of flow such as spread and slump measurement[124], [160], and thixotropic effects[161], [162]. Fewer methods have been employed to measure yield stress of concrete after long periods at rest. Notable examples of this are compressive strength[8], [39], vane[62], [61], [163] or penetration[164] measurements carried out at fixed times upon casting. A common ground for these methods is their (at least partially) destructive nature and the need for an individual sample for each measurement. The reason for this is that failure in such measurements is based on a transitional flow state with the development of a surface, on which shear strain is concentrated, leading to partial breakdown of the supporting structure of the material[50], [63], the recovery of which takes time[123].

A continuous and simple to carry out method to measure the build-up of strength at rest by mechanical loading would be ideal, as only one sample is required, which reduces the labour time and offers measurements in real time. Among non-mechanical methods, there are non-destructive indirect methods. One of these is calorimetry [55], which gives (indirect) information on growth of hydration products. Its drawback for the problem at stake however is that it does not directly measure physical interactions and their mechanical consequences. Mechanical non-destructive methods such as ultrasound travel speed[164]–[166] or small amplitude oscillatory strain measurements[50], [107],

[128], [167] and settling [168] also exist. Ultrasound can also measure dynamic shear moduli [166], but, for yield stress calculation, a constant critical deformation needs to be assumed and the measurement does not occur at the onset of flow. It therefore also presents a number of limitations.

Continuous methods measuring at the onset of flow are mainly limited by the transitional flow state on a fixed shear surface. Examples of this are compression, vane and penetration tests. In compression tests, sample layers can be directly loaded at the rate of the building process, detecting failure and relating it to yield stress at the time of failure [39]. Vane measurements involving multiple discontinuous measurements have been studied [62]. However, the structural breakdown from one such measurement to the next may not be fully recovered. In addition, vane geometries are prone to other phenomena such as wall slip [169], shear localisation and fracturing in the shear zone, which leads to a permanent change in measuring conditions [63]. Attempts at continuous penetration measurements related different penetration geometries and methods, to yield stress. Among these, some could measure continuously, but their application was limited to cement pastes [170].

In the field of digital fabrication, the processes in most direct need of a real-time measuring technique are layered extrusion and slip-forming. In both cases, their overall processing and especially their pumping, defines that they must be matrix-rich mortars. Additionally, an important requirement of digital fabrication methods is the possibility of geometrical detailing, generally limiting the maximum grain sizes to 4mm at most. For this reason, the measuring technique needs to be most adequate in this range of matrix rich mortars.

Finally, it should be noted that, for these new building processes, the strength upon placing should evolve from values as low as 100 Pa – sufficient to self-support a single placed layer – up to 0.1 MPa – sufficient to self-sustain a structure of several meter height [26], [28]. This is therefore the range of values that we seek to determine with a continuous measurement method, suitable for matrix rich - fine mortars.

4.2. Materials and methods

The cement pastes used in this study consist of Ordinary Portland Cement CEM I 52.5R mixed with tap water, without admixture additions and have a w/c ratio of 0.35. The goal of the study being to relate physical characterization methods, only one cement paste composition is used.

The mortar mixes for characterisation consist of the same OPC, of 0-2mm crushed limestone aggregates and a commercial PCE based superplasticizer. These mortar mixes have solid volume fractions of 20, 40 and 48% with the sand having a dense packing fraction of 65% (measured based on volume and weight of vibrated aggregates.[171], [172])

Additionally, the slow penetration test is used on mortars for digital fabrication processes, with the intention of assessing how strongly slow penetration measurements are affected by composition. In addition to the components of the mortar mixes for characterisation, these application mortars additionally contain a set retarder, silica fume and optionally a viscosity modifier and/or set accelerator. As for the application, they include a self-compacting mortar with long open time and set accelerated mortars for layered extrusion and for slip-forming of formulations similar to [103], [173]. The self-compacting mortar and the mortar for slip-forming use siliceous 0-4mm aggregates, and the mortar used for layered extrusion used calcareous 0-2 mm crushed aggregate.

All materials are mixed for 1min at slow speed and 2min at medium speed using a Hobart mixer, adding fluids to solids in volumes of 4L for pastes and 6L for mortars.

The conical penetration tip used in this study has a 30mm height and 10mm radius and is attached to a load cell of 1kN on a Zwick universal testing machine. Cylindrical containers of 9cm diameter and 12cm height filled with cement paste or mortar are used unless specified otherwise. The penetration tip is inserted into the sample with 1mm/s before measurement until the conical part is level with the sample surface (step 3 in figure 4.2). For fast penetration measurement, the tip keeps penetrating at a rate of 1mm/s. For slow penetration measurement, the penetration rate is 20mm/h.

Vane tests are carried out on a rotational rheometer (MCR501) using a Vane tool with 4 blades, being 40mm high, and 11mm wide. The cement paste is poured in a cylinder of diameter 27mm immediately after mixing and the vane tool is introduced immediately. After a specified resting time, a 0.05 1/s shear rate is applied and the peak shear stress is considered as yield stress, assuming a cylindrical shear surface (*i.e.* the so-called “Couette analogy”) [174].

Uniaxial compression tests are carried out on cylinders 18cm high and 9cm in diameter. The samples are cast immediately upon mixing. They are later demoulded and placed for testing 10 minutes before the measurement. The loading is displacement controlled at a rate of 0.2mm/s. Between the top surface and the steel calotte, a foam sheet is added. The yield stress is calculated considering the von Mises criterion.

In some complementary tests, a flat penetration tip with diameter 18.8mm and height 4mm is used as well as the penetration sample geometry studied by Mettler et al[170] (sample height 40mm).

4.3. Understanding penetration experiments in concrete and soil

4.3.1. A soil mechanics approach to fresh concrete

As for any material, the stability of soils or concrete depends on the relation of applied load to resistance. In soil mechanics, the approach to describing the mechanical resistance depends on the type of soil under study. The main points of distinction are drainage state, consolidation degree, saturation with water, pore water pressure and microstructure[175], [176]. The presence of water is an essential factor in the mechanical behaviour of soils, expressed by the concept of saturation and is typically considered as an environmental variable, while in concrete the water content is defined at mixing and decreases as hydration progresses.

To use geo-mechanical approaches, a qualitative conceptual understanding of the state of concrete at early age, its strength build-up and hydration is useful. For concrete as used in digital fabrication, processing requires a microstructure saturated with matrix material at early age, which itself is saturated with water [108], [137], [172]. As such, its mechanical behaviour is governed by colloidal interactions, hydration products growing

at the contact points of particles at rest [50] and hydrodynamic interactions under flow [172]. This behaviour is usually approximated as a yield stress fluid using the Bingham or the Herschel-Bulkley model [48], [49]. In the field of soils, the most comparable materials are fine-grained clay and silt, exhibiting similar colloidal interactions and a flow behaviour linked to their saturation degree and classified by Atterberg limits [177]. Soils consolidate, losing water through drainage and increase their shear resistance in the process, which especially for clays and silts is a long-term process.

The open time of concrete is typically shorter than the typical timeframe for the occurrence of consolidation, which is referred to as bleeding for concrete, and is generally an undesired behaviour that is prevented by proper formulation [143], [178]. With bleeding as the physical origin of drainage and consolidation excluded, drainage will nevertheless occur during the onset of hydration. Indeed, during hydration, free pore water is consumed to form hydration products. This increases the solid content and strengthens interparticle bonds/cohesion [123]. It also fills the pore space, reaching eventually the solid percolation threshold and leading to a state in which the material's rheology is governed by frictional particle interactions [108], [179]. This was demonstrated by Mettler et al [170], who showed that at very early age failure is localised at shear bands and that tensile and compressive strengths are of similar magnitude. They also reported that in the course of hydration the ratio of tensile to compressive strength tends to the value of about 1:10 known for hardened concrete, with the occurrence of distributed cracks and an increase of internal friction angle [170]. In terms of soil mechanical analogy, this marks the transition to an undersaturated or drained soil. In SCC the same general phenomenon is observed for increasing aggregate contents [172].

Additionally, with hydration occurring, pore water pressure becomes negative at a similar time as final set by Vicat needle penetration. This can be explained by the lower volume required by hydration products compared to water and cement, causing chemical shrinkage, in addition to producing a high enough solid volume for frictional contacts. In the presence of negative water pressure, an effective normal stress between particles of the soil or concrete exists even in absence of external loading [176], implying a frictional contact. Using pore pressure measurements could therefore be a simple approach to estimate the transition of concrete from undrained to drained conditions.

While the cementitious matrix is water saturated it can be considered as an undrained soil, with the key property being yield stress. With the progress of hydration, a drained state is reached, in which failure is dominated by cohesion and the angle of internal friction. In terms of mechanical description for materials with external normal stresses essentially in compression, the first phase of the undrained behaviour is one of a fully plastic behaviour. It can be described by the Tresca failure criterion or as a Bingham fluid, where all shear stresses experienced by the material have to be lower than its cohesion/yield stress (figure 4.1).

With the occurrence of a drained state, internal friction influences the shear resistance. This second phase of drained behaviour may be described by a failure criterion according to Mohr-Coulomb. In this case, the resistance to failure depends on the effective normal stresses between the particles. Generally, the material is stable if shear stresses in all directions remain within the space delimited by the Mohr-Coulomb failure criterion (figure 4.1), defined by the angle of internal friction, cohesion and effective normal stresses, which depend on pore pressure.

Pore pressure does not affect plastic materials, as yield stress is directly linked to the difference of normal stresses. However, it does influence frictional materials. In the case of a negative pore water pressure u_w , it increases the effective normal stress. This does not fundamentally change the failure mechanism, but represents an added normal stress, increasing the apparent cohesion c_0 . This can be accounted for in terms of the normal stress by increasing the effective material cohesion c' by a term $u_w \tan(\varphi)$:

$$c_0 = c' + u_w \tan(\varphi) \quad (1)$$

where

- c' : Effective material cohesion
- c_0 : Apparent cohesion as measured
- u_w : Negative pore water pressure
- φ : Internal friction angle

To summarize, in the first phase of hardening, concrete is expected to behave like a plastic material, characterized by its yield stress and described by a Tresca criterion. In

the second phase, concrete should behave like a frictional material, characterized by its cohesion, internal friction angle and pore water pressure and described by a Mohr-Coulomb criterion.

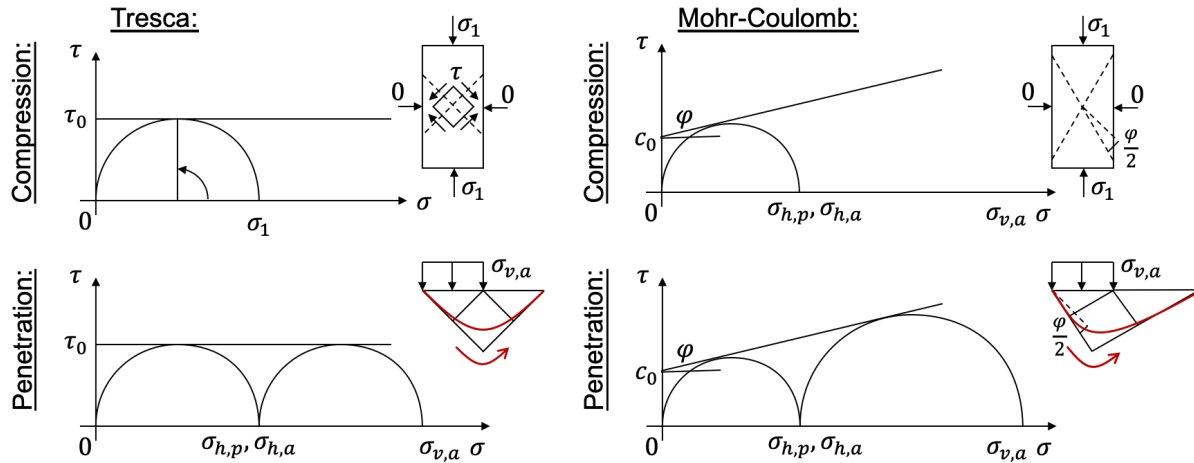


Figure 4.1: Mechanical behaviour of drained and undrained soils. Tresca criterion for plastic material and Mohr-Coulomb criterion for frictional material, with the relationship of normal stresses to shear stress in the Mohr circle. In frictional materials, shear failure stress depends on effective normal stresses. The angle of shear failure in compressive strength measurements and the shape of failure zone in penetration tests depends on the angle of internal friction and is qualitatively indicated in red. The inclination of the shear failure surface is related to internal friction angle via Mohr's circle. In penetration tests in frictional materials high effective normal stress occurs.

4.3.2. Penetration in soil mechanics

The stability of soils has been studied extensively in the field of soil mechanics and is of great importance for many practical applications, such as for the verification of the bearing capacity of foundations and piles [176], [181], [182]. Based on these contributions, the stability of foundations can be assessed, knowing the mechanical properties of soil, or by analogy the resistance of concrete to a penetration tip. Thus, the stress resisting the penetration σ_f of a penetration tip of cross-section area A_{pen} into a mortar sample may be expressed using bearing capacity factors N_i :

$$\frac{F_{pen}}{A_{pen}} = \sigma_f = N_c c_0 + N_q (q + \rho \cdot g \cdot d) + N_\gamma \frac{1}{2} b \cdot \rho \cdot g \quad (2)$$

where

- F_{pen} : Penetration force
- A_{pen} : Penetration tip cross-section area
- σ_f : Penetration stress
- N_c : Cohesion bearing capacity factor
- N_q : Surcharge bearing capacity factors
- N_γ : Soil-weight bearing capacity factor
- q : Applied surcharge
- ρ : Mortar density
- g : Gravity
- d : Penetration depth
- b : Penetration tip width

The cohesion, surcharge and soil-weight bearing capacity factors (N_c, N_q and N_γ respectively) have been derived analytically or empirically and are documented with minor differences between publications [183] (see table 4.1). They are essentially correlation factors between the applied penetration stress and the resisting stress in the soil, such as cohesion. They strongly depend on the angle of internal friction. This affects the bearing capacity of a foundation and by analogy the penetration resistance. The bearing capacity factors define the contribution of the different mechanisms to the resistance to penetration and can serve to assess the influence of penetration depth, penetration tool size, cohesion and internal friction angle on the relationship of the penetration force to cohesion/yield stress.

Equation (2) has been introduced for 2D-wedges of infinite length, but correction factors, or even bearing capacity factors calculated for other geometries exist, including conical and flat penetration tips [184]–[186]. Penetration test approaches using this framework such as the fall-cone test [187] or the cone penetration test for measurements underground [188], [189] have been used to characterise or classify soils (foremost clays). Despite the broad range of publications, assumptions needed to idealise material behaviour for calculations limit the quantitative precision that can be expected from these methods. However, for the study of parameters influencing the bearing capacity of a penetrating geometry at a certain depth and for different material groups, soil mechanical studies can offer valuable insight.

Table 4.1: Bearing capacity factors according to Foundation Engineering Handbook[183] for a 2D-wedge used for the calculations in section 4.3.3 and in figure 3.

$\varphi [^\circ]$	0	5	10	15	20	25	30	35	40
N_c	5.14	6.50	8.35	11.0	14.8	20.7	30.1	46.4	75.3
N_q	1	1.57	2.47	3.94	6.40	10.7	18.4	33.6	64.2
N_γ	0	0.45	1.22	2.65	5.39	10.9	30.2	48.7	109

4.3.3. Bearing capacity factors for conical penetration tests

For an undrained material without a surcharge q , the stress at the penetration tip adopts a simplified form to equation (2), depending essentially on cohesion c_0 , equivalent to yield stress τ_0 . When the penetration tip is pushed into the material, the surcharge of the soil weight is $\rho \cdot g \cdot d$, giving:

$$\sigma_f = N_c \tau_0 + \rho \cdot g \cdot d \quad (3)$$

The cohesion bearing capacity factor N_c for a conical penetration tip as used in this study is approximately 9 as found by Houlsby et al[184]. It considers adhesion between the penetration tip and concrete, as well as the heave exerted by the penetration tip. Houlsby also finds that the shape of the outermost characteristic, the volume in which shearing occurs, has approximately the shape of a cone with an apex angle of 90° extending from the penetration tip towards the surface, in a similar way as shown in figure 4.2. Adhesion was found to double the bearing capacity factor for a rough cone [186].

Using the bearing capacity factor, the penetration setup of this study is assessed. The penetration tip used has a cross-sectional area of $A_{pen} = 314mm^2$. Penetration tests are carried out up to a depth of 8cm, resulting in a surcharge of up to $\rho g d = 2300 \frac{kg}{m^3} 9.8 \frac{m}{s^2} 0.08m \approx 1800 Pa$. This surcharge may increase the penetration resistance by 0.6N for an undrained material ($N_q = 1$) and of 36.2N for a drained material with a friction angle 40° ($N_q = 64$).

In this study the soil weight resisting penetration is $\frac{1}{2} b \rho g = 0.01m 2300 \frac{kg}{m^3} 9.8 \frac{m}{s^2} \approx 225 Pa$. This does not affect penetration resistance in an

Continuous characterisation method for yield stress of fresh concrete at rest

undrained material ($N_\gamma = 0$), but increases the penetration resistance in a drained material with a friction angle of 40° ($N_\gamma = 100$) by 7.1N.

For digital fabrication the lowest yield stress of interest is $\tau_0 = 100Pa$. For undrained conditions ($N_c = 9$), the contribution of cohesion on penetration resistance is 0.28N, while surcharge contributes with 0.6N. If the yield stress is low, the penetration depth strongly affects the measured force. For cohesions larger than 1kPa (contribution to resistance 2.8N), the surcharge contributes to the penetration force by less than 20%, allowing to neglect the effect of penetration depth.

The transition to a frictional fluid with an internal friction angle of 40° is expected to occur at a cohesion of 100kPa for OPC mortars [170]. Considering this combination of highest friction angle and lowest cohesion, the cohesion ($N_c = 75$) contributes to the penetration resistance with a force of 2355N, while surcharge of 36.2N and the soil weight of 7.1N can be neglected.

We find that as long as the yield stress is larger than 1kPa, the penetration resistance is in all cases dominated by the cohesion in mortars. Only for cohesion values below 1kPa, should the effect of surcharge with penetration depth be considered. For slow penetration measurements, yield stress should in most cases increase to at least 1kPa, before any substantial penetration depth is reached for most mortars.

For the conical tip used here, the equivalent shear surface expected from the soil stability calculation is:

$$\frac{F_{pen}}{\tau_0} = N_c \cdot A_{pen} = 9 \cdot 314mm^2 = 2820mm^2 \quad (4)$$

Concerning the range of possible bearing capacity factors, using a kinematically possible failure surface, an upper limit of the bearing factor can be computed. For the conical penetration tip used in this study, a simple approximation of such a failure surface may be a conical shear surface with an apex angle of 90° starting from the cone tip (cf. figure 4.2). This gives a shear failure surface of $4050mm^2$ or equivalently $N_c=13$. The

Continuous characterisation method for yield stress of fresh concrete at rest

lower limit can be derived directly from the main stress difference applied two times in the material, giving $N_c=4$. Soil mechanical approaches contrast with currently documented approaches for yield stress scaling in concrete, where the contact surface is considered, giving in this case (993mm^2) a value $N_c = 3.2$ [164].

A common limitation of wedge stability models is the extension of failure surfaces into the surcharge material as penetration depth increases (figure 4.2 - bottom). For conical penetration tips, depth dependent bearing factors exist [184]. Alternatively, using again a kinematically possible failure surface, a depth dependency correction factor can be calculated, considering the shear surfaces in the dashed lines in figure 4.2 - bottom:

$$\delta = \frac{\min(\sqrt{2}dH, H^2 - R^2)}{H^2} + 1 \quad (5)$$

In this consideration the effect of depth dependency is expected to be most pronounced up to a depth of $H - R$ (as experimentally observed in figure 4.5), while most soil mechanical approaches expect a significant change up to a depth of $4R$ [184], [190], [191], twice the depth for this geometry.

Other effects to consider involve the effect of the cone apex angle α and cone bluntness. The apex angle should further be chosen in a range where the bearing capacity is not strongly affected by it, thus between 40° and 70° [186]. Blunt cones and the effect of heave increase penetration resistance to a minor extent (10% and 9% respectively).

Continuous characterisation method for yield stress of fresh concrete at rest

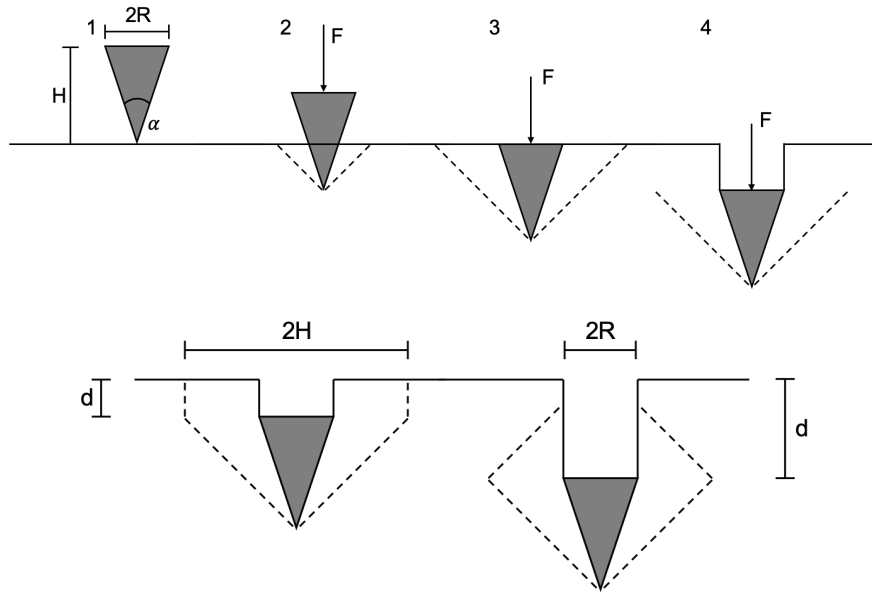


Figure 4.2: (top): Steps of the penetration test and approximation of the outermost characteristic with increasing penetration depth from 1 to 4, without depth correction from equation (5). (bottom): Kinematic shear failure surface used for the calculation of the depth dependency factor δ .

4.3.4. Penetration and compressive strength in fresh concrete

Previous studies have found an excellent linear agreement between compressive strength measurements in the experimental timeframe [170] up to a penetration stress of 520kPa and compressive stress of 190kPa, equivalent to approximately 110kPa yield stress. Using the documented experimental results from compressive strength and penetration tests, the bearing capacity factor of the used penetration tool can be calculated. The study fitted the measurements with exponential functions $\sigma_{pen} = \alpha_{pen} e^{\beta t}$ and $\sigma_{comp} = \alpha_{comp} e^{\beta t}$ with factors $\alpha_{pen} = 0.188kPa$, $\alpha_{comp} = 0.070kPa$ and found the same factor β for the time dependency $e^{\beta t}$. The ratio of normal stresses can be expressed in this specific case as the ratio of fitting factors:

$$\frac{\sigma_{pen}}{\sigma_{comp}} = \frac{\alpha_{pen}}{\alpha_{comp}} \quad (6)$$

To relate uniaxial compression to yield stress, the von Mises criterion is commonly used:

$$\sigma_{comp} = f_y = \sqrt{3} \tau_0 \quad (7)$$

Using this, we can calculate a conversion factor for yield stress from the penetration test (flat penetration tip with $2R = 18.8mm$):

$$\tau_0 [Pa] = \frac{\alpha_{comp}}{\alpha_{pen} \sqrt{3} \pi R^2} \left[\frac{Pa}{N} \right] \cdot F_{pen} [N] = 774 [Pa/N] \cdot F_{pen} [N] \quad (8)$$

The bearing capacity factor in this case can also be derived using the undrained penetration stress and neglecting penetration depth:

$$N_{c,Mettler} = \frac{\alpha_{pen} \sqrt{3}}{\alpha_{compr}} = 4.65$$

The theoretical value for an undrained soil with a flat penetration tip is 5.69 [186], but this is only applicable for a material with a strain-independent cohesion and for shallow penetration. Measurements as done in the study occurred below the surface, slightly increasing the effective bearing capacity factor, while the formed shear surface has to be considered as slightly pre-sheared at the time of measurement, slightly decreasing the bearing capacity factor. Given these uncertainties, the experimentally found factor is within 20% of the theoretical one.

With the onset of flow, shear may localize mainly on pre-damaged shear surfaces, where the lower dynamic yield stress applies (see figure 4.7 at large deformation). This may change the shear surface shape and the material state in the studied surface may be more damaged in some areas than others. This considered, the bearing capacity factor is expected to depend to some extent on the mortar studied, even if a priori saturated undrained conditions can be assumed.

Continuous characterisation method for yield stress of fresh concrete at rest

The relationship of compressive strength to penetration resistance can be used to assess the reliability to be expected for penetration tests as a measurement of yield stress or compressive strength. In general, for a frictional material and neglecting soil weight and penetration depth it writes as follows:

$$\frac{\sigma_{pen}}{\sigma_{comp}} = \frac{\sigma_f}{\sigma_{comp}} = \frac{N_c \cdot c_0}{2 c_0 \left(\tan \varphi + \frac{1}{\cos \varphi} \right)} = \frac{N_c^*}{\sqrt{3}} \quad (9)$$

It appears that the internal friction angle contributes more strongly to penetration resistance than compressive strength (compare Table 4.2). This means that with the transition from undrained to drained state, a linear relationship of penetration to compressive stress cannot be expected. For a given friction angle the ratio is however independent of cohesion. Thus, if the internal friction angle is known, penetration tests may still be used as a measure of cohesion and by extension of compressive strength. The equivalent bearing capacity factor N_c^* to be used in this case needs to consider the internal friction angle, as done in equation (9).

Table 4.2: Ratio of penetration stress to compressive stress for a 2D-wedge. Amplification factor α_{fr} and equivalent bearing capacity factor for a conical tip N_c^ with increasing internal friction angle. The amplification factor estimates the ratio change between penetration and compressive stress, compared to plastic material. The equivalent bearing capacity factor N_c^* is the factor estimating directly the relationship of penetration to compressive stress for a frictional material using a conical tip.*

$\varphi [^\circ]$	0	5	10	15	20	25	30	35	40
N_c	5.14	6.5	8.35	11.0	14.8	20.7	30.1	46.4	75.3
$\frac{\sigma_{pen}}{\sigma_{comp}}$	2.6	3.0	3.5	4.2	5.2	6.6	8.7	12.1	17.6
α_{fr}	1.0	1.2	1.4	1.6	2.0	2.6	3.4	4.7	6.8
N_c^*	9	10	12	15	18	23	30	42	61

$$N_c^* = \alpha_{fr} \cdot N_c(\varphi = 0), \text{ with } \alpha_{fr} = \frac{\sigma_{pen} \sigma_{comp}(\varphi=0)}{\sigma_{comp} \sigma_{pen}(\varphi=0)} \quad (10)$$

Given the difficulty to measure internal friction angles especially in the transition phase from plastic to frictional behaviour as hydration progresses, the penetration

resistance may be difficult to relate to yield stress in the transition zone. Thus, the penetration test seems most suited for undrained conditions. An overview of the expected validity range when neglecting surcharge and soil weight and considering plastic material is shown in figure 4.3 compared to the effective conditions.

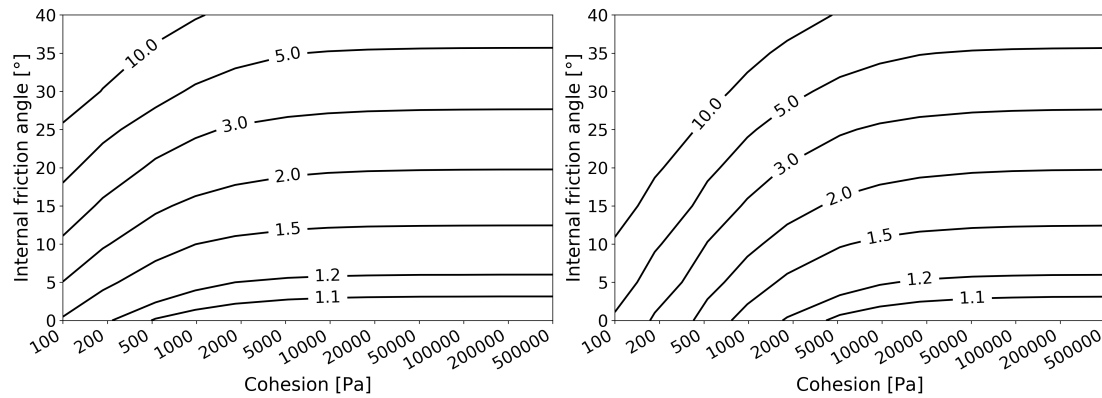


Figure 4.3: Estimation of ratio of penetration stress and compressive stress, normalized with the expected ratio with a plastic material with high cohesion, giving the expected trueness of penetration tests using the plastic material assumption. (left): tip in 1cm depth, (right): tip in 8cm depth. For very low cohesion between 100-500Pa, penetration test overestimate yield stress if surcharge is not considered. For frictional materials penetration tests strongly overestimate shear strength, more drastically for high internal friction angle.

4.4. Discontinuous and continuous methods on cement pastes

4.4.1. Fast penetration

In figure 4.4 the penetration forces of a conical penetration tip pushed into a cement paste placed in cylindrical containers of different diameters (height 12cm) are shown for pastes of the same age. The measurement is started when the tip touches the cement paste surface and is finished once the conical needle is fully inserted after a displacement of 30mm (steps 1-3 from figure 4.2). In this case, the penetration force scales with the square of penetration depth and linearly with the cross-sectional area. The measured penetration stress thus remains constant throughout the measurement. The cylinder diameter has an effect on the measured force. Especially for sample container sizes smaller than 7cm in diameter in this case, the measured penetration force is substantially smaller than for large containers. In this range the outermost characteristic of the sheared zone is close to the container wall, involving an increasing risk of wall slip. The penetration force appears to increase with the surface area of the interface of the container with the cement paste.

In figure 4.5 the penetration force of a fully submerged conical penetration tip for fast penetration is shown as it is further pushed into the sample container (steps 3-4 from figure 4.2). In the first centimeters the penetration force increases with penetration depth. As the tip moves deeper, the penetration force reaches a plateau. This trend is measured for all cement pastes independently of their age. Furthermore, the penetration force increases exponentially with material age. The increase of the force increase with depth is the same for all measurements, indicating that all measurements capture the same physical phenomenon with respect to depth dependency.

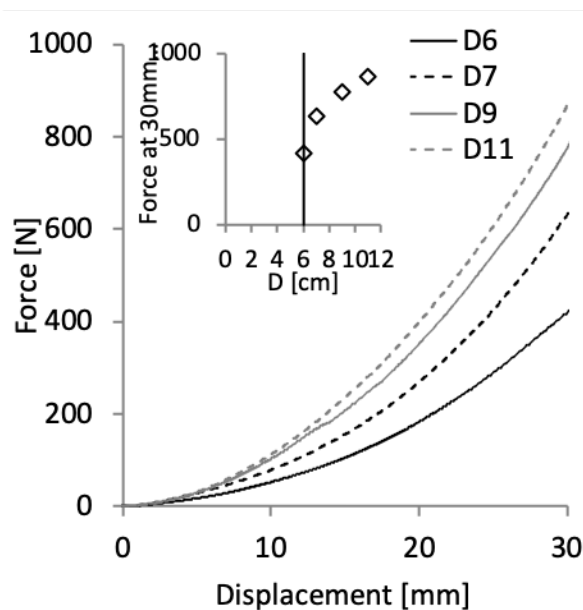


Figure 4.4: Fast penetration. Dependence of depth and container geometry for not fully immersed penetration tip (steps 1-3). Penetration force increases with the square of penetration depth. Inner figure: Force at end of measurement depending on the sample container diameter. The extent of the outermost characteristic of the shear zone is indicated as a line. The container diameter needs to be substantially larger than the outermost characteristic.

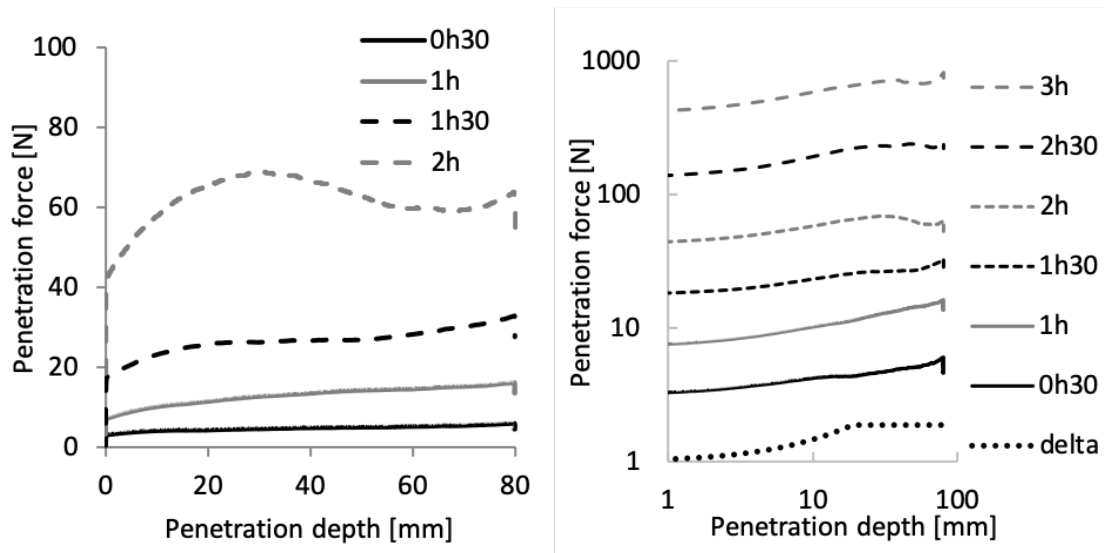


Figure 4.5: Fast penetration for the same geometry at different times and starting from a fully submerged penetration tip (steps 3-4). (left) lin-lin, (right) log-log. The penetration force increases with the age of the material and with the depth up to a depth of 20-30mm. The depth dependency between 0 and 20mm depth follows the same characteristic between all measurements and can be approximated using the shear failure surface introduced in equation (3).

For single point measurements, the experimental configuration used in figure 4.4 appears to be adequate, as the measured stress scales as expected with the cross-sectional area. However, such a configuration is problematic for continuous measurements with an increasing yield stress as initially both the contact surface and yield stress are lowest, which reduces the sensitivity of this test.

As for the relation of force to container size, it cannot be directly accounted for by analytical approaches and rather appears to be associated with wall slip on the container wall. Wall slip on the interface between the container and the cement paste would result in a similar trend, where force increases with the container diameter. The very low penetration force for the smallest container, which has the same size as the asserted outer characteristic of the sheared zone discussed in the previous section seem to confirm this. Thus wall-slip may be more critical for materials with a pronounced tendency of forming a lubrication layer, such as mortars suitable for pumping [137]. From a practical perspective, a minimum container diameter is required and a solution to counteract difficulties of wall-slip may be the roughening of the interface layer in order to ensure that yield stress is reached on this interface or the smoothing of it in order to bring the local stress to zero. In this study, subsequent measurements have been carried out with

container diameter 9cm, and containers with roughened surfaces are only used occasionally for mortars.

For single point measurements at larger depths as shown in figure 4.5, the force increase with depth follows a common characteristic behaviour. The ratio of the maximum force measured to the force obtained at full insertion is generally less than 2. This is substantially less than in the phase of insertion, indicating that this experimental measuring phase is more adequate as a characterization method. In addition, and to further improve characterization quality, the depth dependency can be well captured in a single factor (equation (5)) by considering the size of the shear failure zone forming during penetration (see figure 4.2 - bottom). This factor is used to correct for the depth dependency in both slow and fast penetration tests in mortars and for cement pastes in figure 4.8 (right).

Considering the scaling with contact surface, the increase with resting time and previous studies by Lootens et al. [164] and Mettler et al. [170], the measurement is capturing yield stress. Considering again the scaling with penetration tip cross-section area and the depth dependency, the measurements from figures 4.4 and 4.5 are also in agreement with soil mechanics.

4.4.2.Slow penetration

In figure 4.6, the penetration force of a fully submerged conical tip is shown as it is further pushed into the sample at a rate of 20mm/h. The force evolution is approximately exponential from the measurement start. A good agreement between repetitions of the experiment in the force range 1N-1000N is obtained. The largest difference between repetitions is 30%. Overall, the penetration force measured with the flat tip geometry is similar to the one of the conical tip.

Continuous characterisation method for yield stress of fresh concrete at rest

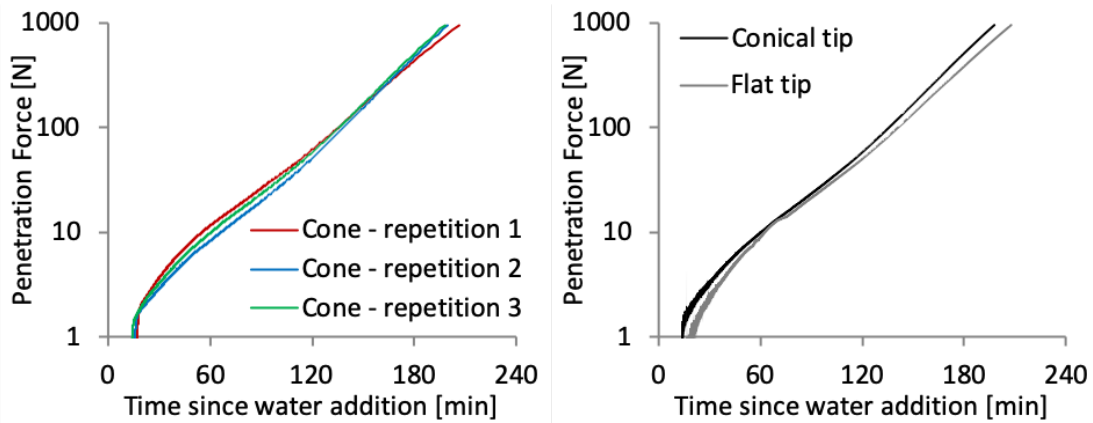


Figure 4.6: Slow penetration (left) Repetitions of the same composition using a conical tip. (right) Comparison of conical and flat tip. Exponential increase of penetration force with time.

The exponential increase of force and yield stress observed in all measurements is in agreement with the ongoing formation of hydration products after the onset of hydration and the resulting strength increase expected in the acceleration phase of hydration [18], [123].

A difference between flat and conical tip can be noted (figure 4.6 - right). Just upon contact of the flat tip with the material, the flat tip measures a force substantially lower than the conical one. It can be considered that, in the case of the conical tip, the material surrounding the tip has previously been deformed and the current failure surface is already deformed up to flow initialization, while the flat tip measures a lower yield stress, before the onset of flow. As evidenced in vane measurements (figure 4.7), the highest shear stress occurs after some displacement. Thus, before onset of flow, a partially destructive deformation is applied, but at a lower stress level. As such, it is expected that a flat tip penetrometer requires some displacement until the transition state is overcome.

Using the soil mechanical approach, the force ratio between flat and conical tip should be $5.69/9=0.63$ based on the theoretical bearing capacity factor. The measured ratio is: 0.76.

4.4.3. Complementary methods

Shear stresses measured in figure 4.7 by vane rheometry are divided into two phases of linear increase. The first is characterized by high stiffness up to 0.3-0.5x of the maximum shear stress, giving a vertical segment in Figure 4.7. It is followed by a second linear increase to the maximum shear stress (yield stress). Beyond the maximum shear stress, a residual resistance is measured. So, the cement paste cannot be described by a simple linear elastic behaviour. The shear stress for onset of deformation, the yield stress and the residual shear stress increase with material age. The critical deformation at which the yield stress is reached, decreases in the first minutes at rest and then appears constant beyond (from 30 minutes on based on figure 4.7).

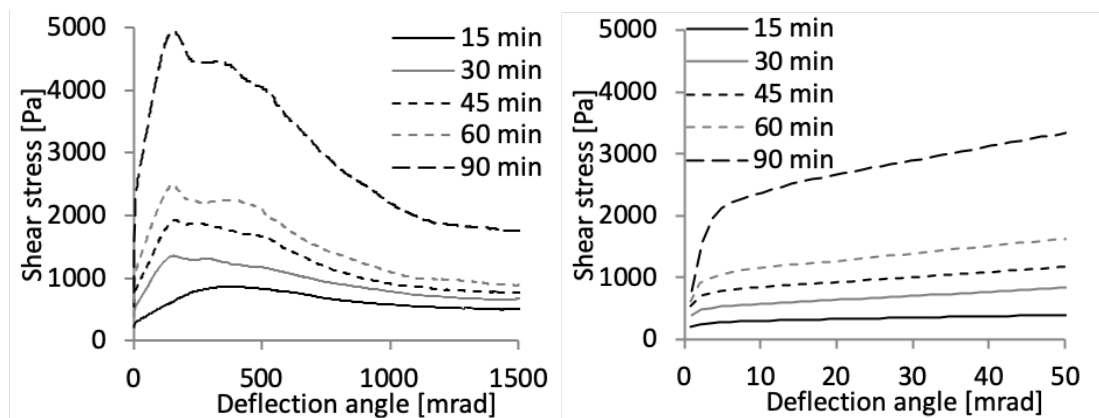


Figure 4.7: (left) Vane measurements at constant strain rate for cement pastes resting for increasing durations before measurement. (right) Zoomed in section of low deformation range.

Measurements of uniaxial compression show a similar exponential increase of compressive strength with material age as those obtained with the vane test (see figure 4.8). With respect to the yield stress conversion of compression force, the contribution of self-weight to compressive stress is smaller than 2% in the weakest samples and is neglected. Compression measurements are acquired at a later age and consequently at larger strengths than for the vane measurements. The fact that they display similar kinetics at different ages, suggests both that the mechanism does not change and that both tests are properly capturing this single strength increase mechanism.

From the vane experiments (figure 4.7) it is evident that a partially destructive deformation is applied before the yield stress is reached, thus some deformation until yield stress is measured occurs, with a decrease of stiffness that captures partial structural breakdown. This characteristic strain dependency should also exist for penetration tests [170].

Owing to the existence of these 3 types of characteristic stress states measured by vane rheometry, it appears that assuming yield stress as the only characteristic stress may limit the validity of analytical approaches to penetration tests. In such experiments, the deformation history (related to shear strain) in the sheared zone is unknown and likely a mix of the characteristic stress states. Furthermore, the shape of the sheared zone may be affected by this. This considered, geo-mechanical approaches describing penetration should underestimate the yield stress, when compared to vane or compressive strength measurements, because shear stresses in penetration tests are an average value of the shear history in the shear zone.

4.4.4. Yield stress from experimental methods

In figure 4.8 (left), a summary of the previous experiments is given with measurements displayed with respect to time since water addition. On the left vertical axis, the penetration force is shown, while on the right the yield stress is shown for uniaxial compression and vane measurements. First, we note the excellent agreement between fast (at a depth of 1mm) and slow penetration tests regardless of hydration time. Secondly, it can be seen that the vane and uniaxial compressive strength measurements complement each other perfectly. Covering respectively the lower and the upper yield stress range, they display a single exponential trend, which additionally matches the one obtained from the penetration tests. This shows that, for the studied cement paste, the penetration test scales linearly with yield stress.

Continuous characterisation method for yield stress of fresh concrete at rest

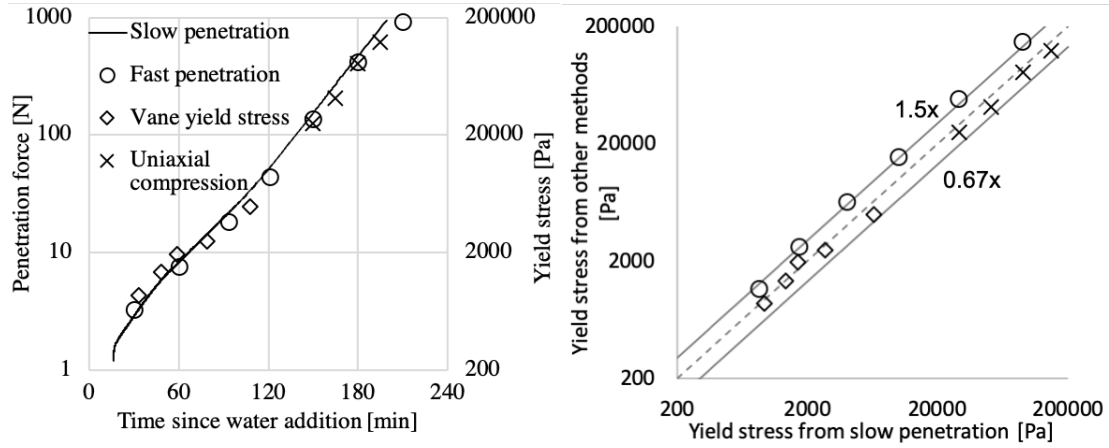


Figure 4.8: (left) Measurements on cement paste, showing penetration force as a function of time and yield stress calculated from vane test and uniaxial compression, with an excellent agreement between methods. (right) Master curve showing, yield stress from all methods compared to the slow penetration test and considering the depth dependency from equation (5).

Using the ratio of calculated yield stress to penetration force of approximately 200 Pa/N (figure 4.8 - left), it is both possible to calculate the bearing capacity factor according to geomechanics and to calculate the size of an associated shear surface. The area of the shear surface is simply the inverse of that ratio and is approximately 5000 mm^2 . As to the bearing capacity factor, it is obtained by (using equation (4)):

$$N_c = \frac{\sigma_f}{c} = \frac{F_{pen}}{A_{tip} \cdot \tau_0} = \frac{1000N}{314mm^2 \cdot 0.2MPa} = 15.9$$

The experimentally measured value is significantly larger than the theoretical value ($N_c = 9$). For the fast penetration tests, this discrepancy could be linked to the high loading rate, while for the slow penetration tests, it could come from not accounting for the depth dependence of the force or induced by the container walls. To check this hypothesis, we apply the depth dependence determined for the fast penetration test to the slow penetration test (equation (5)). Doing this and using the theoretical bearing capacity factor of $N_c = 9$, gives an excellent quantitative agreement between vane, uniaxial compression tests and slow penetration tests. This can be seen from the direct proportionality shown in Figure 4.8 (right). The correlation is also good with the fast penetration test, but yield stresses are overestimated by about 50% (slope of 1.5 in figure 4.8 - right).

Continuous characterisation method for yield stress of fresh concrete at rest

Aside from having to use a pre-factor to account for fast penetration results, it can be stated that continuous and discontinuous penetration, as well as vane and compressive strength all coincide in this measurement range of 1-200kPa yield stress. It is concluded that for cement pastes with similar initial yield stress to the one of this study, penetration experiments are adequate to derive yield stress, either pointwise or continuously. Slow penetration measurements seem to be repeatable from as low as 200Pa, however soil mechanics mandates that such low yield stress measurements should only be acquired at low penetration depth.

Whether depth dependency is accounted for ($N_c = 9$) or is neglected ($N_c = 15.9$), the bearing capacity factor is significantly higher than considering a shear surface on the penetration tip ($N_c = 3.2$). This indicates that the yield stress is measured inside the material volume (along a surface similar to the one asserted in figure 4.2). It is an important consideration to avoid the bias of wall slip in mortars as it allows measurement in a homogenous material section. The existence of such a shear zone is required when a mass flow balance is considered, as the material displaced by the penetration tip can only be displaced towards the free surface and a zone for this to occur is necessary. With the measurement likely occurring in the material volume, the surface of interest is linked to the tip and moves into the sample at constant speed. So, the shear surface should also move into the sample with the penetration tip (see figure 4.2, right). This contrasts with other methods such as compression or vane tests, in which the shear surface is static. Thus, conical penetration tips appear to be a good compromise for continuous penetration tests, measuring yield stress. However, the size of the shear zone should increase with penetration depth (equation (5)) as it should extend into the material above the conical sheared zone, something that fast penetration tests (figure 4.5) corroborate up to a penetration depth of 20 mm.

4.5. Continuous penetration in mortars

In figure 9 (left), the change of penetration force is shown for mortars of different aggregate content (M:20,40,48 in volumetric percent) and different superplasticizer dosage (S:0.0,0.6,1.0 in percent of cement weight) during the first 3 hours after water addition. These mortars are very different, M20 has an aggregate content in the dilute regime, implying that its flow is dominated by the cement paste, while M48 is close to the percolation limit [172] of the used sand (0-2mm crushed limestone). With increasing sand content, the onset of exponential yield stress increase occurs at earlier times. With increasing superplasticizer dosage, this increase occurs later and at a slower rate, which is in good agreement with literature as superplasticizers are well known to retard the onset of hydration and to reduce yield stress at early age [111], [192], [193]. Similarly, the addition of aggregates increases yield stress, as is qualitatively measured here, both for the initial penetration force as for its evolution. [172].

Furthermore, the differences in fluidity and time of onset appear clearly in figure 4.9 (right) where a log-log scale is used. This helps to better differentiate initial yield stresses, the ranking of which matches the qualitative differences observed when placing these different mortars. M48_S1.0 was self-compacting, M20_S0.0 and M40_S0.6 flowing easily, while M40_S0.0 and M48_S0.6 required compaction. The log-log representation additionally highlights a two-step mechanism, involving a slow evolution until approximately the time of 60-90 minutes, followed by exponential increase. This can be associated with the onset of hydration and a rate increasing growth of hydrates [194].

Continuous characterisation method for yield stress of fresh concrete at rest

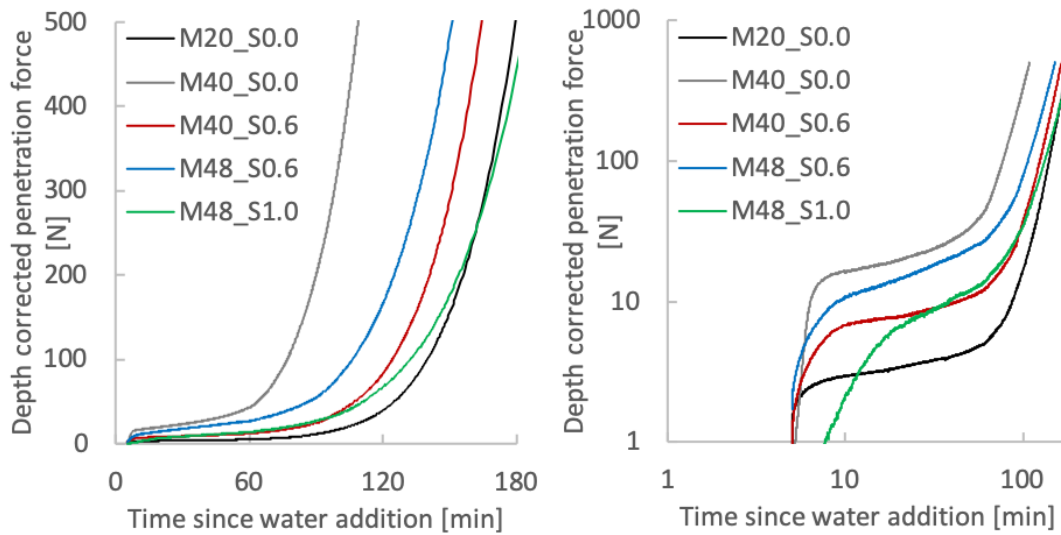


Figure 4.9: Slow penetration evolution for different mortars. (left) lin-lin, (right) log-log

In figure 4.10, the evolution of yield stress calculated from uniaxial compression experiments is shown for the different mortars as a function of time since placing. In general, the same ranking of strength evolution as in slow penetration measurements is observed. The fastest yield stress increase occurring for high solid content without superplasticizer and the slowest for mortars with high superplasticizer dosage and low aggregate solid content. In the case of mortar with high superplasticizer content and high sand content, the measured yield stress remains substantially lower than the value measured with slow penetration and is excluded in the following analysis.

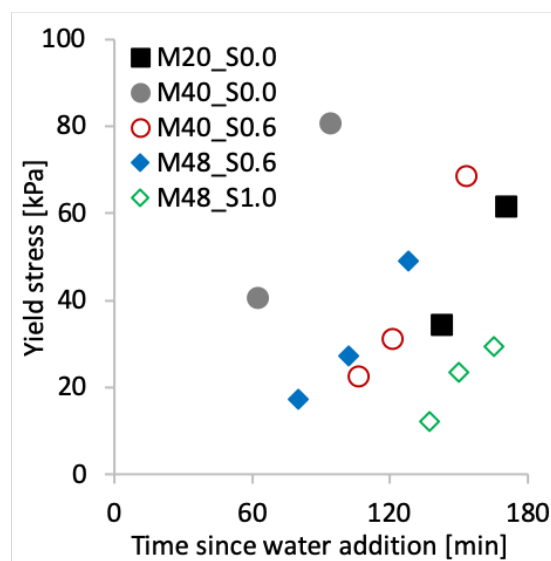


Figure 4.10: Yield stress from compressive strength measurements on mortars from figure 4.9.

The data in figures 4.9 and 4.10 provides the means to compare, now for mortars, the yield stress measurements from different discrete methods to the one obtained from slow penetration. As shown in Figure 4.11, discrete measurements generally give lower values. Nevertheless, there is a good correlation even if the studied mortars are broadly different. The correlation is slightly improved if the best fit bearing capacity factor from table 4.3 (calculated by fitting slow penetration and compression tests) is used. It brings all measurements into agreement within a range of 0.5x-2x of the theoretically predicted value. We also note that using containers with rough surface, appears to bring no substantial improvement (comparing fast penetration and fast penetration with rough container) and that slow penetration can be brought into general agreement with the penetration setup studied by Mettler et al. The failure shape of compressive strength samples further indicates that all measurements remain in the plastic regime.

Given the minor improvement of accuracy by considering the best fit bearing capacity factor, using the theoretical bearing capacity factor can be considered good enough in most applications, as even without fitting, most measurements fall within a range of 2x of the prediction. In this respect, despite the lack of substantial improvement by fitting with compression tests, compression tests are fundamentally important on theoretical grounds for the distinction of plastic and frictional behaviour as this transition significantly affects penetration resistance.

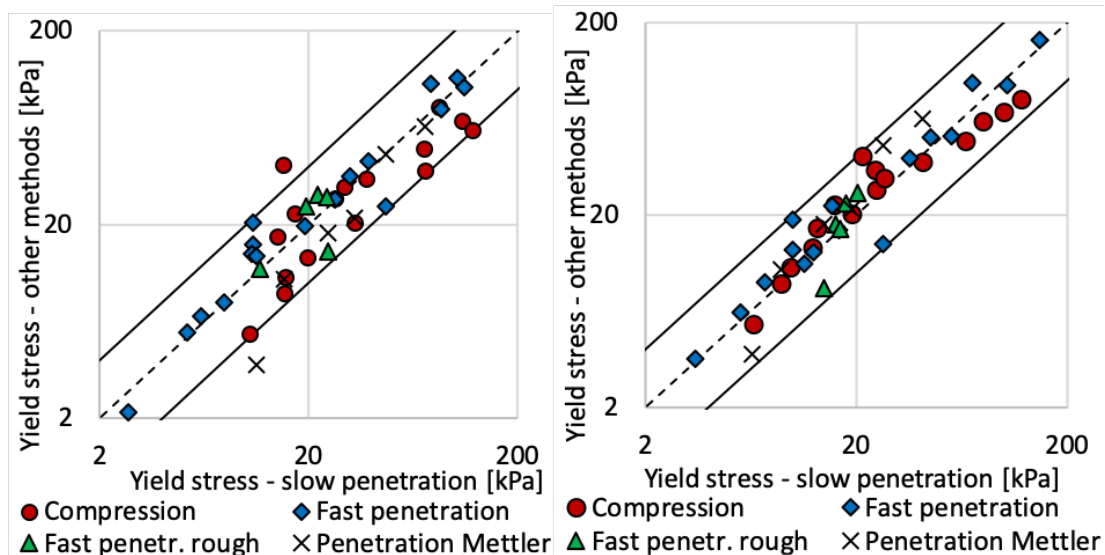


Figure 4.11: Yield stress calculated from slow penetration tests and compared to discrete measurements conducted at the same time for mortars. (left) using the theoretical bearing capacity $N_c^* = 9$. (right) using the best fit bearing capacity factor for each mortar. The lines mark the range of 0.5-2x of the expected values.

The measurements on mortars also show that slow penetration tests measure a higher yield stress than compression tests in all cases. This is something already observed to a lesser extent on cement paste and can be a consequence of demoulding and sample transportation, as this mechanical action can damage the structure built-up at rest, something that may not be fully recovered before the test is started. Especially for samples involving high superplasticizer content, the recovery of static yield stress may take a long time, as seen in figure 4.9 (right) for M48_S1.0.

Table 4.3: Best fit N_C^ for mortars with different aggregate volume fraction ϕ_{Aggr} and superplasticizer (SP) content. Apart from M48_S1.0, the best fit N_C^* is within the range of approximately 1.6x of the theoretical value.*

Composition	ϕ_{Aggr}	SP [%]	Best fit N_C^*
M20_S0.0	20%	0%	13.8
M40_S0.0	40%	0%	6.4
M40_S0.6	40%	0.6%	9.8
M48_S0.6	48%	0.6%	9.7
M48_S1.0	48%	1.0%	23.2

4.6. Discussion

4.6.1. Slow penetration test for yield stress characterisation

The slow penetration test is an easy to use experimental setup that measures structural build-up in pastes and mortars over time on a single sample. As such, this method can provide real-time measurements of yield stress on a material at rest as is the case in digital fabrication applications especially in layered extrusion and slip-forming, where concrete strength build-up at rest is used technologically to support the structure as it is produced[19]. Its measuring range of 1-200kPa is ideal for capturing the yield stress range that is required for such self-support. This measuring method can predict failure, when used during fabrication, acting as a quality control method for the placed concrete, or it can inform the process, giving feedback on how fast the process can build, or how much set accelerator is needed.

As such, knowing that penetration force and yield stress scale linearly, predictably in agreement with soil-mechanical concepts and without a substantial dependency of the mortar formulation, gives confidence in the yield stress calculated from the measurement. This is particularly useful when dealing with variation caused by changes of raw materials, something that digital fabrication processes are rather sensitive to.

In this respect, the predictions of soil-mechanics are particularly useful as they predict the measuring range and clearly show the dominance of cohesion within the entire measuring range as well as the contribution of minor effects such as surcharge, soil-weight, heave, cone bluntness and can be applied on other penetration setups. The soil-mechanical approach also shows that the measurement is carried out essentially away from the penetration tip surface in a homogenous sample section that is constantly reaching previously undeformed material, allowing continuous measurements without wall slip and not on a single shear surface. Beyond this, for fully immersed penetration tips, the depth dependency can also be approximated with soil-mechanical concepts and the relationship of penetration to compression stress can be predicted for materials beyond the range of plastic behaviour. From the significant increase of penetration resistance at the transition to frictional behaviour, it is shown that comparative uniaxial compression tests should be carried out for all unknown mortar matrices.

4.6.2. Measuring recommendations

Measuring conditions:

For measurements in conjunction with a building process, either for development or process control, the sample is required to be measured off-line. Initial yield stress and hydration kinetics need to be equivalent to the material from the process, meaning that the conditioning should be as close as possible to the process conditions (temperature, resting times, shear rate history, etc.). Plastic mortars are sensitive to mechanical shock and compression samples can be damaged when demoulded, something that needs time to recover. Also, the time of sample casting can strongly affect measurements. Thus, material samples should be placed into the measurement container at a similar time as in the building process, where they are intended to be used.

Continuous characterisation method for yield stress of fresh concrete at rest

Depending on composition, the measurement range in which slow penetration scales with compressive strength can vary. Comparative compressive strength measurements, validating the measurement range, are essential for compositions, without previous experimental evidence.

Size of sample container and penetration tip

The outermost characteristic defines the minimum container diameter. For conical tips, assuming an apex angle of 90° , the outermost characteristic has a radius equivalent to the penetration tip height H . The minimum container diameter for the outermost characteristic to form regularly is thus $2H$. This minimum diameter is also the minimum size for a container with a rough surface. However, a container diameter of at least $3H$ is warranted to reduce the risk of wall slip on the container walls. For homogeneous measuring conditions the penetration tip diameter should be at least $5x$ the size of largest aggregate.

Shape of penetration tip

The penetration tip geometry should ensure failure in homogenous material and for the shear failure zone to consistently change with penetration depth. In this way measurement occurs over the entire depth in previously resting zones. This study finds that this can be achieved with conical tips with an apex angle α smaller than 90° .

In other penetration geometries, penetration tips should not have surfaces parallel to penetration (pile shape) in order to prevent wall slip. Penetration tips for continuous measurements should also not be flat. Upon penetration of a flat tip, some displacement is required for the failure regime to be established, involving transient regimes.

Yield stress calculation

Yield stress can be calculated from penetration force measurements by using equation (4), using the bearing capacity factor N_c for a conical tip and dividing the found yield stress by the correction factor from equation (5). To consider surcharge for deeply immersed penetration tips, equation (3) can be used as an alternative to equation (4).

4.6.3. Checklist for measurements

To further facilitate the use of slow penetration tests, we provide here a short checklist of important aspects to consider:

Sample:

- Sample does not bleed or sediment
- Sample is well compacted and container is completely filled
- Aggregate solid content causes no frictional contacts

Setup:

- Sample container is large enough (Container radius is at least 1.5x penetration tip length)
- Penetration tip is large enough for aggregates (diameter 5 times largest grain)

Measurement:

- Full submersion of penetration tip at start
- Measuring range is verified for combination of initial fluidity and solid fraction
- Measuring range is verified for the main hydration product forming

4.6.4. Application to mortars used for digital fabrication

To show the potential of the slow penetration test for applications, mortars of broadly different compositions are measured (see figure 4.12 and table 4.4), involving different paste matrixes, water content, initial yield stress and targeted application. The compositions targeted for layered extrusion and slip-forming are mortars prepared with blended cements. They contain several different admixture types and have their onset accelerated. Both of these mixtures show the earliest increase of penetration force among the tested materials (compared to figure 4.9), the increase being immediate and approximately linear. An SCC mortar containing a strongly retarding superplasticizer designed for transport concrete, shows only minor penetration force increase in the measuring timeframe. Furthermore, in table 4.4 additional mortars for slip-forming and layered extrusion not measured in this study are listed. Apart from the excluded M48_S1.0, only the mortar for layered extrusion activated with an ettringite forming

activator [173] showed brittle failure and a significantly increased N_c^* , while all other mortars show a slightly elevated bearing capacity factor.

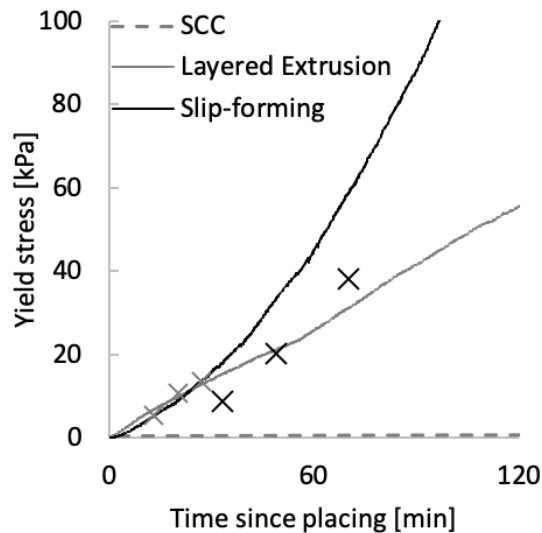


Figure 4.12: Yield stress from penetration and compressive strength measured on mortars as used for layered extrusion, slip-forming and casting (SCC).

Table 4.4: Best fit N_c^* for a large range of mortars with different aggregate volume fraction ϕ_{Aggr} , superplasticizer (SP) content, accelerated mortars and the failure type of the compressive strength test.

Composition	ϕ_{Aggr}	SP [%]	Best fit N_c^*
Slip-forming (fig 4.12)	52%	0.8%	24
Layered Extrusion (fig 4.12)	48%	1.0%	14.4
UHPFRC for slip-forming[195]	23%	3.65%	14.6
Mortar for slip-forming[195]	52%	0.8%	12.2
Mortar for layered extrusion[173]	48%	1.0%	35

4.6.5. Effect of hydration

For any unknown mortar matrix, preliminary measurements comparing to compressive strength should be conducted to verify the bearing capacity factor and define the yield stress from which penetration deviates from compressive stress due to increasing internal friction angle.

The origin of this transition from plastic to frictional material is from a fundamental perspective related to the saturation of microstructure with water. The

saturation with water itself depends on the degree of hydration in the mortar as water is consumed with the formation of hydration products. The microstructure in mortars can be broadly different as can be the hydration products forming. In general, the transition from plastic to frictional material should occur when the percolation packing fraction is reached [108]. Above this solid content, close particle to particle contacts occur.

Hydration products modify the particle size distribution and can have different compositions. In Portland cement at early age mainly calcium silicate hydrates, portlandite and ettringite are expected to form [194]. Early age C-S-H is considered to grow at pseudo-contact points between grains [50], but this may change in presence of superplasticizers [55], [196], [197]. Ettringite however is understood to grow in the pore solution. With C-S-H growing at contact points, its contribution to cohesion is expected to be stronger than the one of ettringite, which is expected to mostly fill the microstructure. Thus, the transition is expected to occur at lower cohesion.

Considering the complexity involved in early age hydration steps and hydration products, a simplified approach may involve pore pressure. Indeed, the onset of negative pore pressure from a microstructural perspective may be understood as the state in which positive normal pressure can be applied on the particle network and this transition is associated with direct particle to particle contacts. The occurrence of negative pore pressure may be understood as a result of hydration, in which the microstructure cannot freely shrink anymore when hydration products occupying less space than the clinker and water they are formed from. The advantage of this approach is the ease of measurement and interpretation [138], [198] and the independence from complex microstructural considerations. Pore pressure measurements should be an ideal complementary measurement to define the upper limit for penetration tests on plastic materials.

4.7. Conclusion

The studied slow penetration test is an easy to use experimental setup that measures the structural build-up of cement pastes and mortars over time on a single sample. The penetration force and yield stress are experimentally found to scale linearly in the range of 1-200kPa in cement pastes and in the range of 6-200kPa in mortars, the range of greatest interest for structural build-up of concrete in digital fabrication during production.

By modelling penetration as a geo-mechanical soil stability problem, it is possible to predict the relationship of penetration force to yield stress for plastic materials. Penetration tests in this approach provide cohesion measurements from a yield stress of 1kPa upwards or from 100Pa at shallow depth, but are limited to early age strength range with plastic behaviour.

Penetration tests with a conical tool moving at slow rate are adequate to measure the structural build-up of both cement pastes and mortars over time on a single sample. The shear surface on which yield stress is measured, appears to have a homogenous microstructure and corresponds to a surface that is constantly moving with the penetration tip. This theoretical finding is substantiated by the good agreement of all characterization methods with the slow penetration measurements.

In materials with interactions dominated by frictional interactions, the penetration force increases faster than compressive strength. The ratio between both depends on internal friction angle, which cannot be directly determined in a penetration test. Measurements on cement pastes explain the effects of setup parameters and give a basis for recommendations for testing. Measurements on broadly different mortar compositions indicate some need for verification of the bearing capacity factor for each type of mortar used. For many mortars it is found that the theoretically derived bearing capacity factor is within 2x the measured value, a precision that may be close enough in many cases. It has to be underlined, that comparative verification of bearing capacity factors has to occur for any compositions not covered in this study, this being namely products forming large quantities of hydrates other than calcium silicate hydrates, as well as for measurements beyond the yield stress range studied here.

Chapter 5 Distinguishing flocculation and hydration effects on structuration

This chapter studies the effect of flocculation and hydration on the structural build-up in cement pastes at rest, or in simpler terms how strength evolves in cement pastes that are not deformed. It makes the link between the mechanical requirements of building processes in chapter 3 and the control of hydration in chapter 6 by studying a cement paste model system. In this system the time scales of the fundamental mechanisms of colloidal interactions and growth of hydration products leading to structural build-up can be separated.

- Section 5.3.2

ICP measurements were performed by Sara Mantellato, based on samples prepared by the author.

- Section: 5.3.4

Characterisations of the model material for flocculation, specifically the adsorption of sucrose on portlandite and competitive adsorption have previously been published in similar form in a conference paper [79]:

Lex Reiter, Marta Palacios, Timothy Wangler, Robert J. Flatt, “Putting concrete to sleep and waking it up with chemical admixtures“, Canmet, 2015.

Measurements of adsorption isotherm and calcium increase have been carried out by Marta Palacios. Calorimetry measurements were conducted by the author, as was the writing of the paper, apart from adsorption isotherms.

- Other parts of section 5.3.

The characterisation of the model system is part of a journal paper in preparation on the mechanism of sucrose retardation.

- Sections 5.4.1 and 5.5. have previously been published in a non-peer reviewed conference paper:

Lex Reiter, Timothy Wangler, Nicolas Roussel, Robert J Flatt., “Distinguishing flocculation and hydration effects on the thixotropy of cement pastes”, SCC2016, 2016 Measurements and paper writing were entirely done by the author under the guidance of Timothy Wangler, Nicolas Roussel, Robert J. Flatt.

Abstract

The structural build-up of cementitious materials at rest is of importance for multiple building processes in digital fabrication. Its partially reversible nature is however not fully understood. Using sucrose as a set retarder, the main mechanisms underlying structuration, namely colloidal interactions building a flocculated network are studied separately from the growth of hydration products.

Apart from causing retardation, sucrose is found to not significantly modify the pore solution, the microstructure and the apparent viscosity throughout the induction period. In this period structural build-up tends towards a slow asymptotic increase of a flocculated structure independently of sucrose dosage, but depending on the solid content/number of particle-to-particle contacts. Increasing the interstitial viscosity by introducing non-adsorbing polyethylene glycol (PEG) does not modify structuration showing that build-up at rest is not associated with large displacements of particles but rather localised ones.

At long resting times, the structuration rate is dominated by the formation of hydration products showing a build-up at rest that is directly proportional to the amount of hydrates formed since the last deformation. The amount of hydration products formed before the last deformation event has a minor effect on the rate of structuration, showing that growth at pseudo-contact points is the main contributor to structural build-up. For building processes requiring similar kinetics for each placed layer as well as fast continuous structuration, this shows that structural build-up should be controlled through hydration.

The results on working mechanisms of sucrose indicate that interactions with aluminates play a minor role in sucrose retardation as early ettringite formation is unchanged. A steady increase of pH in pore solution is observed, which is driving sucrose dissociation and its following adsorption. Furthermore, the maximum saturation degree with respect to portlandite is found to be relatively independent of sucrose dosage, excluding an inhibition of portlandite formation. The results rather suggest a slower C_3S dissolution by direct inhibition and/or a slowing down of nucleation and/or growth of C-S-H.

5.1.Introduction

In the context of the development of new processing techniques relying on early age strength build-up, understanding of the origin of strength gain is of essential importance for its tailoring [19]. For such processes concrete is pumped or otherwise placed, involving a shearing event, followed by a time of stays during which no further deformations are applied.

In colloidal suspensions, the rheological behavior during the early period of rest is controlled by 3 basic types of forces, these being Brownian, colloidal (electrostatic and van der Waals) and hydrodynamic forces [199], [200]. A flocculated structure can develop as a consequence of these interactions involving an attractive force between cement particles. This is believed to occur together with the growth of hydration products taking place in part on the surface of cement grains [194], [201], including at the contact zones between particles, which strengthens the colloidal network [50]. All of this is often referred to as thixotropy, when the material is subjected to flow [202] and referred to as structural build-up when it occurs at rest.

Measurements involving small amplitude oscillatory strain on cement pastes are able to capture this type of structural build-up as demonstrated by Nachbaur et al and by Schultz and Struble [107], [128]. The measurements of Nachbaur et al were performed on samples kept at rest for multiple hours. They found a two-step process at early age with a first structure forming within minutes, followed by a plateau of slow evolution. In particular, they found a small critical strain of the order of 0.03%, associated with physical interparticle forces. In their study a direct link to an underlying process could however not be concluded. More recently, progress on such oscillation methods notably by Mostafa et al [121], [203] as well as the evolution of general understanding [50] has allowed to substantiate these findings. Mostafa et al found a strong relationship between the number of contact points, the nucleation rate and consequently the rigidification rate. This is in line with previous findings for yield stress and its evolution [119], [123], however a lack of separation of flocculation and hydration processes remains.

Distinguishing flocculation and hydration effects on structuration

Typically, the distinction between the contributions of flocculation and hydration to the structuration of cementitious materials is difficult to measure with simple flow experiments, as both phenomena have a comparable impact on the structuration rate in the timeframe of such experiments. Using sucrose as a set retarder [204], [205], the main mechanisms underlying structuration, namely flocculation and hydration are separated, studying the network of colloidal interactions building a flocculated network separately from the growth of hydration products. In the following, the structuration in a resting cement paste is followed using strain oscillation rheometry. Strains are kept well below the critical strain (above which partial damaging occurs) in order to follow the structuration of the studied cement pastes without damaging them.

The rheometric measuring protocol should for this purpose follow the main processing steps, involving a pre-shearing event of constant rotation rate, followed by non-destructive probing at very low oscillation strain. More potent methods for structural breakdown involving large strain oscillation exist to ensure full separation of flocs at the measuring start [206], [207]. However perfect structural breakdown before the measurement start is not specifically targeted here, but rather a situation similar to flow in a pumping system before concrete placing.

5.2. Materials and Methods

A commercial portland cement CEM I 52.5R according to the European standard EN 197-1:2000 is used. The specific surface area measured by nitrogen adsorption (BET model) is $1.12 \text{ m}^2/\text{g}$ following the procedure described elsewhere [208]. The cement is sourced from two batches, leading to substantial differences in retardation at high sucrose dosage. Results of the first batch are used in figures 5.1 top, 5.5, 5.7-5.14. Results of the second batch are used in figures 5.1 middle and bottom, 5.2, 5.4, 5.6. D(+)-Sucrose (99.7% for biochemistry – Sigma Aldrich) is used as set retarder at dosages varying between 0.2 and 0.86 mg/g of cement, equivalent to an initial dosage of up to 6.3 mM in pore solution. The portlandite used for figures 5.3 and 5.6 has a specific surface of $15 \text{ m}^2/\text{g}$ (purum p.a Fluka).

Distinguishing flocculation and hydration effects on structuration

Preparation of pastes

The cement pastes have a water to cement ratio of 0.4 unless differently stated and are prepared in batches of 200 g cement, mixing with a blade stirrer for 3 minutes at 500 rpm. Dosages of 0, 0.2, 0.4 and 0.8 mg of sucrose/g cement are added as 30% solution to the mixing water (direct addition) or after 20 minutes of hydration (delayed addition and mixing 1min at 500 rpm). The resulting mix is sealed and stored at 23°C in a water bath until the measurement. For characterisations of pore solution and TGA, the prepared mass of 1000 g of cement and 400 g water is mixed in a Hobart mixer, mixing 1min at slow speed and 2min at middle speed.

Methods

Structuration rates of cement paste suspensions using rheometry. Oscillation rheometry measurements are carried out in an Anton Paar MCR 501 rheometer using serrated parallel plate geometry with a diameter of 25mm of the upper plate, a diameter of 50mm of the lower plate and approximately 5g of paste placed in a gap of 1mm without trimming and using a solvent trap containing demineralised water.

The experiment cycle is divided in three phases. First the sample is pre-sheared until a shear stress of 400 Pa is reached at a shear rate of 50 1/s. Second the pre-shear is stopped and a small shear strain oscillation of 0.0005% is applied at a frequency of 1Hz for 20 minutes, sampling at a rate of 2 s. Third a stepwise strain sweep oscillation is applied from 0.001% to 10% strain amplitude at 1Hz at a step and sampling rate of 2 s. Oscillation measurements at constant strain are treated with a moving average over 5 measurement points.

Isothermal calorimetry. Isothermal calorimetric measurements are carried out in a TAMAIR calorimeter at 23 °C on cement pastes with 5g of cement paste sample. This technique is used to monitor the kinetics of the hydration reaction of the cementitious systems under study.

Pore solution extraction, ICP and TOC:

Pore solution extraction occurs from 150g of cement paste using a 0.45 μm filter with pressurized air. ICP measurements are carried out using a method described in

[209]. Organic carbon measurements are carried out on a Shimadzu TOC-VCSH/CSN total organic carbon (TOC) analyser. The amount of adsorbed sucrose on $\text{Ca}(\text{OH})_2$ is measured by depletion method, considering the difference between the initially added amount and the amount in the liquid phase.

Stop of hydration and TGA:

The hydration was stopped following a procedure by Mantellato et al. [210], conducting a solvent exchange with isopropanol at 5°C and using 100 mL isopropanol for 5 g cement paste. Drying occurred in a desiccator with anhydrous calcium chloride. TGA measurements were carried out using 20 mg of dried powder in an open crucible subjected to a temperature profile of 10°C/minute up to 1000°C.

Saturation index by GEMS:

The saturation index is calculated based on the pore solution composition measured by ICP. The calculation is done in GEMS using all the elements from the ICP measurements, using the database cemdata18, turning off precipitation of all solid phases, following a method described in [211].

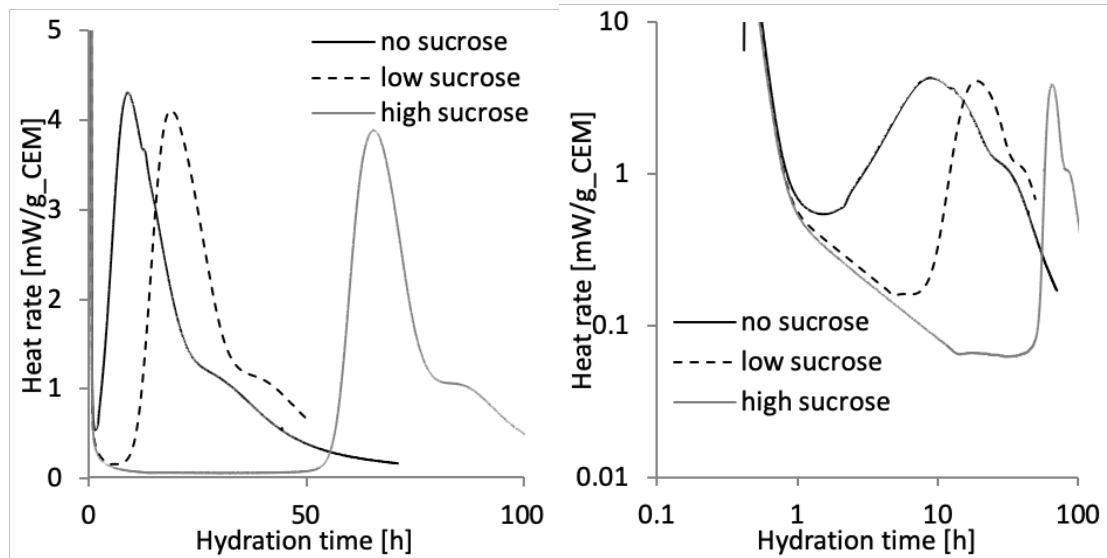
5.3. Model system for study of flocculation

5.3.1. Retarding cement hydration

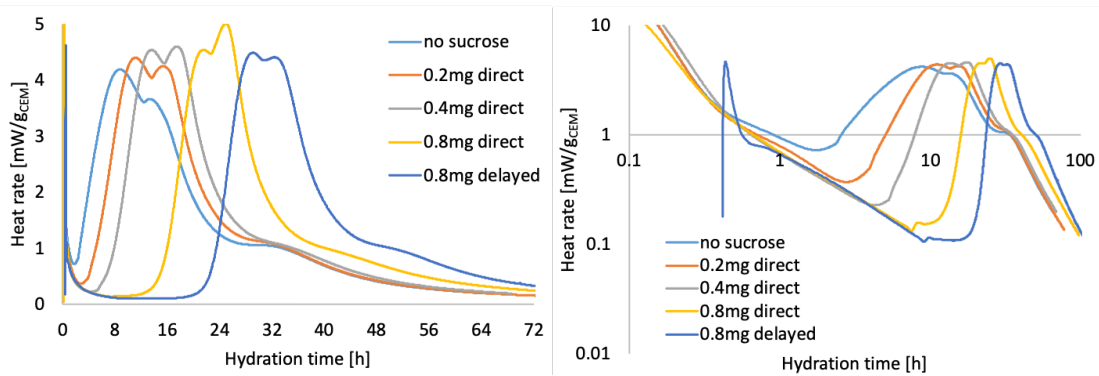
Figure 5.1 shows a strong delay of hydration caused by the addition of sucrose to the cement paste, delaying the onset of the acceleration phase of hydration by as much as 50 hours. Sucrose here mainly delays cement hydration, not affecting the silicate hydration peak. Most analysis of the acceleration period conclude to a process controlled by nucleation and growth, with a slope which depends on the number of nuclei formed before. Thus, these very similar peaks suggest that the number of nuclei is not changed much during the induction period. In cement pastes, sucrose does lead to a merging of the main peak with the sulphate depletion point at high sucrose dosages occurs for one system (figure 5.1 top) and not for the other (figure 5.1 middle).

Distinguishing flocculation and hydration effects on structuration

Top



Middle



Bottom

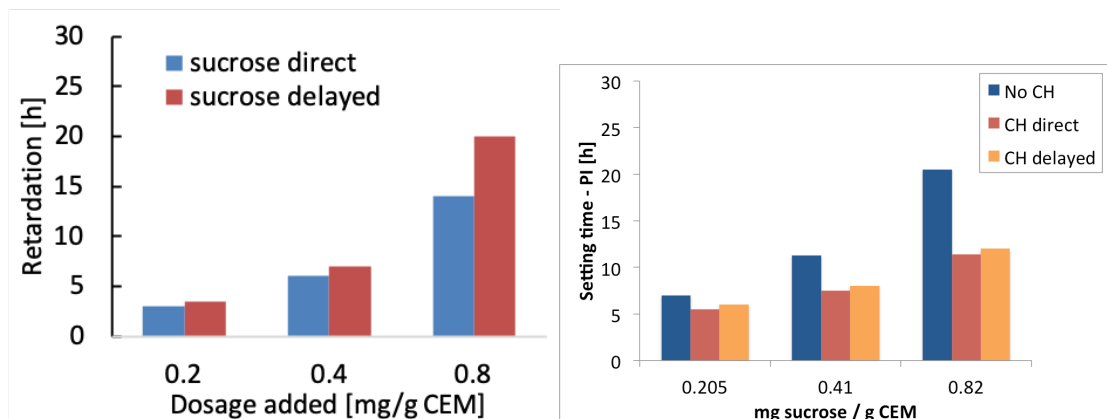


Figure 5.1: (top and middle) Heat rate as a function of hydration time for increasing sucrose dosage for two different cements and direct and delayed addition. (left) Lin-lin, (right) log-log. (bottom): Setting time measured at the inflection point of silicate hydration for direct and delayed addition of sucrose and of portlandite. The heat rate in the induction period follows a power law with an exponent of -0.85. (Top row: [167])

Distinguishing flocculation and hydration effects on structuration

In figure 5.1 (right top and middle) the evolution of the heat rate in the induction period is the same no matter the dosage of sucrose (between 0.5 and 10h), but its duration is changed. This suggests that the main reactions in this period are independent of the sucrose dosage, in particular dissolution which controls the heat release and for which we find a power law dependence on time with an exponent of -0.85. Additionally, it is observed for different sucrose dosages that delayed addition of sucrose affects retardation slightly, with the largest difference occurring at high dosage. This more effective retardation in delayed addition and documented retardation of sucrose in C₃S systems [212] suggests mainly a retardation causing interaction with silicates.

Using the delayed hydration with sucrose, the rheology of a chemically inactive cementitious system can be studied during a prolonged induction period, which makes it possible to specifically study the contribution of flocculation to structural build-up. For this purpose, isothermal calorimetry measurements are complemented by pore solution and the microstructure measurements, all of which are not found to be modified by sucrose.

5.3.2.Changes to pore solution

In figure 5.2 the quantity of sucrose adsorbed on cement surfaces or hydrates, as well as the proportion of sucrose adsorbed are shown. For all concentrations studied, the majority of the admixture is adsorbed on cement surfaces, the proportion being the same for all cases of direct addition with an affinity increasing from 80 to 100% with hydration time. The dosage independent adsorption affinity (figure 5.2 - right) is typical for adsorption with dosages below the adsorption plateau, however the same affinity would be expected for both direct and delayed addition. In delayed addition, adsorption is not as effective. This rather indicates an interaction of sucrose which changes in nature or intensity during the first 20 minutes of hydration. It could be adsorption on a temporary or permanent hydrate forming at high rate in the first minutes after water contact.

Distinguishing flocculation and hydration effects on structuration

With the majority of sucrose adsorbed in all direct addition cases, only a low amount remains in pore solution (1.2mM at 80% affinity in the highest direct addition dosage), so that no significant quantities of complexes are expected in solution. Which cementitious phase adsorbs sucrose or precipitates with it cannot be concluded from these measurements.

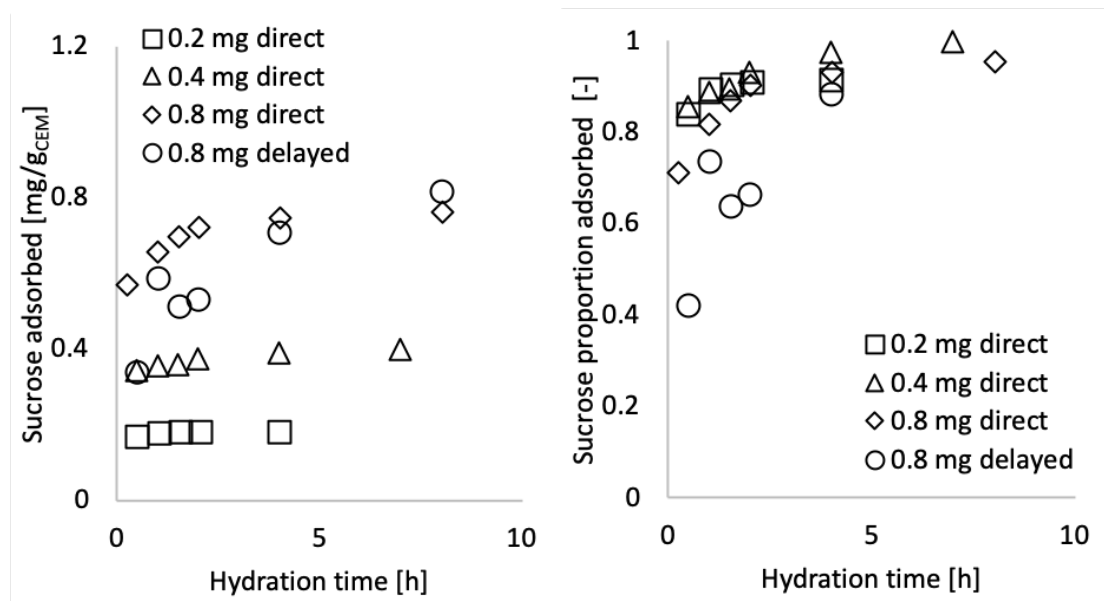


Figure 5.2: Adsorption of sucrose in Portland cement pore solution, increasing over time (left) absolute adsorption (right) adsorption relative to added sucrose indicating almost full adsorption.

In a calcium hydroxide (CH) suspension (water to CH = 2) sucrose is almost completely adsorbed at low dosage (affinity 85%) and a plateau is reached at high dosage (7.5 mg/g CH) both in ultrapure water and in a solution of 0.1M NaOH (figure 5.3 (left)). This shows that in presence of portlandite, sucrose adsorption from a cement paste solution is expected to occur once portlandite forms, and the affinity does not strongly depend on the pH (12.5 compared to 13.0). This is despite expecting a rather large change of dissociation degree of sucrose in this range (pK = 13.1) [213]. In addition, when a sucrose excess is dosed to a CH suspension, the equilibrium Ca concentration in solution qualitatively increases with the excess of sucrose left in solution, indicating the formation of a Ca-sucrose complex (figure 5.3 (right)).

Distinguishing flocculation and hydration effects on structuration

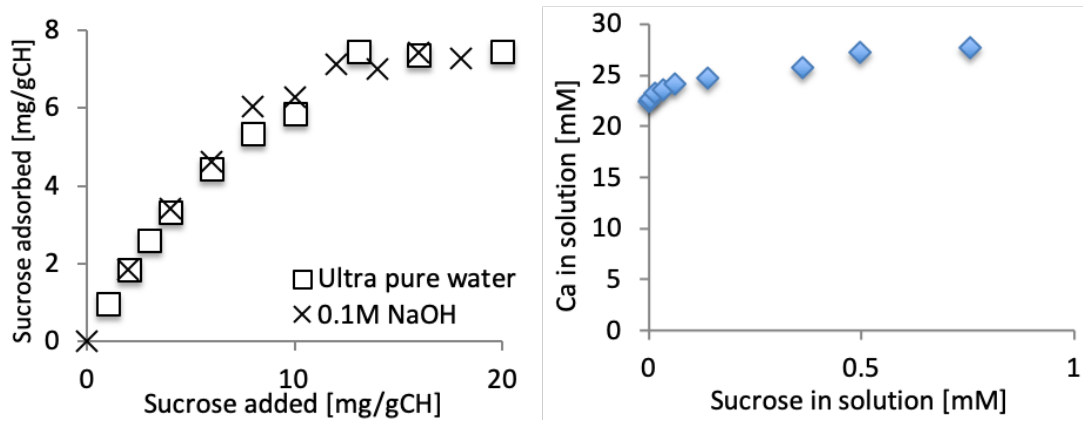


Figure 5.3: (left) Adsorption isotherm of sucrose in a calcium hydroxide suspension (pH 12.5) and pore solution with 0.1M NaOH, with a high affinity (85%) and a plateau formed at 7.5 mg/m². (right) Ca concentration in CH pore solution as a function of the sucrose concentration in solution.

Figure 5.4 shows ICP analysis of Ca, Na, K, S, Si, Al, Fe, Mg from ions in solution (Ca^{2+} , Na^+ , K^+ , SO_4^{2-} , $\text{H}_2\text{SiO}_4^{2-}$, $\text{Al}(\text{OH})_4^-$, $\text{Fe}(\text{OH})_4^-$, Mg^{2+}), as well as OH^- determined by charge balancing considering full dissociation of the major ions. All evolve in a similar way over time, with no significant differences between the major ions (Ca, Na, K, S, OH) and only a minor increase of Si depending on the addition mode. Over time, Ca, Na, K and OH^- concentrations increase to a minor degree in solution, while the concentration of S decreases. Al is close to the detection limit, while Fe and Si can be detected with confidence and are found to decrease over time. Given that no significant differences are observed in the aqueous phase, we conclude that sucrose is not affecting dissolution kinetics, which is the rate controlling mechanism in the induction period.

In support of this, we note that the saturation degree with respect to CH increases with time, while it barely changes for C-S-H, gypsum (see figure 5.5). The negative saturation index of syngenite indicates that this phase doesn't form, while the positive index indicates oversaturation. Unfortunately, the saturation degree with respect to Aft is not quantifiable due to the too low amounts of Al in solution. However, the decreasing SO_4^{2-} concentration along with the increase of pH indicates a slow formation of Aft during the induction period.

Importantly, the increase of the saturation degree with respect to CH indicates a hindrance of precipitation or growth of CH. The same trend is however also observed in the induction period of cement paste not containing sucrose. This indicates that sucrose

Distinguishing flocculation and hydration effects on structuration

does not act here, as by an action on CH precipitation/growth, we would expect an increase of saturation index compared to the non-delayed paste. Similarly, for delayed addition, we also observe that the saturation index is also not increasing for C-S-H when sucrose is added to the paste, indicating that its nucleation/growth is also not hindered. Additionally, a minor reduction of the Ca concentration in pore solution compared to the non-retarded cement paste is observed, not allowing however conclusive statements.

The increased Si concentration in solution depends on the addition mode. As previously mentioned, this suggests an interaction of sucrose with Si ions in the first 20 minutes of hydration, with the Si ions remaining in solution beyond this timeframe if sucrose is added with the mixing water. However, since retardation by delayed sucrose addition is equally or even more strongly retarding cement hydration (compare figure 5.1) than direct addition, we cannot conclude that a Si-sucrose complex is hindering C-S-H precipitation/growth.

Summarising, it appears that a significant hindrance of Aft formation is not occurring and that all cement pastes pore solutions evolve similarly with respect to both C₃A and C₃S hydration.

Distinguishing flocculation and hydration effects on structuration

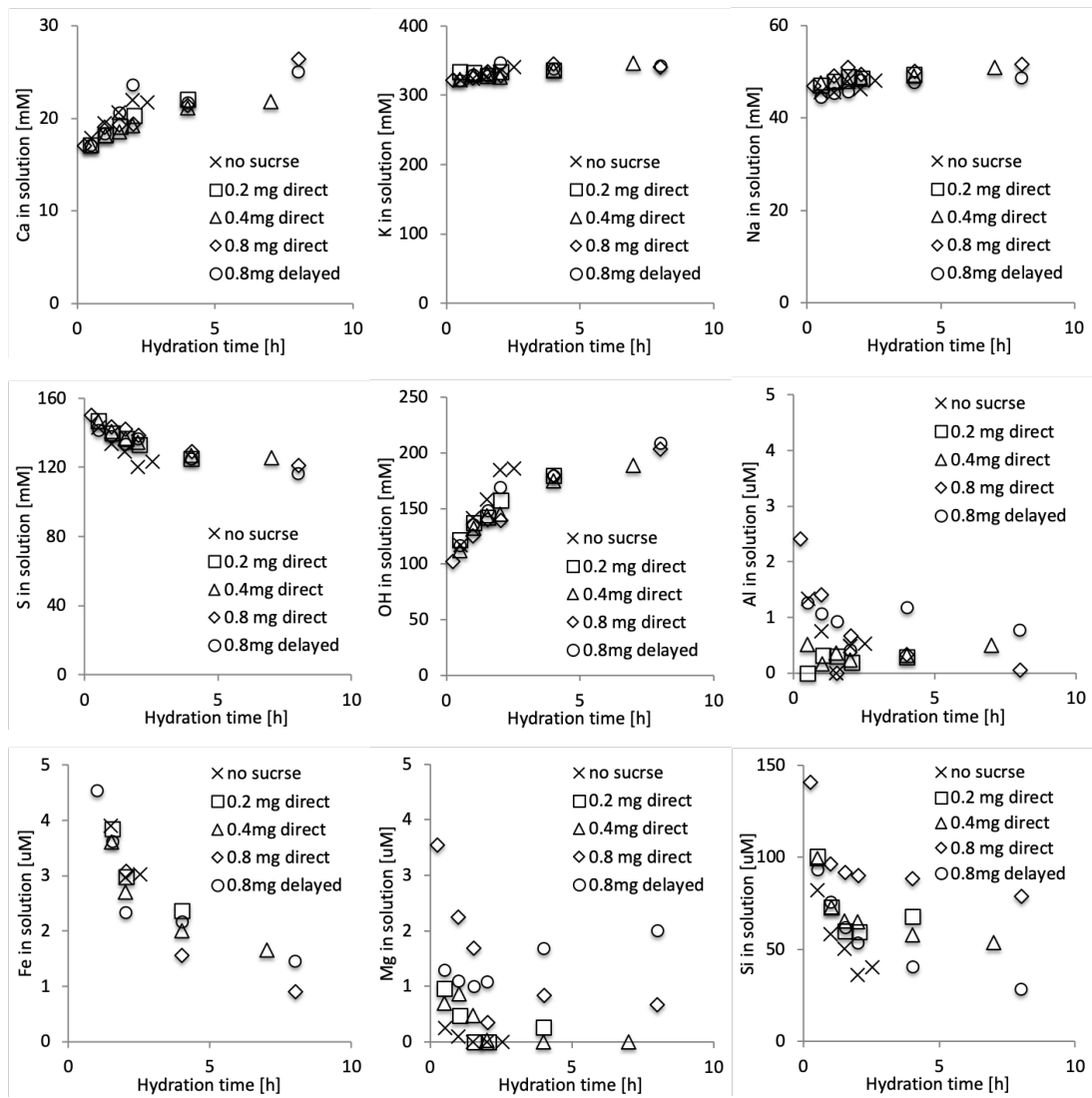


Figure 5.4: Ion concentration in pore solution of the major ions Ca, K, Na, S (being SO₄) and OH and of the minor ions Al, Fe, Mg and Si by ICP. Limit of quantification (LOQ): Al: 4 μM, Fe: 0.3 μM, Mg: 0.2 μM, Si: 11 μM[209].

Distinguishing flocculation and hydration effects on structuration

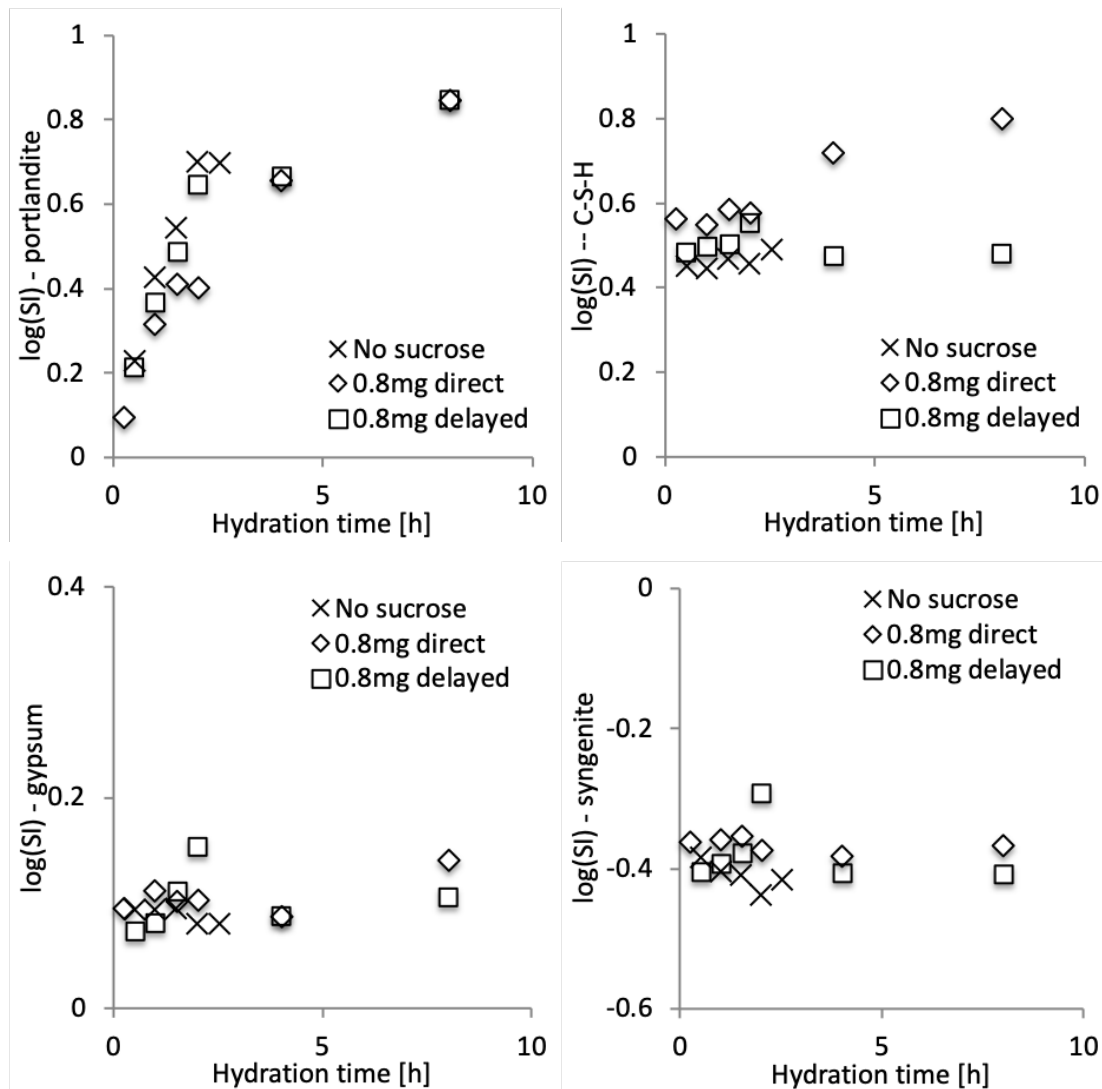


Figure 5.5: Saturation index of pore solutions with respect to portlandite, C-S-H, gypsum and syngenite, following a method described in[211]. Values larger than 0 indicate oversaturation and indicate that this phase can form.

5.3.3.Changes to hydrates

Figure 5.6 (left) shows that the total amount of sulfo-aluminates formed as a function of time does not change with the dosage of sucrose measured by TGA. The mass of this product, mainly ettringite, is a power law of time with an exponent 0.14. This also means that the rate at which this product forms decreases rapidly with time, specifically as $t^{-0.86}$, indicating that most of the ettringite present in the induction period is formed during the initial dissolution of clinker. More importantly, the value of this exponent is equivalent to the one describing the decreasing heat rate in the induction period (figure 5.2 (top-right)). This implies that the heat rate is proportional to the amount of ettringite formed and therefore more or less also proportional to the amount of C_3A reacting. The

Distinguishing flocculation and hydration effects on structuration

fact that the relation works so well over long periods of time, confirms that the degree of reaction of C_3S must be very low. Also, even with some C_3S reaction, the fact that C_3A dissolution is much more exothermic than C_3S explains this result.

Over time the quantity of portlandite measured by TGA is increasing (figure 5.6 (right)). The rate of this depends on the dosage of sucrose in the cement paste, with lower rates for higher sucrose dosage. This shows that C_3S hydration is slowed down, but does not provide clues as to the involved mechanism. As is expected, the amount of portlandite formed in the induction period is very low, less than 0.5%. The corresponding increase of solid content is approximately 0.6% (including both CH and C-S-H), a value later shown not to increase the instantaneous yield stress by more than 10%.

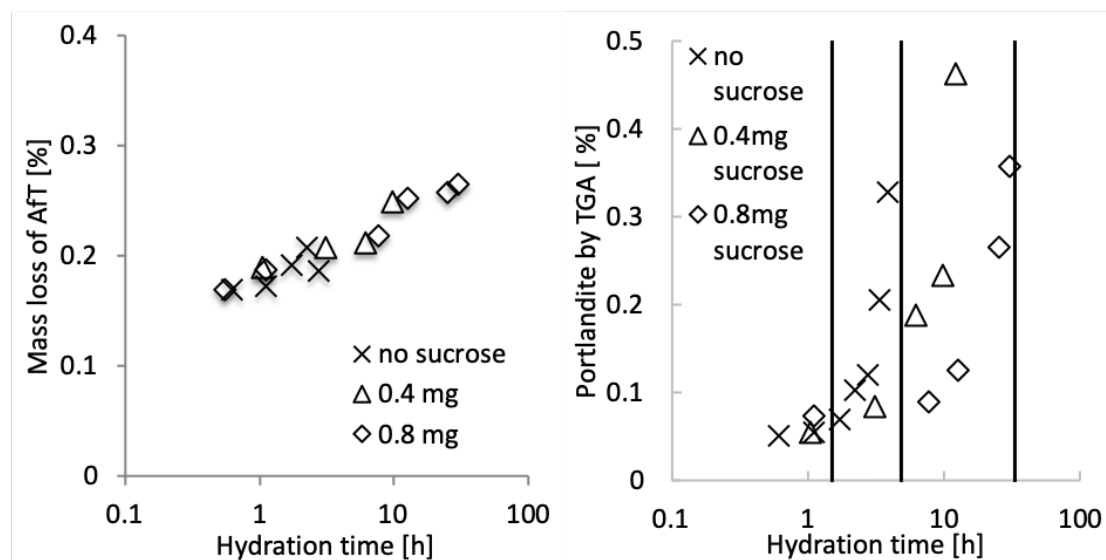


Figure 5.6: (left) Mass loss 200-350°C. The formation of ettringite follows a power law with an exponent of 0.14, so that its formation rate has an exponent of -0.86, very similar to what is found for the heat rate in figure 5.2 (top-right). (right) CH formed, measured by weight loss between 370-400°C. The vertical lines indicate the onset of hydration, from left to right for no sucrose, 0.4 mg and 0.8 mg. The formation of portlandite occurs at a slower rate in presence of sucrose and in presence of sucrose some portlandite formation is detected before the onset of hydration.

5.3.4. Competitive adsorption

By adding calcium hydroxide with high specific surface to a cement paste containing sucrose, the retardation caused is reduced (figure 5.6 (left)). With a sufficient portlandite dosage, this retardation can be almost entirely cancelled. This in similar quantitative terms whether portlandite is added directly or with a delay of 1h (compare

figure 5.1 bottom). The absence of effect of addition time indicates that sucrose retardation does not involve an impact on the initial aluminate reactivity. The retardation reduction by adding CH further shows that an interaction between sucrose and portlandite occurs, independently of how much sucrose is present in pore solution (difference between direct and delayed sucrose addition). It suggests a preferential adsorption of sucrose on portlandite, displacing sucrose away from the surfaces it is initially adsorbed on.

More importantly, retardation in the combined system can be quantitatively predicted from the adsorption plateau introduced in figure 5.3 (left). By considering sucrose to adsorb onto the introduced portlandite surface to the extent observed in a portlandite suspension. The remaining sucrose that is not adsorbed on portlandite remains available to cause retardation (figure 5.7 (right)). With this hypothesis, the observed combinations of sucrose and portlandite dosages fall onto a common master curve relating the retardation to the sucrose that is not adsorbed on portlandite (figure 5.7 - right). This shows that if possible, sucrose adsorbs on portlandite in a cement paste and does so with a high affinity occupying a surface determined at the plateau of the adsorption isotherms measured in pure portlandite suspensions. We thus infer that adsorption on portlandite is strongly favoured over other phases present in the cement.

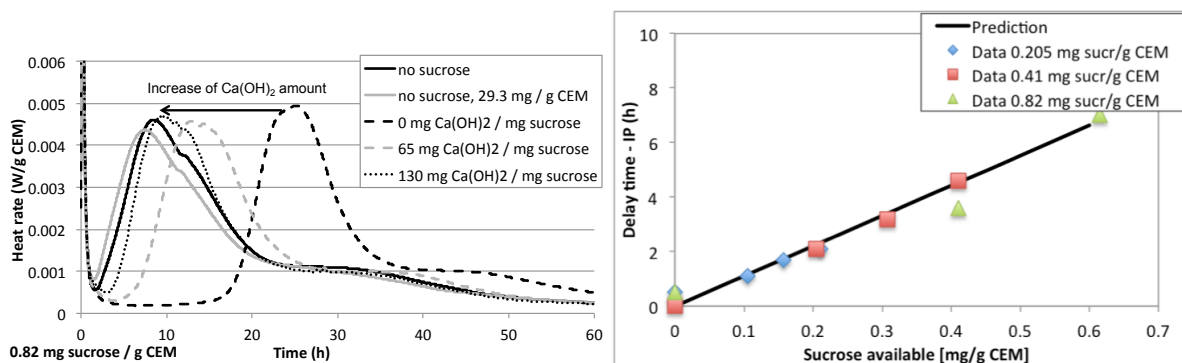


Figure 5.7: (left) Heat rate in cement pastes containing both sucrose and CH. The addition of portlandite reduces the retardation caused by sucrose, the addition of CH alone accelerates hydration to a minor extent. (right) Delay of hydration onset for combinations of sucrose and CH, subtracting the quantity of sucrose adsorbed on CH calculated from the plateau of the adsorption isotherm of sucrose and CH[79].

5.3.5. Rheological consequences of sucrose addition

The results in figure 5.8 - left further confirm that the resulting macroscopic rheological behavior of the suspension is unchanged by the presence of sucrose in the induction period. Indeed, the steady state flow viscosity reached at the end of the pre-shear is independent of sucrose dosage. This suggests that volume fraction, particles roughness and particles interactions in steady state flow are not affected by sucrose. Also, despite a long hydration time, the initial flocculated state when flow is stopped is comparable and the built structure can be entirely broken down to the original state.

It should be noted that by applying a pre-shear at constant rate does not break down the entire structure of colloidal interactions, something that could be much more effectively achieved by large strain oscillations [206]. Nevertheless, the applied shear is capturing a deformation event more similar to what would occur in a pumping, printing or mixing process before the concrete is placed. In this sense, recovering the initial state means recovering the viscosity and yield stress after the material has remained at rest.

By changing the time period of the pre-shearing phase, we additionally tested the recovery of storage modulus, after different apparent viscosities are reached at the end of the pre-shearing event (see figure 5.8-right). This was done in the induction period of a retarded cement paste in random sequence between 2 and 4 hours of hydration (in paste with 0.8 mg sucrose per g cement). We find that structural recovery is rather insensitive to the intensity of structural breakdown in the pre-shearing phase.

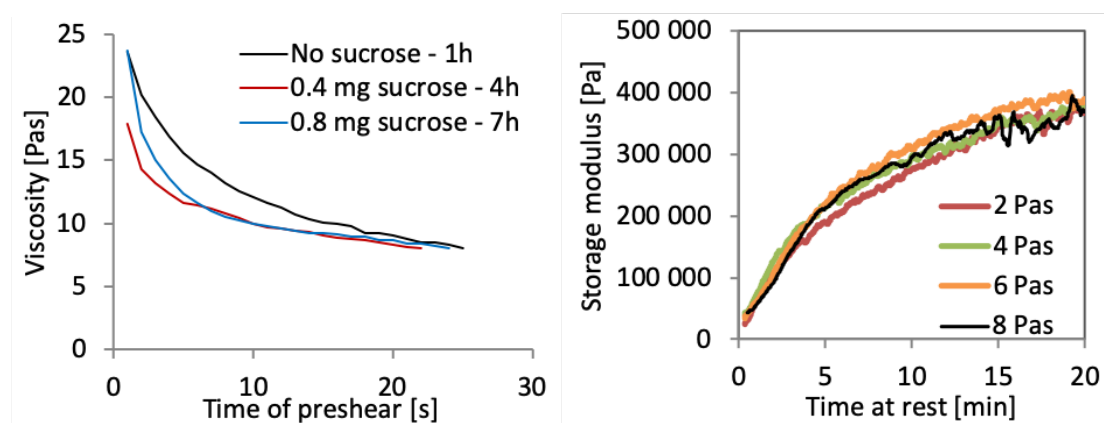


Figure 5.8: (left) Apparent viscosity evolution in pastes with a w/c 0.4 during a pre-shear event in the induction period of hydration, with the starting time of measurement indicated in the legend. (right) Structuration at rest in the induction period of a retarded cement paste with the pre-shear applied until different levels of apparent viscosity are reached.

5.4. Structuration from flocculation

5.4.1. Measuring at different times in the induction period

When measuring the storage modulus as a function of time (see figure 5.9), the initial storage modulus is approximately the same between all measurements (time scales of the order of a few hundreds of seconds). The evolution is however affected by the presence of sucrose. If the system contains sucrose, all structuration measurements in the dormant period follow the same characteristic kinetics, reaching a slow asymptotic rate for long times at rest (after 20 minutes for w/c 0.4). The storage modulus reached after 20 minutes is the same independently of sucrose dosage, reaching 500 kPa. This applies for any retarded cement pastes of the same solid volume fraction in the induction period, independently of dosage (within this range) and independently of the age of the cement paste at the beginning of the measurement. Without sucrose, structural buildup reaches a higher value after 20 minutes and shows a linear increase at long timescales. The similarity of all retarded suspensions suggests that with sucrose the system is not aging but following a fully reversible structuration cycle caused by flocculation. The time to reach half of the storage modulus after 20 minutes, is of the order of 200-250 seconds with sucrose. As the first 20 seconds of oscillation are dominated by relaxation of the sample from the pre-shear event, these measurement points have been discarded.

Given the small hydrodynamic radius of sucrose (approximately 0.5 nm) [214], sucrose is expected to interact with flocculation kinetics by steric hindrance or by depletion to a minor degree as the hydrodynamic radius is smaller than the expected separation between pseudo-contact points (approximately 2 nm) [119], [143], [215] between cement particles due to Van der Waals attraction. For this reason, the dosage independent structural buildup in both timing and asymptotic rate is expected to be the same for all retarded cement pastes, as observed in figure 5.9. However, owing to the adsorption of sucrose, some steric hindrance between particles can occur (increasing the separation between particles by the hydrodynamic radius). As Van der Waals forces scale with $1/H^2$ [216] with H being the minimum separation between particles, interparticle forces may be reduced by a factor 1.6 ($H=2.5\text{nm}$) in presence of sucrose, together with the flocculation taking more time. A difference between natural and

Distinguishing flocculation and hydration effects on structuration

retarded cement pastes of similar magnitude is indeed observed in the timescale up to 300 s. In order to verify the source of this discrepancy between neat and retarded pastes, a measurement on neat paste at lower temperature (e.g. 5°C) could be helpful, as this would also slow hydration, but without affecting interparticle separation.

Additionally, as the heat rate is low in the induction period, in the timespan of 20min, only a small quantity of hydration products is expected to form (0.1 J/g cement in 20min) in the retarded mixes. For this reason, as hydration is excluded for the retarded system, the same kinetics and asymptotic rate is expected due to flocculation dominating the kinetics and this is what is found independently of sucrose dosage. We will in the following consider that in retarded cement pastes, the storage modulus reached after 20 minutes at rest is dominated by flocculation.

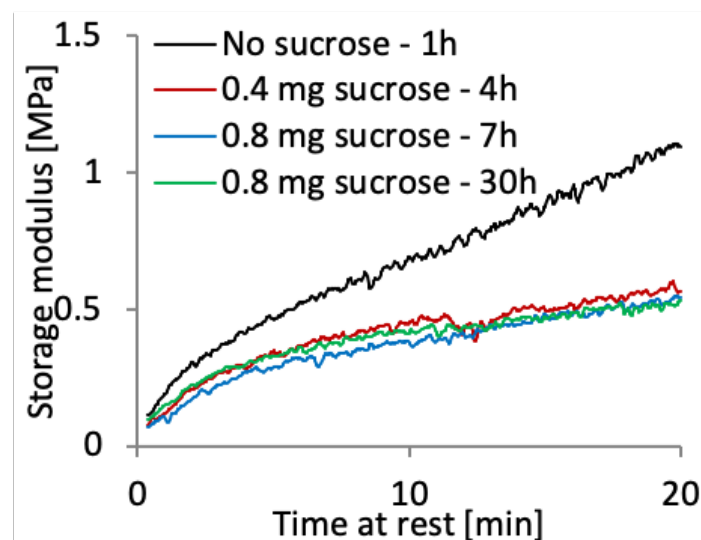


Figure 5.9: Evolution of structural build-up at rest and at low heat rates for cement pastes without sucrose at the lowest heat rate in the induction period and for systems with sucrose at different times.

5.4.2. Changing the solid volume fraction

Structural build-up depends on the solid volume fraction of cement particles in a retarded cement paste (see figure 5.10 - left). With increasing solid volume fraction ϕ , the storage modulus reached after 20 min at rest increases (from 180 kPa to 2600 kPa) and the characteristic structuration time (time to reach storage modulus at 20 minutes) decreases (from 400 s to 150 s). The characteristic kinetics of this process depend on the

Distinguishing flocculation and hydration effects on structuration

solid volume fraction, the exponent of the time dependent storage modulus increase being between 0.38 and 0.42 for all ϕ apart from $\phi = 0.50$, where the exponent is 0.32. This asserts that the flocculation process follows two distinct kinetic slopes of different exponent for the densely packed system and the more dilute system. The power law scaling of solid volume fraction with final storage modulus from the measurements in figure 5.10 (left) follows a power law behavior of $\phi^{14.8}$.

Alternatively, by using the YODEL model[118], [119] with a maximum random close packing fraction of 0.57 and a percolation threshold of $\phi_0 = 0.04$, the storage modulus can be scaled with the packing factor of the YODEL model (see figure 5.10 – right), this being the factor:

$$\frac{\phi^2(\phi - \phi_0)}{\phi_{\max}(\phi_{\max} - \phi)}$$

This factor is expected to scale with yield stress, provided that its pre-factor m_1 describing the interaction on the scale of individual particles remains constant, which is expected in absence of hydration. The agreement found between storage modulus at long resting times and packing factor is linear as expected but has an offset. Such an offset is logical in view of the different size scales to be addressed by the YODEL model (essentially derived based on individual contacts), while in the dense regime a percolated network of particles exists. For such networks, a minimum contact probability is needed to establish a connected floc spanning the entire volume, the percolation threshold [217]. Given the linear fitting parameters found here, this occurs at a YODEL packing factor of 0.669, equivalent to a solid volume fraction of 0.408, equivalent to a w/c of 0.457.

Distinguishing flocculation and hydration effects on structuration

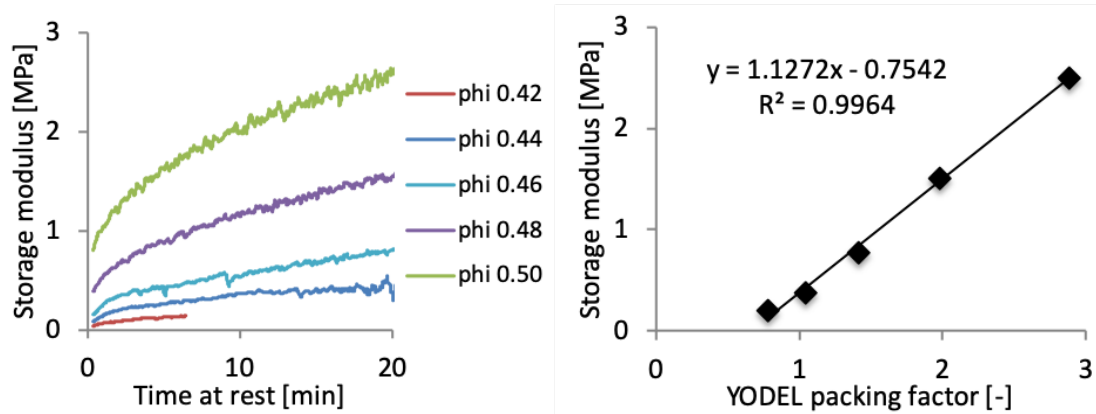


Figure 5.10: (left) Shear elastic modulus as a function of resting time for five cement solid volume fractions in a retarded system. All values tend towards a plateau of final storage modulus. The exponent of this evolution lies between 0.38 and 0.42 for all solid contents, apart from the highest solid content, where it is 0.32. (right) Final storage modulus after 20 minutes at rest as a function of the YODEL packing factor.

5.4.3. Changing the interstitial viscosity

When the interstitial viscosity of the cement paste is modified by the addition of non-adsorbing PEG molecules (PEG1: average molar mass: $1.3 \cdot 10^6$ g/mol, radius of gyration 138nm, PEG2: average molar mass: $1.6 \cdot 10^5$, radius of gyration 38nm [218]), no significant modifications of the flocculation kinetics are observed (see figure 5.11), despite an increase of the interstitial viscosity by more than 100x for the PEG1 and of 15x for PEG2 as measured by rotational rheometry with a Couette geometry. This indicates that long-range motion of particles in the interstitial fluid is not the phenomenon responsible for the flocculation process, as the flow of liquid out of the gap between particles would be slow due to the higher viscosity [110], slowing the flocculation process.

The fact that the kinetics of structural buildup are barely modified by the presence of PEG, while the interstitial viscosity increases drastically, indicates that neither Brownian motion nor gravity forces, leading to segregation/ sedimentation/ bleeding are responsible for structural build up. Smaller scale rearrangements involving these forces among closely neighbouring particles, may however be involved to some extent.

Distinguishing flocculation and hydration effects on structuration

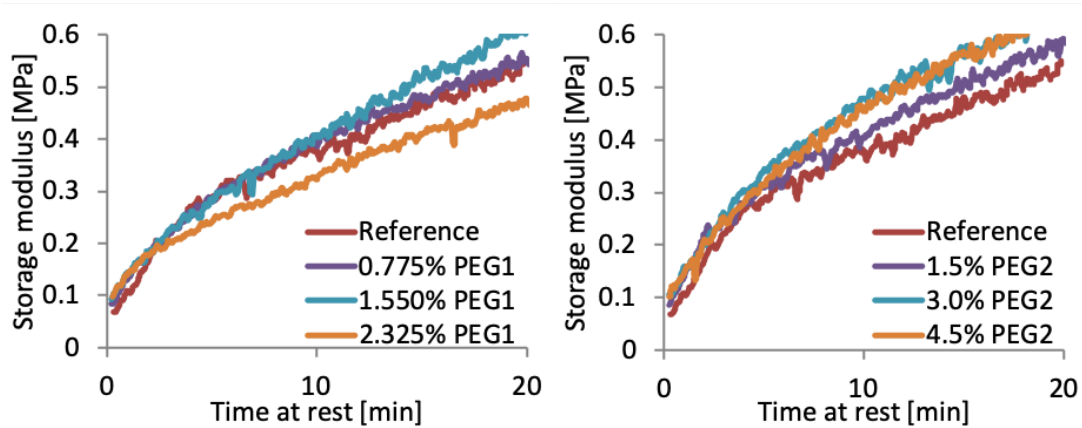


Figure 5.11: Storage modulus evolution with added PEG at increasing dosage. No systematic slowing of structural build-up is observed. (left) PEG1 with radius of gyration of 38nm, the interstitial viscosity of the pore solution increasing up to 680 mPas. (right) PEG2 with radius of gyration of 138nm, the interstitial viscosity of the pore solution increasing up to 15 mPas.

5.5. Structuration from hydration

5.5.1. Measuring at different times from induction to acceleration period

Figure 5.12 shows the evolution of the storage modulus of a non-delayed cement paste for measurements started at different times of cement hydration. In the first 5 minutes at rest the rate of structuration is decreasing (see figure 5.12 – right). This trend continues for the early measurements, while for measurements conducted up to an age of 1h40 (in the induction period), and then tends to an asymptotic rate up to 20 minutes at rest. For measurements occurring thereafter, the rate of structuration increases. Thus qualitatively, an interval between 30 seconds and 5 minutes, as well as between 5 minutes and 20 minutes can be distinguished, in which the structuration rate is dominated by different physical phenomena, the first one being similar to the retarded cement paste and associated with a flocculation process, the second being the effect of hydration. In the last measurement in Figure 5.12 the sample shows a higher initial storage modulus. This can be explained by permanent changes to the cement paste, especially an increase of solid content, increasing the number of contact point forming the network of interactions.

Distinguishing flocculation and hydration effects on structuration

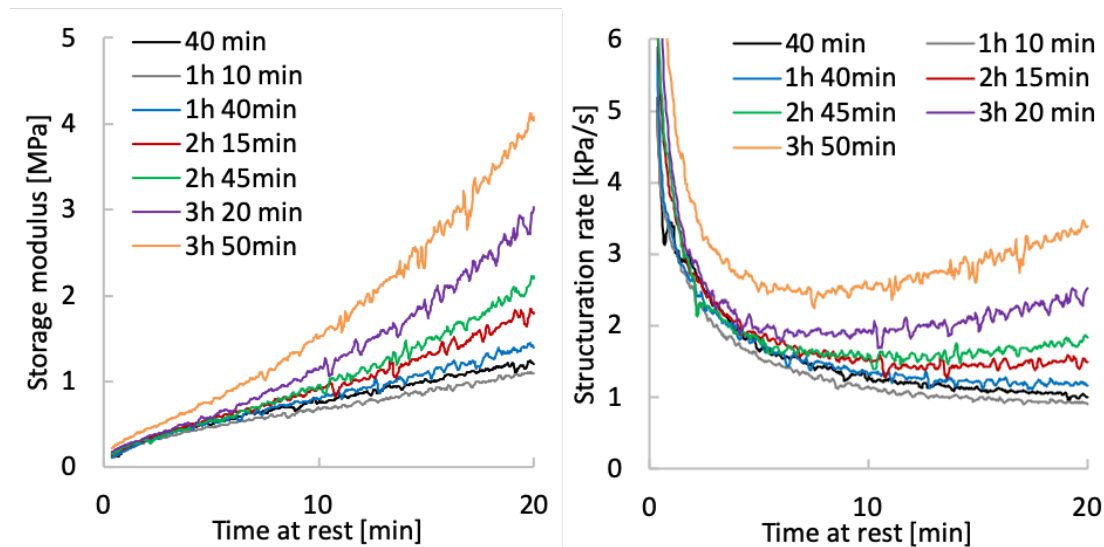


Figure 5.12: Storage modulus evolution at rest, capturing structural build-up and measured for a hydrating paste at different placing times. (left): storage modulus evolution[167]. (right) rate of storage modulus increase (storage modulus divided by time at rest). In the first 5 minutes structuration rate evolves approximately with exponent 0.5, while on longer timescales structuration rate increases for older samples.

5.5.2. Yield stress at long resting times

Figure 5.13 (left) shows the shear stress and storage modulus recorded by increasing the oscillation strain at the end of a 20 min resting time. We observe a storage modulus plateau at very small deformations between 0.001 and 0.01 % strain. When the peak shear stress is reached (yield stress), we observe that the storage modulus is substantially lower, something showing structural breakdown. Structural breakdown occurs well before yield stress is reached (maximum shear stress) and is initialised approximately at a stress half a decade below the measured yield stress. The measured characteristic strain can be strongly affected by shear localisation in a zone in which structural breakdown is initialised and may not capture the effective local strain[113]. It can however be stated that at a strain as low as 0.01% the structure behaves as a linear elastic material and beyond this point some damaging occurs.

Figure 5.13 (right) shows a non-perfect linear relationship between the storage modulus measured at the end of the 20 min long oscillation period and the yield stress (peak shear stress from figure 5.13 - left) measured by oscillation sweep after this period. This shows that the structure formed during the non-destructive oscillation period is

Distinguishing flocculation and hydration effects on structuration

directly associated with the yield stress measured at the onset of flow. This observation is important, as yield stress is measured at the onset of flow and after substantial structural breakdown, while storage modulus describes the undamaged structure. This also shows that storage modulus measurements at long resting times, can be associated to yield stress, which is the more commonly measured property used in building processes. The discrepancy in the linear relationship between storage modulus and yield stress is probably associated with a change of characteristic strain in the material.

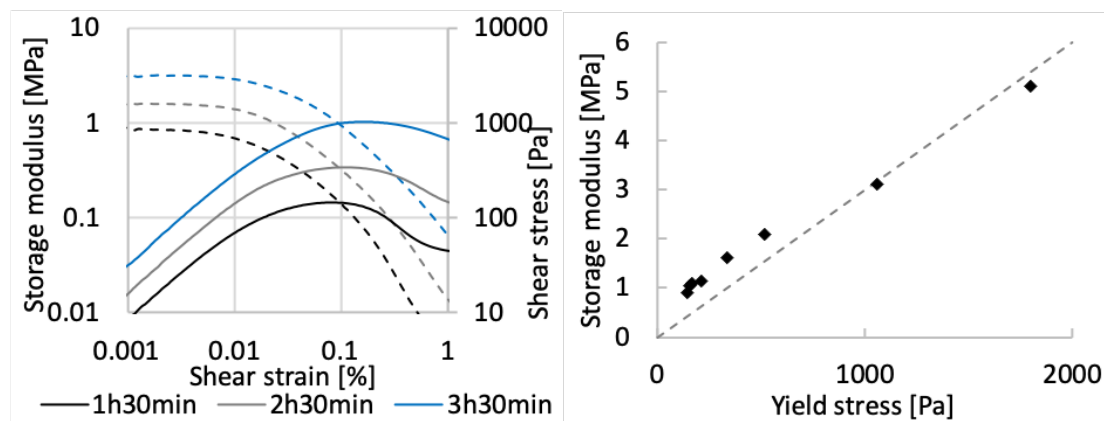


Figure 5.13: (left) Shear stress (full line) and storage modulus (dashed line) after 20 minutes at rest measured by oscillation sweep. Structural damaging occurs well before yield stress is reached and characteristic strain varies to a minor degree (right) Storage modulus after 20 minutes at rest compared to yield stress by oscillation sweep, with an arbitrary dashed line indicating proportionality. Direct linear proportionality is not found.

5.5.3. Relating structural build-up to the rate of hydration

The oscillation measurements in figure 5.12 clearly show that beyond a resting time of 5 minutes the structuration rate increases strongly with the time at which the specimen is placed. To examine this closer, figure 5.14 shows the series of measurements of structural build-up along with the hydration rate. It is observed that the storage modulus after 20 minutes of each oscillation measurement is directly proportional to hydration rate. Qualitatively, the higher storage modulus can thus be explained by and associated to the increased formation and growth of hydration products between the cement grains as a consequence of C_3S reaction. This increasing rate at which hydration products form, is considered to strengthen the network of colloidal interactions, previously built during the first minutes of rest.

Distinguishing flocculation and hydration effects on structuration

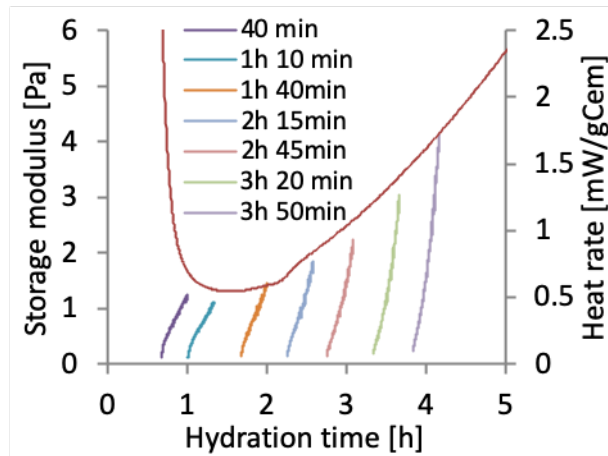


Figure 5.14: Structuration on the left axis compared to the rate of hydration by isothermal calorimetry on the right axis. The storage modulus reached at the end of the oscillation measurement is directly proportional to heat rate[167].

Figure 5.15 (left) complements the measurements on neat cement pastes, with retarded pastes reaching a slow asymptotic rate modulus after 20 minutes at rest as in figure 5.9 and a transition for an intermediate sucrose dosage. This finding is summarised in figure 5.15 (right), showing the rate of structuration in relation to the heat of hydration at the time of measurement. A linear relationship is found.

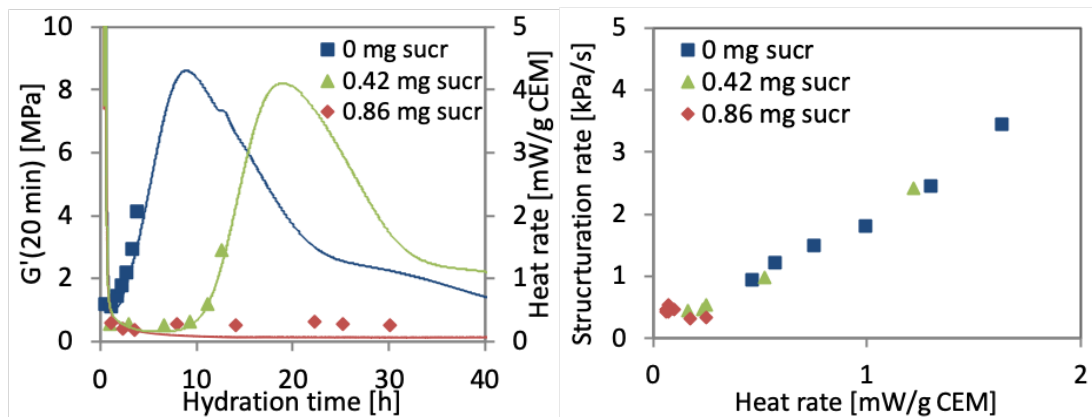


Figure 5.15: (left) Storage modulus after 20 minutes compared to the heat rate, including retarded cement pastes. (right) Relationship of structuration rate after long periods at rest and average heat rate during rest. Strongly retarded, intermediately retarded and neat cement pastes follow the same trend[167].

5.6.Discussion

5.6.1.Understanding sucrose retardation

Background information

Sucrose is well known as a strong set retarder in concrete technology. While the role of molecular structure of sucrose and other sugars has been studied over decades [204], [212], [219]–[224], the physico-chemical mechanisms causing and ending the retardation remain debated.

Thomas and Birchall [204] studied the effect of different sugars at rather high concentration in dilute suspensions and observed a significant increase of ion concentrations (Ca, Si, Al, Fe) in solution over time, but did not find a Si-sucrose complex. Instead they generally explained sugar retardation by a mechanism of adsorption on hydrates and poisoning of hydrate surfaces.

Thomas et al [222] studied the effect of combinations of sucrose with C-S-H seeds in pastes and proposed again an interference with the nucleation/growth process through adsorption on a particle surface. Similar studies by Peterson et al [223] and by Bishop and Barron [224] largely supported these findings.

Luke and Luke [220] showed a correlation of sucrose in solution and ettringite formation. Smith et al [219] concluded rather that sucrose affected C_3S dissolution, while Young [221] inferred an effect on CH nucleation. In line with this, Juilland et al [212] concluded more recently that sucrose inhibits portlandite nucleation and growth.

Adsorption

In most interpretations above, the dissociation degree of sucrose in the aqueous phase plays an important role and as shown by Popov et al [213] this changes a lot above pH 11-12 since one hydroxyl group of sucrose has a pKa of 13.1. This means that in cementitious systems approximately half the species is dissociated and that the extent varies in relation to the exact alkalinity.

Distinguishing flocculation and hydration effects on structuration

The role of pH deserves further investigation and should be considered when considering results obtained in dilute suspensions. In this thesis, we found that sucrose has a very high affinity for portlandite, with about 85% adsorbing until the plateau (figure 5.3 - left) and no modification of this behavior at higher pH. Whether this behavior is the same or not on C_3S and C-S-H remains to be studied. However, in any case we find that sucrose has a high adsorption in cement paste (figure 5.2), which suggests that only very few calcium complexes are to be found in solution. Such complexes may however be relevant at high dosages since in such cases there is indeed an increase in calcium in the aqueous phase (figure 5.3 -right).

Impact on aluminates

Isothermal calorimetry shows a characteristic decreasing heat rate in the induction period (Figure 5.1) which is the same independently of sucrose dosage. This together with TGA results showing unchanged formation rates of ettringite (section 5.3.3, Figure 5.6) and Al concentration below the detection limit (figure 5.4) suggests that sucrose is not affecting the hydration of aluminate phases. Luke and Luke had however observed an increasing adsorption of sucrose with the ettringite formation and we suggest that this reflects a pH increase that increases sucrose dissociation and thereby its adsorption on some phases (see figure 5.4, OH in solution). This remains to be investigated as so far, we only looked at the pH effect on portlandite and did not find an effect.

In terms of pore solution, the decreasing sulfate concentration, with a lack of Al ions indicates ettringite formation, this being similar independently of sucrose dosage (figure 5.4), which on longer timescales could suggest a risk of sulfate-silicate-aluminate imbalance. However, this does not appear to be the case from the calorimetry curve, so that once again we do not conclude that sucrose acts through its impact on aluminates.

An open question of this concern is however that sucrose causes more retardation in delayed addition (figure 5.1 - middle). This could suggest an impact on nucleation of the first hydrates, in particular ettringite, leaving less sucrose available if it is added in the mixing water, something that appears to occur in TOC measurements in figure 5.2,

Distinguishing flocculation and hydration effects on structuration

where adsorption is stronger for direct addition cases. Measurements of specific surface would be useful to elucidate this point.

Impact on Portlandite

The evolution of calcium and silicate concentrations in solution provide important clues to how sucrose may modify hydration reactions (see figure 5.4). However, here it is important to underline that the mechanism of retardation may change with dosage. In particular, at high dosages, we expect an excess of sucrose, so that its concentration in solution will increase and that the presence of complexes in the aqueous phase could start playing an important role on retardation (as in the work of Thomas and Birchall [204]). Therefore, we underline that we have used dosages that remain “reasonable” giving retardation from about 1 to 10 hours, with even a value of 30h for delayed addition.

For these dosages, we note that to one exception, the calcium concentration to not rise about a concentration of about 23 mM, but that the average rate at which these values are reached decreases with the dosage of sucrose. Similar trends are observed for the hydroxyls (see figure 5.16). Looking at the saturation index, we observe an oversaturation with respect to portlandite and C-S-H, with an increase of saturation index over time in the case of portlandite (see figure 5.5). However, the saturation index evolution is independent of the presence of sucrose. These results suggest that Portlandite saturation is not exceeded and this observation is very important because, in the “Portlandite inhibition” mechanism proposed by Bullard and Flatt [225], the dissolution of C_3S is turned off because of an increasing concentration of calcium and hydroxide in the pore solution. The present study does not show any evidence of this and therefore suggests that retardation is not coming from an inhibition of Portlandite.

Results do however show that calcium concentrations do not necessarily stop to increase at the setting time (taken as the minimum in the heat rate and indicated as vertical line in figure 5.16). This observation is supported by a similar conclusion for CH formation, which tends to accelerate before the setting time is reached (see figure 5.6 - right). Unfortunately, a direct comparison between both data series is not possible, because these measurements were done at different times with a slightly modified

Distinguishing flocculation and hydration effects on structuration

cement. However, using relative comparisons with respect to the calorimetry remains possible.

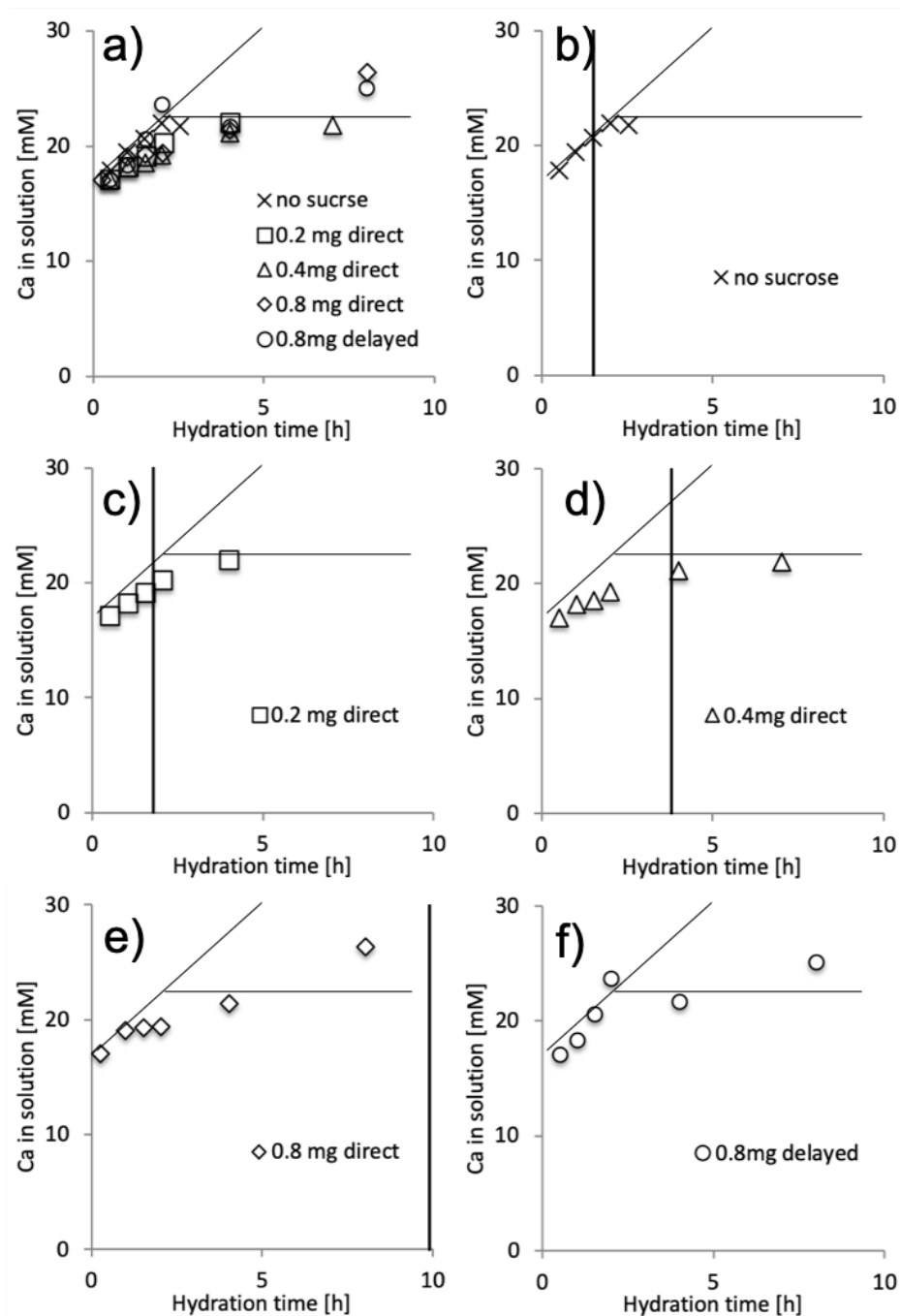


Figure 5.16: Calcium concentration from figure 5.4. a) All figures, b-f) individual subfigures for different cement pastes. The vertical line indicates the time of onset of hydration for the respective cement paste, the inclined line indicates the calcium concentration evolution for non-delayed cement paste and the horizontal line indicates the calcium concentration peak value reached for non-delayed cement paste. b,c,d) Calcium concentration increases after the onset of hydration. c, d,e) Calcium concentration increases slower than in the non-retarded paste.

Impact on silicates

In the initial reaction stages of C_3S , calcium and silicon are released in solution in stoichiometric proportions. However, almost instantaneously, C-S-H begins to precipitate because of its very low solubility, so that the silicate concentration decreases rapidly, while that of calcium and hydroxides continues to increase [109]. While this is easy to explain qualitatively, doing so in quantitative terms is much more challenging and can only be done if some form of mechanism is introduced to slow down the dissolution of C_3S .

One of the first mechanism proposed for this was the formation of a diffusion layer, but failure to observe it has led it to loss of popularity. An alternative interpretation was to argue that the hydroxylated surface should be treated as a separated phase with a very different equilibrium constant (with a value of about 10^{-17} instead of about 3...). Combined the role of etch pits, kinks and step retreat impact this has led to a new school of thought in which dissolution rates are considered to change in direct response to the pore solution [226].

Based on the changes in calcium concentration, our results do suggest a decrease in the rate of C_3S dissolution (see figure 5.16). However, the question is what the reason for these changes is. One possibility is a direct impact of sucrose on dissolution of C_3S . The recent study of Juilland et al seems to exclude this. However, it should be noted that their measurements were conducted at a pH where sucrose dissociation is limited. Another possibility, is that C_3S dissolves more slowly in response to the impact of sucrose on C-S-H. This effect is subtle and deserves a separate discussion.

Indeed, if sucrose prevented C-S-H from forming, it would lead to a massive increase of silicates in solutions, up to the level of calcium, which is not the case (see figure 5.4). However, a slowing down of nucleation and/or growth kinetics would cause less dramatic increases in silicon concentrations in solution, that would nevertheless influence dissolution kinetics of C_3S by reducing its undersaturation. To evaluate the credibility of this mechanism would require accurate quantification of activity products and would only be possible by properly accounting for all possible sucrose complexes in solution, including in particular those with silicate ions. While this is beyond the scope of

Distinguishing flocculation and hydration effects on structuration

this PhD, we can comment on the fact that in the first hours of hydration, the silicate concentrations are indeed increased in solution for cases of direct addition (figure 5.4). More research is ongoing in collaboration with other PhD students to resolve this question.

Deactivating sucrose retardation

A novel result in this chapter is to show how using portlandite additions can be used to deactivate retardation by sucrose (figure 5.7). Importantly, it was shown that this resulting retardation can be quantitatively predicted on the basis of separately measured adsorption isotherms of sucrose on Portlandite. From the above our current interpretation of this process is that sucrose transfers through solution from the surface of C_3S and/or C-S-H to that of Portlandite for which it has a higher affinity.

This sucrose transfer reduces the ability of sucrose to either directly inhibit the dissolution of C_3S , or to do so indirectly by slowing down the nucleation and/or growth of C-S-H. The ability to predict the change in retardation based on portlandite and sucrose dosage was a first quantitative approach to the topic of setting on demand, which is called to play a major role in digital fabrication and to which a separate chapter is dedicated.

5.6.2. Understanding flocculation

The main observations in cement pastes without the occurrence of hydration are: In absence of hydration, storage modulus measured by small amplitude oscillatory strain is tending to a slow asymptotic rate (figure 5.9). The kinetics at which this is reached depend to a minor degree on the presence of sucrose (figure 5.9) and are not affected by the presence of PEG molecules (figure 5.11). The characteristic structuration time decreases slightly with increasing solid volume fraction and the storage modulus reached after 20 minutes at rest scales with solid volume fraction according to a power law behaviour (section 5.4.2 and figure 5.10 - left). Furthermore, as a storage modulus can be measured in all cases, the flocs forming during structuration are percolated and able to transfer a shear stress through the sample. When comparing the YODEL model and final storage modulus, a linear scaling is found, with an offset indicating that a minimum solid volume fraction is needed in order to establish a macroscopic floc (figure 5.10 - right).

Distinguishing flocculation and hydration effects on structuration

In colloidal suspensions, 3 basic types of forces determine the rheological behavior, these being Brownian, colloidal (electrical static and van der Waals) and hydrodynamic forces [199], [200]. As long as hydration does not allow for nucleation of hydrates, the van der Waals attractive force between cement grains surface defects [119], [215] is expected to be the dominating particle interaction in the system. Given the lack of effect of PEG on structuration (section 5.4.3 and figure 5.11), we can say that particle movements beyond the size scale of the PEG molecules do not contribute to flocculation. This statement is based on the fact that PEG does not adsorb and strongly increases the viscosity of the pore solution, which raises hydrodynamic forces are slows down flocculation. Additionally, non-adsorbed PEG can cause attractive depletion forces. Overall, the absence of a measurable effect of PEG on flocculation rates implies that flocculation is not driven by combinations of hydrodynamic and gravity forces (sedimentation) or by combinations of hydrodynamic and Brownian forces.

Concerning the flocculation kinetics (section 5.4.2), the changing exponent asserts that the flocculation process follows two distinct kinetic slopes of different exponent for the densely packed system and the more dilute system. By using the maximum random close packing fraction of $\phi_{max} = 0.57$ found typically for cement, a percolation limit (80% of maximum random close packing) distinguishing an initial state at rest of closer contact between particles or larger separation, predicts a change of characteristic kinetics at a solid volume fraction of $\phi = 0.46$, however the transition in this case appears to occur at $\phi = 0.50$.

The very small critical deformation found in figure 5.13 (section 5.5.2), is likely the consequence of structural breakdown occurring locally at weak contacts between flocs. As such its quantification may depend strongly on the measurement setup. However, the deformation applied until first contacts are broken (around 0.01%) may be more directly linked to the DLVO theory, considering a concentration of the deformation on the gap separating two particles. As such, the macroscopic shear strain γ_{cr} is linked to local shear strain γ_{local} in the gap by a factor depending on the radius of the hard particles a and their separation R , according to:

$$\gamma_{cr} \approx \gamma_{local} R/2a$$

Distinguishing flocculation and hydration effects on structuration

Given an average particle size of the order of $5 \mu m$ and a separation of the order of $2 nm$ (and γ_{local} assumed as 1), the critical deformation is expected to be of the order of 0.02%. With such an approach, the very small critical deformations as frequently found in oscillatory strain measurements may be justified, independently of the presence of hydration products.[50], [107], [121], [128], [203]

5.6.3.Understanding structural build-up from hydration

The main observations in cement pastes with the occurrence of hydration are: During the resting time within an oscillation measurement, the heat of hydration is directly proportional to the rate of structuration (see section 5.5.3). In other words, for any amount of hydration product formed during the resting period, the structure is strengthened proportionally. It is particularly important to realise that the structural build-up is reversible by shearing as done in the pre-shearing phase of each measurement (see figure 5.8). This shows that the quantity of hydration products formed before the last flow event plays a minor role with respect to the structural build-up occurring at rest. The very good agreement between structuration rate and heat rate of hydration both in the induction period and at the beginning of the acceleration period shows that the structuration rate of cement pastes at rest is quantitatively proportional with the formation and/or growth of hydration products. These findings are in agreement with a study of Jiang et al[123] in which strength increase at rest could be negated by mixing up to a time equivalent to the final set as measured by Vicat needle and they are also consistent with the constant yield stress period in the induction period in the work of Mantellato[227].

Concerning the physical origin of structural build-up through hydration, two contributing mechanisms need to be distinguished: growth of hydration products at pseudo-contact points and space filling by hydration products [50]. Indeed, it is understood that some hydration products such as C-S-H are growing preferably on the surface of cement particles [194], [201], with some exceptions such as with the introduction of seeds [228]. With this growth occurring at the surface of particles, it is implied that it also occurs at the contact points between particles, increasing the strength of these contacts. This explanation agrees with the found linear relationship of

Distinguishing flocculation and hydration effects on structuration

structuration rate with hydration rate (see figure 5.15). The pure increase of solid volume fraction in the pore space can be excluded as the main origin of structural build-up at rest, as build-up can be fully reversed in this time period and the solid fraction increase by hydration is small, not warranting a significant change of colloidal interactions. Chemical shrinkage could increase the interactions at contact points between particles by lowering the pore solution pressure (as discussed in chapter 4), leading to a positive pressure on the particle network. Measurements of Lecompte et al [179] show a rather insignificant reduction of pore solution pressure over similar timescales, indicating that this mechanism has a minor effect for Portland cement. The experimental evidence of this study thus favours a mechanism involving growth at pseudo-contact points.

5.6.4. Consequences for building processes

For building processes this means that as flocculation only contributes to yield stress buildup on a timescale of some 5 minutes, the main contribution in additive manufacturing processes has to come from the formation of crystallization products at the pseudo-contact points of particles, thus from hydration. As shown by Mantellato[227], in presence of admixtures these additional cohesive contact points come both from the nucleation of additional hydrates as well as from the reduction of the surface coverage of cement grains (and hydrates) by chemical admixtures.

Additionally, as most processes in additive manufacturing require a substantially long processing window of multiple hours, with similar rheological properties and controlled structuration rates, the rate of hydration at the moment of concrete placing is to be kept constant (for multiple hours). A number of different approaches can achieve this, such as continuous mixing from dry components (e.g. traditional slip-forming or dry-process shotcrete) or chemical control of hydration, by either mixing a set accelerator into the concrete shortly before placing (e.g. wet-process shotcrete)[13], [229], [230] or using a combination of set retarder and accelerator[231], [232], with the benefit of prolonging the open time substantially (e.g. Smart Dynamic Casting), which is a concept called Set on Demand.

Distinguishing flocculation and hydration effects on structuration

Given the linear relationship of structuration and hydration, any characteristic structuration kinetics needed for building processes, should be found in their equivalent hydration kinetics in a continuous mixing or Set on Demand system. In this way, using the requirements defined in chapter 3, if an immediate linear structural build-up is required, this should be ensured by an immediate and continued hydration mechanism, while if an induction period is required in a casting application, this should be ensured by a hydration step providing some induction period.

As the characteristics on the paste level dominate the properties for such generally pumpable concrete systems as shown by Yammine et al[172], despite not having studied the influence of aggregates, equivalent time-dependent structuration is expected. For the influence of superplasticizers, we refer to the work of Mantellato et al[227] in which the same general exponential dependency of yield stress with solid volume fraction was found in systems with and without superplasticizer, scaling again with the number of contact points between particles in a given volume. Based on this it can be inferred that in superplasticised systems similar initial interactions occur, at lower attractive forces due to steric hindrance [117], [233]. The interplay of hydration and such non-flocculated states is something that will deserve special attention.

5.7.Conclusions

The ability to predict strength development of cementitious materials is essential for several advanced fabrication processes such as the prediction of building rates in slip-forming, in layered extrusion and for formwork pressure control. Structural build-up is a reversible process involving the formation of a network of colloidal interactions along with the permanent formation of hydrates and their partially reversible connection to cement particles.

Using sucrose as a set retarder, it is possible to distinguish the contributions of flocculation and hydration to the structural build-up in cement pastes without substantially changing the strength and kinetics of flocculation (network of colloidal interaction). For this purpose, small amplitude oscillation rheometry and isothermal calorimetry have allowed quantifying the extent of hydration during rheometric

Distinguishing flocculation and hydration effects on structuration

measurements. Sucrose in this study puts the cementitious system to rest, strongly delaying the nucleation and/or growth of hydration products. It is shown here that apart from causing retardation, sucrose does not significantly modify the pore solution, the microstructure and the apparent viscosity throughout the induction period. In the induction period the structuration levels reaching a certain value of G' , indicating that the system's structuration is governed by a diffusion/flocculation process. Additionally, it is shown that increasing the interstitial viscosity with PEG does not modify structuration, indicating that build-up at rest is not associated with large displacements of particles but rather localised ones.

For cement pastes without superplasticizers, it is found that at long resting times, the structuration rate is dominated by the formation of hydration products and quantitatively proportional to the heat rate, showing a build-up at rest linearly proportional to the amount of hydrates formed since the last deformation, while on short time scales it is dominated by flocculation. Additionally, it is found that the amount of hydration products formed before the last deformation has a minor effect on the rate of structuration, indicating that growth at pseudo-contact points is the main contributor to structural build-up. The structuration can be associated to the growth of hydration products bridging the cement particles in the flocculated network.

Furthermore, advancements to the understanding of the working mechanism of sucrose retardation are presented. The measurements described here indicate that interactions with aluminates play a minor role in sucrose retardation as early ettringite formation is unchanged. In addition, dissociation of sucrose and its following adsorption is driven by a steady increase of pH in pore solution. The maximum saturation degree with respect to Portlandite is relatively independent of sucrose dosage, which should exclude the "Portlandite inhibition mechanism". Results presented suggest that C3S dissolution is slowed down, either by sucrose directly inhibiting it or by slowing down the nucleation and/or growth of C-S-H. More work is however needed to draw definitive conclusions on this question.

For building processes, this chapter shows that for sustained yield stress increase at rest, hydration is needed. For processes requiring similar kinetics for each layer placed,

Distinguishing flocculation and hydration effects on structuration

and fast structuration, this means that controlling structural build-up should be done through the control of hydration. Additionally, as the quantity of hydration products formed at rest is linearly proportional to the strength build-up at rest, the mechanical criteria of chapter 3 can be linearly applied to hydration kinetics. This gives clear requirements for hydration control over long timescales of concrete at rest, approaches of which are presented in chapter 6.

Chapter 6 Set on Demand systems for digital fabrication with concrete

This chapter is a draft of a review paper for a special issue on Concrete 3D Printing and Digitally-Aided Fabrication in the journal Materials.

In its current state, this chapter presents different strategies for the control of cement hydration for digital fabrication processes. It offers a perspective to achieving the needed strength build-up illustrated in chapter 3 by employing the relationship of hydration and strength build-up outlined in chapter 5.

The work presented is tied to different collaborations and the author's contributions to these are summarized below:

- Section 6.3.2
 - Alone: “negating retardation by consuming retarder”, “negating retardation by precipitation” by using CAC as accelerator for OPC, “negating retardation by changing the C/A/S/\$ balance”
 - With Anna Szabo (Gramazio & Kohler Research)
 - “negating retardation by precipitation” by using an accelerator for OPC
 - Own contribution: Help with analysis of the measurements
 - With Arnesh Das (PCBM):
 - “negating retardation by precipitation” by using CAC as OPC accelerator with C\$ addition.
 - Own contribution: Help with analysis of the measurements
 - With Mariana Popescu (Block Research Group)
 - Own contributions: concept of stiffening with cementitious materials, choice of cementitious systems in different development steps and development of processing technology.

- Section 6.3.3

Set on Demand systems for digital fabrication with concrete

- Alone: Acceleration on demand of pure CAC systems and their tailoring
- With Ana Anton (Digital Building Technologies): Layered extrusion. Own contributions:
 - analysis of hydration processes
 - measurement of strength build-up for OPC/CAC combinations
 - collaborative development of a first-generation mixing reactor for layered extrusion.
- Own contributions in section 6.4
 - With Ena Lloret Kristensen, Collaborative development of a first-generation mixing reactor for slipforming for which they also changed the accelerator compound used for the process.
 - With Ana Anton: Collaborative development of a mixing reactor for layered extrusion
 - With Mariana Popescu: Developed the mixing reactor of paste spaying for KnitCrete.
 - With Anna Szabo: Analysis of time dependent effectiveness of accelerators.
- Other sections: Alone.

Abstract

Some building processes rely on specific rates of strength build-up during fabrication and this can be achieved by controlling hydration kinetics, in particular by using set retarders and set accelerators. By combining these admixtures, both long open times, allowing prolonged processing, and rapid hardening after the onset of hydration are possible. A particular embodiment of such combinations is the retardation of a large concrete batch that can be processed over multiple hours, with the subsequent activation achieved by adding an accelerator just before placing. We refer to this concept as Set on Demand. This chapter lays out the basic concepts for a Set on Demand system and implements it for processing with multiple mineral binders and for multiple processes.

The kinetics of such Set on Demand activators and the extent of the reaction are governed by the underlying mechanisms and the mineral binder system. Set accelerators allowing rapid precipitation and growth of hydration products, such as shotcrete accelerators and C-S-H seeding products are interesting candidates for Portland cement. Besides this, set on demand can also be implemented for calcium aluminate cement, including binary and ternary blends of calcium silicates, calcium aluminates and calcium sulfates. In such systems, adding CAC to an OPC mortar shows potential for layered extrusion, while activation of CAC-rich mixes with shotcrete accelerators shows potential for coatings.

6.1.Goals for the set on demand system

For building processes as studied in chapter 3, the strength build-up after concrete placing is crucial. As the strength build-up at early age is directly proportional to the rate of hydration (chapter 5), we conclude that the nature of hydration kinetics (linear, power law or exponential) should be adjusted to match the corresponding kinetics in the considered building process. As such, if linear strength build-up is required, a linear hydration process is sufficient. Similarly, if a rate accelerating strength gain is needed, then the hydration process should also exhibit an acceleration of its rate over time. For processes where only a limited strength build-up is needed, as in layered-extrusion, a limited but rapid first strength gain can also be useful. For processes where an immediate strength build-up is to be avoided, as in slip-forming, strategies for a delay of the action of activators is required. This shows that different modifications to hydration kinetics are needed, depending on the process.

An added requirement for these building processes is to have the same behaviour for all placed layers (chapter 3). Again, given the proportionality of strength and hydration (chapter 5), this means that with respect to the time of placing the hydration rate needs to stay constant for a prolonged amount of time, something that cannot be achieved directly in the acceleration phase of hydration. This leads to the apparent conflict of having to have a single mixture with both a long open time (without changes to fluidity) and a fast strength build-up after placing (see chapter 5).

In this chapter, we present strategies that resolve this dichotomy through the set on demand concept. For similar short-term modifications of rheology using thickeners we refer to chapter 2 [19] as well as to a review by Marchon et al [111].

6.2. Concepts for hydration control

6.2.1. Fundamentals of hydration

Cement hydration is a process of complex coupled chemical reactions, involving the dissolution of several anhydrous phases into a pore solution, the nucleation of hydration products from pore solution and their subsequent growth [234]–[236]. Hydration is governed by intricate interactions of all these mechanisms and is not fully understood despite decades of intensive research. More importantly for Portland cement the detailed mechanism responsible for the transition from the induction to the acceleration period is still an open question, even when no admixtures are present [81], [235]. For advanced building processes, the main periods of interest in cement hydration are the induction period, or open time, during which concrete can be processed, and the acceleration period, in which strength builds-up. Ideally, it is at the time of placing that the transition from induction to acceleration period should be made to occur.

6.2.2. Types of mineral binders

While Ordinary Portland cement is the most used binder for concrete, it is not the only one that can be used. Alternative cements include Calcium Sulfo-Aluminate cements (CSA), Calcium Aluminate Cements (CAC), Calcium Sulfate (C\$), geopolymers or alkali activated cements and magnesia cements (e.g. Sorel cement) [237]. With respect to hydration kinetics some of these cements can be interesting.

Ordinary Portland cement consists of 3 groups of phases, the silicates (C_3S and C_2S), the aluminates (C_3A and C_4AF) and the calcium sulfates (C\$, typically gypsum, in some cases hemihydrate or anhydrite) [238]. The main phases involved in the beginning of hydration are C_3A and calcium sulfate, leading to ettringite precipitation. Additionally, C_3S dissolution leads to precipitation of calcium silicate hydrate (C-S-H) and portlandite (CH). In OPC, the hydration of the main phase C_3S is the main contributor to strength build-up, as the hydrate C-S-H fixes a lot of water, substantially increasing the volume of solids, in addition to providing a good cohesion between cement grains when it forms at their contact points [12], [123].

Owing to their rapid hydration in the acceleration phase, CAC and CSA are used for fast repair applications, such as the exchange of airport runways or for dry mix repair and reprofiling mortars. CAC's are a range of fast hardening cement used as a refractory cement or for applications requiring abrasion and chemical resistance [239]–[241]. They can have different compositions, ranging from crystalline C_3A , $C_{12}A_7$, CA, CA_2 to amorphous ones, with their general hydration being faster for higher calcium oxide contents and for amorphous cements. In contrast, CA and CA_2 have a prolonged open time. A particular use of CAC is their combination with other mineral binders, especially with OPC and C\$ promoting the precipitation of ettringite, something referred to as ettringite binders or binary and ternary binders [242]–[245]. Similar blends with the main hydration product ettringite also exist for CSA [148], [157], [246], [247]. Owing to the fast precipitation of ettringite in these blended cements, one way to achieve rapid hardening is by using CAC as an OPC accelerator [243].

In general terms, combining OPC, CAC and C\$ (and CSA as a substitute for the combination of CAC and C\$) can be represented in a ternary binder diagram, in which the range of possible formulations is shown in figure 6.1. The main hydration process in these mixed systems is dominated by the main ingredient. As such, a high CAC content can be associated in general with a fast rate of hydration. The fastest general hydration and strength build-up kinetics are thus found for CAC-rich formulations, while in the range of OPC-rich formulations, hydration kinetics can be modified by using CAC as an additive.

It has to be noted here, that not the entire ternary binder diagram offers viable formulations. A summary of this is given by Lamberet [242]. A high calcium sulfate content has to be avoided, as it can cause expansion, a process that can cause a rapid deterioration by cracking [248], [249]. In OPC-rich formulations, without the addition of C\$, sulfate depletion can occur, severely delaying silicate hydration in the OPC [243], [250]. Pure CAC systems form metastable hydration products, leading to a reduction of bound water, increasing porosity and leading to a reduction of strength between 28 days and 1 year [239]. Furthermore, for blended systems the use of set retarders is essential to provide even a short open time [251], [252].

To summarise, for the context of this thesis, ettringite binder systems can be used either as aluminate rich systems by modifying the general hydration kinetics in the acceleration phase of hydration, or as silicate rich systems by using aluminates as set accelerator.

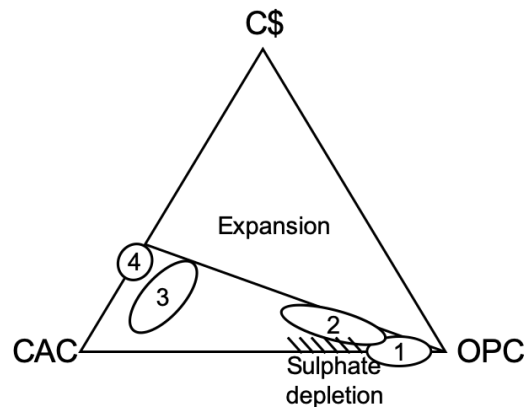


Figure 6.1: Ternary binder diagram. 1: Binary OPC rich-binder, with small substitutions not leading to sulphate depletion, 2: Ternary OPC-rich binder with sulphate balancing. 3,4: Binary and ternary CAC-rich binders. For ratios of CAC/C\$ larger than 2, expansion can occur. (Modified from Lamberet [242])

6.2.3. Delaying the time of hydration onset

In order to achieve a long open time, the onset of hydration needs to be delayed. This can be achieved with dedicated set retarders or with admixtures for which set retardation is a side effect, such as superplasticizers [205], [253]. In general, these admixtures either act on dissolution of clinker (reducing dissolution rate) or on the precipitation and growth of hydration products (preventing nucleation and/or growth). The mechanisms of action for each admixture are often still subject of debate and their effectiveness partially depends on the cementitious system in which they are used. The purpose of these compounds shall be to reduce the hydration rate in the induction period as much as possible, while causing the least possible change of fluidity, thus extending the processing time without impacting other important properties.

Dedicated set retarders for Portland cement can be found in a variety of sugars [254], [255], organic acids, phosphates, phosphonates [192], [256] and lignosulfonates. Besides set retarders, especially superplasticizers are also retarding cement hydration. Polycarboxylate ether (PCE) superplasticizers are widely used as water reducers in the

concrete industry, but it is known that at very high dosages, they retard the hydration of cement, leading to very long setting times [257], [258]. A more in depth overview is given in various review papers [19], [111], [205]. In CAC systems, similar admixtures exist with particularly potent retarders being gluconic [259], [260], phosphoric, citric [261] and tartaric acids [262], their alkaline salts and polycarboxylates [263].

For binary and ternary CAC binders and for CSA systems involving a sulphate source, the use of citric, tartaric and phosphoric acid is a common way to achieve retardation [264]. A particularly effective path for this is the combined use of tartaric acid and lithium salts [252]. In this combination, tartaric acid is understood to adsorb on calcium aluminate surfaces, precipitating a layer of calcium tartrate on its surface and preventing further dissolution [224]. At the same time lithium aluminium hydrate precipitates [252], depleting the solutions of the ingredients needed for ettringite to form. This specific combination leads to a more effective retarding effect, with less change of flow behaviour in the induction period.

6.2.4. Causing onset and accelerating cement hydration

Admixtures to accelerate hydration exist in different forms. Useful reviews of commercially available admixtures exist [13], [265]. These admixtures act through different mechanisms, generally improving the precipitation and/or growth rate of hydration products and an overview of such accelerators deemed useful for digital fabrication has been given in chapter 2 [19] and by Marchon et al. [111]. For OPC, inorganic salts exist (such as CaCl_2) that enhance precipitation by providing more ions to the pore solution, a specific case being shotcrete type accelerators [13] that provoke the precipitation of ettringite. Additionally, seeds are used to provide growth surfaces for C-S-H [266]. For CAC systems, similar seeding products exist in the form of lithium salts, provoking the precipitation of lithium aluminium hydrate.

6.3. Setting on Demand

6.3.1. Achieving the strength requirements

To achieve the strength build-up kinetics needed by advanced building processes, the hydration rate is required to be equal at the time of placing and thereafter for each layer with respect to when it was placed (chapter 5). The common ground of providing the same kinetics for each layer is achievable with two different approaches, the continuous preparation of small quantities of concrete with high early age strength development (controlled setting) [32], or the continuous activation of small quantities of concrete taken from a larger retarded batch [9], [31], [147], [267]. The later approach is what we refer to as Set on Demand. Both methods have specific advantages and challenges for processing, something not covered here.

Generally, for continuous concrete preparation, the strength requirement kinetics can be achieved by using the correct binder system (as in 6.3.2) and/or by the right choice of accelerators (as in 6.3.4) [148]. For Set on Demand, where a single large batch of concrete is used, one must first extend the open time (as in 6.3.3). This ensures that the cementitious system does not change substantially in terms of workability in the timeframe of manufacturing. To achieve the strength requirements, an activator (as in 6.3.4) is added shortly before placing, which is the method mainly investigated here (see figure 6.2) and which we have implemented for the building processes slipforming, for layered extrusion and for coatings. This can be achieved by negating retardation, by precipitating a minor phase or by accelerating the main hydration phase. Each of the methods gives different types of strength build-up characteristics.

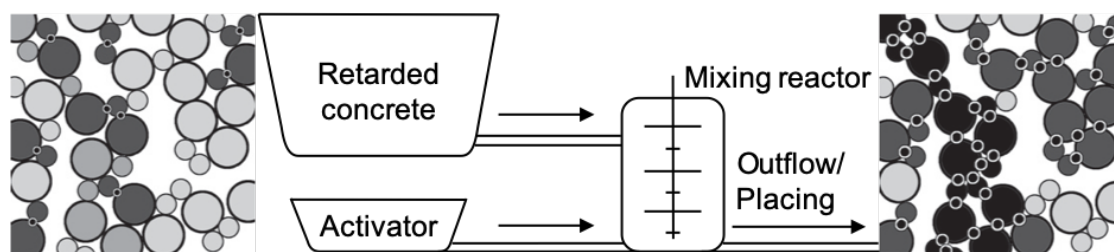


Figure 6.2: Set on Demand application concept with a retarded concrete batch and an activator, pumped into a mixing reactor, homogenized and then placed. With this approach, structural build-up can occur on demand from a retarded concrete batch (microstructure development subfigures taken from [12]).

6.3.2. Negating retardation on demand

Negating retardation by consuming the retarder

As shown in chapter 5, we have shown that a Portland cement can be retarded by sucrose addition, the effect of which can be negated by introducing a sufficient quantity of portlandite [77]. In this case, adsorption on portlandite is used to decrease or eliminate the retarding action of sucrose, restoring the non-retarded hydration kinetics.

We have also shown that the same type of behaviour can also be achieved by using PCE based superplasticizers as retarders and using their affinity for swelling clays such as bentonite (see figure 6.3) [77]. In this case, the intercalation of polyethylene oxide side chains into the interlayer region, is used to move the PCEs off cement grains, thus negating their inhibiting effect on C_3S dissolution [268]–[270].

The advantage of these methods lies in the consumption of the retarder, merely restoring the neat Portland cement hydration kinetics, something that in consequence is not prone to cause excessive acceleration when the activator is overdosed. However, both of these specific combinations have proved to be unpractical due to the rather large quantities of activator and water they call for [19].

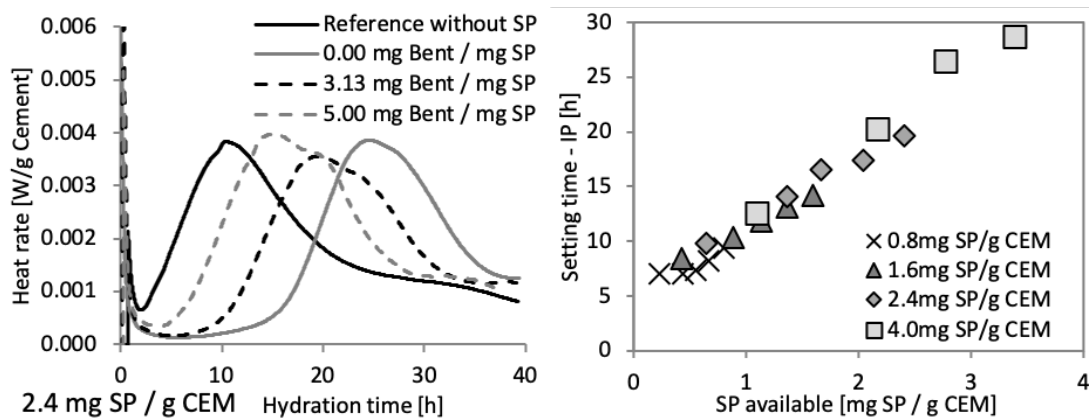


Figure 6.3: (left) Heat release of cement pastes retarded with a PCE based superplasticizer with the subsequent addition of bentonite, causing a partial cancellation of the superplasticizer retardation. (right) Setting time as a function of the superplasticizer content remaining in solution, allowing a control of the onset of hydration [77].

Negating retardation by precipitation

In retarded Portland cement systems, the action of the retarder can also be partially or fully negated by introducing a species causing the precipitation of hydration products [173], [195]. This can be achieved with different types of activators, prominent products being solutions containing aluminates and suspensions of calcium aluminate cement [13], [157]–[159], [243], [244]. In our work we have demonstrated this previously undocumented behaviour in multiple instances, first in the work of Anna Szabo (figure 6.4.a), where an accelerator is consuming the retarding action of sucrose [195], and where this is used for the fabrication of thin folded structures, as well as work original to this thesis (figure 6.4.b), where the addition of a CAC suspension to a retarded OPC mortar 1 hour after mixing is studied and used for layered extrusion processing. Additionally, in the work of Arnesh Das (figure 6.4.c) we have shown that the same approach of adding a CAC suspension to a mixed system of OPC and C\$ as introduced in figure 6.1, gives similar results, mainly causes ettringite precipitation and leads to a ternary OPC-binder as introduced in figure 6.1, in which OPC can be substituted up to 20%, without causing silicate retardation.

The accelerator acts here in two ways. In the first phase, it increases the precipitation of hydrates and causes a yield stress increase (needed for a building process such as slipforming or layered extrusion). This phenomenon is of temporary nature and the heat rate decreases towards a low and steady state value, characteristic of an induction period, about 1 hour after activation. The yield stress gain is however maintained as it depends on the cumulated amount of hydrates produced. This initial phase is followed by an acceleration phase of the silicate hydration, which occurs earlier than in the retarded mortar. Both these effects are intensified by increasing accelerator dosage. In terms of underlying mechanisms, it can be inferred that the retarding admixture is consumed by adsorption on a hydration product or that more nucleation/growth sites become available for hydration onset.

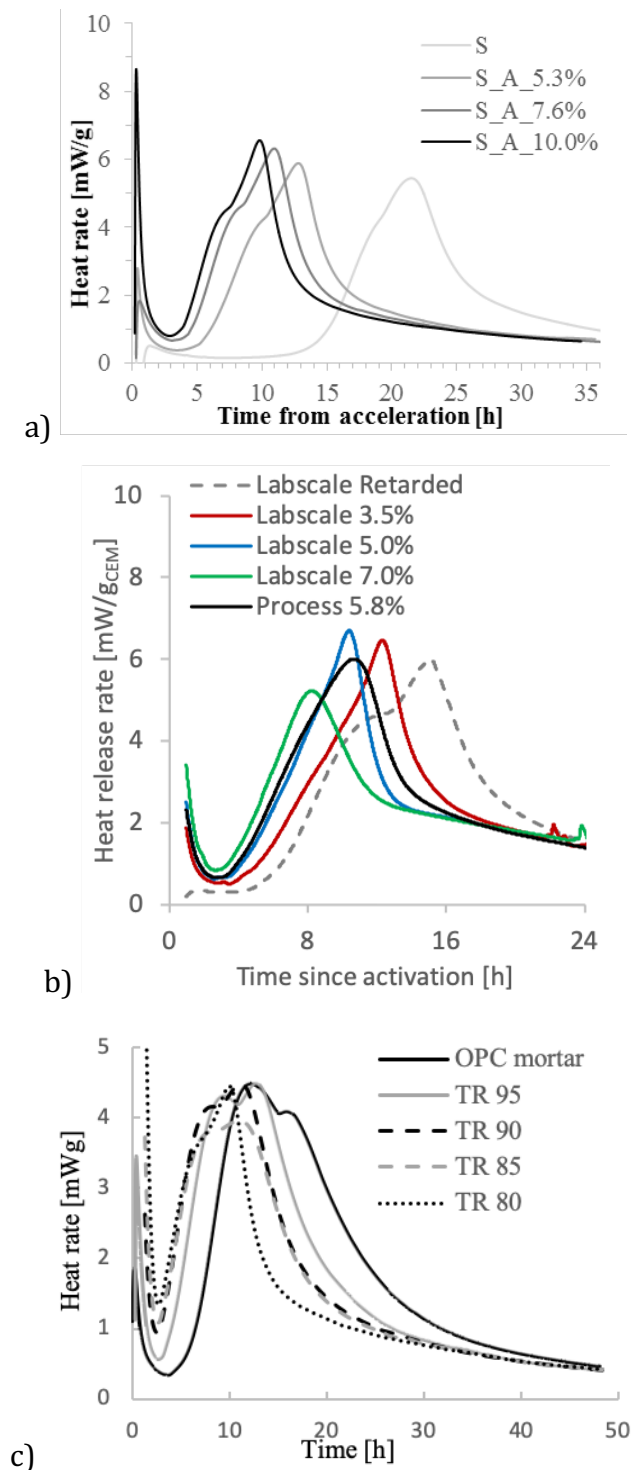


Figure 6.4: Heat release rate of OPC mortar retarded with sucrose and containing PCE based superplasticizer, and activated 1h after water addition. a) with an accelerator solution,[195] b) with a CAC suspension retarded with sodium gluconate, c) with a CAC suspension retarded with sodium gluconate, but where the OPC mortar contains anhydrite (C\$) at a final mass ratio of CAC/C\$ of 2[173]. The activator addition leads to a precipitation in the first 2 hours after activation, and a partially negated retardation, compared to the non-accelerated mortar. With increasing dosage this negating effect is more pronounced, as more hydration products are formed (higher heat rate in first hour). Sulfate depletion is not observed in any of the above examples.

The advantage of this method lies in the combined precipitation of a hydration product, leading both to a yield stress increase and the faster onset of Portland cement hydration. Importantly, when ettringite is precipitated (as with shotcrete accelerators and CAC), sulphate depletion should not occur before the main hydration of silicates. This means that the silicate hydration will not suffer the massive retardation that aluminium ions could otherwise cause in the so-called situation of silicate-aluminate-sulphate imbalance [230], [244], [250] In the example given in figure 6.4.b, this is not occurring up to an OPC substitution of 7%.

Negating retardation by changing the C/A/S/\$ balance

In set regulated CAC systems (as introduced in 6.3.3) retardation is achieved in parts by consuming Al in a hydration product LA_2H_{10} , creating a pore solution similar to the one found during the induction period in a Portland cement, something used in practice for the casting of fast drying screed underlays. A possibility to reverse this effect lies in the addition of aluminium salts, such as sodium aluminate, providing the previously consumed ions, to form ettringite, something not currently documented in academic literature. With this method, the main hydration kinetics of the CAC system can be triggered (see figure 6.5).

The advantage of this method lies in the activation of the main hydration kinetics of a rapid hardening cementitious system and is as such of greatest interest for coatings, where hydration competes with drying. Work on this approach is preliminary, but has nevertheless contributed to enable the realisation of KnitCandela, a homage pavilion built in a collaboration between ETH Zürich and Zaha Hadid Architects, based on the KnitCrete technology [151]. KnitCrete is a building process, where a bespoke knitted textile is tensioned into shape and stiffened with a coating. In this project the binary binder from figure 6.5 was sprayed as a stiffening coating on the textile, subsequently allowing concrete placing [271].

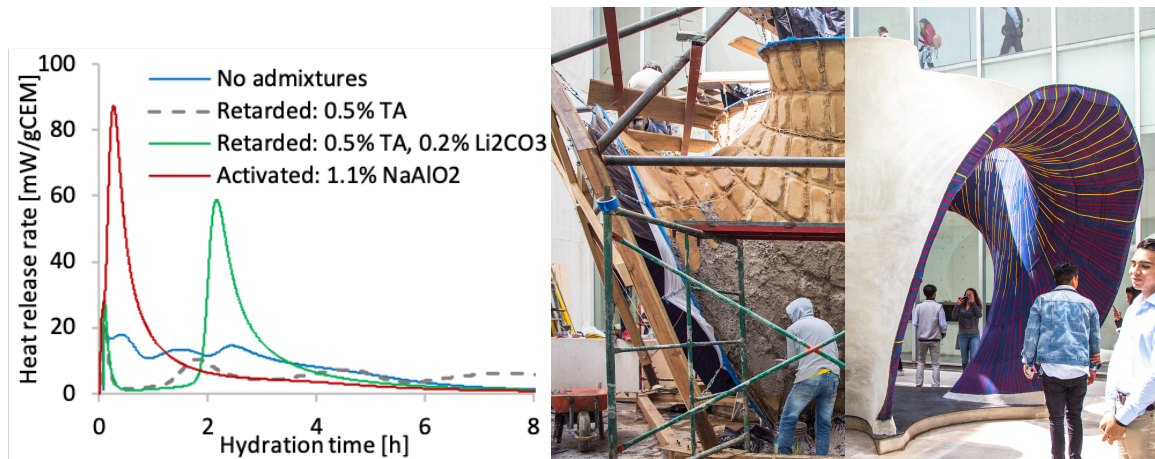


Figure 6.5: (left) Heat release of a binary binder paste, consisting of the main phases $C_{12}A_7$ and hemihydrate. The set regulated cement paste contains Li_2CO_3 and tartaric acid for retardation. In the activated paste a solution of $NaAlO_2$ is added, 15 minutes after initial water addition, negating the retardation with the entirety of the main hydration phase occurring within the first hour upon activation. (right) KnitCandela, a flexibly formed thin concrete shell, built on an ultra-lightweight knitted formwork (during construction and finished). We have used a binary binder based coating as a stiffening element between textile and concrete (visible as an orange coating during construction), (pictures by Mariana Popescu) [271].

6.3.3. Acceleration on demand

Precipitation of a secondary phase

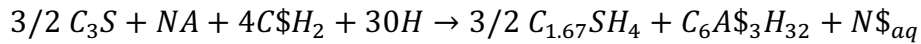
Instead of triggering the start of massive hydration, in many cases it can be sufficient to induce the faster formation of a small quantity of hydration products. This can be achieved by adding compounds that can release the aluminates and/or silicates missing in the aqueous phase to form hydration products. Prominent examples of this are shotcrete accelerators, which are commonly used in delayed addition with a similar set on demand goal [13]. While they are most often concentrated solutions of aluminium salts, they work through an overall similar principle as CAC suspensions, as they also provide aluminium or aluminate ions to the aqueous phase.

Bringing together the concrete and its pore solution with the activator, the ingredients needed to precipitate ettringite are combined and this phase can precipitate. However, unless C_3A is the source of aluminates, an additional calcium source is needed to form exclusively ettringite. In Portland cement systems, this balancing occurs through the silicates, with C_3S as the most reactive phase. Therefore, depending on the product

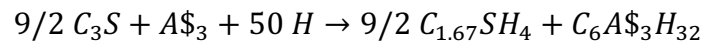
Set on Demand systems for digital fabrication with concrete

used, the kinetic path and ratio of hydration products may vary. In this regard, we note that depending on the additive used, the following reactions are expected to occur.

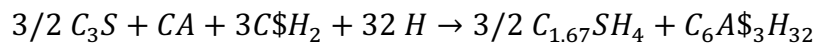
For alkali-rich shotcrete accelerators (example $NA = 2 NaAlO_2$, with $N = Na_2O$) the following reaction should take place:



For alkali-free shotcrete accelerators (example aluminium sulphate: A_3) the following reaction is expected:



For activators consisting of CAC suspensions (main phase CA) the following reaction is expected:



This simple analysis shows how aluminate rich accelerators, as CAC suspensions or alkali-rich shotcrete accelerators, can consume the gypsum from an OPC, possibly leading to the issues of sulfate depletion explained above. It also shows how similar all these activators are and that all of them need some silicate hydration to take place. Especially aluminium sulphate may be interesting in this respect as it leads to a larger quantity of C-S-H than other activators, a phase that due to its growth on the surface has good cohesive properties [12], [123].

Another very promising candidate are CAC's as they provide largely the same hydration products as alkali-rich activators, with the added advantage that not all aluminate ions are immediately available to form ettringite, giving a priori a slower initial reaction. As shown in figure 6.6, this type of accelerator leads to a strength build-up that starts directly from the time of addition. Moreover, we note that for this type of accelerator, the strength build-up in the first hour is largely linear.

The general advantage of this method is that it leads to a rapid precipitation of hydration products, which is particularly useful for processes needing strength to build-up from the time of placing, examples thereof being layered extrusion and shotcrete. We found that the combination of CAC and OPC had the added advantage of a comparably slow initial build-up, making it particularly useful for layered extrusion. We have implemented the approach using CAC as accelerator for the layered extrusion process at ETH in collaborative work with the group of digital building technologies and in particular Ana Anton and we achieve characteristic strength build-up shown in figure 6.6 [105], [272]. At the time of writing this manuscript, a series of columns 2.7 meters high has been produced as a proof-of-concept (see figure 6.7) for a tower to be built in the East of Switzerland with a height of 27 meters.

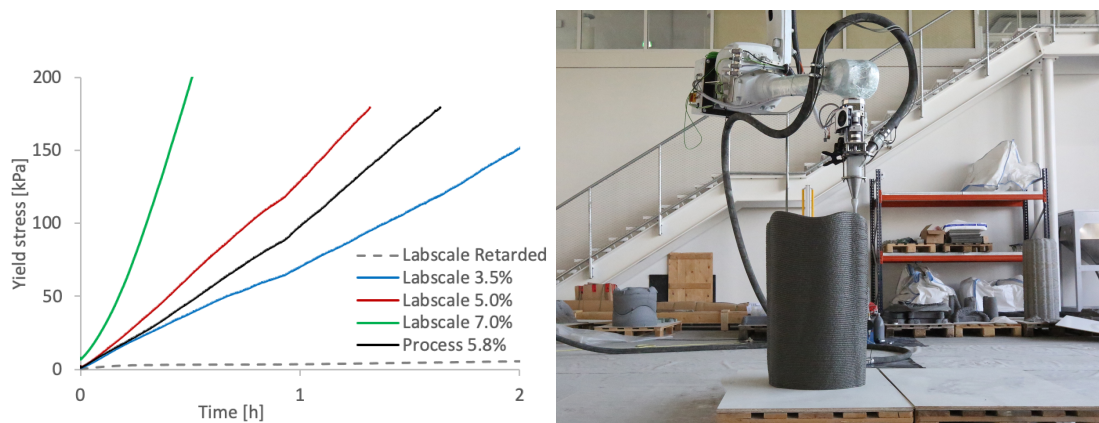


Figure 6.6: (left) Strength build-up of the mortar from figure 6.4 in the first 2 hours since activation, measured with the slow penetration test from chapter 4, showing a linear strength build-up from the time of activation. (right) We are using this approach for the realisation of articulated concrete columns and it has allowed a vertical building rate of 3m/h.[272].



Figure 6.7: Fabrication of 2.7m high articulated columns, by layered extrusion, using a retarded OPC mortar and a CAC suspension as accelerator, with previously fabricated columns in the background for reference of process robustness (picture by Axel Crettenand). Fabrication time per column is approximately 2 hours, with all mortar coming from a single batch. At the time of placing, this mortar can self-support not more than 10cm.

Accelerating the main hydration kinetics

Contrary to negating the retarding action of a set retarder, activation can also occur by accelerating the main hydration kinetics of the mineral binder. For Ordinary Portland cement this was studied by Thomas et al [273] using a combination of sucrose (set retarder) and C-S-H seeds (set accelerator). As shown in figure 6.8 (left) this allowed to extend the open time of Portland Cement by more than 30 hours (from blue to green curve) and activating hydration by adding the seeds (from green to red curve). This principle was used successfully in the project Smart Dynamic Casting by Lloret et al [33]. A practical drawback of this specific combination is the rheology change owing to the large quantities of added superplasticizer and water contained in the accelerator as already mentioned in chapter 2.

In CAC mortars, the same principle can be employed. Here sodium gluconate is used as an effective retarder and acceleration is achieved by adding a lithium hydroxide solution on demand (see figure 6.8 – right) [260]. This is known to cause a massive precipitation of aluminium hydroxide [252], [260] and thereby to significantly increase the rate of reaction in the main hydration phase, the combined action for a set on demand

process is however again not documented in academic literature. A practical drawback of this specific combination is the long-term conversion of metastable aluminate phases leading to a long-term strength loss [239]. For this reason, we have used pure CAC binder systems mainly as proof of concept materials. The simplicity of the binder system, with essentially only one mineral phase (CA) and the existence of powerful set retarders and accelerators has proven to be invaluable for early development steps for a set on demand spraying application, which then evolved into the system shown in figure 6.5. We have also tried this same principle for printing CAC mortars by layered extrusion, with promising results on lab scale (see figure 6.9 - right), but that couldn't be applied in the process (insufficient retardation leading to hardening in the pump).

The general advantage of accelerating the main hydration kinetics lies in the exponential strength increase typically observed in the acceleration phase of hydration, something that for all building processes appears to be beneficial (see chapter 3).

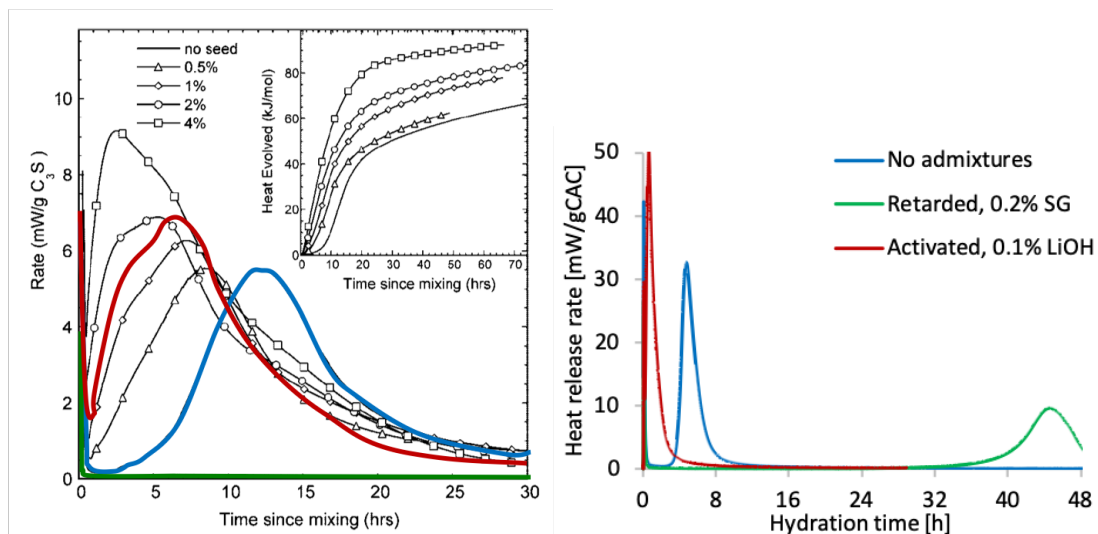


Figure 6.8: (left) Heat release rate of an OPC paste retarded with sucrose and activated with C-S-H seeds, adapted from Thomas et al. [273] (blue: no admixtures, green: retarded, red: activated). (right) Heat release rate of a CAC mortar retarded with sodium gluconate and accelerated with a LiOH solution. In both cases, a long retardation is cancelled by accelerating the main hydration mechanism.

Tailoring of activation

When an immediate strength build-up upon activation needs to be avoided, such as during the time in the formwork for slipforming or inside the mixing reactor, results from this thesis show that interactions of set accelerators and retarders may be utilised. As an example of such a behaviour, for CAC systems, this can be achieved by formulating the set activator as a combination of the set accelerator LiOH, known to cause the precipitation of aluminium hydroxide, with the set retarder sodium gluconate (SG), known to prevent the precipitation of that phase (see figure 6.9). We can show that the onset of hydration can then be controlled by modifying the ratio of sodium gluconate to lithium hydroxide. Again, here we merely show a proof of concept for a non-immediately acting accelerator, something that would be most useful if achieved in an OPC system.

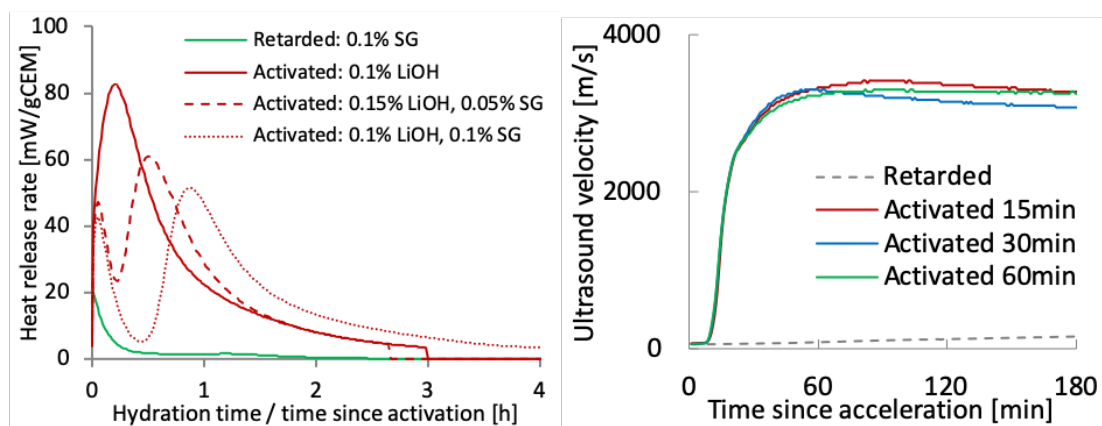


Figure 6.9: (left) Heat release rate of a CAC mortar retarded with sodium gluconate to which an activator is added consisting of a blend of sodium gluconate and lithium hydroxide. With 0.1% sodium gluconate hydration is delayed for 24 hours. Upon activator addition, the main peak of hydration occurs within one hour. With 0.1% LiOH the onset is immediate and a single hydration peak occurs. By adding a small quantity of sodium gluconate into the activator, the open time is prolonged after activation. (right) Strength build-up qualitatively measured by ultrasound travel speed, for the activated mortar (0.15% LiOH, 0.05% SG) from the figure on the left, activated at different times. The time hydration onset is robust despite the change of acceleration time and strength build-up occurs rapidly.

6.4. Practical aspects

6.4.1. Set on Demand processes at work

An early embodiment of set on demand systems is wet process shotcrete, where an airflow containing accelerator is intermixed with concrete [229]. For applications in digital fabrication, intermixing with airflow was not possible. A technology having developed Set on Demand strategies early on, was Smart Dynamic Casting, a robotic

slipforming process developed at ETH Zürich [33]. At the time, when this thesis started, SDC was the only documented process in digital fabrication to have used a Set on Demand approach, but intermixing of concrete and accelerator occurred manually in a laboratory mixer and could not be automated, owing to a significant yield stress drop with the addition of C-S-H seeds (section 6.3.3). With the change to a different commercial accelerator, maintaining a similar yield stress before and after activation and being used in most work since, we were able to implement a mixing reactor into the process [9], [103], [274].

For processes, other than slipforming, academic literature with respect to Set on Demand approaches is scarce. An early example of combinations of retarders and accelerators used in layered extrusion can be found in the work of Lee et al, however this appears to not have been used for setting on demand as defined here [7]. In academic literature, the work of Gosselin et al [31] shows a processing setup with two pumps feeding to a nozzle (shown in chapter 2 and similar to figure 6.2) but does not describe the composition of the activator. The work of Esnault et al [147] shows a lab scale processing setup and gives an example of an alkali-free shotcrete accelerator being used. In patent literature, the Set on Demand approach is notably claimed by Sika, showing a mixing reactor [275], protecting a range of accelerators [276] and using an alkali-free shotcrete accelerator for acceleration in the examples given. At the time, when work at ETH started on layered extrusion (beginning of 2018), only the publication of Gosselin and the Sika patent on intermixing were available. For spraying of CAC-rich binders, academic publications of set on demand materials are not known to us. In both cases, we developed the mixing reactors based on lessons learnt from work on slipforming.

6.4.2. Mixing chamber

For Set on Demand activation in building processes, concrete is activated in a mixing chamber. The design of such a chamber is very important as it must in particular provide for a good homogenisation of both components. At present, all accessible documents concerning a Set on Demand approach [9], [31], [147], [275] indicate that homogenisation is best achieved by active mechanical mixing in a chamber and by positioning the mixing chamber close to where concrete is placed, as explained in chapter 2. It appears that at least three companies have integrated set on demand processing in their layered extrusion process, these being XTreE (publications of Gosselin et al [31] and

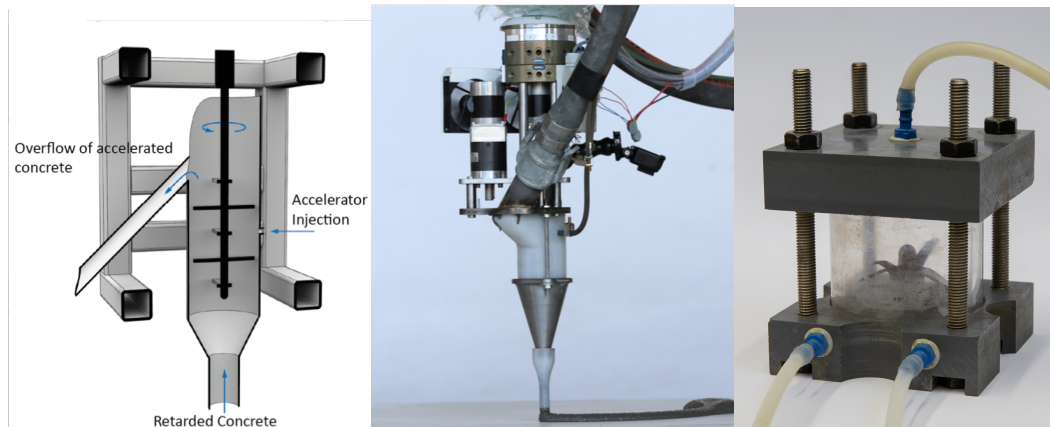


Figure 6.11: Mixing chambers in use at ETH for the processes:

a) Slipforming (SDC): Retarded concrete and accelerator are pumped into the mixing reactor and are mixed with a pin mixer type tool. Activated concrete slides on a chute into the formwork positioned below.[274] (collaboration with Ena Lloret Kristensen)

b) Layered Extrusion: Retarded concrete and accelerator are pumped into the mixing reactor from the top (large pipe for mortar and dark pipe going into the white cylindrical mixing chamber) and are mixed with a pin mixer type tool. The setup weights approximately 4kg (collaboration with Ana Anton).

c) Spraying coatings: Retarded cement paste and accelerator are pumped into the mixing reactor through the pipes from below, are mixed with a blender type tool. The outflow occurs at the top. This type of setup is used for Set on Demand coatings for KnitCrete.

6.4.3. Dealing with time dependent effectiveness of activators

During development for slipforming, we (measurements by Anna Szabo in ongoing work) have observed that certain admixtures are more effective when added earlier in the process (e.g. 1 hour after mixing, compared to 3 hours after mixing), while others become less effective[104]. To understand this variation, we consider that in the induction period of hydration, hydration is not entirely stopped, but rather very slow. A small change of pore solution ion concentration occurs, as shown in chapter 5. This can lead to a decreasing availability of certain ions such as $\text{Al}(\text{OH})_4^-$ and SO_4^{2-} . If these ions are less available at later age, we can expect that an accelerator needing these ions to form hydration products becomes less effective. This trend is what we observed for a commercial accelerator containing among other calcium nitrate. The contrary trend should occur when we consider that for retarded concrete, as it hydrates in the induction period, the retarder will become less effective over time. Therefore, lower amounts of activator should be needed to achieve the same kinetics, when it is added later in time. This is what we observed when we used shotcrete accelerators [104]. Such issues can have major effects on the effectiveness of some activators as shown by Szabo et al [103],

[104]. The selection of efficient accelerators that work well in delayed addition, with low sensitivity to the time of addition of the activator and low sensitivity to composition variability remains a challenge.

6.4.4. Applying Set on Demand systems

In the scope of this thesis, I developed different Set on Demand compositions which, most often in collaboration with other groups, were applied in multiple building processes. While the applications might seem weakly connected, the enabling technology for these processes is the same, this being a controlled transition from fluid to solid. This also shows in the use of the same concepts for processing, specifically the intermixing with an accelerator in a mixing reactor. These concepts will remain true for any process and highly viscous material for which such a phase transition from fluid to solid will be needed for future processes.

With respect to the use of admixtures, the right choice of compounds, giving the desired kinetics needs to be found case by case. The concepts for distinction of chemical processes that I introduced in section 6.3.3 can help finding promising candidates by informed trials. An example of such considerations is the choice of CAC suspensions for layered extrusion, a system in which aluminate ions are not immediately available to form ettringite, as the clinker dissolves over some period of time, this giving a rather linear strength build-up response with a negligible rheology change on contact of mortar and accelerator, achieving exactly the desired behaviour.

An important lesson learnt for development in cementitious systems is the need for reliable and simple measurement methods of the target properties, such as introduced in this thesis in chapter 4 (penetration test) for strength build-up. Such methods are needed in our material systems, as we use "messy" ingredients, involving non-spherical particles, polydispersity, multiple hydrating phases and more, all of which affect processing properties. In such systems, using simplified conceptual descriptions can help bridge some of the gap from fundamental understanding to application but pre-tests will remain essential. This subject will become ever more important, as we transition from having understood the subject to wanting to reliably use the materials in practice.

6.5. Conclusions

For building processes relying on strength build-up during fabrication, the strength development can be achieved by controlling hydration kinetics. This can be done by using set retarders and set accelerators. Using combinations of such admixtures, both a long open time, allowing prolonged processing, and a rapid hardening upon onset of hydration are possible. A particular embodiment of such combinations is the retardation of a large concrete batch that can be processed for multiple hours, with the subsequent activation caused by adding an accelerator just before concrete is placed, a concept referred to as Set on Demand.

The kinetics of such Set on Demand activators and the extent of the reaction are governed by the underlying mechanisms and the mineral binder system. Set accelerators allowing rapid precipitation and growth of hydration products, such as shotcrete accelerators and C-S-H seeds are interesting candidates for Portland cement systems. Besides this, set on demand systems can also be implemented for calcium aluminate cements as well as binary and ternary binders of calcium silicates, calcium aluminates and calcium sulfates. In these systems, using the blended system directly for set activation, as when adding CAC to an OPC mortar shows potential for layered extrusion and the activation of CAC-rich mixes with shotcrete accelerators shows potential for coatings.

This thesis, has given support to using C-S-H seeds and shotcrete accelerators for Portland cement for slip-forming and digital casting. I have also developed and used CAC pastes as accelerator for Set on Demand layered extrusion and supported in the process implementation, which allowed to build 2.7m high columns using only one concrete batch. Finally, I have developed and used a Set on Demand CAC-rich system for the KnitCrete process, in which a cementitious material stiffens a textile to form a stay in place formwork.

Chapter 7 Conclusions and Outlook

7.1. Main outcome

The main outcome of this thesis has been the establishment of a direct link between hydration control methods and the structural build-up needed for digital fabrication processes. This was achieved by understanding the needs for structural build-up during fabrication, their relationship to hydration kinetics, and by outlining the possibilities to modify hydration on demand. Thereby, it was possible to achieve the structuration rates sought in various advanced building processes. The fundamental knowledge that I was able to gain through this work, was then applied in the development of slip-forming, layered extrusion and spraying applications. For this I tailored the strength evolution specifically required for the building process by causing hydration with Set on Demand approaches.

In particular, this was achieved by expressing the building processes and its requirements in a common theoretical framework, which makes it possible to define structuration rate requirements based on physical failure criteria. With this, it was possible to show that generally, strength-based criteria, including self-support, structural breakdown and formwork pressure lead to a requirement for a linear strength build-up after concrete placing, while to avoid self-weight induced buckling, the strength needs to grow with the third exponent of height. In addition, for shotcrete, it is shown that increase of instantaneous yield stress is required, while for thin coatings it is a rapid binding of mixing water into hydrates that is most needed. Both processes are linked to a rapid increase of solid volume fraction, but with different kinetic requirements, which may or not be achieved with similar families of chemical compounds.

For the characterisation of strength increase at rest, a slow penetration test capturing yield stress evolution at continuously over time and in the range of interest has been introduced. This method shows a good agreement with discrete methods such as Vane and uniaxial compressive strength. Also, the conversion factor from the penetration force to yield stress can be predicted with a soil mechanical approach. With this, the basis

Conclusions and Outlook

is set to use this characterisation method as a quality control and feedback tool during fabrication.

With the finding that structural build-up at rest is largely proportional to hydration product growth, with much of hydration before placing being negligible, a basic strategy for controlling hydration and thereby structural build-up was devised. With this, it is possible to relate linear strength build-up requirements to a constant rate of hydration, something possible to achieve with a minor hydration step, while kinetics with an exponent of 3 require the onset of the main hydration step to be reached, after which hydration kinetics are known to progress exponentially. With this basic finding, the right accelerators and cementitious systems can be selected for various digital fabrication processes. It is also shown that when the same structuration rate is required for every layer placed, the hydration rate has to remain constant for an extended timeframe, something that is achievable with a Set on Demand based processing.

The strategy for structuration control is finally substantiated by an outline of hydration control strategies. These involve different cementitious material combinations, offering a wide range of possible hydration kinetics that can be further levered by set retarders and accelerators. The concept mainly investigated here, is the preparation of a large quantity of set retarded concrete that is activated on demand shortly before placing, by either accelerating hydration with a set accelerator or by removing the effect of the set retarder. This concept is referred to as Set on Demand. It is achieved for Portland cement and for faster setting cements of the calcium aluminate family, depending on the kinetics needed by the building process, including some first tools for the tailoring of activation kinetics.

Using the Set on Demand approach, I developed different Set on Demand compositions in collaborative with other groups, for which the building process requires a fluid to solid transition. For slip-forming, we have developed a mixing reactor setup and material system that is compatible with rheology requirements before pumping and while casting. With this process, we have built reinforced facade elements of variable geometry installed in the dfab house at NEST in Dübendorf. For layered extrusion, we have developed a continuous processing setup, with a material system giving linear

strength build-up after activation and we have built articulated columns of 2.7m height with a single concrete batch, without interruptions and within 3 hours of printing. These columns are as of 2019 on exhibition in Riom as part of an open-air theatre. Finally, for spraying of coatings, we have developed the process KnitCrete, for which I developed a CAC-rich Set on Demand system for the stiffening of textiles. These textiles are then used as a stay in place formwork for freeform concrete structures. With this process, we have built KnitCandela inside the museum MUAC in Mexico City as part of an exhibition of Zaha Hadid Architects.

7.2.Importance of structural build-up

Structural build-up is found to be a make or break property for a multitude of building processes currently in development. It is tied to strength requirements during fabrication governed by many failure criteria and must not be achieved while the material is in the processing line. Given this apparent incompatibility, this strength build-up has to occur over time and after placing.

The way to achieve this structural build-up involves multiple steps of understanding and implementation. Given a building process and its manufacturing rate, from chapter 3 the requirements of strength evolution can be derived. To fulfil these, the general linear relationship between strength evolution and hydration can be used, knowing from chapter 5 that strength build-up at rest is dominated by hydration product growth. Selecting the correct combination of set retarders and accelerators to achieve the desired kinetics and by extension the desired strength build-up is made possible by the material combinations described in chapter 6 (Set on Demand). Processing such admixture combinations can be done with mixing chambers built for a specific range of processing rates and application. Finally, strength build-up characterisation and quality control measurements can be performed using the method described in chapter 4. With this a framework is established for building with Set on Demand materials in digital fabrication with concrete for cases where early-age strength build-up is of interest.

7.3.Outlook

Despite the rapid development in digital fabrication with concrete and the contributions from different disciplines, the research field appears to only just grasp the

challenges to overcome in order to bring these new advanced building processes into practice.

Applying structuration control in practice

The results documented in this thesis show the potential of hydration control methods for achieving the type of early age strength build-up needed during fabrication. In the long-term, for these advanced building processes to find widespread **applicability**, concrete processing has to become as **simple** and **reliable** for a practitioner as the casting of regular concrete. This means having **robust** formulations that are able to **deal with** raw material **variability**, especially with respect to yield stress at placing time and combined hydration and strength development after that. Beyond this, formulations need to be reliably and robustly compatible with processing equipment. For this we need simple and reliable tests to assess mixing times, pumping, stability under pressure and stability after placing. For some of these cases of “yes-no” answers, I will pursue simple rheological testing methods accessible to practitioners.

If advanced building processes involving early age strength should reach any form of competitiveness with traditional fabrication techniques, reliance on specific formulation ingredients required in large quantities has to be eliminated as much as possible. This means, accepting that the main ingredients cement, gravel and sand but also fillers and supplementary cementitious materials must be locally sourced and not specially treated, such as dried aggregates. A strategy for effective mix design adaptations to **local ingredients** without relying on too extensive pre-testing is needed as well as simple and reliable testing of transport concrete when this is the selected option. For smaller scale applications, robustness may be gained through dry mortar packaging, something commonly used for similar compositions such as repair mortars, but at higher cost.

While development of structural build-up methods is targeted for digital fabrication processes, the advancements on **hydration control**, structural build-up and processing setups can be rescaled **for traditional casting** processes. The most obvious example of this would be the introduction of Set on Demand processing as developed for Smart Dynamic Casting and applied to traditional slip-forming, enabling smaller

characteristic cross-sections. Other applications may involve quicker mould removal in pre-fabrication or more control for the onset of hardening in road slab repairs.

Where to apply digital fabrication in practice

It remains an open question if these novel processes will develop into **on site** fabrication processes **or** remain in **pre-fabrication**. The answer to this question is tied to the approach of either fabricating transportable elements in a more controlled environment or aiming at full structures in-situ. Different levels of **environmental control** in this respect need to be considered: controlling formulations (material mixed inhouse or ordered based on required properties), controlling logistics (transport concrete or inhouse), dealing with temperature (minor fluctuations, possibly compensated by heating versus larger fluctuations difficult to buffer without building a large enclosure), controlling worksite (level factory floor versus irregular conditions on a job site in-situ). Delivering robust concrete formulations for advanced building processes with local ingredients to a worksite will be a major challenge considering the narrowness of acceptable properties. Generally, the most ambitious application of on site in-situ fabrication with transport concrete ordered by properties will clearly remain problematic at best, at least as long as pre-fabrication continues to struggle with material control despite its much more favourable conditions. The current focus of the research effort at ETH and the work in this thesis is in prefabrication, however a transition to on-site conditions may be an interesting future challenge.

As for the possible uses of advanced building processes, the **competition with traditional fabrication techniques** will dictate the range of meaningful applications. The types of concrete used for digital fabrication cannot compete in price directly with regular concrete due to their more limited aggregate packing fraction. Indeed, this means that more cement and admixtures are needed per unit volume, so that the corresponding price increases. However, there is some potential to compete with pumped concrete on these terms. More broadly however, building the same wall sections as with standard modular formwork systems is unlikely a viable perspective as the price savings of assembling formwork and casting regular concrete is probably easily offset by more expensive concrete formulations, investments in processing equipment and currently unknown solutions for reinforcement. This challenge for market entry is still faced by the

substantially better understood self-compacting concrete formulations. **Viable** applications are more likely found in **difficult to mould geometries**, where moulding dominates the structure's total costs, where moulds are used only once, are geometrically complex or where moulding is geometrically impossible. Academic advancements should keep this perspective of geometrical complexity in mind as a targeted goal.

As such, advanced building processes can open doors to previously unrealistic geometric detailing, such as structural geometry optimisations, funicular structures, shells, other weight optimisations or functional integration[15], [27], [277]. Material savings would then be enabled by the leaner structures that could be produced. Moreover, rather than trying to hide artefacts of advanced building processes, such as the layer interfaces of layered extrusion, these features can be used to add to the expression. Adding also to the expression of building components, the possibility of including ornaments at little added costs, can provide the added value to justify higher construction costs, compared to traditional geometries.

Making processes work

On more technological and scientific grounds, knowing in advance if a building component can be manufactured with advanced building processes represents an essential basis for industrial applications. Here, the research field will have to **combine material characterisation** techniques **with** material **models** capable of simulating the evolution of material properties from the time of placing and during fabrication. First steps in this direction have been proposed by Wolfs et al [8] using FEM tools with material strength and Young's modulus as input data. Their approach however largely avoids the question of material evolution, while Suiker [278] has included minor material evolutions. In both cases however, the work is still restricted to rather simple straight geometries and linear elastic behaviour. In the present PhD, the material evolution kinetics and process requirements were studied constitutively, defining the general target evolutions, but avoiding again more complex geometric features such as cantilevering. Combining yield stress measurements from the penetration test with a FEM tool accounting for non-linear material and calculating with the material evolution should make it possible to **predict** strength or stability induced failure, this being something that could later be integrated into planning and fabrication tools. We will try

Conclusions and Outlook

to combine measurements of strength build-up, physical models and full-scale processing tests in a systematic way using simple sample geometries. These will be a basis for predictive analysis of the process, instead of our current trial-based knowledge of what can and can't be built.

For this purpose, measurement techniques of not only yield stress, but also Young's modulus, capturing correctly creep occurring under load and accounting for partial structural breakdown may turn out to be essential. To further gain confidence in the penetration test, its validity needs to be substantiated for materials as they transition to frictional interactions. Especially a criterion, such as pore solution pressure could show useful to mark this transition.

Concerning **processing**, a systematic **methodology for scaling** processing rates and setups to a given application is needed. More clearly, methods for selecting and designing processing equipment such as continuous **mixing chambers** are needed, especially when it comes to the choice of minimum spatial geometries, residence and homogenisation time, process flow rate. Moreover, knowing and optimising for the mixing energy and time needed for activation of concrete in the mixing chamber can help limiting tool weight. At the current state, mixing of concrete with low yield stress together with an accelerator not immediately causing a strong yield stress increase appears to be optimal in this respect. We will however need to optimise the mixing chambers for higher flow rates with larger aggregates and for higher concrete yield stress.

Dealing with novel admixture systems

In the **early state**, better **understanding** of the physico-chemical interactions of concrete **admixtures** is direly needed as a basis for predictions on how sensitive admixture systems, especially for hydration control, are to variations in ingredients and environmental conditions. Besides the search for reliable hydration control admixtures by direct testing, we need to understand why certain admixtures perform more reliably than others, allowing for knowledge-based rather than empirical selection. Beyond this, mortar or concrete waiting in the delivery line, is simplistically considered as non-hydrating or "sleeping". However, hydration is nevertheless taking place at a slow rate during the induction period and this can substantially affect the performance of

Conclusions and Outlook

accelerators upon activation. Finding admixture systems **insensitive** to slow progress of hydration and systematically testing for said changes remains an open topic. Besides the quest for reliable hydration control admixtures, admixtures necessary for other properties, such as air entrainers, might have desired or undesired effects on processing and could interact with hydration control admixtures. Such interactions are a common issue in industry and are expected to be more critical in digital fabrication as more properties need to be controlled at the same time.

In the **hardened state**, mechanical properties are considered, such as interface bond strength and the effectiveness of reinforcement[14], [16]. With respect to the work presented in this thesis, concrete durability issues caused by the use of some set accelerators have not been addressed and ought to be examined in the future. This involves especially admixtures containing chlorides and nitrates, which can attack reinforcement and cause salt crystallisation in the cementitious matrix, as well as aluminate containing accelerators, which can delay silicate hydration and create conditions in which concrete becomes more prone to sulfate attack[13], [19], [111]. Beyond this, with aluminate additions, less portlandite should form, potentially increasing the carbonation rate. However, this is a complex problem in which microstructure details, in particular the breakthrough pore radius have been shown to play a dominant role, so that a detailed investigation would clearly be needed to examine this. Also, as some accelerators are alkali-rich, the risk of alkali-silica reaction should be kept in mind. For those containing aluminium however, there may be a beneficial effect in this regard. Again, this deserves further investigation.

Concerning the more detailed scientific contributions, the advancements to the **sucrose mechanism** of retardation have helped getting a better understanding of interactions and changes occurring in its presence. However where exactly the molecule acts by adsorption and a definitive proof of the preferential adsorption and transfer over the course of hydration are missing. These gaps concerning the interacting cementitious surface can only be filled by NMR. While the **scaling of structural build-up** with ongoing hydration is now established for neat cement pastes, systems containing **superplasticizer** in which interparticle forces are modified by steric hindrance or in which hydration is not dominated by silicate hydration may show substantially different

Conclusions and Outlook

structuration kinetics with ongoing hydration. This deserves a dedicated study. Furthermore, we will try to distinguish to which extent which hydration product contributes to structural build-up and by which physical mechanism. This is particularly important, when the ratios of C-S-H to ettringite growth might change by accelerator addition.

References

- [1] K. Oosterhuis, H. H. Bier, C. Aalbers, and S. Boer, "File to Factory and Real Time Behavior in ONL-Architecture," in *Fabrication: Examining the Digital Practice of Architecture, Proceedings of the 23rd Annual Conference of the Association for Computer Aided Design in Architecture and the 2004 Conference of the AIA Technology in Architectural Practice Knowledge Community, Cambridge, November 8-14, 2004*, 2004.
- [2] B. Kolarevic, *Architecture in the digital age: design and manufacturing*. Taylor & Francis, 2004.
- [3] B. Kolarevic, "Digital fabrication: manufacturing architecture in the information age," 2001.
- [4] I. Agustí-Juan and G. Habert, "Environmental design guidelines for digital fabrication," *J. Clean. Prod.*, vol. 142, Part 4, pp. 2780–2791, Jan. 2017.
- [5] I. Agustí-Juan, F. Müller, N. Hack, T. Wangler, and G. Habert, "Potential benefits of digital fabrication for complex structures: Environmental assessment of a robotically fabricated concrete wall," *J. Clean. Prod.*, vol. 154, pp. 330–340, Jun. 2017.
- [6] C. Llatas, "A model for quantifying construction waste in projects according to the European waste list," *Waste Manag.*, vol. 31, no. 6, pp. 1261–1276, Jun. 2011.
- [7] T. T. Le, S. A. Austin, S. Lim, R. A. Buswell, A. G. F. Gibb, and T. Thorpe, "Mix design and fresh properties for high-performance printing concrete," *Mater. Struct.*, vol. 45, no. 8, pp. 1221–1232, 2012.
- [8] R. J. M. Wolfs, F. P. Bos, and T. A. M. Salet, "Early age mechanical behaviour of 3D printed concrete: Numerical modelling and experimental testing," *Cem. Concr. Res.*, vol. 106, pp. 103–116, Apr. 2018.
- [9] E. Lloret, L. Reiter, T. Wangler, F. Gramazio, M. Kohler, and R. J. Flatt, "Slipforming with flexible formwork - inline measurement and control," presented at the 2nd Concrete Innovation Conference, Tromso, 2017.
- [10] G. De Schutter and K. Lesage, "Active control of properties of concrete: a (p)review," *Mater. Struct.*, vol. 51, no. 5, p. 123, Sep. 2018.
- [11] A. M. Neville, *Properties of concrete*. Pearson Education India, 1963.
- [12] N. Roussel, G. Ovarlez, S. Garrault, and C. Brumaud, "The origins of thixotropy of fresh cement pastes," *Cem. Concr. Res.*, vol. 42, no. 1, pp. 148–157, Jan. 2012.
- [13] P.-C. Aïtcin, "19 - Accelerators," in *Science and Technology of Concrete Admixtures*, Woodhead Publishing, 2016, pp. 405–413.
- [14] R. A. Buswell, W. R. L. de Silva, S. Z. Jones, and J. Dirrenberger, "3D printing using concrete extrusion: A roadmap for research," *Cem. Concr. Res.*, vol. 112, pp. 37–49, 2018.
- [15] G. De Schutter, K. Lesage, V. Mechtcherine, V. N. Nerella, G. Habert, and I. Agusti-Juan, "Vision of 3D printing with concrete — Technical, economic and environmental potentials," *SI Digit. Concr. 2018*, vol. 112, pp. 25–36, Oct. 2018.
- [16] D. Asprone, C. Menna, F. P. Bos, T. A. M. Salet, J. Mata-Falcón, and W. Kaufmann, "Rethinking reinforcement for digital fabrication with concrete," *SI Digit. Concr. 2018*, vol. 112, pp. 111–121, Oct. 2018.
- [17] F. P. Bos, Z. Y. Ahmed, R. J. M. Wolfs, and T. A. M. Salet, "3D Printing Concrete with Reinforcement," in *High Tech Concrete: Where Technology and Engineering Meet*, 2018, pp. 2484–2493.

References

- [18] A. Perrot, D. Rangeard, and A. Pierre, "Structural built-up of cement-based materials used for 3D-printing extrusion techniques," *Mater. Struct.*, pp. 1–8, Feb. 2015.
- [19] L. Reiter, T. Wangler, N. Roussel, and R. J. Flatt, "The role of early age structural build-up in digital fabrication with concrete," *SI Digit. Concr. 2018*, vol. 112, pp. 86–95, Oct. 2018.
- [20] I. Gibson, D. W. Rosen, and B. Stucker, *Additive Manufacturing Technologies*. Boston, MA: Springer US, 2010.
- [21] A. Gebhardt and J.-S. Hötter, "Additive Manufacturing," in *Additive Manufacturing*, Hanser, 2016, pp. I–XX.
- [22] S. Lim, R. A. Buswell, T. T. Le, S. A. Austin, A. G. F. Gibb, and T. Thorpe, "Developments in construction-scale additive manufacturing processes," *Autom. Constr.*, vol. 21, no. Supplement C, pp. 262–268, Jan. 2012.
- [23] F. Bos, R. Wolfs, Z. Ahmed, and T. Salet, "Additive manufacturing of concrete in construction: potentials and challenges of 3D concrete printing," *Virtual Phys. Prototyp.*, vol. 11, no. 3, pp. 209–225, Jul. 2016.
- [24] P. Wu, J. Wang, and X. Wang, "A critical review of the use of 3-D printing in the construction industry," *Autom. Constr.*, vol. 68, no. Supplement C, pp. 21–31, Aug. 2016.
- [25] B. P. Conner *et al.*, "Making sense of 3-D printing: Creating a map of additive manufacturing products and services," *Inaug. Issue*, vol. 1–4, pp. 64–76, Oct. 2014.
- [26] N. Roussel, "Rheological requirements for printable concretes," *SI Digit. Concr. 2018*, vol. 112, pp. 76–85, Oct. 2018.
- [27] I. Agustí-Juan and G. Habert, "Environmental design guidelines for digital fabrication," *J. Clean. Prod.*, vol. 142, Part 4, pp. 2780–2791, Jan. 2017.
- [28] T. Wangler *et al.*, "Digital Concrete: Opportunities and Challenges," *RILEM Tech. Lett. Vol 1 2016*, 2016.
- [29] B. Khoshnevis, "Automated construction by contour crafting—related robotics and information technologies," *Best ISARC 2002*, vol. 13, no. 1, pp. 5–19, Jan. 2004.
- [30] R. A. Buswell, R. C. Soar, A. G. F. Gibb, and A. Thorpe, "Freeform Construction: Mega-scale Rapid Manufacturing for construction," *Autom. Constr.*, vol. 16, no. 2, pp. 224–231, Mar. 2007.
- [31] C. Gosselin, R. Duballet, Ph. Roux, N. Gaudillière, J. Dirrenberger, and Ph. Morel, "Large-scale 3D printing of ultra-high performance concrete – a new processing route for architects and builders," *Mater. Des.*, vol. 100, pp. 102–109, Jun. 2016.
- [32] W. R. L. Da Silva, "3d concrete printing: from material design to extrusion. Presented slides.," in *Annual Civil Engineering Workshop at Ecole Centrale de Lille (ACE Workshop 2017)*, 2017.
- [33] E. Lloret *et al.*, "Complex concrete structures: Merging existing casting techniques with digital fabrication," *Mater. Ecol.*, vol. 60, pp. 40–49, Mar. 2015.
- [34] A. R. Shahab, E. Lloret, P. Fischer, F. Gramazio, M. Kohler, and R. J. Flatt, "Smart dynamic casting or how to exploit the liquid to solid transition in cementitious materials.," *Proc. CD 1st Int. Conf. Rheol. Process. Constr. Mater. 7th Int. Conf. Self-Compact. Concr. Paris Fr.*, 2013.
- [35] M. A. Meibodi, M. Bernhard, A. Jipa, and B. Dillenburger, "The smart takes from the strong," in *Fabricate 2017: Rethinking Design and Construction*.
- [36] A. Jipa, M. Bernhard, N. Ruffray, T. Wangler, R. J. Flatt, and B. Dillenburger, "skeLETHon Formwork," presented at the SIGraDi 2017, Concepcion, Chile, 2017.

References

- [37] M. Popescu, M. Rippmann, T. Van Mele, and P. Block, "Complex concrete casting: knitting stay-in-place fabric formwork," in *Proceedings of the International Association for Shell and Spatial Structures (IASS) Symposium 2016*, Tokyo, Japan, vol. 2016.
- [38] G. Ovarlez and N. Roussel, "A Physical Model for the Prediction of Lateral Stress Exerted by Self-Compacting Concrete on Formwork," *Mater. Struct.*, vol. 39, no. 2, pp. 269–279, Mar. 2006.
- [39] A. Perrot, D. Rangeard, and A. Pierre, "Structural built-up of cement-based materials used for 3D-printing extrusion techniques," *Mater. Struct.*, pp. 1–8, Feb. 2015.
- [40] R. J. M. Wolfs, F. P. Bos, and T. A. M. Salet, "Early age mechanical behaviour of 3D printed concrete: Numerical modelling and experimental testing," *Cem. Concr. Res.*, vol. 106, pp. 103–116, Apr. 2018.
- [41] A. S. J. Suiker, "Mechanical performance of wall structures in 3D printing processes: Theory, design tools and experiments," *Int. J. Mech. Sci.*, vol. 137, pp. 145–170, Mar. 2018.
- [42] E. Lloret Fritschi, L. Reiter, T. Wangler, F. Gramazio, M. Kohler, and R. J. Flatt, "Smart Dynamic Casting - Slipforming with Flexible Formwork - Inline Measurement and Control," in *2nd Concrete Innovation Conference*, 2017.
- [43] L. Reiter, T. Wangler, N. Roussel, and R. J. Flatt, "Distinguishing flocculation and hydration effects on the thixotropy of cement pastes," in *8th International RILEM Symposium on Self-Compacting Concrete*, 2016.
- [44] M. Schultheiss, T. P. Wangler, L. Reiter, and R. J. Flatt, "Feedback control of Smart Dynamic Casting through formwork friction measurements," presented at the 8th International RILEM Symposium on Self-Compacting Concrete, Washington, DC, USA, 2016.
- [45] N. Roussel and F. Cussigh, "Distinct-layer casting of SCC: The mechanical consequences of thixotropy," *Cem. Concr. Res.*, vol. 38, no. 5, pp. 624–632, 2008.
- [46] B. Zareiyan and B. Khoshnevis, "Effects of interlocking on interlayer adhesion and strength of structures in 3D printing of concrete," *Autom. Constr.*, vol. 83, no. Supplement C, pp. 212–221, Nov. 2017.
- [47] B. Zareiyan and B. Khoshnevis, "Interlayer adhesion and strength of structures in Contour Crafting - Effects of aggregate size, extrusion rate, and layer thickness," *Autom. Constr.*, vol. 81, no. Supplement C, pp. 112–121, Sep. 2017.
- [48] P. Coussot, "Introduction to the rheology of complex fluids," in *Understanding the Rheology of Concrete*, Woodhead Publishing, 2012.
- [49] A. Yahia, S. Mantellato, and R. J. Flatt, "7 - Concrete rheology: A basis for understanding chemical admixtures," in *Science and Technology of Concrete Admixtures*, Woodhead Publishing, 2016, pp. 97–127.
- [50] N. Roussel, G. Ovarlez, S. Garrault, and C. Brumaud, "The origins of thixotropy of fresh cement pastes," *Cem. Concr. Res.*, vol. 42, no. 1, pp. 148–157, Jan. 2012.
- [51] L. K. Mettler, F. K. Wittel, R. J. Flatt, and H. J. Herrmann, "Evolution of strength and failure of SCC during early hydration," *Cem. Concr. Res.*, vol. 89, pp. 288–296, Nov. 2016.
- [52] P. H. Billberg *et al.*, "Field validation of models for predicting lateral form pressure exerted by SCC," *Spec. Issue Self-Consol. Concr.*, vol. 54, no. Supplement C, pp. 70–79, Nov. 2014.

References

- [53] A. Perrot, A. Pierre, S. Vitaloni, and V. Picandet, "Prediction of lateral form pressure exerted by concrete at low casting rates," *Mater. Struct.*, vol. 48, no. 7, pp. 2315–2322, 2014.
- [54] G. Gelardi and R. J. Flatt, "11 - Working mechanisms of water reducers and superplasticizers," in *Science and Technology of Concrete Admixtures*, Woodhead Publishing, 2016, pp. 257–278.
- [55] S. Mantellato, "Flow loss in superplasticized cement pastes," ETH Zürich, 2017.
- [56] D. Marchon, S. Mantellato, H. Bessaies, S. Kawashima, and S. Br, "Hydration and rheology control of concrete by admixtures for digital fabrication," *Cem. Concr. Res.*, no. this issue.
- [57] A. Perrot, T. Lecompte, H. Khelifi, C. Brumaud, J. Hot, and N. Roussel, "Yield stress and bleeding of fresh cement pastes," *Cem. Concr. Res.*, vol. 42, no. 7, pp. 937–944, Jul. 2012.
- [58] D. Marchon, S. Mantellato, A. B. Eberhardt, and R. J. Flatt, "10 - Adsorption of chemical admixtures," in *Science and Technology of Concrete Admixtures*, Woodhead Publishing, 2016, pp. 219–256.
- [59] D. Lootens, P. Jousset, L. Martinie, N. Roussel, and R. J. Flatt, "Yield stress during setting of cement pastes from penetration tests," *Cem. Concr. Res.*, vol. 39, no. 5, pp. 401–408, May 2009.
- [60] E. Lloret Fritschi, "Smart Dynamic Casting A digital fabrication method for non-standard concrete structures," Doctoral thesis, ETH Zürich, Switzerland, 2016.
- [61] H. A. Barnes and Q. D. Nguyen, "Rotating vane rheometry — a review," *J. Non-Newton. Fluid Mech.*, vol. 98, no. 1, pp. 1–14, Mar. 2001.
- [62] P. Billberg, "Form pressure generated by self-compacting concrete : influence of thixotropy and structural behaviour at rest," KTH, Civil and Architectural Engineering, 2006.
- [63] A. Pierre, A. Perrot, A. Histace, S. Gharsalli, and E.-H. Kadri, "A study on the limitations of a vane rheometer for mineral suspensions using image processing," *Rheol. Acta*, vol. 56, no. 4, pp. 351–367, Apr. 2017.
- [64] M. Palacios and R. J. Flatt, "Working mechanism of viscosity-modifying admixtures," in *Science and Technology of Concrete Admixtures*, .
- [65] C. Brumaud, R. Baumann, M. Schmitz, M. Radler, and N. Roussel, "Cellulose ethers and yield stress of cement pastes," *Cem. Concr. Res.*, vol. 55, pp. 14–21, Jan. 2014.
- [66] H. Bessaies-Bey, R. Baumann, M. Schmitz, M. Radler, and N. Roussel, "Organic admixtures and cement particles: Competitive adsorption and its macroscopic rheological consequences," *Cem. Concr. Res.*, vol. 80, no. Supplement C, pp. 1–9, Feb. 2016.
- [67] A. Mechaymech, "Effets des viscosants sur la rhéologie et la stabilité des systèmes cimentaires fluides," Université de Sherbrooke., 2010.
- [68] K. H. Khayat and N. Mikanovic, "Viscosity-enhancing admixtures and the rheology of concrete," in *Understanding the Rheology of Concrete*, .
- [69] J. Assaad, K. H. Khayat, and H. Mesbah, "Assessment of thixotropy of flowable and self-consolidating concrete," *Mater. J.*, vol. 100, no. 2, pp. 99–107, 2003.
- [70] J. J. Assaad and K. H. Khayat, "Effect of viscosity-enhancing admixtures on formwork pressure and thixotropy of self-consolidating concrete," *Mater. J.*, vol. 103, no. 4, pp. 280–287, 2006.

References

- [71] S. Kawashima, J. H. Kim, D. J. Corr, and S. P. Shah, "Study of the mechanisms underlying the fresh-state response of cementitious materials modified with nanoclays," *Constr. Build. Mater.*, vol. 36, no. Supplement C, pp. 749–757, Nov. 2012.
- [72] N. Tregger, M. Pakula, and S. Shah, "Influence of Micro- and Nanoclays on Fresh State of Concrete," *Transp. Res. Rec. J. Transp. Res. Board*, vol. 2141, pp. 68–74, May 2010.
- [73] L. J. A. A. Jeknavorian C. C. Ou, H. Koyata, and K. Folliard, "Interaction of Superplasticizers with Clay-Bearing Aggregates," *Spec. Publ.*, vol. 217, Sep. 2003.
- [74] E. Sakai, D. Atarashi, and M. Daimon, *Interaction between superplasticizers and clay minerals*. 2006.
- [75] S. Ng and J. Plank, "Interaction mechanisms between Na montmorillonite clay and MPEG-based polycarboxylate superplasticizers," *Cem. Concr. Res.*, vol. 42, no. 6, pp. 847–854, Jun. 2012.
- [76] L. Lei and J. Plank, "A study on the impact of different clay minerals on the dispersing force of conventional and modified vinyl ether based polycarboxylate superplasticizers," *Cem. Concr. Res.*, vol. 60, pp. 1–10, Jun. 2014.
- [77] L. Reiter, R. Käßmann, A. R. Shahab, T. Wangler, and R. J. Flatt, "Strategies to wake up sleeping concrete," in *Proceedings of the 14th International Congress on the Chemistry of Cement*, Beijing, China, 2015.
- [78] D. Marchon, P. Juilland, E. Gallucci, L. Frunz, and R. J. Flatt, "Molecular and submolecular scale effects of comb-copolymers on tri-calcium silicate reactivity: Toward molecular design," *J. Am. Ceram. Soc.*, vol. 100, no. 3, pp. 817–841, 2017.
- [79] L. Reiter, M. Palacios, T. Wangler, and R. J. Flatt, "Putting concrete to sleep and waking it up with chemical admixtures," in *Proceedings 11th CanmetACI International Conference Superplast. Chem. Admix. Concr.*, ACI, Ottawa, Ottawa, ON, Canada, 2015, vol. SP-302, pp. 145–154.
- [80] P. Juilland, E. Gallucci, R. Flatt, and K. Scrivener, "Dissolution theory applied to the induction period in alite hydration," *Cem. Concr. Res.*, vol. 40, no. 6, pp. 831–844, Jun. 2010.
- [81] J. W. Bullard *et al.*, "Mechanisms of cement hydration," *Conf. Spec. Cem. Hydration Kinet. Model. Quebec City 2009 CONMOD10 Lausanne 2010*, vol. 41, no. 12, pp. 1208–1223, Dec. 2011.
- [82] P.-C. Aïtcin, "19 - Accelerators," in *Science and Technology of Concrete Admixtures*, Woodhead Publishing, 2016, pp. 405–413.
- [83] C. Paglia, "The influence of calciumsulfoaluminate as accelerating component within cementitious systems," 2000.
- [84] Q. Xu and J. Stark, "Early hydration of ordinary Portland cement with an alkaline shotcrete accelerator," *Adv. Cem. Res.*, vol. 17, no. 1, pp. 1–8, 2005.
- [85] D. Lootens, B. Lindlar, and R. J. Flatt, "Some peculiar chemistry aspects of shotcrete accelerators," in *Proceedings of the 1st International Conference on Microstructure Related Durability of Cementitious Composites*, 2008.
- [86] N. Tenoutasse, "The Hydratation Mechanism of C3A and C3S in the Presence of Calcium Chloride and Calcium Sulphate," in *Proceedings of the 5th International Symposium on the Chemistry of Cement*, 1968.
- [87] P. Juilland, "Early hydration of cementitious systems," in *EPFL*, 2009.
- [88] L. Nicoleau, "New Calcium Silicate Hydrate Network," *Transp. Res. Rec. J. Transp. Res. Board*, vol. 2142, pp. 42–51, May 2010.

References

- [89] L. Nicoleau, "Accelerated growth of calcium silicate hydrates: Experiments and simulations," *Conf. Spec. Cem. Hydration Kinet. Model. Quebec City 2009 CONMOD10 Lausanne 2010*, vol. 41, no. 12, pp. 1339–1348, Dec. 2011.
- [90] M. Balonis, M. Mędala, and F. P. Glasser, "Influence of calcium nitrate and nitrite on the constitution of AFm and AFt cement hydrates," *Adv. Cem. Res.*, vol. 23, no. 3, pp. 129–143, 2011.
- [91] G. W. Scherer, "Stress from crystallization of salt," *Cem. Concr. Res.*, vol. 34, no. 9, pp. 1613–1624, Sep. 2004.
- [92] K. Zehnder and A. Arnold, "Crystal growth in salt efflorescence," *J. Cryst. Growth*, vol. 97, no. 2, pp. 513–521, Sep. 1989.
- [93] B. Y. Lee and K. E. Kurtis, "Effect of pore structure on salt crystallization damage of cement-based materials: Consideration of w/b and nanoparticle use," *Cem. Concr. Res.*, vol. 98, pp. 61–70, Aug. 2017.
- [94] U. Angst, B. Elsener, C. K. Larsen, and Ø. Vennesland, "Critical chloride content in reinforced concrete — A review," *Cem. Concr. Res.*, vol. 39, no. 12, pp. 1122–1138, Dec. 2009.
- [95] U. M. Angst and B. Elsener, "Chloride threshold values for corrosion in concrete—a myth?," *Concr. Solut.*, p. 391, 2016.
- [96] D. Marchon and R. J. Flatt, "8 - Mechanisms of cement hydration," in *Science and Technology of Concrete Admixtures*, Woodhead Publishing, 2016, pp. 129–145.
- [97] P.-C. Nkinamubanzi, S. Mantellato, and R. J. Flatt, "16 - Superplasticizers in practice," in *Science and Technology of Concrete Admixtures*, Woodhead Publishing, 2016, pp. 353–377.
- [98] B. Sencer, K. Ishizaki, and E. Shamoto, "A curvature optimal sharp corner smoothing algorithm for high-speed feed motion generation of NC systems along linear tool paths," *Int. J. Adv. Manuf. Technol.*, vol. 76, no. 9, pp. 1977–1992, Feb. 2015.
- [99] "Projects XTree," *Projects XTree*. [Online]. Available: <http://www.xtreee.eu/projects/>. [Accessed: 28-Oct-2017].
- [100] B. Ouriev and E. J. Windhab, "Rheological study of concentrated suspensions in pressure-driven shear flow using a novel in-line ultrasound Doppler method," *Exp. Fluids*, vol. 32, no. 2, pp. 204–211, Feb. 2002.
- [101] J. Wiklund, I. Shahram, and M. Stading, "Methodology for in-line rheology by ultrasound Doppler velocity profiling and pressure difference techniques," *Chem. Eng. Sci.*, vol. 62, no. 16, pp. 4277–4293, Aug. 2007.
- [102] R. Teillet, S. Bruneaud, and Y. Charonnat, "Suivi et contrôle de la fabrication des mélanges-une nouvelle jeunesse pour le wattmètre différentiel," *Bull. Liaison Lab. Ponts Chaussées*, no. 174, 1991.
- [103] A. Szabo, L. Reiter, E. Lloret-Fritschi, F. Gramazio, M. Kohler, and R. J. Flatt, "Adapting Smart Dynamic Casting to Thin Folded Geometries," in *First RILEM International Conference on Concrete and Digital Fabrication – Digital Concrete 2018*, 2019, pp. 81–93.
- [104] A. Szabo, E. Lloret-Fritschi, L. Reiter, F. Gramazio, M. Kohler, and R. J. Flatt, "On the potential and limitations of thin folded structures produced by Smart Dynamic Casting," *Mater. Struct.*, no. in preparation.
- [105] L. Reiter, A.-M. Anton, T. Wangler, B. Dillenburger, and R. J. Flatt, "Layered extrusion - Processing and Set on Demand," no. in preparation.

References

- [106] D. Lowke, E. Dini, A. Perrot, D. Weger, C. Gehlen, and B. Dillenburger, "Particle-bed 3D printing in concrete construction – Possibilities and challenges," *Cem. Concr. Res.*, Jul. 2018.
- [107] L. Nachbaur, J. C. Mutin, A. Nonat, and L. Choplin, "Dynamic mode rheology of cement and tricalcium silicate pastes from mixing to setting," *Cem. Concr. Res.*, vol. 31, no. 2, pp. 183–192, Feb. 2001.
- [108] P. Coussot and C. Ancey, "Rheophysical classification of concentrated suspensions and granular pastes," *Phys Rev E*, vol. 59, no. 4, pp. 4445–4457, Apr. 1999.
- [109] J. W. Bullard *et al.*, "Mechanisms of cement hydration," *Conf. Spec. Cem. Hydration Kinet. Model. Quebec City 2009 CONMOD10 Lausanne 2010*, vol. 41, no. 12, pp. 1208–1223, Dec. 2011.
- [110] M. Palacios and R. J. Flatt, "Working mechanism of viscosity-modifying admixtures," in *Science and Technology of Concrete Admixtures*, .
- [111] D. Marchon, S. Kawashima, H. Bessaies-Bey, S. Mantellato, and S. Ng, "Hydration and rheology control of concrete for digital fabrication: Potential admixtures and cement chemistry," *SI Digit. Concr. 2018*, vol. 112, pp. 96–110, Oct. 2018.
- [112] T. Lecompte and A. Perrot, "Non-linear modeling of yield stress increase due to SCC structural build-up at rest," *Cem. Concr. Res.*, vol. 92, pp. 92–97, Feb. 2017.
- [113] S. Jarny, N. Roussel, S. Rodts, F. Bertrand, R. Le Roy, and P. Coussot, "Rheological behavior of cement pastes from MRI velocimetry," *Cem. Concr. Res.*, vol. 35, no. 10, pp. 1873–1881, Oct. 2005.
- [114] A. Pierre, A. Perrot, A. Histace, S. Gharsalli, and E.-H. Kadri, "A study on the limitations of a vane rheometer for mineral suspensions using image processing," *Rheol. Acta*, vol. 56, no. 4, pp. 351–367, Apr. 2017.
- [115] G. Ovarlez, F. Mahaut, F. Bertrand, and X. Chateau, "Flows and heterogeneities with a vane tool: Magnetic resonance imaging measurements," *J. Rheol.*, vol. 55, no. 2, pp. 197–223, Jan. 2011.
- [116] S. Mantellato, M. Palacios, and R. J. Flatt, "Relating early hydration, specific surface and flow loss of cement pastes," *Mater. Struct.*, vol. 52, no. 1, p. 5, Jan. 2019.
- [117] G. Gelardi and R. J. Flatt, "11 - Working mechanisms of water reducers and superplasticizers," in *Science and Technology of Concrete Admixtures*, Woodhead Publishing, 2016, pp. 257–278.
- [118] R. J. Flatt and P. Bowen, "Yield Stress of Multimodal Powder Suspensions: An Extension of the YODEL (Yield Stress mODEL)," *J. Am. Ceram. Soc.*, vol. 90, no. 4, pp. 1038–1044, 2007.
- [119] R. J. Flatt and P. Bowen, "Yodel: A Yield Stress Model for Suspensions," *J. Am. Ceram. Soc.*, vol. 89, no. 4, pp. 1244–1256, Apr. 2006.
- [120] Z. Zhou, M. J. Solomon, P. J. Scales, and D. V. Boger, "The yield stress of concentrated flocculated suspensions of size distributed particles," *J. Rheol.*, vol. 43, no. 3, pp. 651–671, Apr. 1999.
- [121] A. M. Mostafa and A. Yahia, "Physico-chemical kinetics of structural build-up of neat cement-based suspensions," *Cem. Concr. Res.*, vol. 97, pp. 11–27, Jul. 2017.
- [122] S. Mantellato, M. Palacios, and R. J. Flatt, "Reliable specific surface area measurements on anhydrous cements," *Cem. Concr. Res. Accept.*
- [123] S. P. Jiang, J. C. Mutin, and A. Nonat, "Studies on mechanism and physico-chemical parameters at the origin of the cement setting. I. The fundamental processes involved during the cement setting," *Cem. Concr. Res.*, vol. 25, no. 4, pp. 779–789, May 1995.

References

- [124] N. Roussel and P. Coussot, "'Fifty-cent rheometer' for yield stress measurements: From slump to spreading flow," *J. Rheol.*, vol. 49, no. 3, pp. 705–718, 2005.
- [125] W. R. L. Da Silva, "3d concrete printing: from material design to extrusion. Presented slides.," in *Annual Civil Engineering Workshop at Ecole Centrale de Lille (ACE Workshop 2017)*, 2017.
- [126] S. P. Timoshenko and J. M. Gere, *Theory of elastic stability*. Courier Corporation, 2009.
- [127] G. Greenhill, "Determination of the greatest height consistent with stability that a vertical pole or mast can be made, and the greatest height to which a tree of given proportions can grow.," *Proc Camb Philos Soc*, no. 4, pp. 65–73, 1881.
- [128] M. A. Schultz and L. J. Struble, "Use of oscillatory shear to study flow behavior of fresh cement paste," *Cem. Concr. Res.*, vol. 23, no. 2, pp. 273–282, Mar. 1993.
- [129] F. Mahaut, S. Mokéddem, X. Chateau, N. Roussel, and G. Ovarlez, "Effect of coarse particle volume fraction on the yield stress and thixotropy of cementitious materials," *Cem. Concr. Res.*, vol. 38, no. 11, pp. 1276–1285, Nov. 2008.
- [130] G. Schmidt and E. Schlegel, "Rheological characterization of C-S-H phases–water suspensions," *Cem. Concr. Res.*, vol. 32, no. 4, pp. 593–599, Apr. 2002.
- [131] C. Brumaud, R. Baumann, M. Schmitz, M. Radler, and N. Roussel, "Cellulose ethers and yield stress of cement pastes," *Cem. Concr. Res.*, vol. 55, pp. 14–21, Jan. 2014.
- [132] N. Hack and W. V. Lauer, "Mesh-Mould: Robotically Fabricated Spatial Meshes as Reinforced Concrete Formwork," *Archit. Des.*, vol. 84, no. 3, pp. 44–53, 2014.
- [133] L. Gebhard, R. J. Flatt, and N. Roussel, "Spaghetti and meatball concrete or the art of engineered jamming," presented at the 1st International Conference on Concrete and Digital Fabrication (RILEM 2018), Zurich, Switzerland, September 10-12, 2018, 2018.
- [134] D. Leith, "Drag on nonspherical objects," *Aerosol Sci. Technol.*, vol. 6, no. 2, pp. 153–161, 1987.
- [135] N. Roussel, "A Theoretical Frame to Study Stability of Fresh Concrete," *Mater. Struct.*, vol. 39, no. 1, pp. 81–91, Jan. 2006.
- [136] M. Choi, N. Roussel, Y. Kim, and J. Kim, "Lubrication layer properties during concrete pumping," *Cem. Concr. Res.*, vol. 45, pp. 69–78, Mar. 2013.
- [137] D. Feys, "13 - Understanding the pumping of conventional vibrated and self-compacting concrete," in *Understanding the Rheology of Concrete*, N. Roussel, Ed. Woodhead Publishing, 2012, pp. 331–353.
- [138] K. T. Fosså, "Slipforming of Vertical Concrete Structures. Friction between Concrete and Slipform Panel," 2001.
- [139] A. Gregori, R. P. Ferron, Z. Sun, and S. P. Shah, "Experimental simulation of self-consolidating concrete formwork pressure," *ACI Mater. J.*, vol. 105, no. 1, p. 97, 2008.
- [140] K. H. Khayat and J. J. Assaad, "Measurement systems for determining formwork pressure of highly-flowable concrete," *Mater. Struct.*, vol. 41, no. 1, pp. 37–46, Jan. 2008.
- [141] P. Billberg, "Form pressure generated by self-compacting concrete : influence of thixotropy and structural behaviour at rest," KTH, Civil and Architectural Engineering, 2006.
- [142] J. Assaad and K. H. Khayat, "Kinetics of formwork pressure drop of self-consolidating concrete containing various types and contents of binder," *Cem. Concr. Res.*, vol. 35, no. 8, pp. 1522–1530, Aug. 2005.

References

- [143] A. Perrot, T. Lecompte, H. Khelifi, C. Brumaud, J. Hot, and N. Roussel, "Yield stress and bleeding of fresh cement pastes," *Cem. Concr. Res.*, vol. 42, no. 7, pp. 937–944, Jul. 2012.
- [144] N. Massoussi, E. Keita, and N. Roussel, "The heterogeneous nature of bleeding in cement pastes," *Cem. Concr. Res.*, vol. 95, pp. 108–116, May 2017.
- [145] E. Keita, "Physique du séchage des sols et des matériaux de construction," Université Paris-Est, 2014.
- [146] E. Lloret, F. Gramazio, M. Kohler, and S. Langenberg, "Complex Concrete Structures: Merging existing casting techniques with digital fabrication," presented at the CAADRIA, Singapore, 2012, pp. 613–622.
- [147] V. Esnault, A. Labyad, M. Chantin, and F. Toussaint, "Experience in Online Modification of Rheology and Strength Acquisition of 3D Printable Mortars," in *First RILEM International Conference on Concrete and Digital Fabrication – Digital Concrete 2018*, 2019, pp. 24–38.
- [148] N. Khalil, G. Aouad, K. El Cheikh, and S. Rémond, "Use of calcium sulfoaluminate cements for setting control of 3D-printing mortars," *Constr. Build. Mater.*, vol. 157, pp. 382–391, Dec. 2017.
- [149] J. Amdahl, "Tmr4205 buckling and ultimate strength of marine structures," *Dep. Mar. Struct. NTNU Nor.*, 2005.
- [150] L. Reiter, T. Wangler, N. Roussel, and R. J. Flatt, "Continuous characterisation method for yield stress in concrete at rest," no. in preparation.
- [151] M. Popescu, L. Reiter, A. Liew, T. Van Mele, R. J. Flatt, and P. Block, "Building in Concrete with an Ultra-lightweight Knitted Stay-in-place Formwork: Prototype of a Concrete Shell Bridge," *Structures*, vol. 14, pp. 322–332, Jun. 2018.
- [152] H. Lindemann *et al.*, "Development of a Shotcrete 3D-Printing (SC3DP) Technology for Additive Manufacturing of Reinforced Freeform Concrete Structures," in *First RILEM International Conference on Concrete and Digital Fabrication – Digital Concrete 2018*, 2019, pp. 287–298.
- [153] D. Beaupre, "Rheology of high performance shotcrete," University of British Columbia, 1994.
- [154] M. Jolin, "Mechanisms of placement and stability of dry process shotcrete," University of British Columbia, 1999.
- [155] K.-K. Yun, P. Choi, and J. H. Yeon, "Correlating rheological properties to the pumpability and shootability of wet-mix shotcrete mixtures," *Constr. Build. Mater.*, vol. 98, pp. 884–891, Nov. 2015.
- [156] Y. Y. Kim, H.-J. Kong, and V. C. Li, "Design of engineered cementitious composite suitable for wet-mixture shotcreting," *Mater. J.*, vol. 100, no. 6, pp. 511–518, 2003.
- [157] C. Paglia, "The influence of calciumsulfoaluminate as accelerating component within cementitious systems hydration, microstructure, strength development, and sulfate resistance of the cement-based mixtures," Doctoral thesis, ETH Zürich, Zürich, 2000.
- [158] Q. Xu and J. Stark, "Early hydration of ordinary Portland cement with an alkaline shotcrete accelerator," *Adv. Cem. Res.*, vol. 17, no. 1, pp. 1–8, 2005.
- [159] D. Lootens, B. Lindlar, and R. J. Flatt, "Some peculiar chemistry aspects of shotcrete accelerators," in *Proceedings of the 1st International Conference on Microstructure Related Durability of Cementitious Composites*, 2008.
- [160] A. Pierre, C. Lanos, and P. Estellé, "Extension of spread-slump formulae for yield stress evaluation," *Appl. Rheol.*, vol. 23, no. 6, p. 63849, Nov. 2013.

References

- [161] J. Assaad, K. H. Khayat, and H. Mesbah, "Assessment of thixotropy of flowable and self-consolidating concrete," *Mater. J.*, vol. 100, no. 2, pp. 99–107, 2003.
- [162] J. J. Assaad and K. H. Khayat, "Effect of viscosity-enhancing admixtures on formwork pressure and thixotropy of self-consolidating concrete," *Mater. J.*, vol. 103, no. 4, pp. 280–287, 2006.
- [163] A. F. Omran, S. Naji, and K. H. Khayat, "Portable Vane Test to Assess Structural Buildup at Rest of Self-Consolidating Concrete.," *ACI Mater. J.*, vol. 108, no. 6, 2011.
- [164] D. Lootens, P. Jousset, L. Martinie, N. Roussel, and R. J. Flatt, "Yield stress during setting of cement pastes from penetration tests," *Cem. Concr. Res.*, vol. 39, no. 5, pp. 401–408, May 2009.
- [165] R. J. M. Wolfs, F. P. Bos, and T. A. M. Salet, "Correlation between destructive compression tests and non-destructive ultrasonic measurements on early age 3D printed concrete," *Constr. Build. Mater.*, vol. 181, pp. 447–454, Aug. 2018.
- [166] D. Lootens, R. J. Flatt, and P. Juilland, "Pragmatic (and) scientific characterization of the early ages properties of cementitious materials," in *Creep, Shrinkage and Durability Mechanics of Concrete and Concrete Structures, Two Volume Set: Proceedings of the CONCREEP 8 conference held in Ise-Shima, Japan, 30 September-2 October 2008*, 2008, vol. 1, p. 305.
- [167] L. Reiter, T. Wangler, N. Roussel, and R. J. Flatt, "Distinguishing flocculation and hydration effects on the thixotropy of cement pastes," in *8th International RILEM Symposium on Self-Compacting Concrete*, 2016.
- [168] S. Amziane, A. Perrot, and T. Lecompte, "A novel settling and structural build-up measurement method," *Meas. Sci. Technol.*, vol. 19, no. 10, p. 105702, Aug. 2008.
- [169] H. A. Barnes, "A review of the slip (wall depletion) of polymer solutions, emulsions and particle suspensions in viscometers: its cause, character, and cure," *J. Non-Newton. Fluid Mech.*, vol. 56, no. 3, pp. 221–251, Mar. 1995.
- [170] L. K. Mettler, F. K. Wittel, R. J. Flatt, and H. J. Herrmann, "Evolution of strength and failure of SCC during early hydration," *Cem. Concr. Res.*, vol. 89, pp. 288–296, Nov. 2016.
- [171] H. Hafid, G. Ovarlez, F. Toussaint, P. H. Jezequel, and N. Roussel, "Effect of particle morphological parameters on sand grains packing properties and rheology of model mortars," *Cem. Concr. Res.*, vol. 80, pp. 44–51, Feb. 2016.
- [172] J. Yammine, M. Chaouche, M. Guerinet, M. Moranville, and N. Roussel, "From ordinary rheology concrete to self compacting concrete: A transition between frictional and hydrodynamic interactions," *Cem. Concr. Res.*, vol. 38, no. 7, pp. 890–896, Jul. 2008.
- [173] A. Das, L. Reiter, T. Wangler, and R. J. Flatt, "Hydration control of ternary cements for digital fabrication with concrete," in *RheoCon2*, Dresden, 2019, vol. submitted.
- [174] G. Ovarlez, "2 - Introduction to the rheometry of complex suspensions," in *Understanding the Rheology of Concrete*, N. Roussel, Ed. Woodhead Publishing, 2012, pp. 23–62.
- [175] D. Taylor, *Fundamentals of soil mechanics*. Chapman And Hall, Limited.; New York, 1948.
- [176] K. Terzaghi, *Theoretical soil mechanics*. Chapman And Hall, Limited.; London, 1951.
- [177] A. Atterberg, "Die Plastizität der Tone (The plasticity of the clays)," *Int Mitt Bodenkd*, vol. 1, pp. 10–43, 1911.
- [178] S. A. Jefferis, "Grouts and grouting," 2003.

References

- [179] T. Lecompte, A. Perrot, V. Picandet, H. Bellegou, and S. Amziane, "Cement-based mixes: Shearing properties and pore pressure," *Cem. Concr. Res.*, vol. 42, no. 1, pp. 139–147, Jan. 2012.
- [180] T. Craipeau, T. Lecompte, F. Toussaint, and A. Perrot, "Evolution of Concrete/Formwork Interface in Slipforming Process," *Cham*, 2019, pp. 12–23.
- [181] L. Prandtl, "Über die härte plastischer körper," *Nachrichten Von Ges. Wiss. Zu Gött. Math.-Phys. Kl.*, vol. 1920, pp. 74–85, 1920.
- [182] J. B. Hansen, "A revised and extended formula for bearing capacity," 1970.
- [183] H.-Y. Fang, *Foundation engineering handbook*. Springer Science & Business Media, 2013.
- [184] G. T. Houlsby and C. M. Martin, "Undrained bearing capacity factors for conical footings on clay," *Géotechnique*, vol. 53, no. 5, 2003.
- [185] T. Koumoto and G. T. Houlsby, "Theory and practice of the fall cone test," p. 12.
- [186] G. T. Houlsby, "Theoretical analysis of the fall cone test," *Géotechnique*, vol. 32, no. 2, pp. 111–118, 1982.
- [187] S. Hansbo, *A new approach to the determination of the shear strength of clay by the fall-cone test*. Royal Swedish Geotechnical Institute, 1957.
- [188] Juang C. Hsein, Yuan Haiming, Lee Der-Her, and Lin Ping-Sien, "Simplified Cone Penetration Test-based Method for Evaluating Liquefaction Resistance of Soils," *J. Geotech. Geoenvironmental Eng.*, vol. 129, no. 1, pp. 66–80, Jan. 2003.
- [189] P. K. Robertson, "Soil classification using the cone penetration test," *Can. Geotech. J.*, vol. 27, no. 1, pp. 151–158, Feb. 1990.
- [190] A. S. Vesic, "Bearing capacity of shallow foundations, Foundation Engineering Handbook," *Ed. By*, 1975.
- [191] A. W. SKEMPTON, "The bearing capacity of clays," *Proc Build. Res. Congr.*, vol. 1, pp. 180–189, 1951.
- [192] J. Cheung, A. Jeknavorian, L. Roberts, and D. Silva, "Impact of admixtures on the hydration kinetics of Portland cement," *Conf. Spec. Cem. Hydration Kinet. Model. Quebec City 2009 CONMOD10 Lausanne 2010*, vol. 41, no. 12, pp. 1289–1309, Dec. 2011.
- [193] D. Marchon and R. J. Flatt, "—Impact of Chemical Admixtures on Cement Hydration," in *Science and Technology of Concrete Admixtures*, Woodhead Publishing (an imprint of Elsevier), 2015.
- [194] K. L. Scrivener, P. Juilland, and P. J. M. Monteiro, "Advances in understanding hydration of Portland cement," *Keynote Pap. 14th Int. Congr. Chem. Cem. ICC 2015*, vol. 78, Part A, pp. 38–56, Dec. 2015.
- [195] A. Szabo, L. Reiter, E. Lloret-Fritschi, F. Gramazio, M. Kohler, and R. J. Flatt, "Processing of set on demand solutions for digital fabrication in architecture," in *RheoCon2*, Dresden, 2019, vol. submitted.
- [196] C. Hirsch, "Untersuchungen zur Wechselwirkung zwischen polymeren Fließmitteln und Zementen bzw. Mineralphasen der frühen Zementhydratation," Dissertation, Technische Universität München, München, 2005.
- [197] G. Artioli, L. Valentini, M. Voltolini, M. C. Dalconi, G. Ferrari, and V. Russo, "Direct Imaging of Nucleation Mechanisms by Synchrotron Diffraction Micro-Tomography: Superplasticizer-Induced Change of C–S–H Nucleation in Cement," *Cryst. Growth Des.*, vol. 15, no. 1, pp. 20–23, Jan. 2015.

References

- [198] A. Radocea, *A study on the mechanism of plastic shrinkage of cement-based materials*. Chalmers University of Technology, 1992.
- [199] M. Yang, C. M. Neubauer, and H. M. Jennings, "Interparticle potential and sedimentation behavior of cement suspensions: Review and results from paste," *Adv. Cem. Based Mater.*, vol. 5, no. 1, pp. 1–7, Jan. 1997.
- [200] W. B. Russel, W. B. Russel, D. A. Saville, and W. R. Schowalter, *Colloidal dispersions*. Cambridge university press, 1991.
- [201] A. Bazzoni, "Study of early hydration mechanisms of cement by means of electron microscopy," EPFL, 2014.
- [202] J. Mewis and N. J. Wagner, "Thixotropy," *Colloids Polym. Surfactants Special Issue Honour Brian Vincent*, vol. 147–148, pp. 214–227, Mar. 2009.
- [203] A. M. Mostafa and A. Yahia, "New approach to assess build-up of cement-based suspensions," *Cem. Concr. Res.*, vol. 85, pp. 174–182, Jul. 2016.
- [204] N. L. Thomas and J. D. Birchall, "The retarding action of sugars on cement hydration," *Cem. Concr. Res.*, vol. 13, no. 6, pp. 830–842, Nov. 1983.
- [205] D. Marchon and R. J. Flatt, "12-Impact of chemical admixtures on cement hydration," in *Science and Technology of Concrete Admixtures*, Woodhead Publishing, 2016, pp. 279–304.
- [206] A. M. Mostafa and A. Yahia, "Performance evaluation of different rheometric shearing techniques to disperse concentrated cement suspension," *Appl. Rheol.*, vol. 25, no. 3, pp. 45–53, 2015.
- [207] J. E. Wallevik, "Rheological properties of cement paste: Thixotropic behavior and structural breakdown," *Cem. Concr. Res.*, vol. 39, no. 1, pp. 14–29, Jan. 2009.
- [208] S. Mantellato, M. Palacios, and R. J. Flatt, "Reliable specific surface area measurements on anhydrous cements," *Cem. Concr. Res.*, vol. 67, pp. 286–291, Jan. 2015.
- [209] F. Caruso, S. Mantellato, M. Palacios, and R. J. Flatt, "ICP-OES method for the characterization of cement pore solutions and their modification by polycarboxylate-based superplasticizers," *Cem. Concr. Res.*, vol. 91, pp. 52–60, Jan. 2017.
- [210] S. Mantellato, M. Palacios, and R. J. Flatt, "Impact of sample preparation on the specific surface area of synthetic ettringite," *Cem. Concr. Res.*, vol. 86, pp. 20–28, Aug. 2016.
- [211] B. Lothenbach, G. Le Saout, E. Gallucci, and K. Scrivener, "Influence of limestone on the hydration of Portland cements," *Cem. Concr. Res.*, vol. 38, no. 6, pp. 848–860, Jun. 2008.
- [212] Patrick Juilland and Emmanuel Gallucci, "Hindered Calcium Hydroxide Nucleation and Growth as Mechanism Responsible for Tricalcium Silicate Retardation in Presence of Sucrose," *Spec. Publ.*, vol. 329, Sep. 2018.
- [213] K. I. Popov *et al.*, "¹³C NMR and electrospray ionization mass spectrometric study of sucrose aqueous solutions at high pH: NMR measurement of sucrose dissociation constant," *Food Chem.*, vol. 96, no. 2, pp. 248–253, May 2006.
- [214] S. G. Schultz and A. K. Solomon, "Determination of the effective hydrodynamic radii of small molecules by viscometry," *J. Gen. Physiol.*, vol. 44, no. 6, pp. 1189–1199, 1961.
- [215] N. Roussel, A. Lemaître, R. J. Flatt, and P. Coussot, "Steady state flow of cement suspensions: A micromechanical state of the art," *Cem. Concr. Res.*, vol. 40, no. 1, pp. 77–84, Jan. 2010.
- [216] J. N. Israelachvili, *Intermolecular and surface forces*. Academic press, 2011.
- [217] D. Stauffer and A. Aharony, *Introduction to percolation theory*. Taylor & Francis, 2014.

References

- [218] E. Pustovgar, "Mechanism of action of viscosity modifying admixtures," Master thesis, ETH Zürich, 2012.
- [219] B. J. Smith, L. R. Roberts, G. P. Funkhouser, V. Gupta, and B. F. Chmelka, "Reactions and Surface Interactions of Saccharides in Cement Slurries," *Langmuir*, vol. 28, no. 40, pp. 14202–14217, Oktober 2012.
- [220] K. Luke and G. Luke, "Effect of sucrose on retardation of Portland cement," *Adv. Cem. Res.*, vol. 12, no. 1, pp. 9–18, 2000.
- [221] J. F. Young, "A review of the mechanisms of set-retardation in portland cement pastes containing organic admixtures," *Cem. Concr. Res.*, vol. 2, no. 4, pp. 415–433, Jul. 1972.
- [222] J. J. Thomas, H. M. Jennings, and J. J. Chen, "Influence of Nucleation Seeding on the Hydration Mechanisms of Tricalcium Silicate and Cement," *J. Phys. Chem. C*, vol. 113, no. 11, pp. 4327–4334, Feb. 2009.
- [223] V. K. Peterson and M. C. G. Juenger, "Hydration of Tricalcium Silicate: Effects of CaCl₂ and Sucrose on Reaction Kinetics and Product Formation," *Chem. Mater.*, vol. 18, no. 24, pp. 5798–5804, Nov. 2006.
- [224] M. Bishop and A. R. Barron, "Cement Hydration Inhibition with Sucrose, Tartaric Acid, and Lignosulfonate: Analytical and Spectroscopic Study," *Ind. Eng. Chem. Res.*, vol. 45, no. 21, pp. 7042–7049, Sep. 2006.
- [225] J. W. Bullard and R. J. Flatt, "New Insights Into the Effect of Calcium Hydroxide Precipitation on the Kinetics of Tricalcium Silicate Hydration," *J. Am. Ceram. Soc.*, vol. 93, no. 7, pp. 1894–1903, 2010.
- [226] P. Juilland, L. Nicoleau, R. S. Arvidson, and E. Gallucci, "Advances in dissolution understanding and their implications for cement hydration," *RILEM Tech. Lett.*, vol. 2, pp. 90–98, 2017.
- [227] S. Mantellato, "Flow loss in superplasticized cement pastes," ETH Zürich, 2017.
- [228] L. Nicoleau, "New Calcium Silicate Hydrate Network," *Transp. Res. Rec. J. Transp. Res. Board*, vol. 2142, pp. 42–51, May 2010.
- [229] O. W. Blümel and H. Lutsch, *Spritzbeton*. Springer, 1981.
- [230] P. Juilland, "Early hydration of cementitious systems," Verlag nicht ermittelbar, 2009.
- [231] E. Lloret *et al.*, "Complex concrete structures: Merging existing casting techniques with digital fabrication," *Comput.-Aided Des.*, no. 0, 2014.
- [232] E. Lloret, L. K. Mettler, A. R. Shahab, F. Gramazio, M. Kohler, and R. J. Flatt, "Smart Dynamic Casting: A robotic fabrication system for complex structures," in *Proceedings of 1st Concrete Innovation Conference*, Norway, 2014.
- [233] H. Uchikawa, S. Hanehara, and D. Sawaki, "The role of steric repulsive force in the dispersion of cement particles in fresh paste prepared with organic admixture," *Cem. Concr. Res.*, vol. 27, no. 1, pp. 37–50, Jan. 1997.
- [234] K. L. Scrivener and A. Nonat, "Hydration of cementitious materials, present and future," *Spec. Issue 13th Int. Congr. Chem. Cem.*, vol. 41, no. 7, pp. 651–665, Jul. 2011.
- [235] K. L. Scrivener, P. Juilland, and P. J. M. Monteiro, "Advances in understanding hydration of Portland cement," *Keynote Pap. 14th Int. Congr. Chem. Cem. ICCM 2015*, vol. 78, Part A, pp. 38–56, Dec. 2015.
- [236] D. Marchon and R. J. Flatt, "8 - Mechanisms of cement hydration," in *Science and Technology of Concrete Admixtures*, Woodhead Publishing, 2016, pp. 129–145.
- [237] M. C. G. Juenger, F. Winnefeld, J. L. Provis, and J. H. Ideker, "Advances in alternative cementitious binders," *Cem. Concr. Res.*, vol. 41, no. 12, pp. 1232–1243, 2011.
- [238] H. F. Taylor, *Cement chemistry*. Thomas Telford, 1997.

References

- [239] K. Scrivener, "Calcium aluminate," *Adv. Concr. Technol. Set*, p. 1, 2003.
- [240] R. N. Edmonds and A. J. Majumdar, "The hydration of monocalcium aluminate at different temperatures," *Cem. Concr. Res.*, vol. 18, no. 2, pp. 311–320, Mar. 1988.
- [241] C. Gosselin, "Microstructural Development of Calcium Aluminate Cement Based Systems with and without Supplementary Cementitious Materials," EPFL, Lausanne, 2009.
- [242] S. Lamberet, "Durability of ternary binders based on Portland cement, calcium aluminate cement and calcium sulfate," Lausanne, Lausanne, 2005.
- [243] J. Nehring, J. Neubauer, S. Berger, and F. Goetz-Neunhoeffler, "Acceleration of OPC by CAC in binary and ternary systems: The role of pore solution chemistry," *Cem. Concr. Res.*, vol. 107, pp. 264–274, May 2018.
- [244] D. Damidot and A. Rettel, "Study of the interaction between the hydration of CA and of C3S at room temperature," in *Proceedings of the 11th International Congress on the Chemistry of Cement (ICCC), Durban, South Africa, 2003*, pp. 1845–1854.
- [245] L. Xu, P. Wang, and G. Zhang, "Formation of ettringite in Portland cement/calcium aluminate cement/calcium sulfate ternary system hydrates at lower temperatures," *Constr. Build. Mater.*, vol. 31, pp. 347–352, 2012.
- [246] L. Pelletier, F. Winnefeld, and B. Lothenbach, "The ternary system Portland cement–calcium sulphoaluminate clinker–anhydrite: Hydration mechanism and mortar properties," *Cem. Concr. Compos.*, vol. 32, no. 7, pp. 497–507, Aug. 2010.
- [247] J. J. Wolf, D. Jansen, F. Goetz-Neunhoeffler, and J. Neubauer, "Mechanisms of early ettringite formation in ternary CSA–OPC–anhydrite systems," *Adv. Cem. Res.*, vol. 31, no. 4, pp. 195–204, 2019.
- [248] J. Bizzozero, C. Gosselin, and K. L. Scrivener, "Expansion mechanisms in calcium aluminate and sulfoaluminate systems with calcium sulfate," *Cem. Concr. Res.*, vol. 56, pp. 190–202, 2014.
- [249] J. Bizzozero, "Hydration and dimensional stability of calcium aluminate cement based systems," Doctoral thesis, EPF Lausanne, Lausanne, 2014.
- [250] A. Quennoz and K. L. Scrivener, "Interactions between alite and C3A-gypsum hydrations in model cements," *Cem. Concr. Res.*, vol. 44, pp. 46–54, Feb. 2013.
- [251] J. Kighelman, "Hydration and structure development of ternary binder system as used in self-levelling compounds," EPFL Lausanne, 2007.
- [252] F. Goetz-Neunhoeffler, "The function of Li carbonate and tartaric acid in the hydration of mixtures of calcium aluminate cement (CAC) with calcium sulfate hemihydrate CSH0.5 À Á," *Cem Int*, vol. 5, pp. 90–101, 2007.
- [253] M. M. Collepardi, "6 - Water Reducers/Retarders," in *Concrete Admixtures Handbook (Second Edition)*, V. S. Ramachandran, Ed. Park Ridge, NJ: William Andrew Publishing, 1996, pp. 286–409.
- [254] J. F. Young, "A review of the mechanisms of set-retardation in portland cement pastes containing organic admixtures," *Cem. Concr. Res.*, vol. 2, no. 4, pp. 415–433, Jul. 1972.
- [255] C. Nalet and A. Nonat, "Ionic complexation and adsorption of small organic molecules on calcium silicate hydrate: Relation with their retarding effect on the hydration of C3S," *Cem. Concr. Res.*, vol. 89, pp. 97–108, Nov. 2016.
- [256] V. S. Ramachandran, M. S. Lowery, T. Wise, and G. M. Polomark, "The role of phosphonates in the hydration of Portland cement," *Mater. Struct.*, vol. 26, no. 7, pp. 425–432, Aug. 1993.

References

- [257] D. Marchon, U. Sulser, A. Eberhardt, and R. J. Flatt, "Molecular design of comb-shaped polycarboxylate dispersants for environmentally friendly concrete," *Soft Matter*, vol. 9, no. 45, pp. 10719–10728, 2013.
- [258] K. Yamada, T. Takahashi, S. Hanehara, and M. Matsuhisa, "Effects of the chemical structure on the properties of polycarboxylate-type superplasticizer," *Cem. Concr. Res.*, vol. 30, no. 2, pp. 197–207, Feb. 2000.
- [259] A. Rettel, D. Damidot, D. Müller, and W. A. Gessner, "NMR study of gels formed during the hydration of calcium aluminate cements in the presence of citrate or gluconate," *Proc. 10th ICCG Gothenbg. Amarkai AB Congrex Göteb. AB*, vol. 3, pp. 1–8, 1997.
- [260] D. Damidot, A. Rettel, and A. Capmas, "Action of admixtures on Fondu cement: Part 1. Lithium and sodium salts compared," *Adv. Cem. Res.*, vol. 8, no. 31, pp. 111–119, 1996.
- [261] S. A. Rodger and D. D. Double, "The chemistry of hydration of high alumina cement in the presence of accelerating and retarding admixtures," *Cem. Concr. Res.*, vol. 14, no. 1, pp. 73–82, Jan. 1984.
- [262] T. A. Bier, A. Mathieu, B. Espinosa, and C. Marcelon, "Admixtures and their interactions with high range calcium aluminate cement," *UNITECR Jpn.*, 1995.
- [263] N. Ukrainczyk, "Effect of polycarboxylate superplasticiser on properties of calcium aluminate cement mortar," *Adv. Cem. Res.*, vol. 27, no. 7, pp. 388–398, 2015.
- [264] M. Zajac, J. Skocek, F. Bullerjahn, and M. Ben Haha, "Effect of retarders on the early hydration of calcium-sulpho-aluminate (CSA) type cements," *Cem. Concr. Res.*, vol. 84, pp. 62–75, Jun. 2016.
- [265] R. Myrdal, "Accelerating admixtures for concrete. State of the art," 2007.
- [266] L. Nicoleau, "Accelerated growth of calcium silicate hydrates: Experiments and simulations," *Conf. Spec. Cem. Hydration Kinet. Model. Quebec City 2009 CONMOD10 Lausanne 2010*, vol. 41, no. 12, pp. 1339–1348, Dec. 2011.
- [267] T. Wangler, "Digital Concrete Processing: A Review," in *1st International Conference on 3D Construction Printing (3DcP 2018)*, 2018.
- [268] S. Ng and J. Plank, "Interaction mechanisms between Na montmorillonite clay and MPEG-based polycarboxylate superplasticizers," *Cem. Concr. Res.*, vol. 42, no. 6, pp. 847–854, Jun. 2012.
- [269] G. B. S. Ng, "Interactions of Polycarboxylate based Superplasticizers with Montmorillonite Clay in Portland Cement and with Calcium Aluminate Cement," Technische Universität München, 2013.
- [270] L. J. A. A. Jeknavorian C. C. Ou, H. Koyata, and K. Folliard, "Interaction of Superplasticizers with Clay-Bearing Aggregates," *Spec. Publ.*, vol. 217, Sep. 2003.
- [271] M. Popescu, "KnitCrete: Stay-in-place knitted fabric formwork for complex concrete structures," ETH Zürich, 2019.
- [272] A.-M. Anton, A. Yoo, P. Bedarf, L. Reiter, T. Wangler, and B. Dillenburger, "Vertical Modulation - Computational Design for Concrete Extrusion 3D Printed Columns," in *submitted*, Austin, TX, 2019, vol. ACADIA.
- [273] J. J. Thomas, H. M. Jennings, and J. J. Chen, "Influence of Nucleation Seeding on the Hydration Mechanisms of Tricalcium Silicate and Cement," *J. Phys. Chem. C*, vol. 113, no. 11, pp. 4327–4334, Feb. 2009.
- [274] E. Lloret-Fritsch *et al.*, "Challenges of Real-Scale Production with Smart Dynamic Casting," in *First RILEM International Conference on Concrete and Digital Fabrication – Digital Concrete 2018*, 2019, pp. 299–310.

References

- [275] P. Kuhn, A. Brühwiler, R. Bourquin, D. Lootens, and L. Oblak, "Mixer, system for applying a building material and method for producing a structure from building material," WO2017149040.
- [276] D. Lootens, A. Brühwiler, and R. Bourquin, "Additive manufacturing of shaped bodies from curable materials," WO2018115166.
- [277] S. Adriaenssens, P. Block, D. Veenendaal, and C. Williams, *Shell structures for architecture: form finding and optimization*. Routledge, 2014.
- [278] A. S. J. Suiker, "Mechanical performance of wall structures in 3D printing processes: Theory, design tools and experiments," *Int. J. Mech. Sci.*, vol. 137, pp. 145–170, Mar. 2018.

Acknowledgements

This thesis was realized in the group of Physical Chemistry of Building Materials at ETH Zürich and financed by the NCCR for digital fabrication.

First, I would like to thank the jury members for reviewing this work: Prof. Robert Flatt, Prof. Richard Buswell, Prof. Viktor Mechtcherine, Dr. Timothy Wangler and to the chairman Prof. Anastasopoulos Ioannis. Second, I would like to thank all the people who made this dissertation possible, those from the research group and those from the NCCR.

Primarily, I want to thank my supervisor, Prof. Robert Flatt, who gave me the opportunity to explore with substantial freedom the realms of rheology, cement chemistry and admixtures. He trusted that the opportunities pursued in different directions would come back together at the end and allowed for the collaborations in the NCCR that show that the explored concepts are practicable beyond the theoretical framework. I'm also grateful for the on-demand guidance and invaluable scientific exchange.

I also want to particularly thank Timothy Wangler for the constant exchange, the mutual learning process and for sharing the NCCR support tasks in a way that allowed both of us to learn and develop, Nicolas Roussel for learning about many aspects of rheology, Marta Palacios for learning about admixtures, characterizations and hydration, Delphine Marchon for introducing me to the vast field of research on cement and creating my initial interest on the subject.

I was fortunate to work together on projects of different research groups, from which I first want to thank the professors steering the projects: Prof. Philippe Block, Prof. Benjamin Dillenburger, Prof. Fabio Gramazio, Prof. Walter Kaufmann and Prof. Matthias Kohler. In addition, I want to thank Prof. Denis Damidot and Prof. Rafael Pileggi for the exchange during their sabbatical stays.

From the collaborations in the NCCR I want to particularly thank the main collaborators in the respective projects that I could work with and who helped to create and to solve the challenges imposed by what they were assigned to build: Ena Lloret and Anna Szabo in Smart Dynamic Casting/Digital Casting, Ana Anton in layered extrusion and Mariana Popescu in KnitCrete.

With respect to getting the work done, my primary acknowledgements go of course to the technician. Without them no experimental applied work would be possible.

Acknowledgements

Here I first and foremost want to thank Heinz, for the amount of help given over many years and his realistic view of the new ideas for construction processes that we mess with. I also want to thank Mike, who can solve many challenges in the five minutes that he can afford to spend, Andi, who is an invaluable help for all work related to concrete processing, Philippe, who has helped a lot for the integration of our processing equipment into RFL, Martin, who has built components and shakes his head at my tinkered concept-prototypes and Tobias, who is working on the next extruder. This acknowledgement is also extended to the mechanical workshops in civil engineering, chemistry and physics for their manufacturing skills, insight and fabrication consulting, as well as the electronics workshop and the physics shop. I also thank Gaby, Asel and Sara for microscopy and IPC measurements taken, of which only some of which made it to the thesis. I also thank Andrea for many instances where she helps with SAP, booking, payments and reproduction rights.

Then I want to thank the various persons having contributed to demonstration projects that I contributed to. Thank you for your insight, knowledge, skills and helping hands. In SDC: Falk, Linus, Marc, Fabio, Hans. In layered extrusion: Lukas, Angela, Patrick, Yoana, Eleni and the MAS students of 18/19. In KnitCrete: Matthias, Andrew, Minu, Tom, Alessandro, Christian and Nora. I'm equally grateful for the learning opportunities in projects, where my contributions were only short-term, such as in MeshMould, where I'd like to thank especially Norman to learn from early trials, as well as the exchange later with Kathrin and Alex.

Finally, I'd like to thank the many students supervised throughout the years.

Appendix

Calculation of pre-factors for cylinder buckling

These pages describe the calculation of pre-factors in section 3.4.2 and equation (50).

The energy-based equation introduced for a beam in equation (15) writes as equation (49):

$$\Pi = \int_0^{2\pi} \int_0^H (D \nabla w^2 + \frac{Eb}{r^2} w^2 - \sigma_{vb} w'^2) r dz d\theta,$$

With:

$$D \nabla w = D \left(\frac{\partial^2 w}{\partial z^2} + \frac{1}{r^2} \frac{\partial^2 w}{\partial \theta^2} \right)$$

In order to make the next steps, we create a unitless function of the shape of the deflection \tilde{w} and the extent of the deflection at its largest δ :

$$w = \delta \tilde{w}$$

And the substitute in the differential parts:

$$\frac{\partial w}{\partial z} = \frac{\delta}{H} \frac{\partial \tilde{w}}{\partial \xi}$$

$$\frac{\partial^2 w}{\partial z^2} = \frac{\delta}{H^2} \frac{\partial^2 \tilde{w}}{\partial \xi^2}$$

$$\frac{\partial^2 w}{\partial \theta^2} = \frac{\delta}{R^2} \frac{\partial^2 \tilde{w}}{\partial \theta^2}$$

And we will consider the shape of the deflection to be:

$$\tilde{w} = (1 - \cos(\varepsilon \xi)) \sin \theta,$$

which fulfills the boundary condition of a bending stiff base free of displacement and bending angle. This function is a simple approximation of the shape observed by Wolfs et al. as it can capture bulging out on one side, somewhere along an element's height, in a cylinder. For example, we get the case of Wolfs et al. where the material remains held at the top for $\varepsilon = \pi/2$.

Substituting in the above differentials gives:

$$\frac{\partial \tilde{w}}{\partial \xi} = \varepsilon \sin(\varepsilon \xi) \sin \theta$$

$$\frac{\partial^2 \tilde{w}}{\partial \xi^2} = \varepsilon^2 \cos(\varepsilon \xi) \sin \theta$$

Appendix

$$\frac{\partial^2 \tilde{w}}{\partial \theta^2} = -\tilde{w}$$

The trick in the following is to write out the energy-based equation in a form where δ^2 appears in each of the terms, and then to use the criterion for stability that internal energies increase with deflection δ :

$$\frac{\partial^2 \Pi}{\partial \delta^2} \geq 0,$$

Which means that the term independent of δ needs to be larger than 0.

This gives ($\sigma_V = \rho g H(1 - \xi)$, $E = E_0(1 - \xi)^\beta$):

$$\begin{aligned} \Pi = & \frac{b^3}{12(1-v^2)} rH \delta^2 \int_0^{2\pi} \int_0^1 \left(\underbrace{\frac{E}{H^4} \left(\frac{\partial^2 \tilde{w}}{\partial \xi^2} \right)^2}_I + \underbrace{\frac{2E}{r^2 H^2} \frac{\partial^2 \tilde{w}}{\partial \xi^2} \frac{\partial^2 \tilde{w}}{\partial \theta^2}}_{II} + \underbrace{\frac{E}{R^4} \left(\frac{\partial^2 \tilde{w}}{\partial \theta^2} \right)^2}_{III} \right) d\xi d\theta \\ & + \underbrace{\frac{Hbr}{r^2} \delta^2 \int_0^{2\pi} \int_0^1 \left(\frac{E}{H^4} \tilde{w}^2 \right) d\xi d\theta}_{IV} - \underbrace{\frac{Hbr\rho g H}{H^2} \delta^2 \int_0^{2\pi} \int_0^1 (1 - \xi) \left(\frac{\partial \tilde{w}}{\partial \xi} \right)^2 d\xi d\theta}_V \end{aligned}$$

With the stability criterion:

$$\frac{b^2}{12(1-v^2)} (I + II + III) + \frac{1}{r^2} IV \geq \frac{\rho g H}{H^2} V$$

With, $v^2 \approx 0$ and:

$$\begin{aligned} I &= \frac{E_0 \varepsilon^4}{H^4} \underbrace{\int_0^1 ((1 - \xi)^\beta \cos^2 \varepsilon \xi) d\xi}_{c_1} \\ II &= \frac{2E_0 \varepsilon^2}{r^2 H^2} \underbrace{\int_0^1 ((1 - \xi)^\beta (\cos^2 \varepsilon \xi - \cos \varepsilon \xi)) d\xi}_{c_2} \\ III &= \frac{E_0}{R^4} \underbrace{\int_0^1 ((1 - \xi)^\beta (1 - \cos \varepsilon \xi)^2) d\xi}_{c_3} \\ IV &= E_0 \underbrace{\int_0^1 ((1 - \xi)^\beta (1 - \cos \varepsilon \xi)^2) d\xi}_{c_3} \\ V &= \varepsilon^2 \underbrace{\int_0^1 ((1 - \xi) \sin^2 \varepsilon \xi) d\xi}_{c_4} \end{aligned}$$

Now we can calculate the integrals for some cases with the expected buckling shape $\varepsilon = \pi/2$:

Appendix

	β			
	0	1	2	3
c_1	0.500	0.351	0.268	0.215
c_2	-0.137	-0.054	-0.026	-0.015
c_3	0.226	0.041	0.013	0.005
c_4	0.149	0.149	0.149	0.149

Table: pre-factors for the energy-based equation, coming from the integration.

In the final step the inequation above is solved for E_0 :

$$E_0 \geq \frac{c_4 \varepsilon^2 \rho g H}{\frac{c_1 \varepsilon^4 b^2}{12 r^4} + \frac{c_2 \varepsilon^2 b^2}{6 r^2 H^2} + \frac{c_3 b^2}{12 r^4} + c_3 \frac{1}{r^2}}$$

With $\beta = 1$ and $\varepsilon = \pi/2$, this becomes:

$$E_0 \geq \frac{0.368 \rho g H}{0.178 \frac{b^2}{r^4} - 0.022 \frac{b^2}{r^2 H^2} + 0.0034 \frac{b^2}{r^4} + 0.041 \frac{1}{r^2}}$$

Curriculum Vitae

Lex Reiter

Date of birth: 19.01.1989

Nationality: Luxembourgish

Languages: German, French, English, Luxembourgish

E-mail: lreiter@ethz.ch

Research interests:

- Digital fabrication with concrete
- Physics and chemistry of hydration and rheology control
- Set on demand materials
- Rheology and processing of building processes

Education:

05.2014 – 07.2019: ETH Zürich, Doctor of Sciences, “Structural Build-up for Digital Fabrication with Concrete – Materials, Methods and Processes” (CH)

09.2011 – 07.2013: ETH Zürich, Master in Civil Engineering, Majors: Structural engineering, Materials and Mechanics (CH)

09.2008 – 07.2011: ETH Zürich, Bachelor in Civil Engineering (CH)

09.2001 – 07.2008: Athénée de Luxembourg, Lycée Classique (LU)

Work experience:

01.2014 – present: ETH Zürich, Assistant, Physical chemistry of building materials
Teaching: Materials 3 & Concrete material science: lab courses
Teaching: Supervision of student projects

Collaborative research: Digital fabrication with concrete

07.2013 – 12.2013: ETH Zürich, Assistant, Steel, Timber and Composite Structures
Teaching: Steel structures, Research: Cementitious coatings

Publications:

Papers in peer-reviewed international journals

- Wangler T., Lloret E., Reiter L., Hack N., Gramazio F., Kohler M., Bernhard M., Dillenburger B., Buchli J., Roussel N., Flatt R., “Digital Concrete: Opportunities and Challenges.”, RILEM Technical Letters (2016) 1: 67-75.
- Popescu M., Reiter L., Liew A., Van Mele T., Flatt R.J., Block P., “Building in Concrete with an Ultra-lightweight Knitted Stay-in-place Formwork: Prototype of a Concrete Shell Bridge”, Structures 14 (2018) 322-332.
- Reiter L., Wangler T., Roussel N., Flatt R.J., “The role of early age structural build-up in digital fabrication with concrete”, Cement and Concrete Research 112 (2018) 86-95.

Papers submitted to peer-reviewed international journals

- Reiter, Lex, Timothy Wangle, Ana Anton, Robert J. Flatt, “Setting on demand for digital concrete – principles, measurements, chemistry, validation”, Cement and Concrete Research, invited contribution, under review

Curriculum Vitae

- Popescu, Mariana, Matthias Rippmann, Andrew Liew, Lex Reiter, Robert Flatt, Tom Van Mele, Philippe Block, “Structural design, digital fabrication and construction of the cable-net and knitted formwork of the KnitCandela concrete shell”, submitted
- Lloret-Fritschi, Ena, Timothy Wangler, Lukas Gebhard, Jaime Mata-Falcon, Joseph Choma, Fabio Scotto, Joris Burger, Rafael Pileggi, Nicolas Ruffray, Lex Reiter, Anna Szabo, Federica Boscaro, Sara Mantellato, Walter Kaufmann, Matthias Kohler, Fabio Gramazio, Robert Flatt, “From Smart Dynamic Casting to a growing family of Digital Casting Systems”, Cement and Concrete research, invited contribution, under review

Papers in work for peer-review in international journals

- Reiter, Lex, Timothy Wangler, Nicolas Roussel, Robert Flatt, “Continuous penetration test for structural build-up characterization”, special issue of Materials, invited contribution, to be submitted Q1 2020.
- Szabo, Anna, Ena Lloret-Fritschi, Lex Reiter, Fabio Gramazio, Matthias Kohler, Robert J. Flatt, “On the potential and limitations of thin folded structures produced by Smart Dynamic Casting”, special issue of Materials, invited contribution, to be submitted Q1 2020.

Conferences proceedings (first author)

- Reiter, Lex, Marta Palacios, Timothy Wangler, and Robert J. Flatt. “Putting Concrete to Sleep and Waking It up with Chemical Admixtures.” In *Proceedings 11th CanmetACI International Conference Superplast. Chem. Admix. Concr., ACI, Ottawa*, SP-302:145–54. Ottawa, ON, Canada, 2015.
- Reiter, Lex, Rene Käßmann, Amir Reza Shahab, Timothy Wangler, and Robert J. Flatt. “Strategies to Wake up Sleeping Concrete.” In *Proceedings of the 14th International Congress on the Chemistry of Cement*. Beijing, China, 2015.
- Reiter, Lex, Timothy Wangler, Nicolas Roussel, and Robert J. Flatt. “Distinguishing Flocculation and Hydration Effects on the Thixotropy of Cement Pastes.” In *8th International RILEM Symposium on Self-Compacting Concrete*, 2016.
- Reiter, Lex, Timothy Wangler, Nicolas Roussel, and Robert J. Flatt. “Continuous Characterization Method for Structural Build-Up.” In *Rheology and Processing of Construction Materials (RheoCon2)*. Dresden, 2019.

Conferences proceedings (other)

- Schultheiss, Marc, Timothy Wangler, Lex Reiter, Nicolas Roussel, Robert J Flatt, “Feedback control of Smart Dynamic Casting through formwork friction measurements”, SCC2016.
- Lloret, Ena, Lex Reiter, Timothy Wangler, Fabio Gramazio, Matthias Kohler, and Robert J. Flatt. “Slipforming with Flexible Formwork - Inline Measurement and Control.” Tromsø, 2017.
- Hack, Norman, Timothy Wangler, Jaime Mata-Falcón, Kathrin Dörfler, Nitish Kumar, Alexander N. Walzer, Konrad Graser, Lex Reiter, Heinz Richner, and Jonas Buchli. “Mesh Mould: An on Site, Robotically Fabricated, Functional Formwork.” In *Second Concrete Innovation Conference (2nd CIC), Paper*, 2017.
- Szabo, Anna, Lex Reiter, Ena Lloret-Fritschi, Fabio Gramazio, Matthias Kohler, Robert Flatt, “Adapting Smart Dynamic Casting to Thin Folded Geometries”, ICCDC, 2018

Curriculum Vitae

- Lloret Fritschi, Fabio Scotto, Fabio Gramazio, Matthias Kohler, Konrad Grasser, Timothy Wangler, Lex Reiter, Robert Flatt, Jaime Mata-Falcon, “Smart Dynamic Casting: first architectural application”, ICCDC, 2018
- Palacios, Marta, Daniel Sanz-Pont, Ratan Mishra, Federica Boscaro, Delphine Marchon, Lex Reiter, Sara Mantellato, Robert J. Flatt, “Retarding cement hydration by increasing temperature”, CANMET, 2018
- Anton, Ana, Angela Yoo, Patrick Bedarf, Lex Reiter, Timothy Wangler, Benjamin Dillenburger, “Vertical Modulations: computational design for concrete 3D printed columns”, ACADIA, 2019
- Szabo, Anna, Ena Lloret-Fritschi, Lex Reiter, Fabio Gramazio, Matthias Kohler, Robert J. Flatt, “Revisiting Folded Forms with Digital Fabrication”, ECAADE, 2019
- Szabo, Anna, Lex Reiter, Ena Lloret-Fritschi, Fabio Gramazio, Matthias Kohler, Robert J. Flatt, “Processing of set on demand solutions for digital fabrication in architecture”, RheoCon2, 2019
- Das, Arnesh, Lex Reiter, Timothy Wangler, Robert J. Flatt, “Hydration control of ternary cements for digital fabrication with concrete”, RheoCon2, 2019
- Anton, Ana, Patrick Bedarf, Angela Yoo, Lex Reiter, Timothy Wangler, Robert J. Flatt, Benjamin Dillenburger, “Concrete Choreography: Prefabrication of 3D printed columns”, Fabricate, 2020
- Das, Arnesh, Lex Reiter, Robert J. Flatt, “Blended calcium aluminate cements for digital fabrication with concrete”, International Conference on Calcium Aluminates, 2020

Awards:

- 2013 Holcim Beton Preis for master thesis
- 2017 Concrete Innovation Award at Concrete Innovation Conference (Mesh Mould)
- 2018 Best student proceedings paper at Digital Concrete Conference (SDC)